Development of a Novel Class of Multifunctional Virulence-Attenuating Antibiotics

by

Bryan Daniel Yestrepsky

A dissertation submitted in partial fulfillment
of the requirements for the degree of
Doctor of Philosophy
(Medicinal Chemistry)
in the University of Michigan
2013

Doctoral Committee:

Research Professor Scott D. Larsen, Co-chair
Assistant Professor Matthew B. Soellner, Co-chair
Professor Henry I. Mosberg
Professor Ronald W. Woodard

Acknowledgement

The preparation of this document caps an experience that has undoubtedly been the most challenging I've faced so far. Although the level of rigor and time commitment was high, everyone involved contributed to making the pursuit of my doctoral degree a pleasant and rewarding experience.

First and foremost, I need to extend my deepest gratitude to my wife Michelle. On top of being a wonderful partner, you have been my best friend, training coach, therapist, and motivational speaker. I can say that without your companionship and eternal optimism over the last seven years, the course of my graduate work, and indeed my life, would unequivocally have been altered for the worse. I love you more than anything and I'm excited to see what the future holds for us.

As a lifelong resident of southern Michigan, I have been blessed with the almost unfair advantage of being near my family and friends as I progressed through my graduate studies. My mother and father, Dan and Diane, continue to be endless sources of encouragement and kindness. Thank you for your unconditional endorsement of the choices I've made and every dream that I've pursued. Thank you also to my grandparents, Andrew and Margaret Yestrepsky and Albert and Judith Noel. I appreciate your pride in my accomplishments despite the fact I am 27 and just finishing school. Also worthy of a special mention is my brother Adam. Your continued successes have stoked a particularly high-achieving form of sibling rivalry that has contributed greatly to my own motivations. My family support group extends beyond these individuals, and includes my parents-in-law Pat and Jean Wicksall and sister-in-law Rachel; my uncles Paul, Jim, Al, Mitch, David Porteous, and their significant others; and all my cousins and extended family members. It is a true blessing to be surrounded by so many supportive and positive people that have given me nothing but encouragement.

I also need to thank my friends and Med Chem colleagues. I owe a lot to my lab mates in the Larsen group: Dr. Jessica Bell, Janice Sindac, Helen Waldschmidt, and particularly Scott Barraza. We shared a lot, including stupid internet videos, constant jokes, a few beers, and occasional input on each other's project difficulties. Scott, I'd like to say thank you for keeping

me sane in lab, but I think everyone would agree that our part of the lab could not be defined as "sane." Though I was technically the senior student in the lab, I think it's up for debate who taught the other more chemistry over the last 4 years. Other Michigan students I need to acknowledge are Joel McDade, Kristoffer Brandvold, Douglas Hansen, Kyle Heslip, Ronak Shah, Corinne Weisheit, and Dr. Ronald Jenkins. I wish you all the best of luck and expect to meet up with you all at conventions and football games once in a while. I must also mention my friends from outside of the University, including Mike Wiese, Gary Peters, Andrew and Ashley Mirasol, Randy McGrail, Ben McArthur, and many more than I can list here.

My road to a doctoral degree did not begin in the Fall of 2008, but rather years before, when my interest in science was stimulated by several excellent teachers. Thank you to my high school chemistry teachers, Dr. Claudia Heinbuck and the late Edward Cackowski, and my professors at Albion College, in particular Drs. Clifford Harris, Vanessa McCaffrey, Chris Rohlman, and Molly Scheel, for teaching me the scientific tools that I use every day.

This acknowledgement would not be complete without thanking the people directly involved with me on my thesis project. In particular my deepest gratitude goes to Dr. Scott Larsen, who deserves most of the credit for my development into a capable synthetic organic chemist. Between your vast theoretical knowledge of medicinal and organic chemistry and Mr. Mike Wilson's equally broad knowledge of bench chemistry, the Larsen group was the ideal place to learn the ropes of medicinal chemistry research. I must also thank Dr. Walajapet Rajeswaran, Roderick Sorenson, Jenny Ryu, and Meghan Breen for their contributions to the synthetic chemistry portion of this project, and the rest of the VMCC for assistance and advice. The biochemical work performed by my collaborators, led by Dr. Hongmin Sun and Dr. David Ginsburg, made this project possible. In particular, Dr. Yuanxi Xu, Dr. Yibao Ma, and Dr. Colin Kretz put significant portions of their time into this study for which I am very appreciative.

Finally, I would like to extend my gratitude to the faculty that served on my thesis committee, including Dr. Ronald Woodard, Dr. Garry Dotson, Dr. Matt Soellner, Dr. Hank Mosberg, and especially Dr. Jason Gestwicki for all of your thoughtful contributions and critiques of my research plan over the years. The rest of the University of Michigan faculty and staff, including Cherie Dotson, Dr. Scott Woehler, and Sarah Lloyd also deserve mention here.

Putting all of my acknowledgements into writing overwhelms me with thoughts of how much I have received from all of you over the years. In return, I will take it upon myself to achieve to the best of my ability and continue to make you all proud.

-Bryan Yestrepsky

Table of Contents

List of Figures

List of Schemes

List of Tables

Chapter 1: Introduction

Bacterial Infection and Antibiotics

Bacterial infection is a ubiquitous aspect of the human condition, representing one of the most significant sources of human mortality from antiquity to the present day. It is estimated that over 16 million people succumbed to communicable diseases in 2008,[1] despite over 100 years of biomedical research into controlling infection. Though the knowledge that outside agents could be used to control infection has been employed for millennia, modern academic inquiry into anti-infective agents can be thought of as beginning in 1871, when Dr. Joseph Lister noted the antibacterial effect *Penicillium* mold had on urine samples and infected wounds.[2] Although the *Penicillium* family of molds was studied sporadically for the next 50 years, Alexander Fleming's 1928 isolation of an organic residue exuded by *Penicillium notatum* capable of destroying *Staphylococcus aureus* cultures[3] caused a rush of interest. Twelve years later, Chain, Florey, *et al.* demonstrated that a partially purified and stabilized concentrate of this substance, dubbed "penicillin," could reliably treat infection in human patients.[4] The 1930s and 1940s saw the ushering in of the "antibiotic age," characterized by an explosion in the development of several classes of antibiotics, including the sulfonamides,[5] aminoglycosides,[6] and tetracyclines.[7] The ready availability of antibiotic agents was one of the most transformative advances of the 20th century, leading to unprecedented decreases in mortality from infectious disease.[8,9,10] The effectiveness of antibiotics led several prominent infectious disease experts to conclude as recently as 1978 that bacterial infection would soon be eradicated,[11,12] but evidence to the contrary had already been mounting for years. Fleming himself noted the possibility of bacteria developing resistance to antibiotics via exposure to sub-lethal doses in his Nobel lecture in 1945.[13]

In less than 70 years since the widespread availability of antibiotic drugs, bacterial resistance to antibiotics has become a worldwide health crisis. Several multiply-resistant strains of both Gram-positive and Gram-negative bacteria are now commonplace in the human population, especially in the hospital setting.[14,15] Antibiotic resistance generally arises when an

individual bacterium acquires mechanisms to deactivate or evade the action of a given drug, either through random mutation, lateral gene transfer from a resistant individual, or phage-acquired genetic material.[16] Bacterial populations with a few resistant members will have the vast majority of susceptible bacteria wiped out by the antibiotic treatment, allowing the resistant population to quickly become dominant within the host. In spite of the ever-increasing threat of widespread bacterial resistance, the number of new drugs in clinical trials for combating bacterial infection has been on a steady decline for decades, due mostly to the difficulty of their development and the reality that any new antibiotic will be used as an agent of last resort and is thus unlikely to recoup research costs through revenue.[17] The tandem threat of increasing resistance and diminished research into traditional antibiotics prompts the need for focused scientific inquiry into novel antibacterial development.

Anti-Virulence Antibiotics

One promising novel approach to the problem of bacterial resistance is the development of virulence inhibitors. Invasive bacteria produce a number of proteins or secondary metabolites known as virulence factors in order to enhance infectivity and ensure colony survival in a host organism. If the action or the production of these factors can be inhibited, the bacterial colony is rendered into a more vulnerable state and is potentially more easily controlled by the host immune response. More importantly, the specific inhibition of virulence factors with small molecules that do not affect bacterial growth should lower the selective pressure to acquire resistance.[18] Traditional antibiotics, on the other hand, by directly inducing bacterial cell death or preventing bacterial reproduction, exert rapid evolutionary pressure by enriching bacterial populations capable of resisting treatment. Anti-virulence antibiotics have garnered the interest of several research groups over the last fifteen years, targeting a variety of virulence factors, including bacterial toxins,[19] adhesion factors,[20] quorum-sensing systems,[21,22] and virulence-inducing signaling pathways.[23] Though no anti-virulence drugs have yet progressed to use in the clinic, inhibitors of anthrax toxin cell permeability,[24] *N*-acyl homoserine lactone-mediated quorum sensing,[25] and QseC histidine sensor kinase activation[23] have demonstrated efficacy in murine models of infection.

Group A Streptococcus

Streptococcus pyogenes, or Group A Streptococcus (GAS), represents one example of the global threat of bacterial infection. This Gram-positive, hemolytic species of bacteria is a

ubiquitous human pathogen responsible for up to 700 million infections per year worldwide.[26] GAS is most commonly associated with relatively benign clinical presentations, including upper respiratory infection ("strep throat") and superficial skin infections. However, particularly virulent strains can induce far more serious systemic infections. Cases of systemic GAS infection are thought to approach 500,000 annually, with a mortality rate of 15-35%.[27,28] Some of the most dangerous systemic GAS infections include streptococcal toxic shock syndrome (STSS), which induces hyperinflammatory responses, hypotension, and organ failure;[29] acute rheumatic fever induced by cross-reactivity of anti-GAS immunoglobulins with heart tissue;[30] and acute necrotizing fasciitis, characterized by massive invasion of the connective tissue surrounding internal organs.[31]

A considerable body of research to characterize GAS virulence factors has evolved over the last half-century, revealing that its virulence is complex and multifaceted.[32] The most well-studied GAS virulence factors are the M-family of proteins and hyaluronic acid, both of which are responsible for resistance to phagocytosis by leukocytes. M-protein is a dimeric coiled-coil α-helical protein that extends from the cell membrane through the peptidoglycan wall.[33] The environment-exposed end of this protein binds to several circulating factors, most importantly C4 binding protein (C4BP), inhibiting the recruitment of opsonization factors C3b and C4 to the microbial surface.[34] In the absence of M-protein, GAS cells are readily opsonized (marked for phagocytosis) and destroyed.[35] Hyaluronic acid is an aminopolysaccharide polymer secreted by GAS in order to encapsulate its cells, conferring up to 100-fold higher resistance to phagocytosis when compared to unencapsulated strains.[36] GAS also produces a host of adhesin molecules, such as fibronectin binding protein and lipoteichoic acid, which promote association with various host epithelial tissue features. Adhesin presentation on the bacterial protein coat allows GAS to anchor itself to solid tissue and initiate biofilm formation, a process strongly associated with enhanced virulence.[37] The mechanics and clinical importance of biofilm formation in systemic infection is further discussed in Chapter 4. Finally, GAS secretes a number of exotoxins including hemolytic enzyme streptolysin O,[38] cysteine protease SpeB,[39] and the fibrinolysis promoter streptokinase (SK).[40] These exotoxins allow GAS to destroy aspects of host systems that are intended to neutralize infections (e.g. leukocytes, lysosomes, and fibrin clots).

Our collaborators in the Hongmin Sun group at the University of Missouri – Columbia are particularly focused on the contribution of SK to GAS virulence.[40] SK essentially functions

as a chaperone-like protein capable of binding to human plasminogen (Plg) and inducing a conformational change. Plg is the catalytically inactive zymogen of plasmin, a serine protease responsible for the cleavage of fibrin.[41] Fibrin cleavage leads to the dissolution of blood clots, and plasmin is normally activated in response to excessive clotting or in the removal of blood clots that are no longer needed. Plg is normally held in the inactive state until a specific cleavage between Arg561 and Val562, endogenously catalyzed by fibrin-associated protein tissue plasmin activator (tPA) or urokinase plasmin activator (uPA).[42,43] Tight regulation of this cascade gives the body fine control over the equilibrium between excessive and insufficient clotting. However, when Plg associates with SK, a conformational shift is induced that confers catalytic activity without proteolytic cleavage. This activated SK-Plg complex is then capable of efficiently cleaving other molecules of Plg to plasmin, activating its fibrinolytic capability.[44] By increasing local concentrations of plasmin, GAS colonies can evade the host immune response of clotting around foci of infection, thereby maintaining its ability to achieve systemic distribution. Sun *et al.* were instrumental in determining that the specificity of the SK-human Plg interaction is the major biochemical determinant of GAS's exclusive virulence in humans.[40]

Identifying GAS-SK Modulators

Armed with the knowledge of SK's ability to mediate potentially fatal systemic GAS infection, Sun and coworkers initiated a high-throughput screen (HTS) for chemical agents that could attenuate GAS-SK.[45] The direct inhibition of protein-protein interactions with small molecules is very difficult, owing to the typically large amount of surface area of each protein involved in the association. Therefore, the decision was made to identify compounds that inhibit SK production at the transcriptional level, presumably by the disruption of transcription factors or upstream signaling cascades that induce its production. The HTS assay parameters required the combination of datasets from two separate screens (Figure 1.1). In the first screen, GAS colonies transfected with a plasmid coding for a kanamycin (Kan) resistance gene downstream from the *ska* gene promoter region ("SKKanGAS") were incubated with screening library compounds in media containing kanamycin. Therefore, if a small molecule exerted an effect that reduced transcription at the *ska* promoter, the test colony was sensitized to kanamycin and cell death was induced. The second screen employed a separate strain of GAS (UMAA2641) with constitutive kanamycin resistance conferred by the knock-in of the ΩKm-2 viral gene interposon.[46] This second screen was intended to identify any compounds that had innately

bacteriotoxic effects. In keeping with the goal of identifying compounds with strictly anti-virulent effects, we were interested in compounds that had potent effects at the *ska* promoter (>50% inhibition of SKKanGAS strain) while having minimal effects on normal bacterial growth (<10% inhibition of UMAA2641) to avoid inducing selective pressure for resistance.

Figure 1.1. Design of tandem HTS screen for identifying compounds that inhibit GAS-SK transcription.

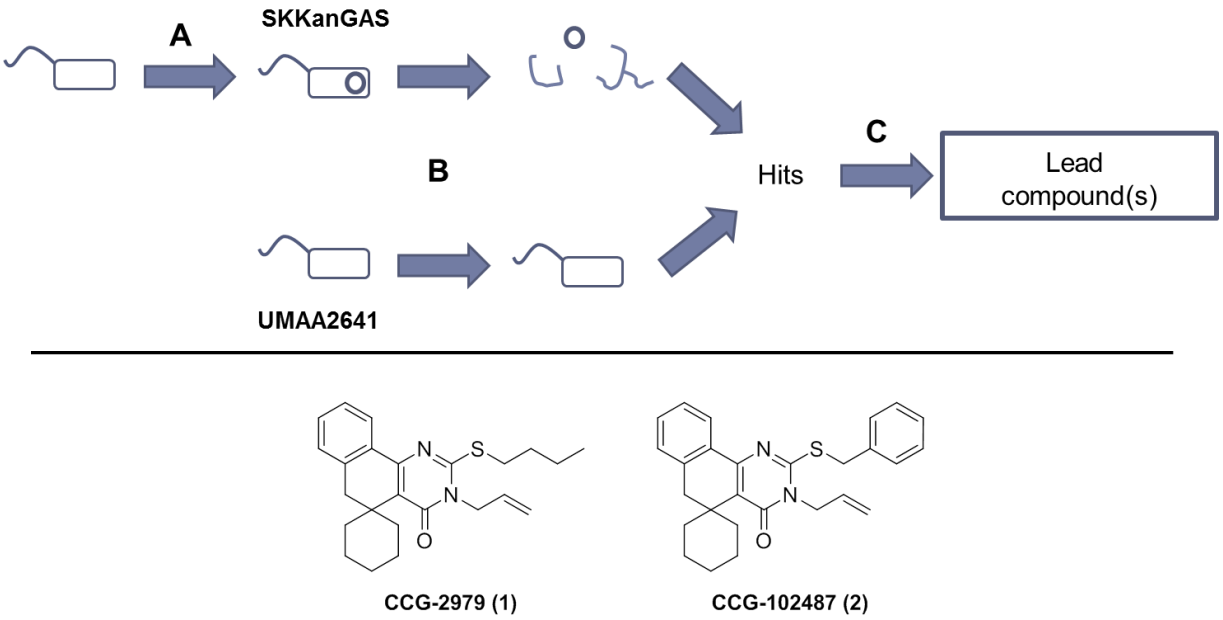

Top pane: HTS design. A: Transfection of plasmid containing Kan resistance gene fused to upstream *ska* promoter. B: SKKanGAS strain (*ska*-dependent Kan resistance) and UMAA2641 (constitutive Kan resistance) incubated in the presence of compounds in Kan+ media. Compounds that sensitize SKKanGAS to Kan >50% affect UMAA2641 growth <10% are considered hits. C: Initial hits are triaged by dose-response confirmation, activity assay with fresh powders, and elimination of hits with structural liabilities. **Bottom pane:** Structures of lead compound 1 and related commercial analog 2.

The screen was performed using the 55,000-compound Center for Chemical Genomics screening collection at the University of Michigan at test concentrations of 5 to 10 µM. After screening both GAS strains and comparing datasets, 95 compounds were identified that satisfied the previously stated activity and selectivity criteria. Dose-response curves were generated for these 95 initial hits, revealing 20 that possessed IC_{50} values of 30 µM or less for SKKanGAS inhibition and at least tenfold higher IC_{50}s against UMAA2641. Of these 20 confirmed hits, 8 were commercially available as fresh powders. 4 of the 8 compounds, when prepared from fresh stock, indicated significant (>30%) inhibition of UMAA2641 at 50 µM, and were dropped from

consideration. Considerations of HTS hit rate, potential for off-target reactivity, and conformity to Lipinski's "Rule of 5"[47] led to the selection of CCG-2979 (**1**) as the lead compound. Follow-up functional assays confirmed that **1** decreased SK activity in wild-type GAS, enhanced GAS susceptibility to phagocytosis in mouse blood, and closely related analog **2** downregulated the expression of SK and several other virulence factors as measured by RNA microarray analysis (Figure 1.2).[45]

Figure 1.2. Summary of GAS RNA levels after incubation with 2 for several important genes, relative to colonies treated with DMSO only.

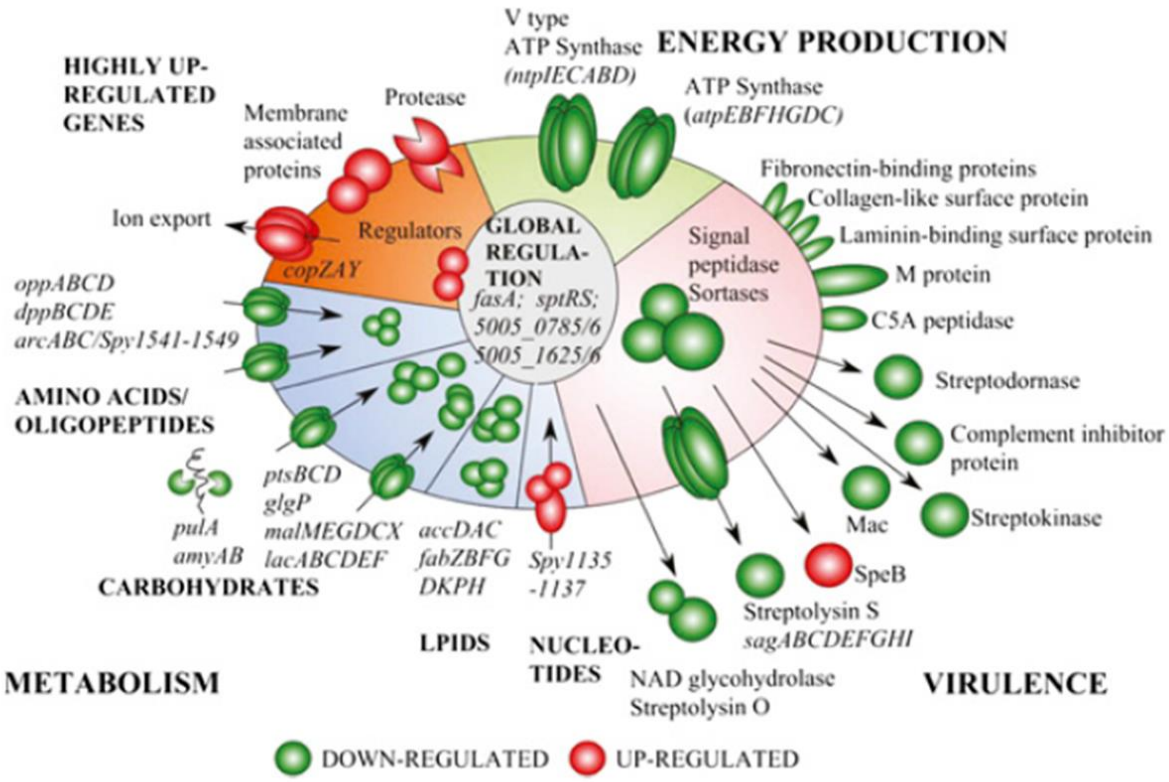

Figure adapted from Sun *et al.*, *PNAS* **2012**, *109* (9), 3469-74.

The encouraging cell-based data collected to this point led Sun *et al.* to characterize the utility of **1** to control GAS infection *in vivo* (Figure 1.3). As previously discussed, human plasminogen is required for systemic GAS infection. Therefore, mice were sensitized to GAS infection via the transfection of the human plasminogen gene into the mouse genome. When the transgenic mice were dosed with 5 or 40 μg of **1** every 24 hours via intraperitoneal injection for

4-5 days after infection with GAS, significant protective effects were observed over the course of the 10-day study.[45] Interestingly, closely related commercial analog CCG-102487 (**2**) did not exert the same protective effect, despite similar activity in cell-based activity assays. A possible explanation for this phenomenon may be related to significant differences in metabolic stability observed between these two compounds, an issue discussed more thoroughly in Chapter 2.

Figure 1.3. Survival curves for mouse populations treated with test compound (dashed lines) or DMSO only (solid lines).

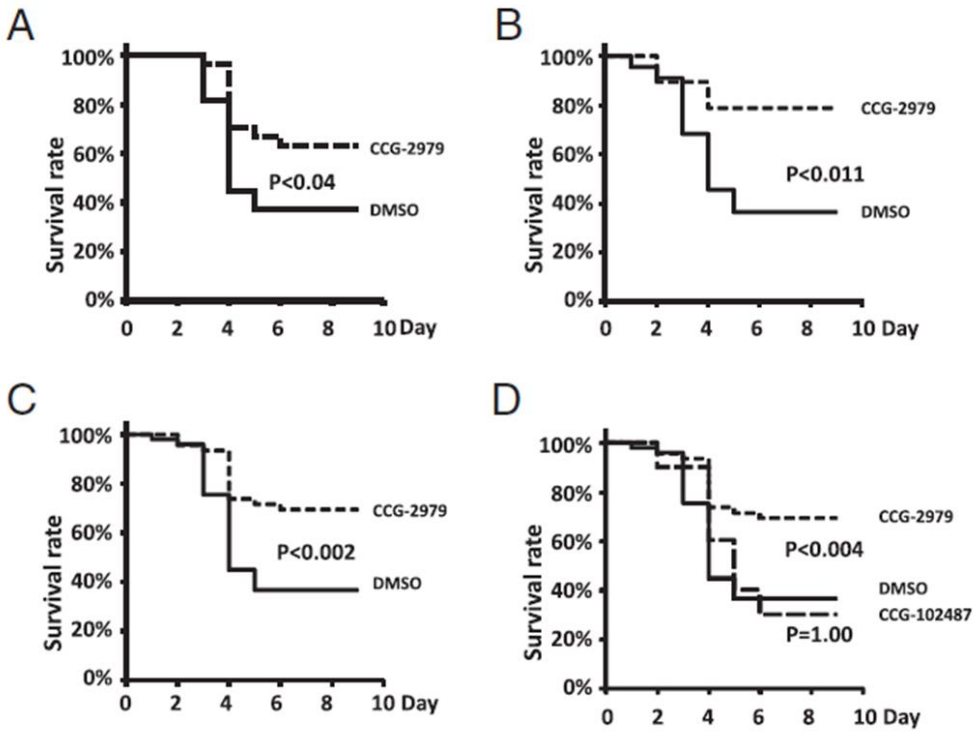

Graph A: Mice treated i.p. with 12.7 nmol **1** every 24 hours for 5 days post-infection with 2.8-8.3 x 10^5 CFU GAS. n = 27 for test and control population. **Graph B*:*** Mice treated i.p. with 101 nmol **1** every 24 hours for 4 days post-infection with 1.2-4.2 x 10^6 CFU GAS. n = 19 for test and 22 for control population. **Graph C:** Pooled data from Graphs A and B. **Graph D:** Mice treated i.p. with 93 nmol **2** every 24 hours for 4 days post-infection with 4.2 x 10^6 CFU GAS. n = 10 for test population. Pooled data from Graph C added for reference. Figure adapted from Sun *et al.*, *PNAS* **2012**, *109* (9), 3469-74.

The completion of several assays suggesting the SK-attenuative properties of **1**, combined with favorable *in vivo* proof-of-concept study data (a relatively rare occurrence for unmodified HTS lead compounds), suggested it was a good starting point for initiating a structure-activity relationship (SAR) study. The SAR study was conceived with the intent of increasing the modest potency (% of plasmin activity at 50 μM = 48 ± 28%) of the lead, and

improving the predicted pharmacokinetic properties of the scaffold. In particular, we were concerned about its high lipophilicity (cLogP = 7.1), which can be associated with poor solubility and metabolic stability.[48] Our efforts toward improving the attenuation of GAS-SK with a compound series based on **1** are discussed at length in Chapter 2.

The results of these pilot studies on **1** also raised the prospects of other studies of academic interest. Cell-based HTS assays are ideal for identifying innately cell-permeable compounds that induce a desired phenotype, but give no insight into the macromolecular target of the lead compound. The identification of the macromolecular target of this compound series could offer great advantages to the SAR effort by supplementing cell-based assays with more direct activity/affinity profiling using the purified target. More broadly, target identification would also help to elucidate potentially novel bacterial mechanisms of virulence control in GAS; any significant findings could have implications for other human bacterial pathogens, depending on the presence of homologous proteins in other species. Our design of chemical probes for the purpose of target identification and the associated preliminary biological data is discussed in Chapter 3. Finally, the mRNA microarray data (Figure 1.2) suggests that this class of compounds exerts activity on other virulence factors, including several genes associated with biofilm formation. The ability for bacteria to form biofilms confers greatly increased colony survival in host organisms, and is thus a very attractive target for anti-virulence antibiotic development. Our efforts toward optimizing this scaffold for biofilm inhibition are detailed in Chapter 4.

Chapter 2: GAS-SK SAR Study

SAR Logic

Lead compound **1**, while showing acceptable activity in the HTS assay and in early *in vivo* trials, exhibited a number of shortcomings that had to be addressed in the structure-activity relationship (SAR) campaign. Though efficacy was indeed observed in mice,[45] the IC_{50} reported by our cell-based assay of SK activity was found to be greater than 50 μM. In addition to its fairly low potency, **1** is also quite lipophilic (cLogP = 7.1), which is indicative of low aqueous solubility and a greater propensity for oxidation by P450 oxidase enzymes, which could lead to instability *in vivo*.[48]

With these observations in mind, we proposed several modifications to the scaffold with the intent of maximizing potency and aqueous solubility while minimizing the number of metabolically labile sites (Figure 2.1). We sought to modify the *n*-butyl sulfide appendage by replacement of the sulfur with smaller heteroatoms (O, N) and incorporation of polar groups to assist in increasing solubility and stability. Smaller alkyl substitutions to replace the spirocyclohexyl substituent of the central ring were intended to serve the same purpose. We were also particularly interested in introducing substitutions around the phenyl ring. With the entire polar functionality of **1** confined to one small region of the molecule, there are likely very few strong intermolecular contacts (e.g. dipole interactions, H-bonds) made with the protein, implying that **1** must rely on relatively weak hydrophobic effects for binding affinity. We reasoned that a more even distribution of polar contacts around the scaffold could lead to significant increases in potency, provided they were sterically allowed by the binding site.

Figure 2.1. Lead compound 1 and proposed alterations to its scaffold for SAR study.

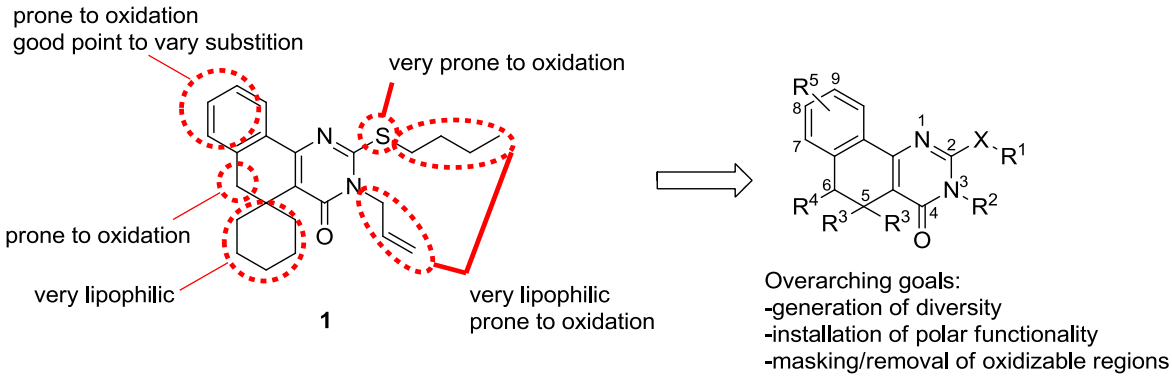

GAS-SK Assay

All new compounds were evaluated by the Sun group at University of Missouri - Columbia for their ability to suppress SK expression using a chromogenic assay of plasmin activity.[45] Briefly, two identical cultures of GAS were grown in the presence of the desired concentration of test compound or DMSO and allowed to grow to $OD_{600} \approx 1.0$. After centrifugation, an aliquot of supernatant was combined with human plasma and synthetic plasmin substrate S-2403. Decreased expression of SK induced by the test compound lowers the amount of activated plasmin, in turn reducing the rate of cleavage of S-2403 to colored product *p*-nitroaniline. The concentration of *p*-nitroaniline was measured by absorbance at 405 nm (A_{405}) and compared to the DMSO control. Activity data is reported as the ratio of A_{405}(test) divided by A_{405}(control) (T/C). To provide an approximate readout of potency, the assay was run initially at both 5 and 50 μM of test compound. An optical density reading at 600 nm (OD_{600}) gave an estimate of cell density and thus overall bacterial growth inhibition; this data is also reported for the higher concentration of compound (50 μM) as a ratio of the OD_{600} of the test culture divided by the OD_{600} of the DMSO control culture. Selected compounds that inhibited SK activity by more than 50% at 50 μM and inhibited growth by less than 25% at 50 μM were subjected to full dose-response titrations to determine approximate IC_{50} values using the same assay.

During the course of evaluating the new analogs, it was observed that there was a relatively high level of inter-assay variability in the activity assay. There are a number of likely contributing factors, most notably the variability inherent to working in a live bacterial system. For example, it has been noted that minimum inhibitory concentration (MIC) values for

determining bacteriotoxicity tend to vary by up to three-fold from assay to assay.[49] Furthermore, the currently unknown macromolecular target of these compounds likely affects a pathway including a transcription factor, which are known to be low-abundance proteins[50] that exhibit significant temporal expression changes, potentially contributing to the variability. It was noted early in the SAR effort that **17** was both moderately active and particularly consistent from assay to assay. In an effort to reduce the number of anomalous data points, **17** was included in each assay as a positive control. Assays in which **17** exhibited activity deviating from the mean activity at 5 and 50 μM by more than one standard deviation (calculated from a total of 35 assays) were discarded.

Synthesis

Spirocyclohexyl tetracyclic analogs

Initial synthetic SAR development was accomplished by Jenny Ryu in the Larsen group using a known 5-step synthetic pathway to access intermediate **6** beginning from cyclohexanone (Scheme 2.1). A Knoevenagel condensation with ethyl cyanoacetate generated Michael acceptor **4**, which was subjected to nucleophilic attack by benzylmagnesium chloride and subsequently cyclized to the tricyclic aminoester **5** in the presence of concentrated sulfuric acid.[51] Addition of the amine to allyl isothiocyanate followed by hydroxide-promoted cyclization provided **6** on multigram scale.[52] From this intermediate a variety of *S*-alkylated analogs (**7**-**13**) could be accessed under basic alkylating conditions. Other heteroatomic substitution at the 2-position of the pyrimidinone ring was achieved via nucleophilic substitution of thiomethyl for the ethyl ether via the action of sodium ethoxide (**12**, Meghan Breen), or through replacement of the methyl sulfone with ethylamine under basic conditions (**13**).[53] Synthetic procedures and spectral characterization of compounds made by other chemists are fully disclosed in our publication on the topic.[54]

Scheme 2.1. Preparation of spirocyclohexyl analogs of 1.[a]

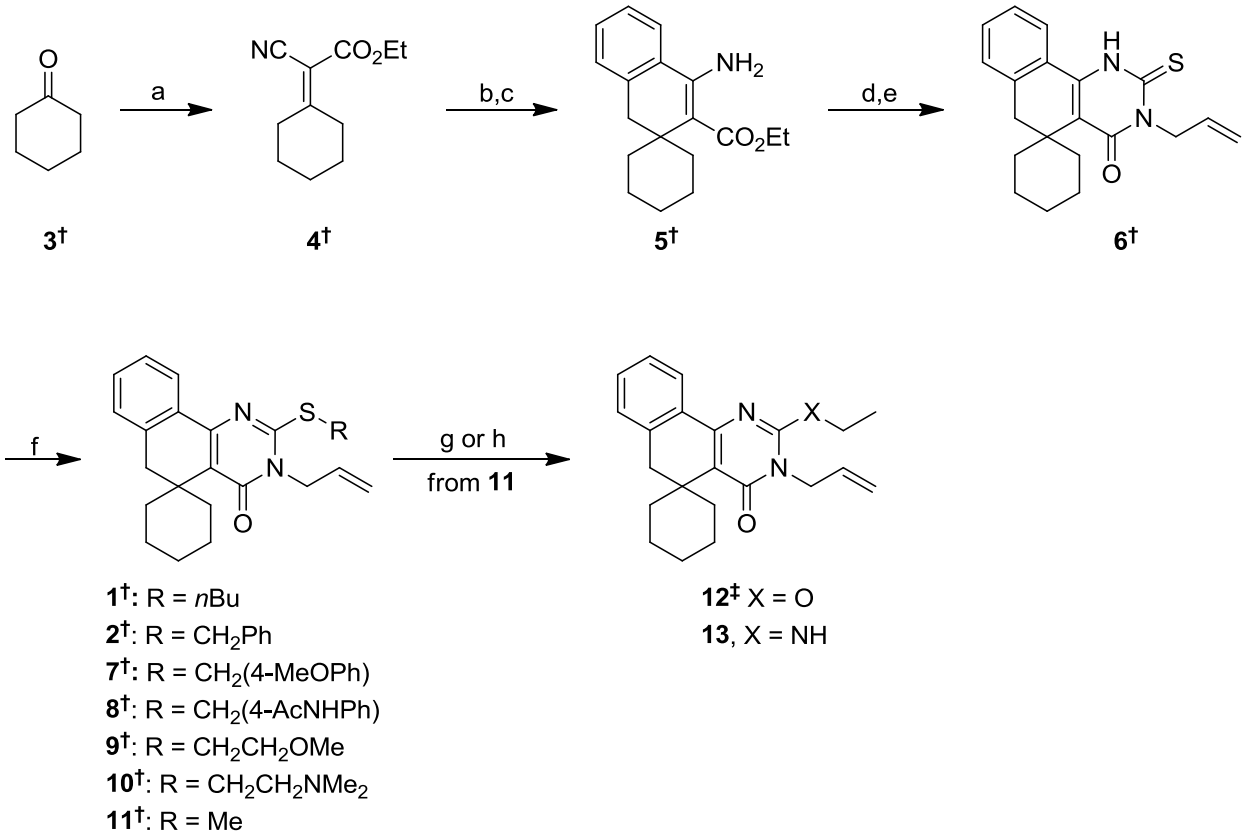

[a]Reagents and conditions: a) ethyl cyanoacetate, AcOH, NH_4OAc, toluene, 150°C, 5h, 89%; b) BnMgCl, Et_2O, RT, 72h; c) H_2SO_4, 0°C-RT, 7h 68% over 2 steps; d) allyl isothiocyanate, EtOH, reflux, 10h; e) KOH, EtOH:H_2O (1:1), reflux, 10h, 30% over 2 steps; f) R-X, base, EtOH or MEK, 0-70°C, 10min-16h, 72-95%; g) NaOEt, EtOH, 40°C, 48h, 73%; h) (i) *m*CPBA, DCM, RT, 16h, (ii) $EtNH_2$, K_2CO_3, THF:DMF (1:1), RT, 5h, 53% over 2 steps. †Compound originally synthesized by Jenny Ryu. ‡Compound originally synthesized by Meghan Breen.

Gem-dimethyl tricycles

Given the relative ease with which the original spirocyclohexyl-substituted analogs were synthesized, we were surprised to find that the generation of gem-dimethyl analogs (e.g. **17-22**, Scheme 2.2) using the chemistry outlined in Scheme 2.1 was extremely unreliable and low yielding. While Michael addition of benzylmagnesium chloride into ethyl 2-cyano-3-methylbut-2-enoate proceeded as desired, the acid-catalyzed cyclization to β-aminoester analogous to **5** proceeded in a yield too low to generate more than a few *S*-alkylated final compounds (Meghan Breen). Likewise, the stepwise addition and cyclization reaction with allyl isothiocyanate shown

in Scheme 2.1 did not proceed in greater than a 25% yield, severely limiting the utility of this synthetic route.

Scheme 2.2. Synthesis of gem-dimethyl substituted analogs 17-24.[a]

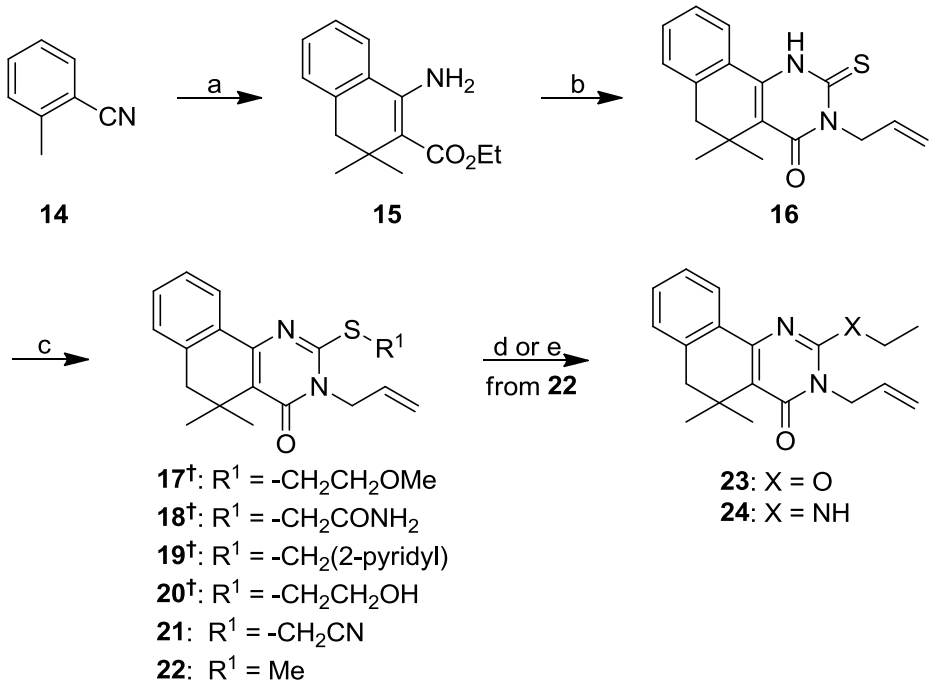

[a]Reagents and conditions: a) LDA, diglyme, -78°C, 1h; then ethyl 3,3-dimethyl acrylate, ZnI_2, -78°C-RT, 2h, 41%; b) allyl-NCS, AcOH, EtOH, 70°C, 16h, 24%; c) R^1-X, Cs_2CO_3, MEK or DMF, 70°C, 16h 71-96%; d) NaOEt, EtOH, 40°C, 48h, 69%; e) (i) *m*CPBA, DCM, 0°C-RT, 16h; (ii) $EtNH_2$, K_2CO_3, THF:DMF (1:1), RT, 5h, 41% over 2 steps. †Compound originally synthesized by Meghan Breen.

Through extensive optimization, it was determined that the β-aminoester **15** could be accessed in one step beginning from commercially available *o*-tolunitrile **14** (Scheme 2.2). In the presence of LDA, smooth addition of the benzyl anion of **14** to the β-position of ethyl 3,3-dimethyl acrylate afforded an enol ester intermediate that readily cyclized in the presence of ZnI_2, providing amino ester **15**.[55] In contrast to the basic conditions used to generate **6**, acid-catalyzed conditions for condensation with alkyl isothiocyanates were found to more efficiently furnish the 2-thioxo-dihydropyrimidinone intermediate **16**. Subsequent alkylation at sulfur ultimately allowed the synthesis of gem-dimethyl analogs **17-22** in a total of 3 steps. Further derivatization of thiomethyl analog **22** to generate ether and amino derivatives **23** and **24** was achieved in the same manner as for **12** and **13**, respectively.

Aryl ethers and phenols

Modification of the synthetic scheme to generate aryl ethers and phenols (**29-39**) was fairly straightforward (Scheme 2.3). The requisite tolunitriles were either purchased from commercial sources (**26c**) or were synthesized via nickel (II) bromide-promoted S_NAr addition of cyanide ion to the corresponding *o*-chlorotoluene aryl methyl ethers **25a**,**b**.[56] The addition of methyl iodide in toluene to the crude reaction isolate allowed for the facile removal of tetraalkyl phosphonium salts and drastically simplified purification of **26a** and **26b**. Elaboration to the *S*-alkylated analogs **29-33** proceeded as previously described. Though we had hoped that the aryl methyl ether of **29** could be cleaved to the free phenol in a regioselective manner, we found that BBr_3-mediated demethylation resulted in a mixture of aryl and alkyl ether removal. When the sulfur appendage was changed to ethyl (i.e. **31-33**), BBr_3 demethylation proceeded smoothly to furnish phenols **34-36**. From these three intermediates, a variety of alkylating agents could be used to generate a library of aryl ether analogs. Our primary concern with these analogs was at first to identify the optimal positioning of a PEG appendage on the molecule for the target identification effort (Chapter 3). Therefore, PEG-like compounds **37-39** were synthesized using 2-methoxyethyl tosylate as the alkylating agent. A full complement of diverse aryl ethers at the 8-position was synthesized by chemist Roderick Sorenson, and a thorough discussion of these analogs can be found in our SAR publication.[54]

Scheme 2.3. Synthesis of aryl ethers 29-39.[a]

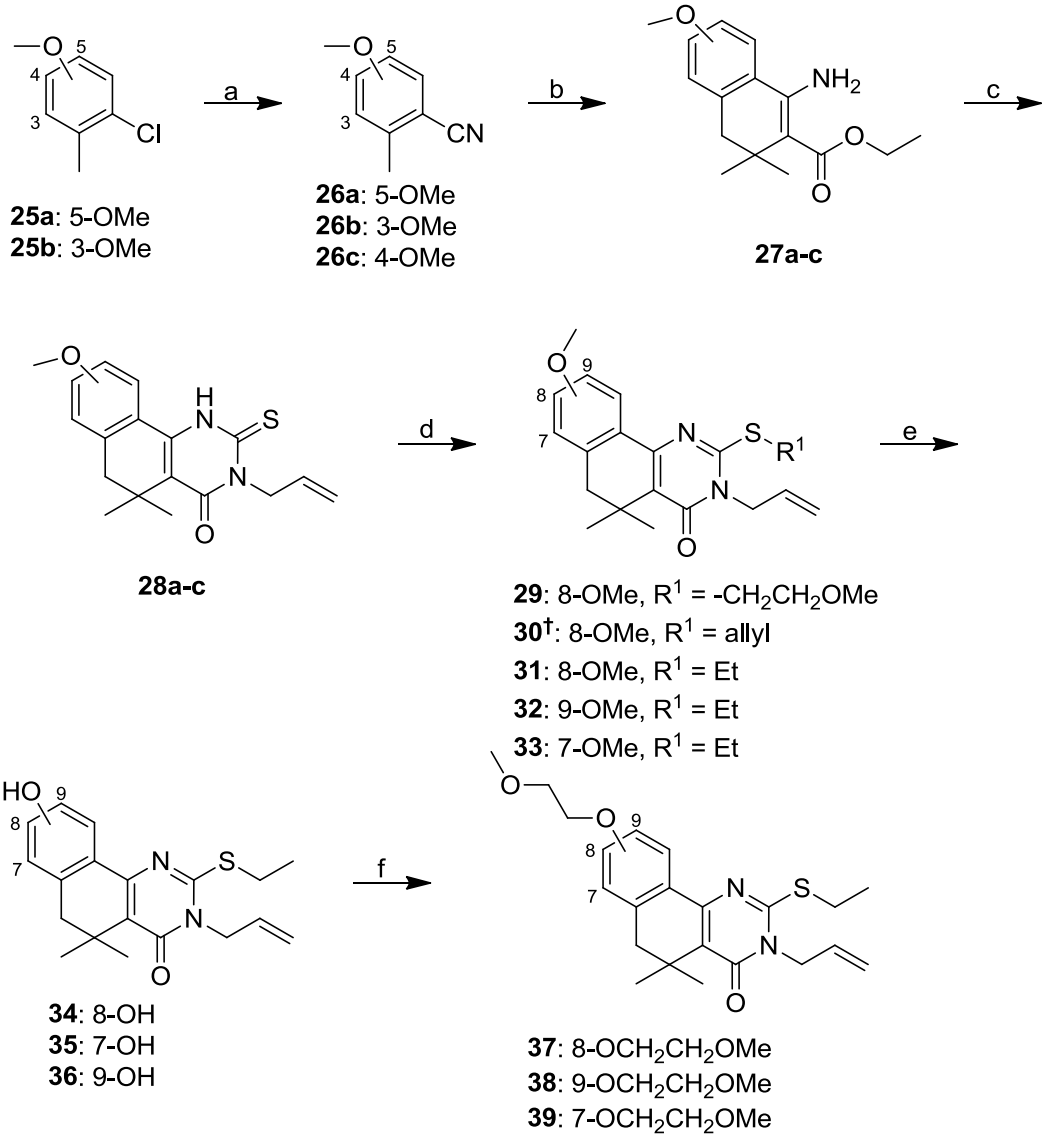

[a]Reagents and conditions: a) (i)$NiBr_2$, Zn (dust), PPh_3, KCN, THF, 50-60°C, 24h; then (ii) MeI, toluene, 0°C, 2h, 68-90%. b) LDA, -78°C, 1h, then ethyl 3,3 dimethyl acrylate, ZnI_2, -78°C-RT, 2h 33-59%; c) allyl-NCS, AcOH, EtOH, 75°C, 16h, 21-59%; d) R^1-X, Cs_2CO_3, MEK or DMF, 70°C, 16h, 69-88%; e) BBr_3, DCM, 0°C-RT, 16h, 43-62%; f) $CH_3OCH_2CH_2OTs$, Cs_2CO_3, DMF, 70°C, 16h, 65-71%. †Compound synthesized by Roderick Sorenson.

Scheme 2.4. Analogs with varied pyrimidinone *N*-substitution.[a]

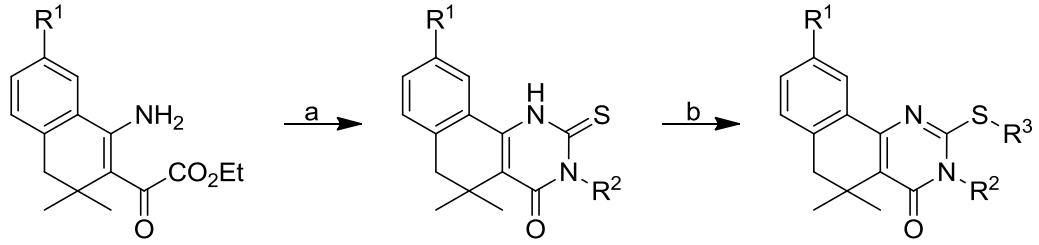

15: R = H
27a: R = OMe

40a: R^1 = H, R^2 = Et
40b: R^1 = H, R^2 = -EtOMe
40c: R^1 = OMe, R^2 = Me

41: R^1 = H, R^2 = Et, R^3 = -EtOMe
42: R^1 = H, R^2 = -EtOMe, R^3 = Et
43: R^1 = OMe, R^2 = Me, R^3 = Et

[a]Reagents and conditions: a) R^2-NCS, AcOH, EtOH, 75°C, 16h, 27-31%; b) R^3-X, Cs_2CO_3, MEK or DMF, 70°C, 16h, 55-71%.

Analogs with varied substitution at the *N*- and *O*- positions of the pyrimidinone ring amide were accessed through two synthetic paths (Schemes 2.4 and 2.5). Beginning from aminoesters **15** and **27a**, treatment with other alkyl isothiocyanates (methyl, ethyl, 2-methoxyethyl) yielded the corresponding pyrimidinones **40a-c**, which could be further elaborated into analogs **41-43** (Scheme 2.4). The synthesis of *O*-alkylated analogs first required the assembly of the unsubstituted thioxo-dihydropyrimidinone ring (Scheme 2.5). Treatment of **15** or **27a** with benzoyl isothiocyanate, followed by ring closure and hydrolysis of the resulting *N*-benzoyl group with aqueous KOH generated intermediates **44a**,**b** (Scheme 2.5).[57] Chemoselective alkylation of the sulfur was achieved under neutral conditions, while subsequent base-catalyzed alkylation of the amide generally gave some mixture of *N*-alkylated (**46**, **47**) and *O*-alkylated (**48-50**) analogs.

Scheme 2.5. Generation of *N*- and *O*-alkylated substitution pairs 46-50.[a]

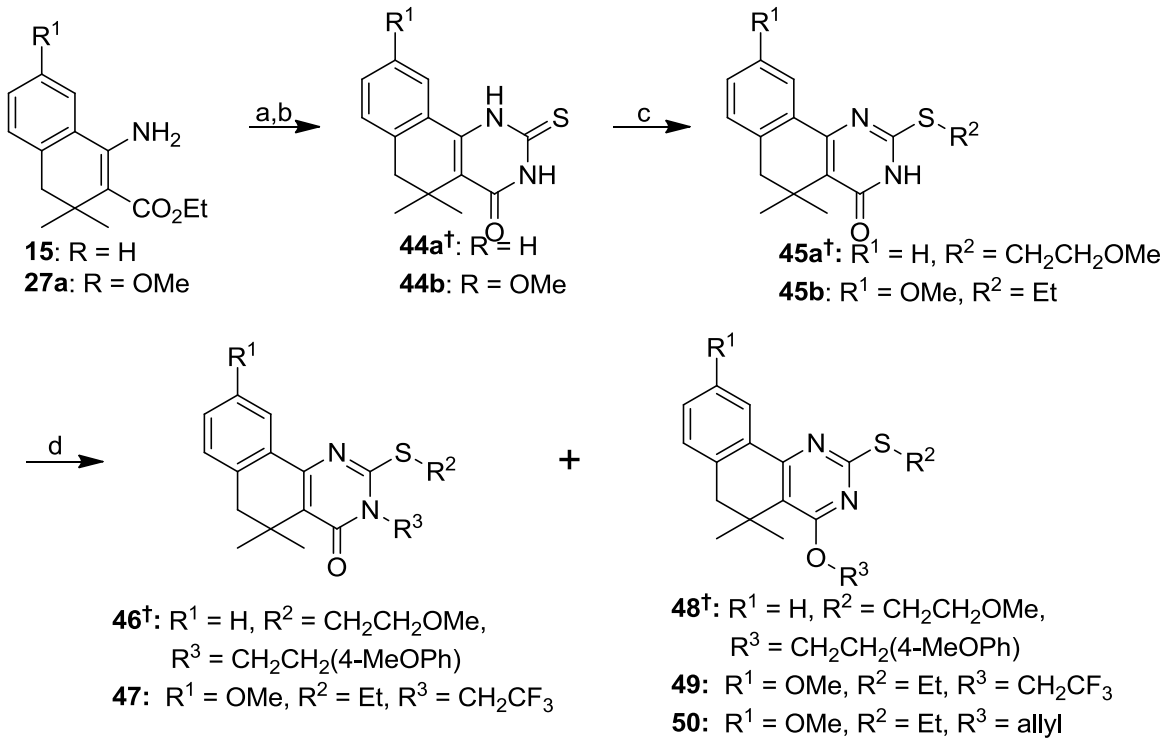

15: R = H
27a: R = OMe

44a†: R = H
44b: R = OMe

45a†: R^1 = H, R^2 = CH_2CH_2OMe
45b: R^1 = OMe, R^2 = Et

46†: R^1 = H, R^2 = CH_2CH_2OMe, R^3 = CH_2CH_2(4-MeOPh)
47: R^1 = OMe, R^2 = Et, R^3 = CH_2CF_3

48†: R^1 = H, R^2 = CH_2CH_2OMe, R^3 = CH_2CH_2(4-MeOPh)
49: R^1 = OMe, R^2 = Et, R^3 = CH_2CF_3
50: R^1 = OMe, R^2 = Et, R^3 = allyl

[a]Reagents and conditions: a) benzoyl isothiocyanate, EtOH, 75°C, 5h; b) KOH, EtOH:H_2O (2:1) 70°C, 2h, 62% over 2 steps; c) R^2-X, $NaHCO_3$, DMF, RT-70°C, 30min-16h, 71%; d) R^3-X, base, EtOH or DMF, 70-80°C, 16-24h, 13-36% yield. †Compound originally synthesized by W.G. Rajeswaran.

Scheme 2.6. Generation of compounds with lower propensity for metabolic oxidation.[a]

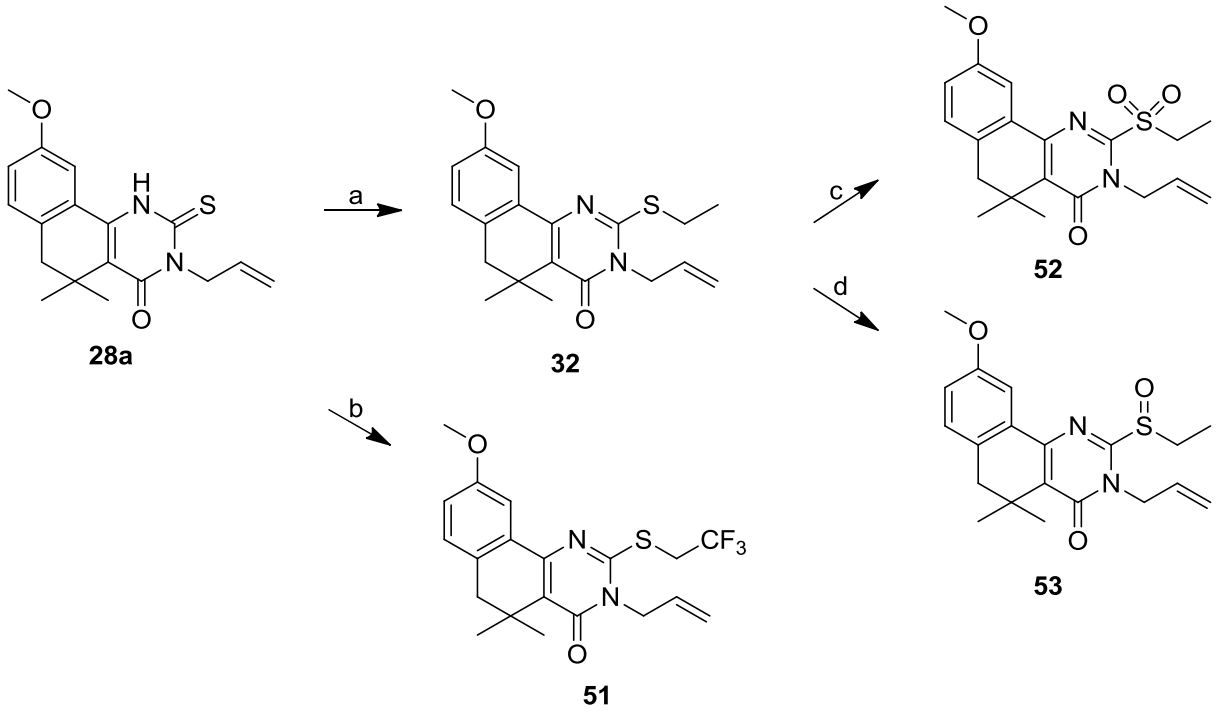

[a]Reagents and conditions: a) CH_3CH_2I, Cs_2CO_3, DMF, 70°C, 16h; b) CF_3CH_2I, Cs_2CO_3, DMF, 50°C, 24h, 24%; c) *m*CPBA, DCM, 0°C-RT, 12h, 62%; d) 1.1 equiv Oxone, THF/H_2O (1:1), 0°C to RT, 16h, 62%.

Metabolic Liability Reduction

As part of an effort to generate analogs of **32** with reduced susceptibility to P450 oxidation, three additional analogs were built beginning from intermediate **28a** (Scheme 2.6). Simple alkylation with 2,2,2-trifluoro-1-iodoethane generated analog **51**. Analog **32**, generated as in Scheme 2.3, could be used as the starting material to prepare sulfone (**52**) and sulfoxide (**53**) derivatives by treatment with *m*CPBA or controlled quantities of Oxone®,[58] respectively. No alkene epoxidation or other off-target oxidation events were observed using either set of conditions.

Template modifications: Scaffold distortion and central ring substitution changes

In addition to the more library-based synthesis of the compounds related above, a variety of prototype compounds were produced to probe significant changes to the central ring. This ring is the least amenable to structural diversity generation in our general scheme, and therefore each analog required significant synthetic departures.

The generation of compound **58** with a 5-membered central ring (Scheme 2.7) proceeded from commercially available 3,3-dimethylindan-1-one **54** once it was determined that β-aminoester **56** could not be generated under acid-catalyzed Friedel-Crafts conditions (see **5**, Scheme 2.1, step c). The indanone was functionalized at the α-keto position via Claisen condensation to yield ketoester **55**,[59] followed by conversion of the ketone to the conjugated enamine via ammonium acetate.[60] With aminoester **56** in hand, it was discovered that our standard set of conditions for generating the thioxopyrimidine ring did not yield any product. After screening a variety of methods, it was eventually found that combining **56**, allyl isothiocyanate, and pyridine in a pressure vessel and heating to reflux was the only set of conditions that furnished **57** in adequate yields.[61] Thioalkyl pyrimidinone **58** was finally synthesized after the alkylation of sulfur under basic conditions.

Scheme 2.7. Synthesis of ring-contracted analog 58.[a]

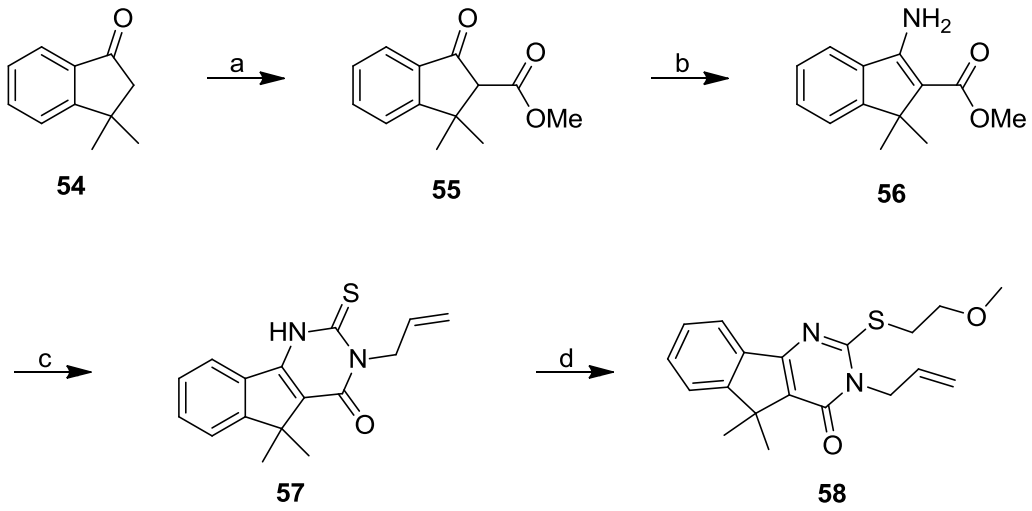

[a]Reagents and conditions: a) NaH, dimethyl carbonate; then **54**, THF, 80°C, 4h, 97%; b) NH_4OAc, MeOH, reflux, 23h, 55%; c) allyl-NCS, pyridine, reflux, 17h, 23%; d) $CH_3OCH_2CH_2OTs$, Cs_2CO_3, MEK, 80°C, 16h, 62%.

A racemic mixture of 6-methylated derivative **63** was synthesized with particular attention focused on using methods that would eventually allow its production in enantiomerically pure form (Scheme 2.8). Beginning from 2-phenylpropan-1-ol, modified Mitsunobu conditions to form a new C-C bond afforded intermediate **60**.[62] Unlike similar substrates in this SAR campaign, it was found that the cyanoester could be effectively cyclized to

61 in the presence of triflic acid in excellent yield.[63] Installation of the pyrimidinone and *S*-alkylation proceeded as normal to furnish **63**. The relatively weak activity of this analog in GAS-SK activity assays led us to abandon synthesis of the corresponding enantiomerically pure analogs.

Scheme 2.8. Synthesis of racemic methylbenzyl analog 63.[a]

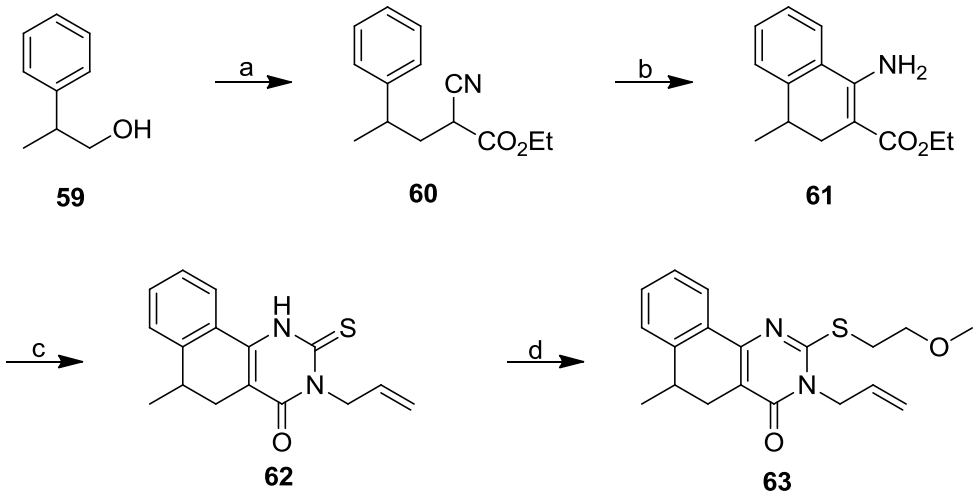

[a]Reagents and conditions: a) DIAD, PPh_3, -20°C, THF, then **59**, ethyl cyanoacetate, THF, -20-0°C, 24h, 82%; b) TfOH, DCM, RT, 24h, 92%; c) allyl-NCS, AcOH, EtOH, 75°C, 16h, 35%; d) $CH_3OCH_2CH_2OTs$, Cs_2CO_3, MEK, 75°C, 16h, 75%.

Two other attempts were made to introduce chiral substitution on the central ring, resulting in compounds **67** and **75**. Compound **67** was synthesized in order to assess whether the LDA/ZnI_2 reaction conditions could be used to diastereoselectively synthesize β-aminoester **65** and possibly other structurally similar intermediates (Scheme 2.9). To this end, 2-ethylbenzonitrile and ethyl crotonate were used as the starting materials in the LDA/ZnI_2 cyclization. The reaction proved to proceed more rapidly than normal, likely owing to the reduced steric bulk around the β-position of the Michael acceptor. It was found that the standard ZnI_2-promoted conditions led to an inseparable mixture of diastereomers in a 1:3 ratio. Omission of the ZnI_2 or addition before the Michael addition step led to 1:1 ratios, albeit in greatly reduced yields. The isothiocyanate cyclization and sulfur alkylation steps followed the standard procedures, eventually furnishing final compound **67**. Unfortunately, the

diastereomeric mixtures were found to be totally inseparable at every stage in the synthetic scheme, leading to the submission of **67** as a 1:3 mixture of diastereomers. It was noted that the final compounds appear to be separable by HPLC (T_R = 6.44 and 6.89 min, HPLC Method B, see Chapter 6), potentially allowing for separation via prep-scale HPLC, but this option was not explored given the relatively low level of activity observed for this compound.

Scheme 2.9. Synthesis of diasteromeric compound 67.[a]

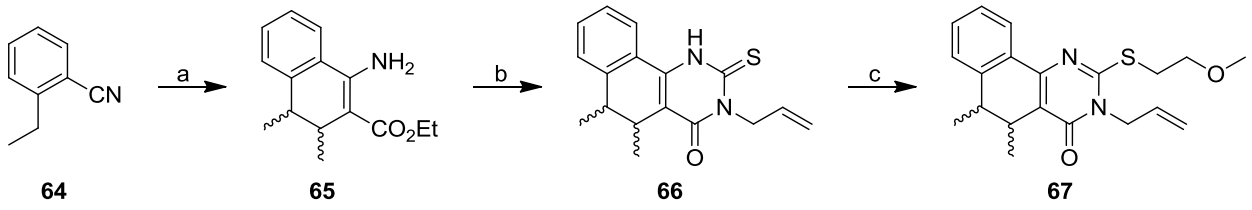

64 **65** **66** **67**

[a]Reagents and conditions: a) LDA, diglyme -78°C, 1h, then ethyl crotonate, ZnI_2, -78°C-RT, 2h, 36%; b) allyl-NCS, AcOH, EtOH, 75°C, 16h, 30%; c) $CH_3OCH_2CH_2OTs$, Cs_2CO_3, MEK, 75°C, 16h, 67%.

Analog **75** was built as part of a campaign to introduce an additional heteroatomic "handle" for diversity generation at the benzyl position of the central ring (Scheme 2.10). Finding substitution amenable to surviving the LDA/ZnI_2 cyclization conditions proved to be quite challenging. A variety of masked oxygen (TBS ethers, acetyl groups) and nitrogen (diphenyl imine, phthalate) substitutions at the benzyl position were found to be incompatible with these rather harsh conditions. Ultimately, only 2-(methoxymethyl)benzonitrile **72** was successfully transformed to its corresponding β-aminoester. This intermediate was synthesized from commercially available phenyl bromide **68** via nucleophilic substitution of sodium acetate at the benzyl position, followed by saponification[64] and methylation to yield intermediate **71**. S_NAr with cuprous cyanide was found to efficiently produce benzonitrile intermediate **72**.[65] After cyclization to **73**, the rest of the synthetic scheme proceeded as usual to generate racemate **75**. Attempts to demethylate **75** to reveal an alcohol amenable to functionalization (**76**) instead led to the immediate aromatization of the central ring via 1,2 methyl shift (**77**), effectively ruling out this strategy for significant diversity generation.

Scheme 2.10. Synthesis of methoxybenzyl substituted analog 75.[a]

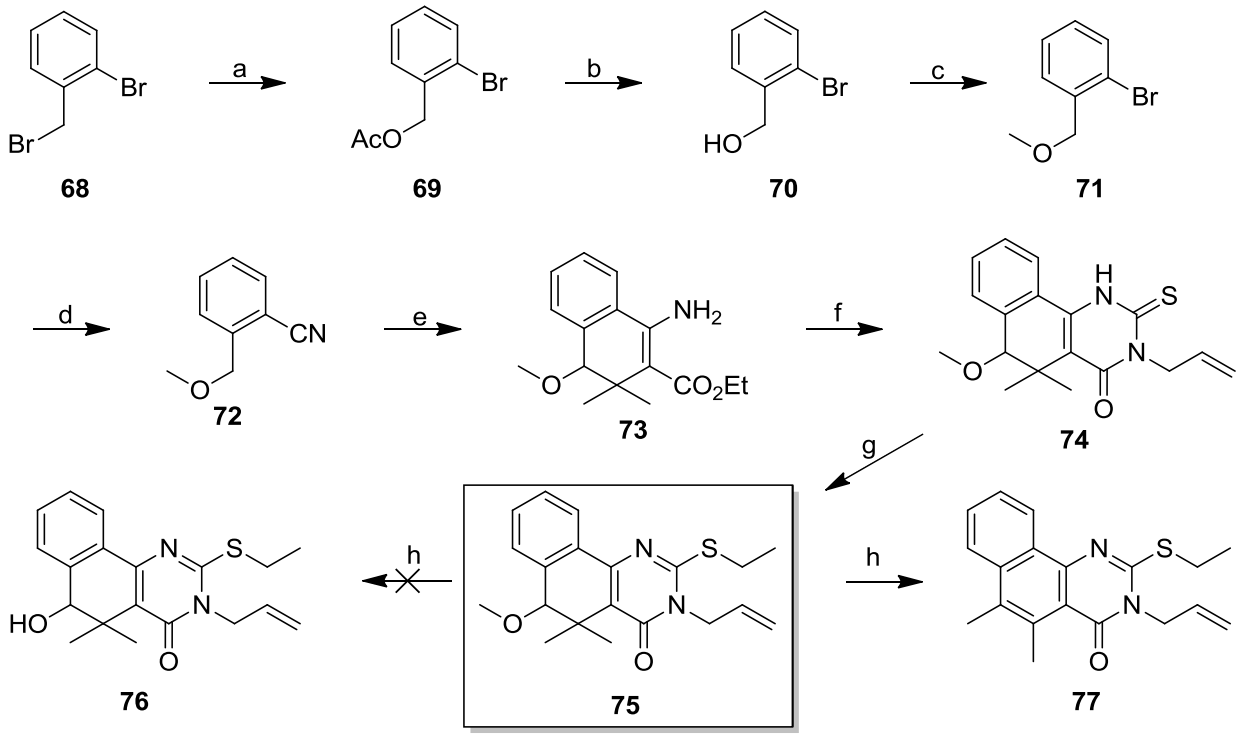

Reagents and conditions: a) NaOAc, DMF, 70°C, 16h, 93%; b) K_2CO_3, MeOH, RT, 60 min, 96%; c) MeI, KOH, DMSO, RT, 90min, 96%; d) CuCN, DMF, 120°C, 16h, 81%; e) LDA, diglyme -78°C, 1h, then ethyl 3,3-dimethyl acrylate, -78°C-RT, 2h, 54%; f) allyl-NCS, AcOH, EtOH, 75°C, 16h, then NaOEt, RT, 30 min, 53%; g) EtI, Cs_2CO_3, DMF, 75°C, 16h, 55%; h) BBr_3, DCM, 0°C-RT, 16h.

SAR Discussion

We first examined the spirocycloalkyl substituted compounds with varied substitution patterns at the 2-position of the pyrimidinone ring system (Table 2.1). Aromatic substitution at R^1 (**2**, **7**, **8**) did not appreciably increase potency over **1,** but methyl substitution (**11**) conferred a modest increase in activity (IC_{50} = 19 μM vs. >50 μM). Interestingly, polar groups were tolerated as part of smaller alkyl groups at the 2-position (e.g. **9**, **12**). The replacement of sulfur with nitrogen (**13**) led to an unacceptable decrease in growth. Similarly, basic amine functionality appended to sulfur (**10**) led to growth inhibition in some trials. We defined acceptable growth inhibition to be no greater than 15% at 50 μM of test compound. The favorable potency of commercially available spirocyclopentyl analog **78** relative to closely related spirocyclohexyl analog **2** led us to hypothesize that the size of the geminal substitution on

the central ring could be reduced, allowing reduction of both the lipophilicity and the molecular weight of future analogs.

Table 2.1. Inhibition of SK activity by spirocycloalkyl analogs.

#	Structure	5 µM SK T/C [a]	50 µM SK T/C [a]	50 µM Growth T/C[b]	IC_{50} (µM)	MLM $t_{1/2}$ (min)[c]	Aq. Sol. (µM)[d]
1†	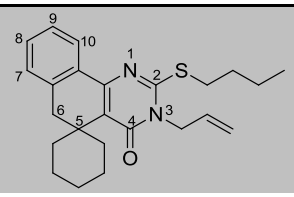	0.84 ± 0.14	0.48 ± 0.28	0.95 ± 0.08	>50	37.2	9 ± 2
2†	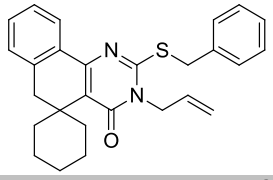	0.74 ± 0.16	0.57 ± 0.21	0.96 ± 0.06	>50	0.6	9 ± 2
7†	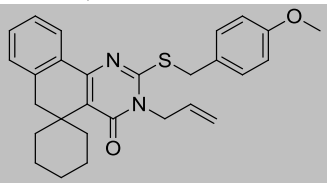	1.00 ± 0.33	0.82 ± 0.44	1.05 ± 0.06			
8†	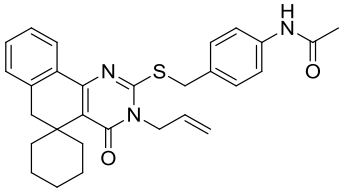	0.96 ± 0.46	0.74 ± 0.28	0.96 ± 0.14			
9†	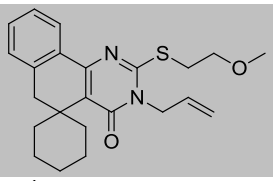	0.47 ± 0.28	0.29 ± 0.15	0.99 ± 0.10		6.4	9 ± 2
10†	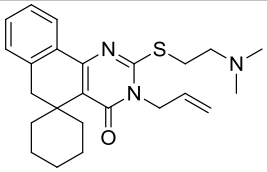	0.72 ± 0.12	0.52 ± 0.37	0.88 ± 0.20			
11‡	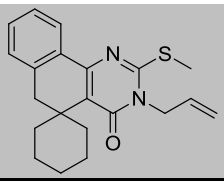	0.60 ± 0.19	0.42 ± 0.03	0.98 ± 0.03	19 ± 6.0	13.5	22 ± 5

#	Structure	5 µM SK T/C [a]	50 µM SK T/C [a]	50 µM Growth T/C[b]	IC_{50} (µM)	MLM $t_{1/2}$ (min)[c]	Aq. Sol. (µM)[d]
12‡	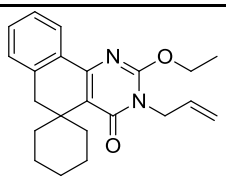	0.53 ± 0.23	0.14 ± 0.05	1.02 ± 0.09			14.5 ± 3
13	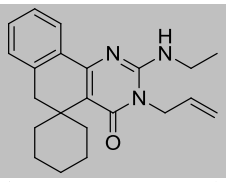	0.78 ± 0.47	0.56 ± 0.70	0.32 ± 0.18			9 ± 2
78	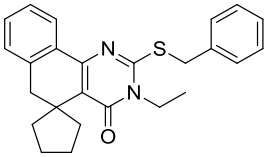	0.44 ± 0.06	0.23 ± 0.16	1.07 ± 0.04			

[a] Ratio of A_{405} of SK-cleaved substrate in GAS culture treated with the indicated concentration of test compound divided by A_{405} of DMSO control (see Chapter 6: Experimental Section). Values are the mean of at least three experiments ± standard deviation. [b]Ratio of OD (600 nm) for growth of GAS in the presence of test compound divided by DMSO control. Values are the mean of at least three experiments ± standard deviation. [c]Half-life of parent compound during incubation with mouse liver microsomes. [d]Kinetic solubility of compound in aqueous Todd Hewitt bacterial media. †Synthesized originally by Jenny Ryu. ‡Synthesized originally by Meghan Breen.

Exploration of analogs with gem-dimethyl substitution of the central ring (Table 2.2) began with the assessment of commercially available analogs **79-81**, all of which showed an increase in potency in comparison to **1**. Polar substitution at the 2-position was generally well-tolerated (**19**, **21**, **17, 81**) except for primary amide **18**. Introducing an alcohol on the sidechain (**20**) to improve solubility led to unacceptable bacteriotoxicity. This toxicity was also observed with heteroatomic analogs **23** and **24** versus sulfur analog **80**, leading us to conclude that retention of the sulfur was necessary to avoid inhibition of bacterial growth. Altering the substitution of the *N*-position of the pyrimidinone was found to lead to bacterial toxicity (**41**) or attenuation of activity (**46**) compared to *N*-allyl (**17**). Overall, the *S*-Et and *S*-CH_2CH_2OMe analogs **80** and **17** were found to be the optimum compounds from this series.

Table 2.2. Inhibition of SK activity by gem-dimethyl analogs.

#	Structure	5 µM SK T/C [a]	50 µM SK T/C [a]	50 µM Growth T/C[b]	IC_{50} (µM)	MLM $t_{1/2}$ (min)[c]	Aq. Sol. (µM)[d]
79	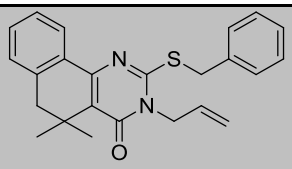	0.65 ± 0.25	0.35 ± 0.14	1.03 ± 0.03	10.8 ± 3.0		9 ± 2
80	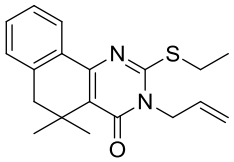	0.24 ± 0.07	0.17 ± 0.08	0.89 ± 0.05	2.0 ± 0.5		
81	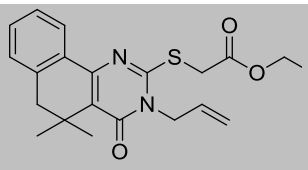	0.54 ± 0.10	0.27 ± 0.12	1.01 ± 0.02			
17‡	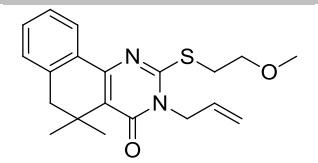	0.35 ± 0.11	0.13 ± 0.07	0.86 ± 0.10	3.2 ± 0.6	1.7	22.5 ± 4.5
18‡	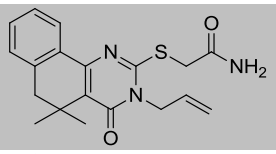	0.79 ± 0.17	0.64 ± 0.16	1.00 ± 0.02		<2	
19‡	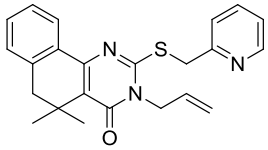	0.40 ± 0.09	0.13 ± 0.07	1.05 ± 0.02			
20‡	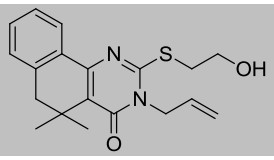	0.48 ± 0.17	-	0.06 ± 0.03			
21	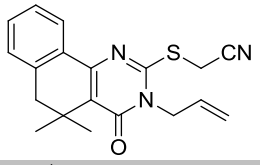	0.37 ± 0.17	0.23 ± 0.06	1.00 ± 0.03		20.6	34.5 ± 7.5
23	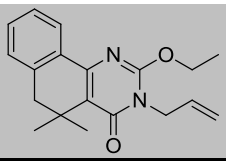	0.34 ± 0.08	0.23 ± 0.10	0.50 ± 0.23		0.9	

#	Structure	5 µM SK T/C [a]	50 µM SK T/C [a]	50 µM Growth T/C[b]	IC_{50} (µM)	MLM $t_{1/2}$ (min)[c]	Aq. Sol. (µM)[d]
24	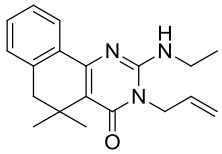	0.48 ± 0.19	-	0.06 ± 0.03		1.1	
41	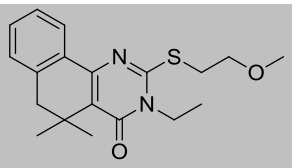	0.41 ± 0.23	-	0.39 ± 0.15		0.8	
42	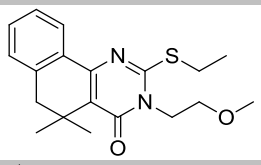	0.20 ± 0.12	0.15 ± 0.20	0.64 ± 0.38			
46¥	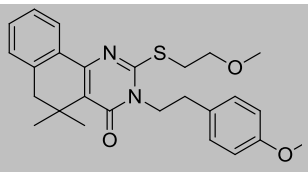	0.71 ± 0.40	0.61 ± 0.32	0.97 ± 0.07		9.4	

[a] Ratio of A_{405} of SK-cleaved substrate in GAS culture treated with the indicated concentration of test compound divided by A_{405} of DMSO control (see Chapter 6: Experimental Section). Values are the mean of at least three experiments ± standard deviation. [b]Ratio of OD (600 nm) for growth of GAS in the presence of test compound divided by DMSO control. Values are the mean of at least three experiments ± standard deviation. [c]Half-life of parent compound during incubation with mouse liver microsomes. [d]Kinetic solubility of compound in aqueous Todd Hewitt bacterial media. ‡Originally synthesized by Meghan Breen. ¥Originally synthesized by W.G. Rajeswaran.

Our attention then turned to exploring substitution of the aromatic ring (Table 2.3) at 3 different positions. Assessment of methyl ether analogs **31-33** revealed that substitution at the 8- and 9- positions conferred a moderate increase in potency over **80**, while substitution of the 7-position did not. Interestingly, *S*-ethoxymethyl compound **29** was observed to be less potent than *S*-ethyl compound **31**, in contrast to similar compounds **17** and **79** which were essentially equipotent. The installation of methoxyethyl ethers (**37-39**) generally led to the attenuation of the potency gains seen with **31-33**. Though unfortunate, this data was valuable for guiding our synthetic strategy for the target ID probes (Chapter 3). Phenol compounds **34-36** (Scheme 2.3) induced acute toxicity in preliminary activity assays and were thus not followed up on. This occurrence was not unexpected, as it is known that many phenols have bacteriotoxic effects.[66] The generation of a larger library of aryl ethers was undertaken by chemist Roderick Sorenson,

but generally displayed low activity, consistent with the trend of increased steric bulk decreasing activity as previously observed with **31-33** vs. **37-39**. Compound **30**, also synthesized by Roderick Sorenson, had moderate activity and low metabolic stability, but was important to the preliminary biofilm effort (Chapter 4). A number of aryl carboxylic acid derivatives (ester, amide; synthesized by Michael Wilson) also proved to be almost completely inactive (*data not shown*). Ultimately, 9-methoxy analog **32** was found to be the optimal compound from this series, exhibiting a 90% reduction in streptokinase activity at 5 μM and an IC_{50} of 1.3 μM, representing a greater than 35-fold improvement in potency over **1**, although some modest inhibition of bacterial growth at high concentrations was introduced.

Table 2.3. Inhibition of SK activity by analogs with 7-, 8-, and 9-position substitution.

#	Structure	5 µM SK T/C [a]	50 µM SK T/C [a]	50 µM Growth T/C[b]	IC_{50} (µM)	MLM $t_{1/2}$ (min)[c]	Aq. Sol. (µM)[d]
29	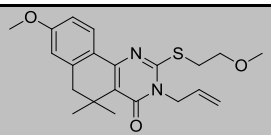	0.47 ± 0.25	0.25 ± 0.18	0.89 ± 0.16			
30†	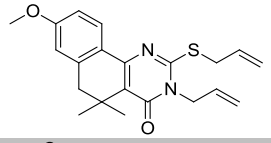	0.33 ± 0.15	0.28 ± 0.16	0.92 ± 0.16	6.9 ± 0.3	0.6	14.5 ± 3.5
31	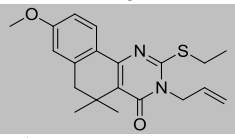	0.18 ± 0.09	0.07 ± 0.01	0.87 ± 0.19	3.1 ± 0.7	0.8	14.5 ± 3.5
32	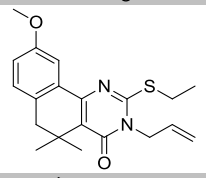	0.10 ± 0.06	0.07 ± 0.02	0.73 ± 0.07	1.3 ± 0.6	2.3	9 ± 2
33	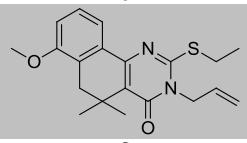	0.26 ± 0.07	0.29 ± 0.18	0.28 ± 0.26			
37	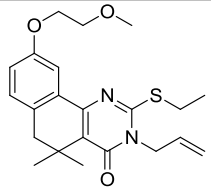	0.58 ± 0.24	0.43 ± 0.15	1.02 ± 0.10			
38	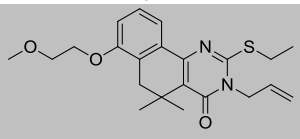	0.84 ± 0.23	0.40 ± 0.21	0.94 ± 0.08			
39	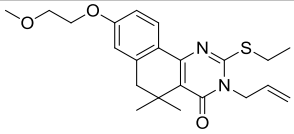	0.46 ± 0.35	0.36 ± 0.41	0.85 ± 0.22			

[a] Ratio of A_{405} of SK-cleaved substrate in GAS culture treated with the indicated concentration of test compound divided by A_{405} of DMSO control (see Chapter 6: Experimental Section). Values are the mean of at least three experiments ± standard deviation. [b]Ratio of OD (600 nm) for growth of GAS in the presence of test compound divided by DMSO control. Values are the mean of at least three experiments ± standard deviation. [c]Half-life of parent compound during incubation with mouse liver microsomes. [d]Kinetic solubility of compound in aqueous Todd Hewitt bacterial media. [†]Compound synthesized by Roderick Sorenson.

Activity data for *N*- and *O*-alkylated compound pairs is summarized in Table 2.4. No general efficacy advantage for *N*- or *O*- alkylation was observed; *O*-alkylated **48** was somewhat more potent than **46**, while **32** remained much more potent than its *O*-alkylated counterpart **50**. Compounds **47** and **49** displayed similarly weak activity.

Table 2.4. Effect of *N*-vs. *O*-alkylation on GAS-SK inhibition and metabolic stability.

#	Structure	5 µM SK T/C[a]	50 µM SK T/C[a]	50 µM Growth T/C[b]	IC_{50} (µM)	MLM $t_{1/2}$ (min)[c]
46¥	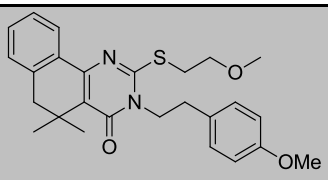	0.71 ± 0.40	0.61 ± 0.32	0.97 ± 0.07		9.4
48¥	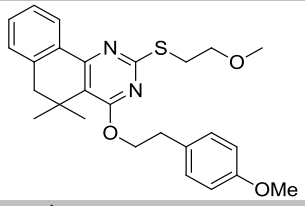	0.46 ± 0.37	0.24 ± 0.15	1.00 ± 0.09	5.5 ± 0.7	45.1
47	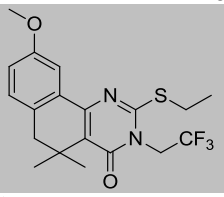	0.78 ± 0.36	0.49 ± 0.17	1.01 ± 0.04		3.0
49	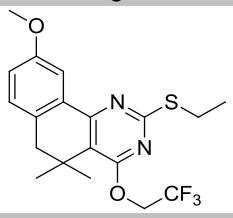	0.51 ± 0.20	0.38 ± 0.23	0.89 ± 0.02		45.5
32	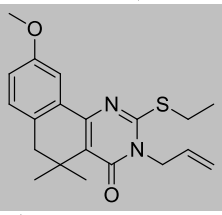	0.10 ± 0.06	0.07 ± 0.02	0.73 ± 0.07	1.3 ± 0.6	2.3
50	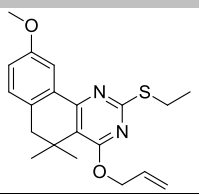	0.89 ± 0.33	0.68 ± 0.39	0.96 ± 0.02		8.3

[a] Ratio of A_{405} of SK-cleaved substrate in GAS culture treated with the indicated concentration of test compound divided by A_{405} of DMSO control (see Chapter 6: Experimental Section). Values are the mean of at least three experiments ± standard deviation. [b]Ratio of OD (600 nm) for growth of GAS in the presence of test compound divided by DMSO control. Values are the mean

of at least three experiments ± standard deviation. [c]Half-life of parent compound during incubation with mouse liver microsomes. [¥]Originally synthesized by W.G. Rajeswaran.

Activity data for the template-modified compounds described in Schemes 2.7-2.10 are summarized in Table 2.5. Although compounds **67** and **75** show reasonable activity, all four of these compounds were found to be quite toxic at 50 µM, suggesting that even small changes to the central ring of the scaffold are not tolerated. The activity data for these four compounds led us to stop exploring the central ring as a point of diversity in the SAR study.

Table 2.5. **GAS-SK activity data for compounds with modified central rings.**

#	Structure	5 µM SK T/C[a]	50 µM SK T/C[a]	50 µM Growth T/C[b]
58	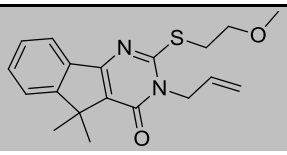	0.61 ± 0.20	-	0.60 ± 0.31
63	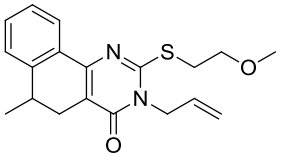	0.74 ± 0.19	-	0.46 ± 0.25
67	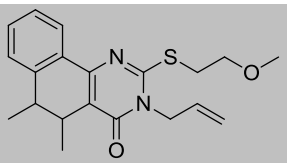	0.40[c]	0.09[c]	0.30[c]
75	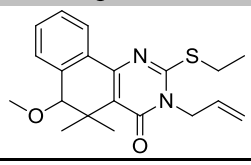	0.38[c]	0.10[c]	0.39[c]

[a] Ratio of A_{405} of SK-cleaved substrate in GAS culture treated with the indicated concentration of test compound divided by A_{405} of DMSO control (see Chapter 6: Experimental Section). Values are the mean of at least three experiments ± standard deviation. [b]Ratio of OD (600 nm) for growth of GAS in the presence of test compound divided by DMSO control. [c]Value derived from only one experiment. Values are the mean of at least two experiments ± standard deviation unless indicated.

Microsomal Stability and Metabolite Identification

In our previous publication identifying **1** and **2** as inhibitors of SK expression, it was determined that **1** displayed efficacy in mouse models of GAS infection while **2** did not, despite having similar activity in bacterial assays.[45] We hypothesized that a difference in susceptibility

to oxidative metabolism might be playing a role in the activity differential between **1** and **2** in mammalian systems. We submitted each of these compounds for stability testing in mouse liver microsomal (MLM) extract (performed by the Duxin Sun group at University of Michigan). The metabolic half-life data from these assays supported our hypothesis, with **1** displaying more than 60-fold higher stability to oxidation than **2** ($t_{1/2}$ = 37.2 min vs. 0.6 min, respectively). A survey of several more compounds in the series (Tables 2.1-2.6) revealed that most were highly unstable ($t_{1/2}$ < 5 minutes), despite several structural modifications that would potentially reduce their propensity to oxidation, including lowered lipophilicity, fewer unsubstituted aliphatic, olefinic, or aryl carbons, and replacement of sulfur with oxygen or nitrogen. Interestingly, we also noted that the spirocyclohexyl compounds were generally more stable than the corresponding gem-dimethyl analogs (e.g. **9**, $t_{1/2}$ = 6.4 min vs. **17**, $t_{1/2}$ = 1.7 min), despite their greater degrees of lipophilicity.

In collaboration with the Duxin Sun group, a metabolite ID study was performed using compound **9** to elucidate the most metabolically labile sites on the scaffold. Possible metabolites were identified by LC-MS analysis, then fragmented via collision-induced dissociation (CID). Further MS analysis of the resulting metabolite fragments allowed us to deduce the structure of each metabolite. This study indicated that the most metabolically labile portions of the molecule were the substitutions on the pyrimidinone ring (Figure 2.2). No oxidation was indicated on the spirocyclohexane ring or any of the four unsubstituted aromatic carbons. Based on the findings of the metabolite ID study, we prepared five analogs of our optimum compound **32** that deactivated this portion of the scaffold to oxidation (Table 2.6); however, these were also found to be quickly metabolized. Interestingly, *metabolic assessment of the O-alkylated compounds **48-50** (Table 2.4) showed that they were consistently more stable (4-15 fold) than their N-alkylated counterparts*. This observation, paired with the generally greater stability of the hindered spirocyclohexyl analogs vs. the corresponding gem-dimethyl analogs, suggests that hydrolysis of the pyrimidinone amide may play a key role in the metabolic breakdown of these compounds. Compound **48**, despite being four-fold less potent than **32** (IC_{50} = 5.5 μM vs. 1.3 μM), demonstrates the potential viability of *O*-alkylated analogs as more metabolically stable alternatives to the *N*-alkylated compounds.

Table 2.6. Analogs of 32 with potentially reduced metabolic liability.

#	Structure	5 µM SK T/C[a]	50 µM SK T/C SD [a]	50 µM Growth T/C[b]	MLM $t_{1/2}$ (min)[c]
32	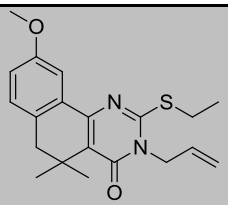	0.10 ± 0.06	0.07 ± 0.02	0.73 ± 0.07	2.3
43	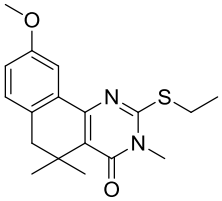	0.66 ± 0.20	0.20 ± 0.14	0.83 ± 0.15	1.7
47	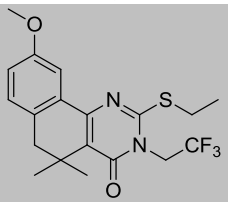	0.78 ± 0.36	0.49 ± 0.17	1.01 ± 0.04	3.0
51	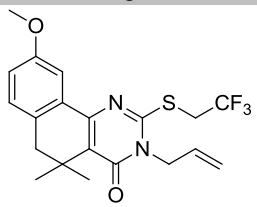	0.45 ± 0.19	0.22 ± 0.08	0.86 ± 0.07	4.8
52	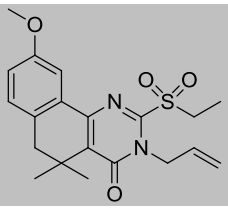	0.83 ± 0.31	0.70 ± 0.13	1.03 ± 0.03	3.8
53	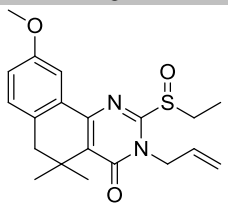	1.00 ± 0.13	0.51 ± 0.31	1.01 ± 0.05	2.8

[a] Ratio of A_{405} of SK-cleaved substrate in GAS culture treated with the indicated concentration of test compound divided by A_{405} of DMSO control (see Chapter 6: Experimental Section). Values are the mean of at least three experiments ± standard deviation. [b]Ratio of OD (600 nm) for growth of GAS in the presence of test compound divided by DMSO control. Values are the mean of at least three experiments ± standard deviation. [c]Half-life of parent compound during incubation with mouse liver microsomes.

Figure 2.2. Potential routes of metabolism identified by MLM incubation and MS analysis. No oxidation of the left-hand side of the molecule was observed.

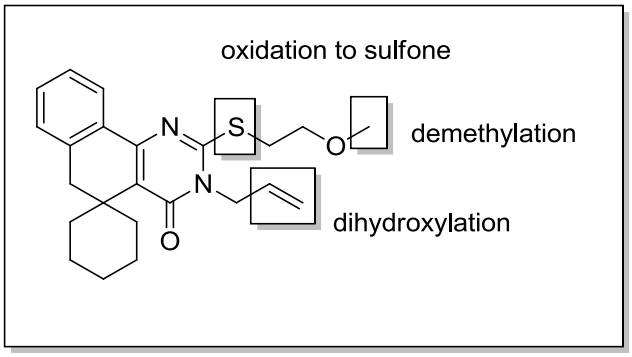

Aqueous Solubility

In addition to microsomal stability, the aqueous solubility of small molecules has been shown to be a critical physicochemical property for predicting the efficacy of compounds in living systems. Lipinski suggests that to achieve oral bioavailability at a dose of 1 mg/kg, a compound needs to achieve a minimum aqueous solubility of 52 μg/mL,[67] corresponding to a concentration of ~150 μM for small analogs similar in size to **32**. Therefore, several key compounds from the SAR library were assessed for kinetic solubility in Todd Hewitt (THY) bacterial media. Taking inspiration from Lipinski's turbidimetric assay of compound solubility and a high-throughput method of solubility determination employed by GlaxoSmithKline,[68] we developed a 96-well plate-based solubility assay that kept DMSO concentrations low (1%) and constant over the range of test compound concentrations.

The solubility of all compounds tested (Tables 2.1-2.3) was equal to or less than 25 μM, with the exception of nitrile **21** (aq. sol. = 34.5 ± 7.5 μM). It was found that the solubility of these compounds was considerably lower in phosphate-buffered saline (PBS) than in THY media (eg. 2 ± 1 vs. 9 ± 2 μM [PBS:THY] for **1**, 3 ± 1 vs. 34.5 ± 7.5 μM [PBS:THY] for **21**), suggesting that the protein and lipid content of THY media may increase the effective aqueous solubility of this compound class. Preliminary activity studies indicated that the activity of **1** (but not **21**) was reduced when human serum albumin (HSA) was added to the bacterial media, reinforcing the hypothesis that some compounds in this series may bind to protein. The measured solubility has a weak negative correlation to the cLogP (R^2 = 0.533), and the most soluble compound **21** does indeed have the lowest cLogP (3.55). Further decreases in cLogP should

logically result in greater aqueous solubility; however, nearly all efforts to significantly decrease lipophilicity, including replacement of the fused phenyl ring with pyridyl and replacement of the central ring with lactones or lactams (Scheme 2.11), have thus far led to the reduction or loss of activity (*data not shown*).

Mammalian Cytotoxicity

A representative subset of compounds (**1**, **32**, **31**, **17**, **46**, **48**, **79**) was assessed by the Hongmin Sun group for toxic effect in HeLa cells using a standard tetrazolium-formazan assay of cell viability (see Chapter 6: Experimental Section). It was found that none of the compounds inhibited growth by more than 35% up to 100 μM, the highest concentration tested.

Scaffold Alteration

A number of alternative scaffolds based on the core structure of **1** were pursued by other chemists in the group. The basic structures of these compounds are delineated in Scheme 2.11. A particular emphasis was placed on decreasing lipophilicity by breaking up the planarity of the ring system (**82**, **83**) or by simply introducing more polar functionality (**84-87**). Though a significant number of compounds were synthesized from these scaffolds (~50 in total), none of them displayed activity comparable to the best compounds identified from the rest of the SAR study, and were not followed up on. Interestingly, the spiropiperidine analogs (entry **86**), although only modestly active in the GAS-SK study, were found to be more metabolically stable and possess another easily functionalized site for diversity generation, which had significant implications for the anti-biofilm study (Chapter 4).

Scheme 2.11. Scaffold modifications explored by other VMCC chemists.[a]

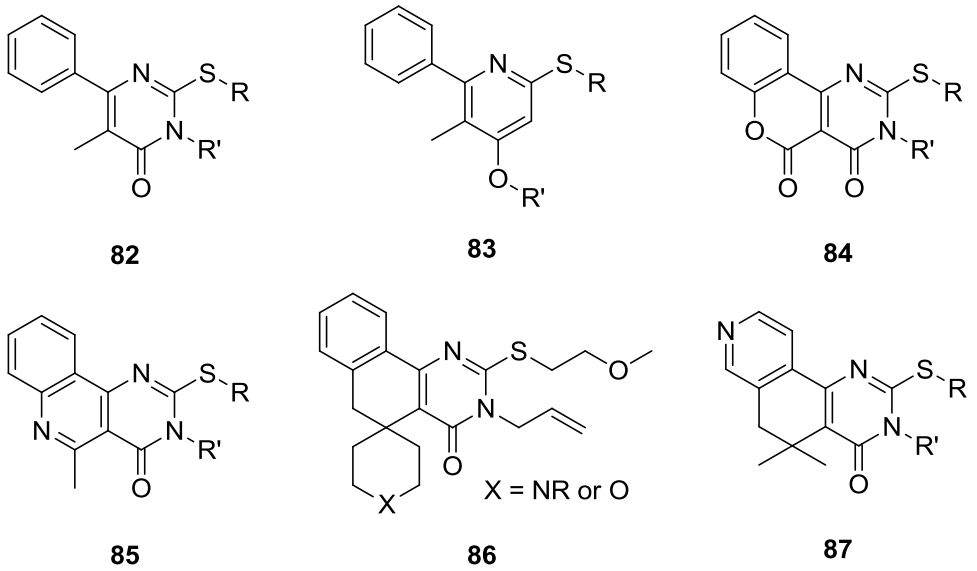

[a]**82-85** developed by Roderick J. Sorenson. **86** developed by W.G. Rajeswaran. **87** developed by Michael Wilson.

Follow-up HTS and Commercial SAR Campaign

Given the high attrition rate inherent to drug development campaigns, our research group and collaborators recognized the importance of evaluating several hit compounds to maximize the probability of developing a potent and pharmacokinetically competent lead. The original screen performed at the Center for Chemical Genomics at the University of Michigan was performed on the modestly sized in-house library of 55,000 compounds, which returned CCG-2979 (**1**) as the only workable lead compound due to issues of reactivity, availability, and reproducibility of the other hits.[45] To find additional hit compounds, the original HTS protocols were used in a second screen, this time employing the 303,000 compound library at the Broad Institute of MIT and Harvard. The second screen returned 7 additional hits from 6 distinct chemical classes (Scheme 2.12). As with the CCG-2979 series, a short round of commercial SAR was initiated to assist in deciding which scaffolds to evaluate further.

Scheme 2.12. Hit compounds identified from follow-up HTS at the Broad Institute.

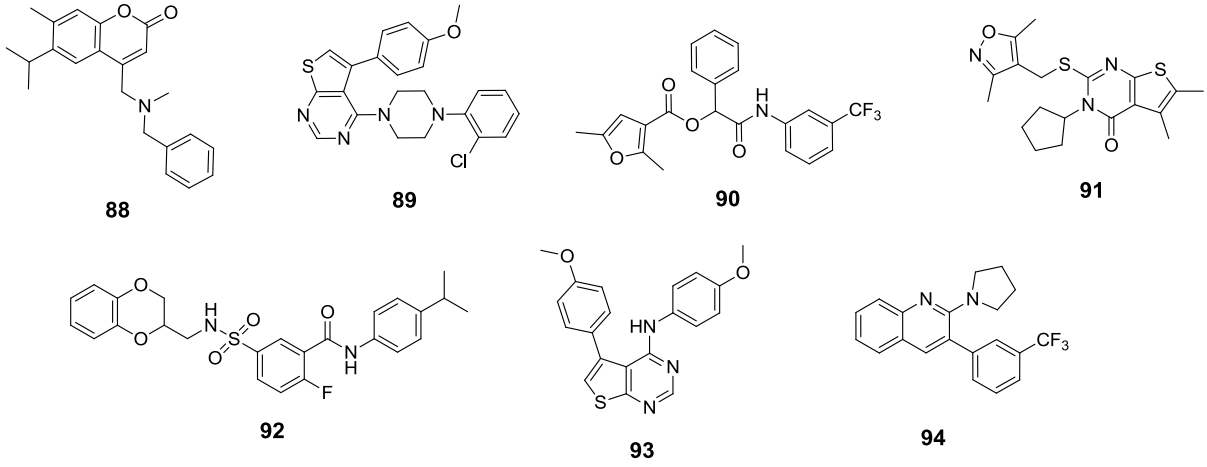

A total of 73 commercially available compounds across the 6 scaffolds were tested for activity in GAS (10-15 compounds per scaffold), sampling a breadth of substitution patterns around the basic skeleton of each hit. The thienopyrimidine (based on **89** and **93**) and quinoline (based on **94**) series showed very little SAR between analogs and were generally low in potency, leading to their removal from consideration. Of the remaining four scaffolds, chromenone-based similar in structure to **88** exhibited the widest range of activity in the GAS-SK assay (Table 2.7), with a few (**103**, **104**) showing exceptional activity on par with potent compound **17**. Furthermore, the aqueous solubility of these compounds, although not tested, is likely enhanced due to the reduced overall planarity of the compound and the presence of a basic amine. Lead compound **88** was not commercially available in sufficient quantities to be included in the commercial SAR study, but several close analogs (**99**, **101**, **102**) were obtained. Although the GAS-SK activity data was encouraging, incubation of representative compound **102** with liver microsomes revealed a severe propensity for rapid oxidation (MLM $t_{1/2}$ = 0.6 min). Given our long-standing issues with metabolic stability in the CCG-2979 series, it was decided the chromenone scaffold would not be pursued as an alternate template. The growing interest in the biofilm arm of the study led us to decide that none of the other 3 potent scaffolds would be assessed further in the GAS study, but the purchased compounds were retained for screening for anti-biofilm activity (Chapter 4).

Table 2.7. GAS-SK Activity data for chromenone-based compounds 95-104.

#	Structure	5 µM SK T/C[a]	50 µM SK T/C[a]	50 µM Growth T/C[b]
95	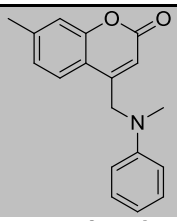	1.48 ± 0.15	1.16 ± 0.01	0.87 ± 0.01
96	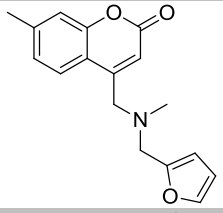	1.28 ± 0.14	0.81 ± 0.01	1.04 ± 0.00
97	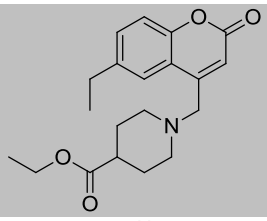	1.27 ± 0.04	0.82 ± 0.07	1.06 ± 0.02
98	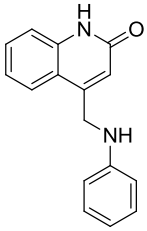	1.25 ± 0.01	1.00 ± 0.04	1.06 ± 0.00
99	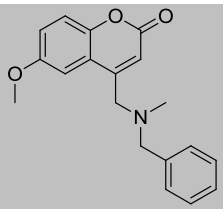	1.19 ± 0.07	0.83 ± 0.01	1.01 ± 0.01
100	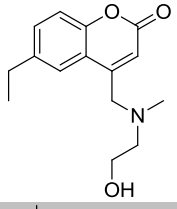	0.75 ± 0.21	0.68 ± 0.04	1.05 ± 0.00
101	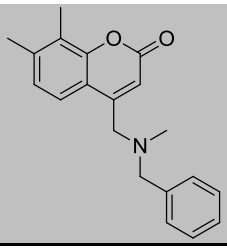	0.73 ± 0.03	0.49 ± 0.02	1.05 ± 0.00

#	Structure	5 µM SK T/C[a]	50 µM SK T/C[a]	50 µM Growth T/C[b]
102	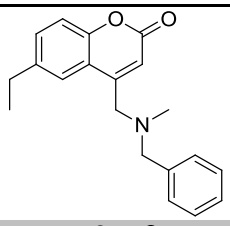	0.69 ± 0.05	0.36 ± 0.07	0.84 ± 0.01
103	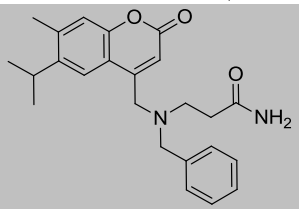	0.58 ± 0.11	0.09 ± 0.04	0.90 ± 0.02
104	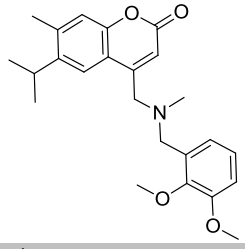	0.34 ± 0.05	0.17 ± 0.01	1.13 ± 0.02
17	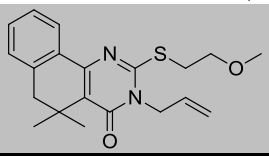	0.44 ± 0.02	0.06 ± 0.04	0.93 ± 0.01

[a] Ratio of A_{405} of SK-cleaved substrate in GAS culture treated with the indicated concentration of test compound divided by A_{405} of DMSO control (see Chapter 6: Experimental Section). Values are the mean of at least three experiments ± standard deviation. [b]Ratio of OD (600 nm) for growth of GAS in the presence of test compound divided by DMSO control. Values are the mean of three replicates within one assay, ± standard deviation.

4. Conclusions

The GAS-SK SAR study ultimately resulted in the synthesis of 123 analogs of **1** developed by myself and five other chemists. Over the course of the study, we discovered several more potent compounds, with **32** identified as the best analog of the series (IC_{50} = 1.3 µM). Despite gains in potency, the overall efficacy of these compounds is no doubt hampered by issues of low metabolic stability and aqueous solubility across nearly all analogs. Careful structure-metabolism relationship analysis identified that alkylating the *O*- position of the pyrimidinone amide (e.g. compounds **48**-**50**) conferred significant (4-15 fold) increases in metabolic stability in comparison to identical *N*-substitution. Unfortunately, compound **50**, the *O*-alkylated isomer of **32**, was much less potent, and is still rather unstable despite a 4-fold

longer MLM half-life ($t_{1/2}$ = 8.3 min vs. 2.3 min for **32**). The aqueous solubility of these compounds remains quite low, and most attempts to increase solubility via the installation of polar functionality were met with severe drops in activity. Ultimately, three factors led to the indefinite suspension of the GAS-SK study: (1) the inability to identify compounds retaining potent activity while enhancing solubility and stability; (2) the overall variable, poorly reproducible, and time-intensive nature of the activity assay; and (3) the discovery of anti-biofilm activity in *S. aureus* with this compound series. While the GAS-SK portion of the study has concluded, the compounds and physicochemical data gleaned from this study are still highly valuable to the ongoing biofilm inhibition effort (Chapter 4).

Chapter 3: Target Identification

Phenotypic Screening and Target Identification

Screening campaigns employing phenotypic assays, like the one used to identify **1**, have the benefit of identifying hit compounds possessing physicochemical properties sufficient for cell permeability and access to intracellular targets. In contrast to target-based screening, phenotypic screening does not rely on *a priori* knowledge of the affected biological pathway to identify hit compounds, making it a useful tool for discovering novel biochemical mechanisms of action.[69] These advantages, taken together with the limited number of successful drug development studies derived from target-based screening of bacterial proteins,[70] demonstrate the potential utility of phenotypic screening for identifying novel antibacterial agents. The benefits of phenotypic screens come at the cost of offering no insight into the macromolecular target of hit compounds. Therefore, the use of some method of target identification is necessary to gain a fuller biochemical understanding of the affected systems. In the context of our project, identifying the target of lead compound **1** would be important for (a) helping to establish a biochemical assay with which to improve the potency and specificity of the compound series, and (b) identifying potentially novel pathways in virulence gene expression.

The potent activity of our compounds against SK expression, combined with RNA microarray data indicating the down-regulation of other important GAS virulence factors (M protein, streptolysins, fibronectin and collagen-like binding proteins, Figure 1.2), suggests that their macromolecular target(s) are involved in the upstream regulation of GAS virulence mechanisms. The control systems governing GAS virulence have been the subject of a considerable body of research that has elucidated the roles of several transcriptional modulators.[71] Various aspects of GAS virulence are controlled by the growth-phase dependent activation of the response regulator (RR) proteins Mga,[72] RALP (also known as RofA),[73] and Rgg.[74,75] In addition, a number of two-component systems (TCSs) have been characterized that

regulate gene expression based on environmental stimuli detected by membrane-embedded sensor proteins. Three TCSs with a role in GAS virulence control have been well-studied: the Ihk/Irr system (leukocyte evasion),[76,77] FasBCAX (RNA-mediated streptokinase induction),[78,79] and CovR/CovS (down-regulation of several virulence factors during stationary phase).[80] More recent studies have identified several other systems that influence GAS virulence, including TCS system *Streptococcus pyogenes* Ser/Thr phosphatase (SP-STP),[81] putative RNase CvfA,[82] and GAPDH, a glycolytic surface-expressed enzyme.[83] It is possible that one of these systems may contain the target of our compound series, but the highly complex nature of GAS virulence and virulence control mechanisms makes this somewhat unlikely. Furthermore, genomic sequencing of multiple virulent GAS serotypes has revealed several well-conserved putative RRs and at least 10 TCSs that have yet to be characterized.[84] The identification of a previously uncharacterized protein would represent an excellent opportunity to expand the current understanding of GAS virulence.

Figure 3.1. A survey of possible methods of chemical probe-based target identification.

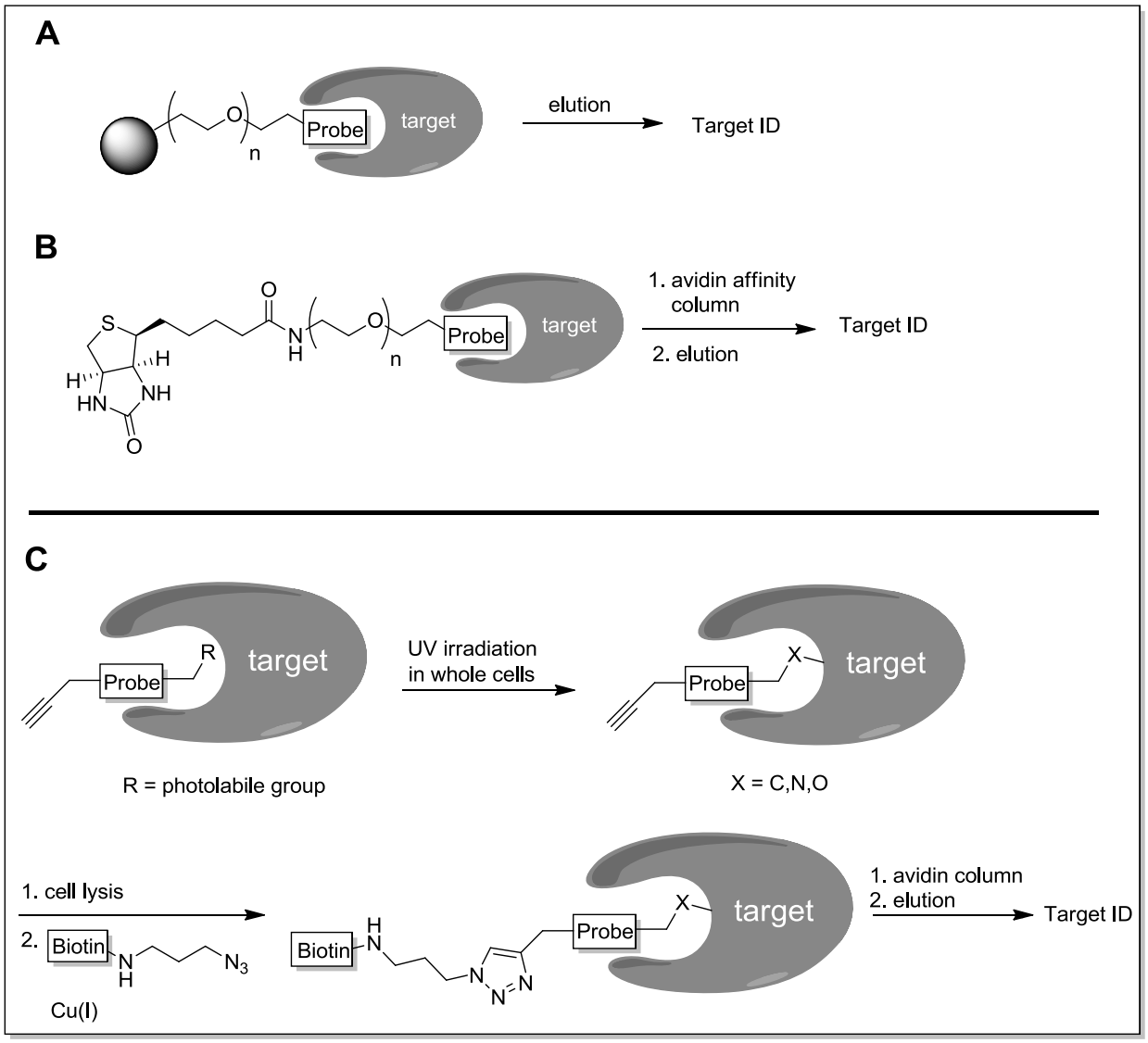

A: An "affinity matrix" column consisting of agarose beads functionalized with probe compound for the selective enrichment of target proteins. **B:** Noncovalent association of probe with target proteins to be enriched via avidin affinity column. **C:** Use of alkyne-modified bifunctional small molecule photoprobes employed to first selectively bind to target proteins, then covalently bond to the binding site under UV irradiation, and finally be modified with a biotin group via click chemistry to facilitate avidin column enrichment.

Chemical probes are commonly employed in target identification studies, and several strategies have evolved for successfully identifying targets (Figure 3.1).[85,86,87,88] Affinity chromatography is a popular method that involves the use of agarose beads conjugated with a small molecule, either directly or through a biotin/streptavidin association, to "pull-down" proteins that interact with the probe compound (Figure 3.1A, 3.1B). Control experiments that add a soluble competitor compound abolishes specific probe-protein interactions, enabling the

differentiation of specific and nonspecific binding events (Figure 3.2). Biotinylated probes most often incorporate a linker region (commonly alkyl amide or polyethylene glycol-derived) of variable length between the biotin and ligand portion of the molecules to avoid steric clashing of the target and streptavidin. Drawing upon previous studies with similar goals, we first decided to pursue the synthesis of biotinylated versions of our more potent GAS-SK compounds.

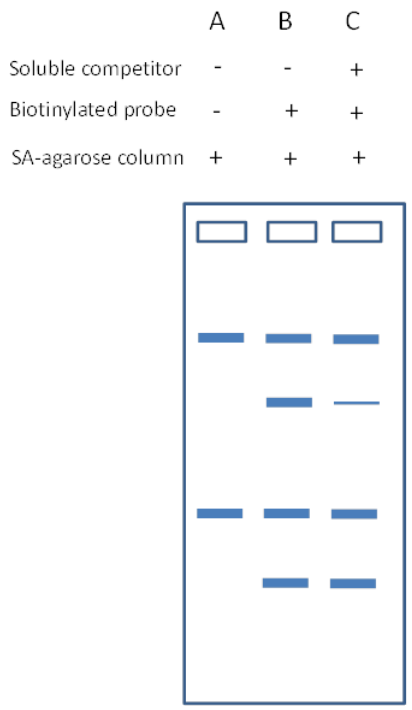

Figure 3.2. Schematic of Western blot indicating a successful target ID using biotinylated probes. Lane A: Proteins that interact nonspecifically with column components are visualized. Lane B: In the presence of probe, proteins are now a mixture of nonspecific protein-column and protein-ligand interactions, as well as possible specific protein-ligand interactions. Lane C: Inclusion of a soluble competitor reduces specific probe-ligand interaction, indicating possible target.

First Generation Probes: Biotinylated Ligands

Before biotinylated probes could be synthesized, we first determined the optimal attachment point for a biotin linker on the scaffold. To do so, we incorporated a methoxyethyl group as a model of the poly(ethylene glycol) spacer at 5 different attachment points on the molecule: three positions on the aryl ring, and one each at the sulfur and amide nitrogen of the pyrimidinone ring. The synthesis of each of these compounds is described in Chapter 2. A comparison of their relative activity in the GAS-SK assay (Table 3.1) indicated that attachment to the aryl ring (**37-39**) led to lower or erratic activity. Compound **42** was found to be essentially equipotent to **17**, but induced bacteriotoxicity in several trials. Therefore, the pyrimidinone sulfur was chosen as the attachment point for the first generation of target identification probes.

Table 3.1. Comparison of 2-methoxyethyl substitution at 5 attachment points.

#	Structure	5 µM SK T/C[a]	50 µM SK T/C[a]	50 µM Growth T/C[b]
17‡	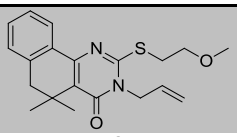	0.35 ± 0.11	0.13 ± 0.07	0.86 ± 0.10
37	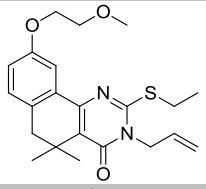	0.58 ± 0.24	0.43 ± 0.15	1.02 ± 0.10
38	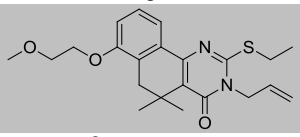	0.84 ± 0.23	0.40 ± 0.21	0.94 ± 0.08
39	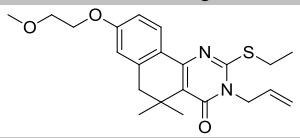	0.46 ± 0.35	0.36 ± 0.41	0.85 ± 0.22
42	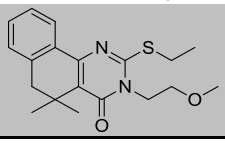	0.20 ± 0.12	0.15 ± 0.20	0.64 ± 0.38

[a] Ratio of A_{405} of SK-cleaved substrate in GAS culture treated with the indicated concentration of test compound divided by A_{405} of DMSO control (see Chapter 6: Experimental Section). Values are the mean of at least three experiments ± standard deviation. [b]Ratio of OD (600 nm) for growth of GAS in the presence of test compound divided by DMSO control. Values are the mean of at least three experiments ± standard deviation. [‡]Originally synthesized by Meghan Breen.

Biotinylated Probe Synthesis

Synthesis of the first generation affinity probe was fairly straightforward. We incorporated a polyethylene glycol-based spacer region derived from hexaethylene glycol (PEG-6) to ensure an adequate distance between the target and the solid-supported streptavidin. Elaboration of PEG-6 to its corresponding monoamine **108** was completed via a known procedure.[89] The monomesylation of the glycol in the presence of silver oxide as a chloride ion sink proceeded in low, but useful yields to furnish **106**. The displacement of the mesylate group with sodium azide followed by Staudinger reduction generated amine **108**, which could then be *N*-protected with a Boc group and mesylated to generate the bifunctional spacer precursor **110**. Treatment of the 2-thioxopyrimidinone intermediate **16** with **110** under standard alkylating conditions furnished ligand-spacer adduct **111**. Acid-catalyzed removal of the Boc group

revealed free amine **112** that was subsequently coupled to the carboxylic acid moiety of biotin to furnish PEG6-biotin probe **113**.

Scheme 3.1. Synthesis of noncovalent biotinylated probe 113.[a]

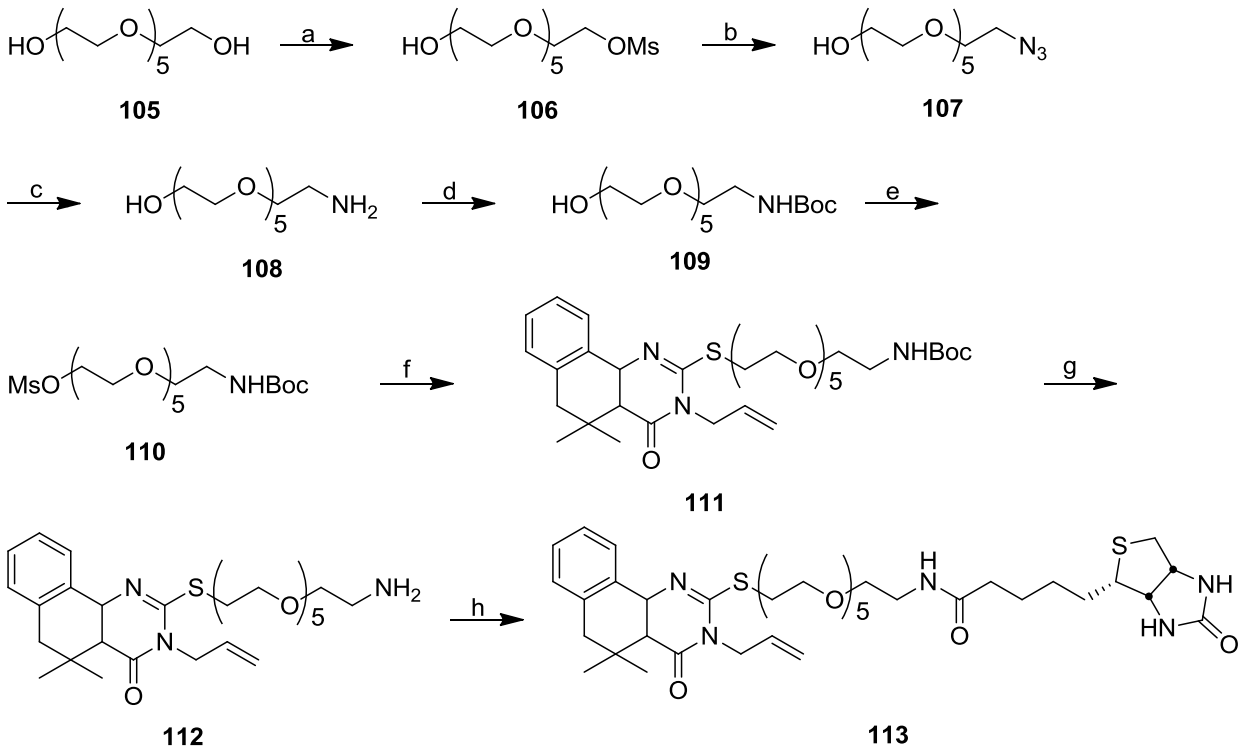

[a]Reagents and conditions: a) MsCl, Ag_2O, DCM, RT, 48h, 26%; b) NaN_3, DMF, 80°C, 6h, 67%; c) PPh_3, THF, 0°C-RT, 12h, then H_2O, RT, 12h, 94%; d) Boc_2O, DIPEA, DMF, 0°C-RT, 16h, 83%; e) MsCl, DIPEA, DCM, RT, 16h, 69%; f) **16**, Cs_2CO_3, DMF, 70°C, 16h, 62%; g) TFA:DCM (1:2), RT, 2h, 81%; h) Biotin-OSu, DIPEA, DMF, RT, 16h, 51%.

With **113** in hand, collaborator Colin Kretz in the Ginsburg group first attempted pulldown assays in whole GAS cells, which indicated the induction of bacteriotoxicity (*data not shown*). This finding was not entirely unexpected given the significantly increased size and TPSA of these compounds. We hypothesized that these two factors likely drastically reduced or abolished the ability of these compounds to permeate the cell membrane, leading subsequent trials to be performed using GAS lysates. Unfortunately, while proteins were indeed pulled down via biotin/avidin affinity column, none of them were likely target compounds, and no selective protein band reduction was evident in competition assays with **17**. It could be that appending the spacer and biotin moieties led to a loss of activity as well as permeability. It was decided the next generation of biotinylated probes would be designed to incorporate photolabile

groups to allow the covalent attachment of probes to the target before enrichment, circumventing potential issues associated with low target-ligand binding affinity.

Second Generation Probes: Photolabile Biotinylated Probes

Biotinylated chemical probes can overcome the issue of low target affinity by incorporating groups that covalently bond to the target, such as amino acrylates,[90] vinyl sulfones,[91] or UV-promoted crosslinking groups.[92] We decided to pursue the incorporation of UV-active photolabile groups over other covalent strategies as they offer control over the initiation of the crosslinking reaction, and are generally irreversible. A number of different photolabile groups are commonly employed in target ID studies, including benzophenones, diazirines, and aryl azides (Scheme 3.4).[92] Upon irradiation with long-wavelength UV light (~365 nm), each of these moieties breaks down into a highly reactive intermediate species conducive to rapid reaction with associated proteins. A synthetic scheme was devised to allow for the production of a basic ligand-spacer-biotin scaffold with an attachment point for photolabile groups built into the spacer. DL-lysine with orthogonally protected amine groups allowed for the late-stage introduction of photolabile groups using a straightforward synthetic route.

Scheme 3.2. Synthesis of photolabile biotin probes 122 and 123.[a]

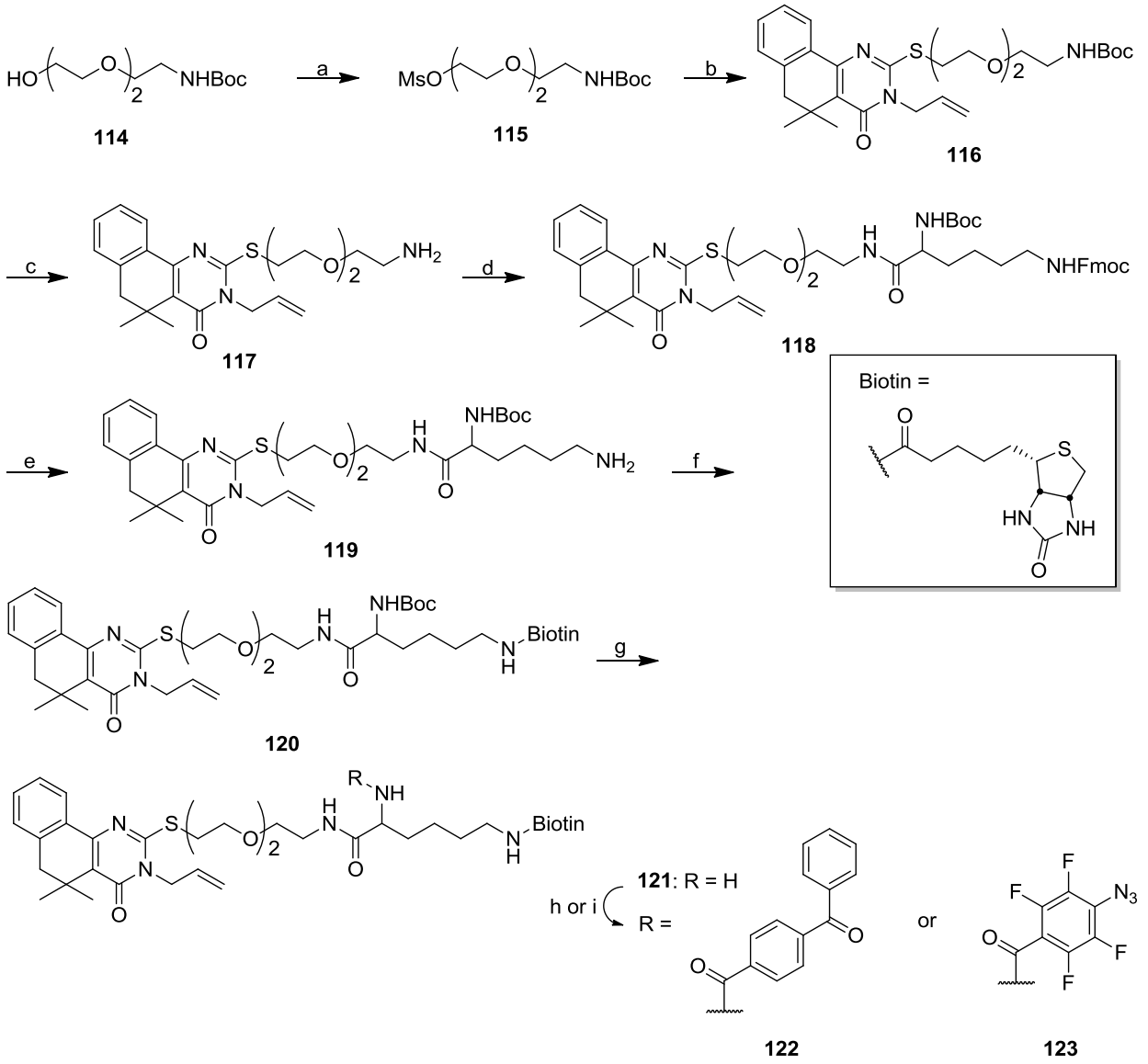

[a]Reagents and conditions: a)MsCl, DIPEA, DCM, RT, 16h, 72%; b) **16**, Cs_2CO_3, DMF, 75°C, 16h; c) TFA:DCM (1:2), RT, 2h; d) Boc-Fmoc-DL-Lysine, HOBt, EDC, DIPEA, DCM, RT, 24h, 58% over 3 steps; e) piperidine, DMF, RT, 60 min, 75%; f) Biotin-OSu, DIPEA, DCM, RT, 16h, 79%; g) TFA-DCM (1:2), RT, 2h, 99%; h) 4-benzoyl benzoic acid, EDC, HOBt, DIPEA, DCM, RT, 16h, 41%; i) **131** (Scheme 3.3), DIPEA, DCM, RT, 48h, 36%.

Beginning from NHBoc-PEG3 (obtained from Mike Wilson), mesylation followed by alkylation with intermediate **16** and Boc deprotection revealed primary amine **117** ready for further elaboration. Installation of the Boc-Fmoc-Lysine proceeded under standard amide coupling conditions to yield **118**. In an effort to introduce the photolabile groups as late as possible in the synthesis, the Fmoc group was removed first with 20% w/v piperidine in DCM,

and the resulting amine was treated with biotin succinimide to furnish biotinylated intermediate **120**. After deprotection under acidic conditions, the resulting common intermediate **121** could be coupled to the desired photolabile group via EDC promoted conditions to yield benzophenone probe **122** or direct addition of the amine to the tetrafluorophenyl azide NHS ester[93] to generate probe **123**.

After the successful synthesis of **122** and **123**, our collaborators performed UV-crosslinking followed by immunoblotting to visualize biotinylated proteins. Briefly, GAS cell lysates were pre-cleared of biotinylated proteins by incubating with avidin-coated beads, then treated with the selected probe. Crosslinking was induced via 365nm UV radiation for 5-90 minutes, then the resulting probe-protein adducts were purified by avidin column. Proteins were separated via SDS-PAGE, transferred to a polyvinylidene difluoride (PVDF) membrane, and treated with horseradish peroxidase (HRP)-avidin fusion protein. Peroxide staining allowed the visualization of proteins conjugated to HRP-avidin.

Crosslinking trials with benzophenone **122** yielded very faint protein bands after 60 minutes of UV exposure, indicating the relatively low UV-induced reactivity of this probe. The inclusion of **17** as a soluble competitor did not lead to the attenuation of any protein bands, which is likely due to a high incidence of nonspecific binding. In addition, the long UV exposure time required for crosslinking (60 minutes) probably allowed the equilibration of binding between **17** and **122**, diminishing the effects of competition-based decreases in specific labeling. Increasing the exposure time to UV radiation from 60 to 90 minutes in an effort to enhance labeling instead resulted in extensive protein aggregation and breakdown. Our inability to find optimal crosslinking conditions led to the dropping of **122** from future trials. Tetrafluorophenyl azide probe **123** on the other hand was extremely reactive, labeling a myriad of proteins after only 5 minutes. The high level of binding observed made the discernment of specific labeling events in competition studies with **17** virtually impossible. Based on this result, we theorized that generating a "dummy probe" (**129**, Scheme 3.3) might enable us to deduce which of the proteins pulled down, if any, were due to specific interactions. This probe retained the photolabile group, spacer, and biotin portions of the molecule, but replaced the ligand portion with a small lipophilic group. The deletion of the ligand portion was intended to abolish interaction at the specific target of **122** and **123**, but retain most of the nonspecific binding capacity of the rest of

the molecule. The dummy probe was synthesized in a manner similar to **123**, using *O*-benzyl ethanolamine **124** as the starting material instead of intermediate **117**.

Scheme 3.3. Synthesis of "dummy probe" 129.[a]

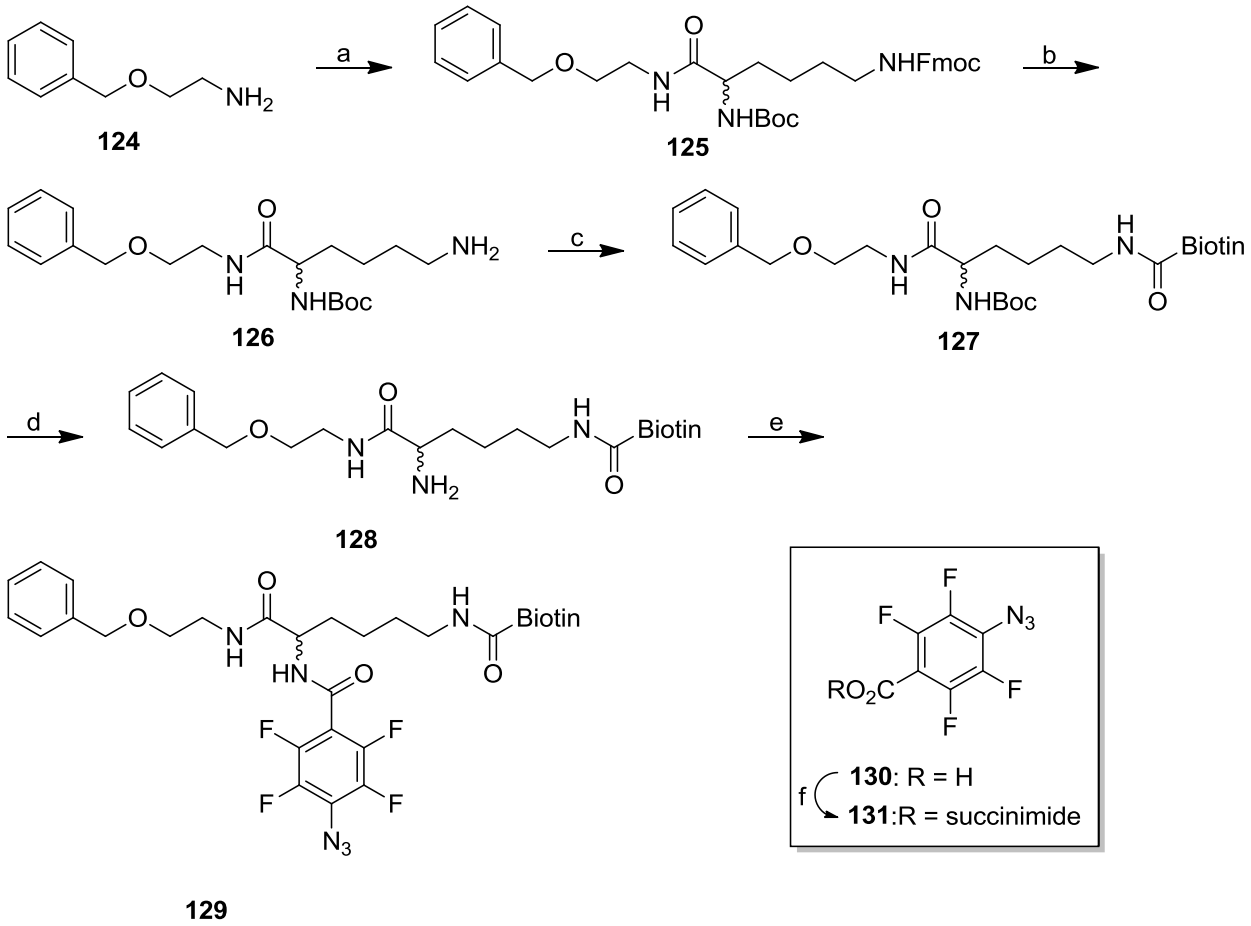

[a]Reagents and conditions: a) Boc-Fmoc-DL-Lysine, HATU, DIPEA, DMF, RT, 90 min, 100%; b) piperidine, DMF, RT, 60 min, 100%; c) Biotin-OSu, DIPEA, DCM, RT, 16h, 76%; d) TFA:DCM (1:2), RT, 2h; e) **131**, DIPEA, DMF, RT, 24h, 36% over 2 steps; f) *N*-hydroxy succinimide, EDC, DCM, 35°C, 16h, 78%.

Studies that employed the active and dummy aryl azide probes in tandem did not meet with much success. When used alone, **123** did indeed pull down a large number of proteins as evidenced by HRP-avidin immunoblot. Unfortunately, when the same conditions were repeated with **129**, the desired diminishment of any protein bands relative to treatment with **123** was not observed. While disappointing, these results do not conclusively rule out the occurrence of specific reactions. The interaction may have been too weak (low potency) or too sporadic (low

target abundance) to be detected in the presence of the noise generated by nonspecific binding events.

Tag-free Photoprobes

The failure of the traditional biotinylated probe study left us searching for alternative methods of target identification. Recently, other groups have demonstrated the utility of combining the advantages of photolabile biotinylated probes with the more biologically suitable properties of conventional small molecule inhibitors by replacing bulky appendages with small "handles" amenable to bioorthogonal click chemistry (Figure 3.1C).[94,95] These probes incorporate a photoreactive group and a terminal alkyne into the scaffold of a potent compound. This probe is then covalently crosslinked to protein in the intact cellular milieu with UV light. An azide-modified fluorescent or biotin-derived moiety can then be appended to the alkyne-functionalized protein(s) via copper(I)-mediated click chemistry after cell lysis, resulting in target proteins with covalently attached tags for visualization or selective purification respectively. The lower molecular weight and TPSA of these "tag-free" probes increases their likelihood of being cell-permeable, allowing them to be used in whole-cell systems rather than lysates. Cell-permeable affinity probes are advantageous in that they enable the confirmation of their activity in phenotypic assays before beginning target identification studies. The probes also have the added benefit of access to all proteins in their native cellular conformations.

To identify the unknown molecular target of our series of GAS anti-virulence compounds, we envisioned the synthesis of several tag-free photoprobes based on structural insights gained from our SAR studies on this scaffold. Although the maintenance of a high level of potency was a primary concern in the synthesis of the probe molecules, the nature and positioning of the UV-active and terminal alkyne groups were equally important to us as they are crucial for ensuring a compatible orientation for labeling.[96,97] A number of different photolabile groups have been employed to positive effect in the literature, varying in their stability, reactivity, and preference for C-C or C-heteroatom bond formation.[92] The presently unknown features of the binding site ultimately determine the features necessary for a functional probe, so we set out to synthesize a diverse series of compounds with one of three photolabile groups (benzophenone, diazirine, aryl azide, Scheme 3.4) at different points on the scaffold to maximize our chances of identifying the target.

Scheme 3.4. Long-wave UV-induced reactivity of benzophenones, diazirines, and aryl azides in the context of molecular target capture. Ketyl radicals (top pane) preferentially form new C-C bonds, while carbenes and nitrenes (middle, bottom pane) more commonly insert into hydrogen-heteroatom bonds.

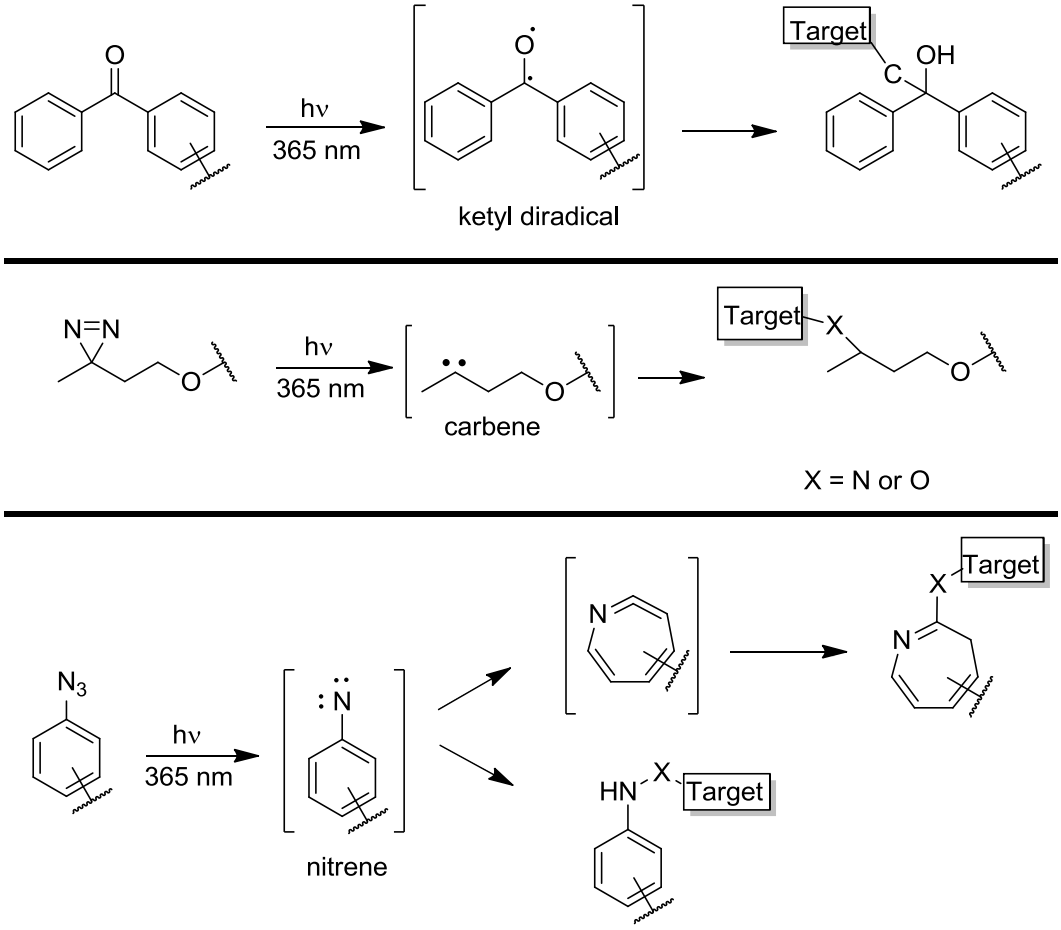

Synthesis

The chemistry to install benzophenone, diazirine, and aryl azide functionality onto the core scaffold of this class of compounds required three distinct synthetic routes. Synthesis of the benzophenone-based probes (Scheme 3.5) began with the LDA-promoted Michael addition of 4-bromo-2-methylbenzonitrile (**132**) to ethyl 3,3-dimethyl acrylate and subsequent ZnI_2-mediated cyclization to afford β-aminoester **133.**[55] Stannylation via halogen-metal exchange[98] followed by carbonylative Stille coupling[99] successfully delivered benzophenone **134**. Acid-catalyzed addition of the amine to allyl isothiocyanate followed by cyclization generated 2-thioxopyrimidinone intermediate **135** that underwent sulfur alkylation with propargyl bromide or

139 (generated by tosylating commercially available propynol ethoxylate, **138**) under mildly basic conditions to generate probes **136** and **137**.

Scheme 3.5. Synthesis of benzophenone-functionalized tag-free probes 136 and 137.[a]

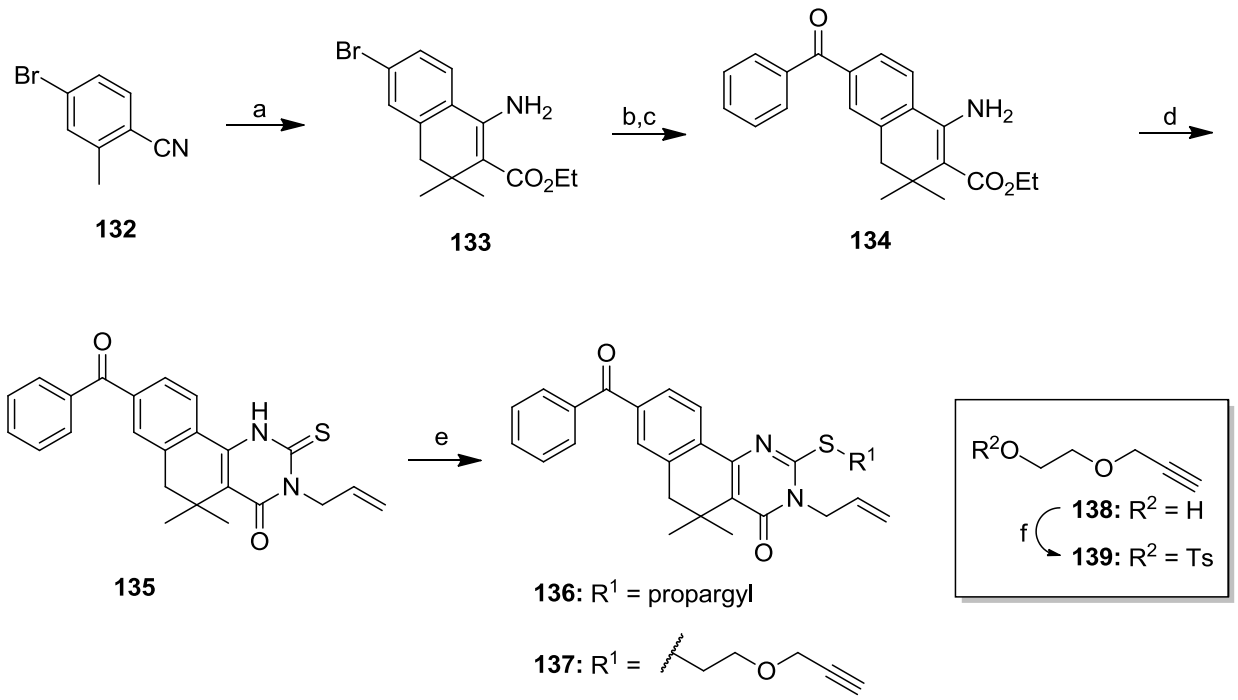

[a]Reagents and conditions. a) LDA, then ethyl 3,3-dimethyl acrylate, ZnI_2, diglyme, -78°C – RT, 50%; b) $(Bu_3Sn)_2$, $Pd(PPh_3)_4$, toluene, reflux, 37%; c) 1 atm CO, $PdCl_2(PPh_3)_2$, iodobenzene, DMF, 60°C, 58%; d) allyl isothiocyanate, AcOH, EtOH, 70°C, 27%; e) propargyl bromide or **139**, Cs_2CO_3, 2-butanone, 70°C, 69-70%; f) TsCl, pyridine, 0-4°C, 24h, 72%.

Diazirine probes **143-146** were synthesized via an analogous route beginning from aryl methyl ether **26c** (Scheme 3.6). Demethylation and protection of the resulting phenol as a silyl ether resulted in **140**, which could be employed in the synthesis of β-aminoester **141** in a manner similar to that for the benzophenone probes. In the course of our investigation, we found that cyclization with allyl isothiocyanate in the presence of cesium carbonate furnished the desired 2-thioxopyrimidinone **142** with the concomitant loss of the silyl ether protecting group. Successive chemoselective alkylations at sulfur and oxygen were exploited to install the diazirine and alkyne linker moieties in four different arrangements, yielding probes **143-146**. Diazirine-containing alkylating agent **149** was synthesized from 4-hydroxy-2-butanone (**147**) via diaziridination of the ketone with 7N methanolic ammonia and hydroxylamine *O*-sulfonic acid[100] followed by oxidation and tosylation.[101]

Scheme 3.6. Synthesis of diazirine-functionalized tag-free probes 143-146.[a]

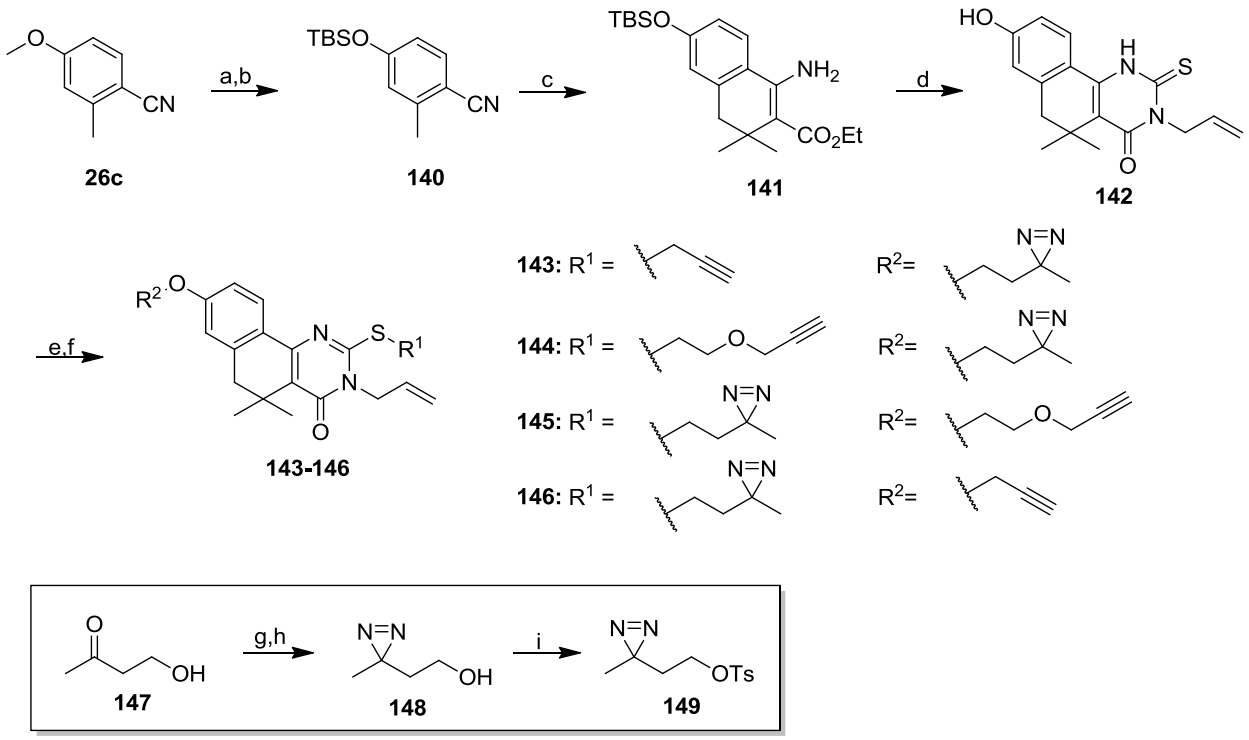

[a]Reagents and conditions. a) BBr_3, DCM, 0°C-RT, 16h; b) TBS-Cl, imidazole, DCM, 0°C-RT, 16h, 96% over 2 steps; c) LDA, then ethyl 3,3-dimethyl acrylate, ZnI_2, diglyme, -78°C-RT, 3h, 63%; d) allyl isothiocyanate, Cs_2CO_3, EtOH, 70°C, 16h, 57%; e) **139**, **149**, or propargyl bromide, $NaHCO_3$, 70°C, DMF, 3-6h, 45-71%; f) **139**, **149**, or propargyl bromide, Cs_2CO_3, 70°C, DMF, 3h, 16-64%; g) 7N NH_3:MeOH, hydroxylamine-*O*-sulfonic acid, 0°C-RT 16h; h) I_2, Et_3N, 0°C, MeOH, 30 min; i) Ts-Cl, pyridine, 0-4°C, 24h, 15% over 3 steps.

Synthesis of the azide probe began with commercially available 2-cyano-3-methylaniline **150** (Scheme 3.7). Masking the aniline functionality of **150** as a mono- or bis-Boc carbamate, diphenyl imine, or azide proved to be incompatible with the LDA/ZnI_2 cyclization conditions. Finally, it was found that modified Sandmeyer conditions to transform the aniline to the aryl iodide[102] permitted the formation of the β-aminoester **151** in modest yields. Gratifyingly, conversion to the corresponding aryl azide **152** via Cu(I)-mediated S_NAr proceeded in excellent yields.[103] Stepwise generation of the unsubstituted 2-thioxopyrimidinone with benzoyl isothiocyanate and potassium hydroxide afforded **153**,[57] which was then selectively *S*-alkylated with TBS-protected alkyne-containing unit **156**.[104] Alkyne protection was necessary to minimize cross-reactivity during the subsequent *N*-allylation under basic conditions to furnish **154**.

Fluoride ion-promoted removal of the silyl group finally yielded the desired aryl azide probe **155**.

Scheme 3.7. Synthesis of aryl azide-functionalized tag-free probe 155.[a]

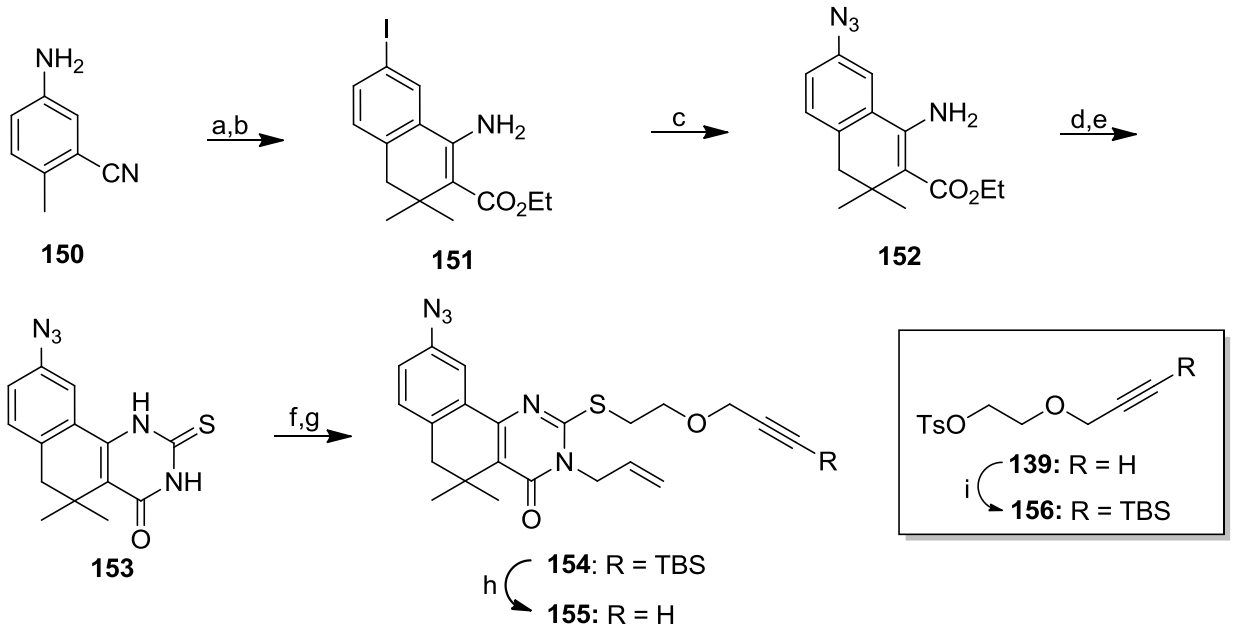

[a]Reagents and conditions. a) $NaNO_2$, HCl, then KI, H_2O, 0°C, 70%; b) LDA, then ethyl 3,3-dimethyl acrylate, ZnI_2, diglyme, -78°C-RT, 3h, 23%; c) NaN_3, CuI, *N*,*N*-dimethyl ethylene diamine, Na-ascorbate, DMSO:H_2O (5:1), RT, 3h, 85%; d) benzoyl isothiocyanate, EtOH, 70°C, 3h; e) KOH, EtOH:H_2O, 2:1, 70°C, 3h, 54% over 2 steps; f) **156**, $NaHCO_3$, 70°C, DMF, 16h; g) NaOMe, allyl bromide, EtOH, 70°C, 3h, 44% over 2 steps; h) TBAF, THF, 0°C, 1h 65%; i) *n*BuLi, -78°C, THF, 2h, then TBS-OTf, -78°C-RT, 1h, 63%.

SK Activity Assay

The 7 tag-free affinity probes were assayed for their inhibitory effects on SK expression (described in Chapter 2) using our previously described chromogenic assay of plasmin activity.[45] Given the critical nature of retaining maximal potency to target identification, 50% SK expression inhibition at 5 μM was used as the cutoff value for further evaluating probe compounds. Compounds meeting this threshold were more completely characterized with full IC_{50} curve generation and were utilized in subsequent crosslinking trials.

SAR Analysis

Benzophenone **137**, with its *S*-propargyloxyethyl click ligation sidechain, was found to be more potent than the corresponding *S*-propargyl analog **136**. This trend was also observed between diazirine probes **143** and **144**. Disappointingly, reversing the positioning of the alkyne and diazirine in probes **145** and **146** resulted in the complete loss of activity. Azide probe **155**, on the other hand, possessed potency slightly greater than lead compound **32**, the most potent compound identified from our prior SAR studies (Chapter 2). Although we were not able to identify active probes with reversed alkyne and photolabile groups, we were gratified to demonstrate a sufficiently active probe containing each of the selected photolabile groups (**137**, **144**, and **155**) for use in target identification studies.

Table 3.2. Activity data for tag-free photoprobes 136, 137, 143-146, and 155.

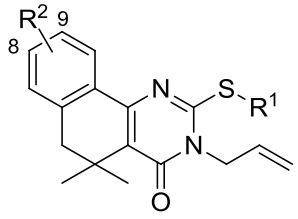

Cmpd	R^1	R^2	T/C (5 μM)[a]	Growth T/C (50 μM)[b]	IC_{50}[c]
136	propargyl	8-Bz	0.77 ± 0.34	1.09 ± 0.04	
137	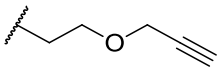	8-Bz	0.51 ± 0.07	0.94 ± 0.18	3.8 ± 0.6
143	propargyl	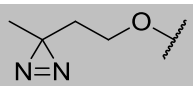	1.07 ± 0.16	0.96 ± 0.09	
144	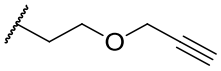	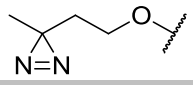	0.49 ± 0.34	1.07 ± 0.02	0.33 ± 0.70
145	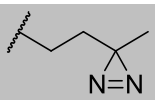	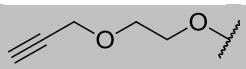	0.71 ± 0.40	1.01 ± 0.09	
146	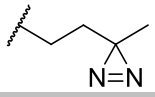	8-O-propargyl	0.89 ± 0.16	1.02 ± 0.01	
155	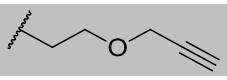	9-N_3	0.30 ± 0.08	0.98 ± 0.04	0.19 ± 0.26
32	Et	9-OMe	0.10 ± 0.06	0.73 ± 0.07	1.3 ± 0.6

[a]Amount of SK activity in GAS culture measured via colorimetric assay after incubation with 5 μM test compound for 24 hours divided by SK activity measured in GAS culture 24 hours after treatment with DMSO +/- standard deviation derived from at least 3 individual experiments. [b]Growth inhibition as measured by OD_{600} of GAS culture 24 hours after treatment with 50 μM test compound divided by OD_{600} of control GAS culture treated with DMSO after 24 hours +/- standard deviation derived from at least 3 individual experiments. [c]Concentration at which 50% maximal inhibitory effect against SK expression was achieved +/- standard deviation. Each data point is derived from the statistical treatment of 3 replicates.

Solvent Capture Study

Representative probe **144** was subjected to crosslinking conditions in methanol to assess whether the core scaffold would exhibit undesired photo-induced reactivity (Scheme 3.8). The methanolic solution of **144** was incubated under a 2.5A 365 nm UV lamp until the parent compound was completely consumed. Conversion of **144** to 2 new compounds (**157** and **158**, Scheme 3.8) was observed within 30 minutes. NMR and ESI-MS analysis of these identified the

major product as **157**, consistent with carbene insertion into the O-H bond of methanol (43% yield). The most prominent minor product consisted of a mixture of alkene isomers resulting from 1,2 hydride shifts[105] (**158**, 27% combined yield).

Scheme 3.8. UV-induced reactivity of probe compound 144 in methanol.

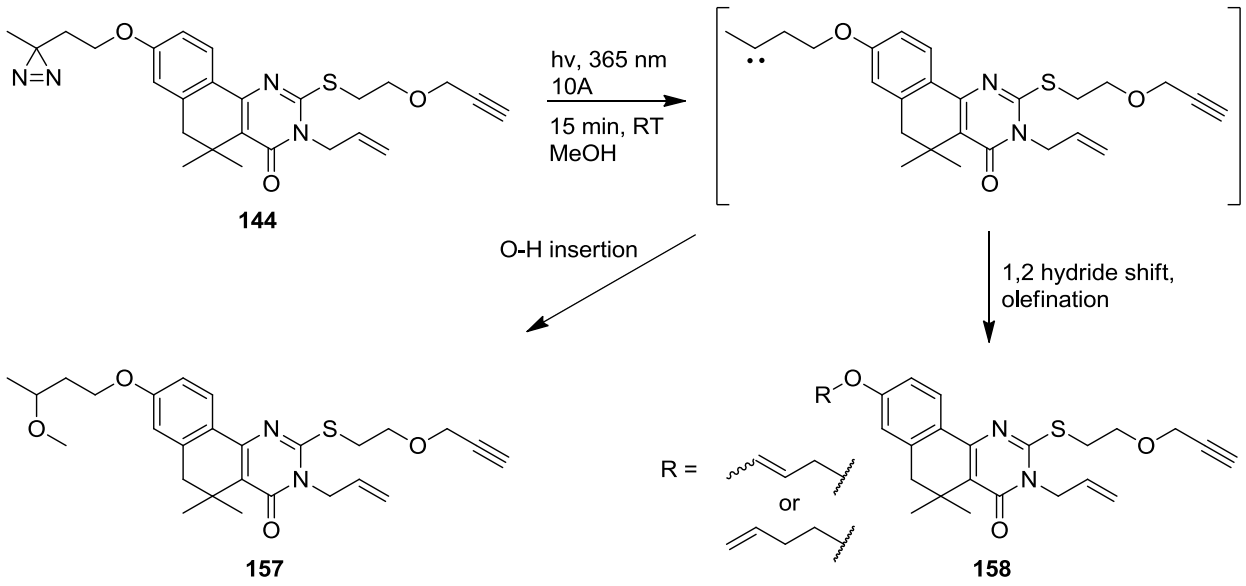

Target Identification Assays

With the identification of a number of active probes and successful photo-mediated solvent capture completed, our collaborators Colin Kretz and Autumn Holmes in David Ginsburg's group initiated protein-probe crosslinking assays. Briefly, GAS cultures were incubated in the presence of probe compounds for 30 minutes, then exposed to long-wave UV radiation for 5 (**144**, **155**) or 10 minutes (**137**) to promote crosslinking. The cells were lysed and pelleted, and the resulting lysates were subjected to click chemistry conditions with azide-functionalized Alexa Fluor 488 fluorescent dye. Proteins were then precipitated via methanol/chloroform/water solution and separated via SDS-PAGE gel. Fluorescent imaging of the gel allowed for the identification of tagged protein, then total protein levels were visualized via staining with Sypro Ruby. Benzophenone probe **137** appeared to crosslink to a distinct population of proteins when separated on a polyacrylamide gel and imaged with Alexa Fluor 488 (Figure 3.3). Tagging was found to be dose-dependent, based on reduced fluorescence with lower compound concentrations. Importantly, an identically treated control omitting the UV

crosslinking step did not fluorescently tag any proteins. Total protein staining of the gel with Sypro Ruby stain confirmed an abundance of protein in the sample, indicating that only a small subset of proteins were crosslinked with **137**. Unfortunately, competition with soluble competitor **17** did not reproducibly reduce the tagging of any protein band on the gel, which suggests a significant degree of nonspecific binding of **137** to protein.

Figure 3.3. Crosslinking trials using benzophenone probe 137.

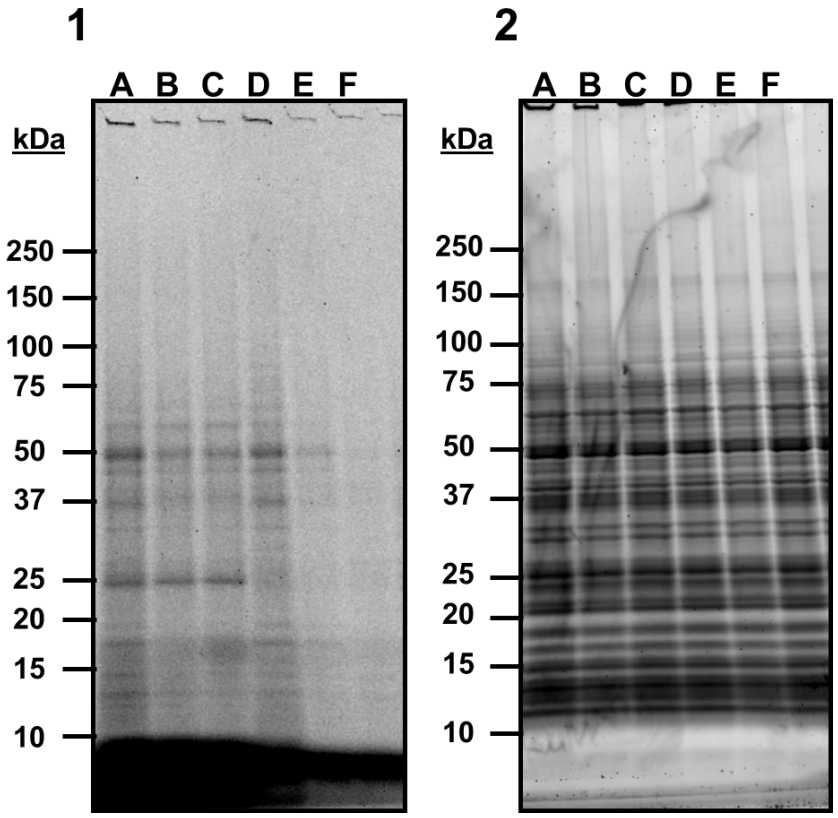

Pane 1: Visualization of crosslinking and competition experiments with Alexa Fluor 488-modified **137**-protein adducts on PAGE gel. **Pane 2:** Total protein stain of gel with Sypro Ruby stain. Lane parameters: A: 100 μM **137**; B: 100 μM **137** + 500 μM **17**; C: 100 μM **137** + 1 mM **17**; D: 10 μM **137**; E: 1 μM **137**; F: 100 μM **137**, no UV crosslinking.

Crosslinking experiments undertaken with diazirine **144** and azide **155** (Figures 3.4 and 3.5) showed similar trends to **137**. In each case the intensity of Alexa Fluor 488-tagged proteins was dependent on both the concentration of the compound and the exposure to UV light.

Qualitative comparison of the fluorescent and total protein stains suggests that the fluorescent intensity was generally proportional to protein abundance. This phenomenon, along with the absence of any reduction of fluorescence observed in the presence of soluble competitor, indicates an even greater degree of nonspecific crosslinking with **144** and **155** than seen with **137**. Interestingly, the addition of **17** to test solutions containing **144** seemed to increase crosslinking efficiency, perhaps owing to increased solubility of the probe in solutions with greater DMSO content.

Figure 3.4. Crosslinking trials using diazirine probe 144.

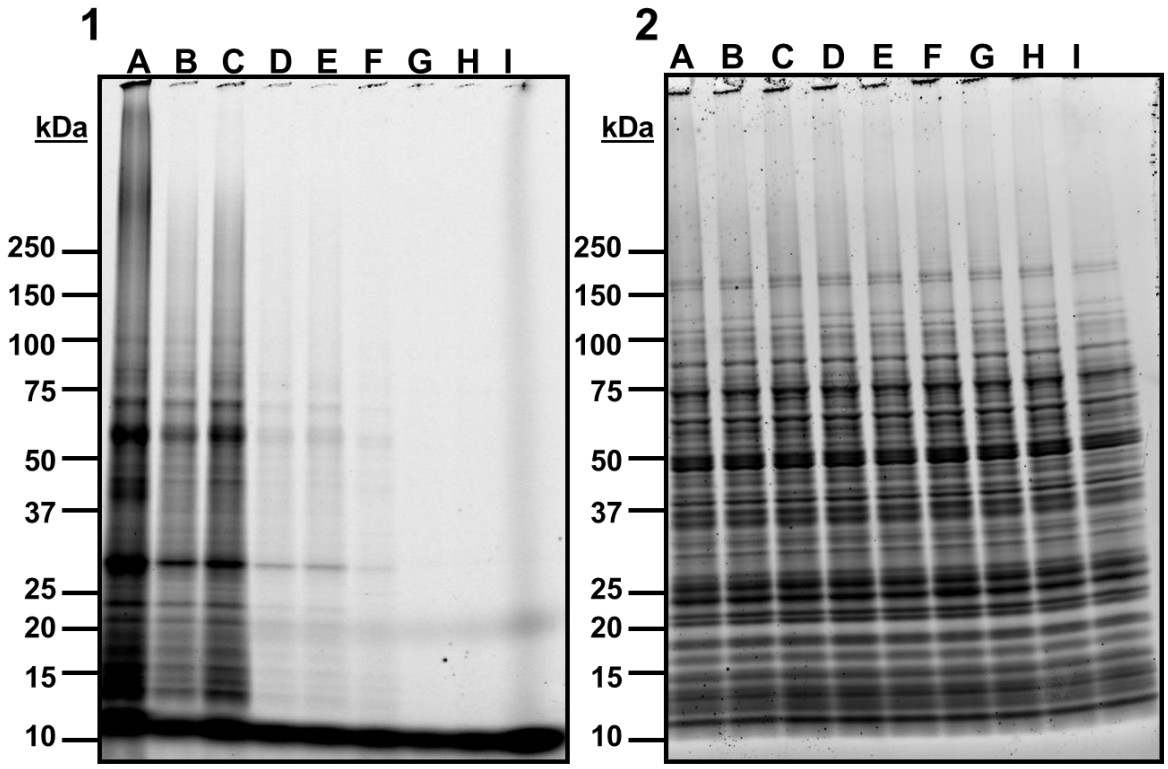

Pane 1: Visualization of crosslinking and competition experiments with Alexa Fluor 488-modified **144**-protein adducts on PAGE gel. **Pane 2:** Total protein stain of gel with Sypro Ruby stain. Lane parameters: A: 100 μM **144**; B: 10 μM **144**; C: 10 μM **144** + 100 μM **17**; D: 1 μM **144**; E: 1 μM **144** + 100 μM **17**; F: 100 μM **144**, no UV crosslinking; G: 100 μM **144**, no click reaction.

Figure 3.5. Crosslinking trials using azide probe 155.

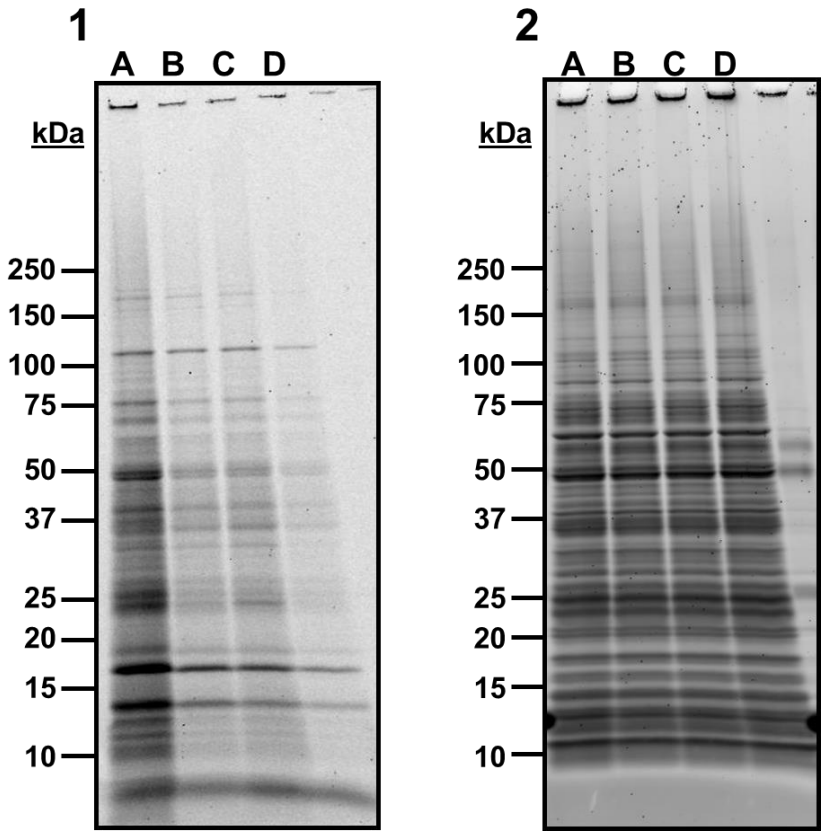

Pane 1: Visualization of crosslinking and competition experiments with Alexa Fluor 488-modified **155**-protein adducts on PAGE gel. **Pane 2:** Total protein stain of gel with Sypro Ruby stain. Lane parameters: A: 100 μM **155**; B: 10 μM **155**; C: 10 μM **155** + 100 μM **17**; D: 1 μM **155**.

Conclusions

Over the course of our efforts toward identifying the target(s) of the CCG-2979 compound series in GAS, three biotinylated probes (1 noncovalent, 2 capable of UV crosslinking) and seven tag-free photoprobes were synthesized. After disappointing results using the full-length noncovalent probe **113** and photolabile biotinylated probes **122** and **123**, we were encouraged by the observation that 3 of the tag-free photoprobes (**137**, **144**, **155**), each with a different photolabile moiety, retained potency in the GAS-SK affinity assay. After confirming clean photoactivation of representative probe **144** without degradation of the scaffold, we performed preliminary target identification studies. Crosslinking in whole cells, followed by

protein isolation and the attachment of a fluorescent tag, led to relatively widespread fluorescent labeling that appears consistent with nonspecific labeling of GAS proteins.

While biotin tagging and SDS-PAGE separation have been used successfully in the past for target identification, the nature of affinity chromatography and PAGE gel visualization confers a natural bias for highly potent interactions with high-abundance proteins.[106] The possibility of the target being a bacterial transcription factor, which are among the least abundant proteins in the cellular milieu,[50] along with the high propensity for nonspecific binding exhibited by these compounds, suggests that visual inspection of SDS-PAGE gels may not be sufficiently sensitive to identify the target with these probes. Future studies will employ proteomic techniques that offer far greater levels of sensitivity and data resolution, namely stable isotope labeling by amino acids in cell culture (SILAC)[106] and GAS genome phage display library screening.[107] These techniques are further discussed in Chapter 5.

Chapter 4: Biofilm Inhibition SAR Study

Biofilms, Virulence, and Clinical Relevance

The ability to form biofilms is an adaptation common to nearly all bacterial species dating back at least 3.5 billion years.[108] In response to certain environmental stimuli (quorum sensing, colony density, nutrient levels, etc.), bacteria can begin to assemble biofilms on biotic or abiotic solid surfaces by secreting a sticky collection of sugar polymers known as exopolysaccharide (EPS) or glycocalyx, which allows for the permanent attachment of bacterial colonies to the substrate.[109] Once attached, the secretion of additional EPS allows for the growth of the solid-supported colony as well as the recruitment of more planktonic bacteria. By encasing themselves in a semi-permeable matrix, these bacterial cultures essentially trade unrestricted access to nutrients, and thus their capacity for exponential growth, for enhanced protection from environmental threats (e.g. host immune responses, other bacteria, viruses, extreme conditions).[109] As biofilms mature, fluid channels begin to form between cell microcultures to alleviate issues of nutrient starvation and waste removal.[110] Mature biofilms can also disseminate planktonic cells back into the aqueous environment, either through external forces or directly via genetic expression changes, and in this way serve as a reservoir for free-floating colonies to establish biofilms on other solid substrates.[111] These aspects both enhance bacterial colony survival and no doubt led to a strong evolutionary selection for bacteria able to efficiently construct robust biofilms.

The ability for bacteria to form biofilms has important implications for human health. Many biological surfaces open to the environment, such as skin, tooth enamel, and the cornea, are hosts to persistent biofilm colonization of a more benign nature. However, biofilm-embedded colonies that access the bloodstream or internal organs, such as *Pseudomonas aeruginosa* colonization of the lungs in cystic fibrosis patients,[112] streptococcal biofilm establishment on platelet aggregates and heart valves,[113] and bacterial invasion of wounds[114] represent a much more serious threat. A number of characteristics of biofilm-mediated infections make them especially hard to clear with antibiotics. The EPS matrix surrounding biofilm-embedded bacteria

can act as a selectively permeable barrier, sequestering the population within from several aspects of the surrounding aqueous environment, including leukocytes and antibiotics. Depending on the nature of the biofilm and the antibiotic agent, up to 1000-fold greater effective resistance against some antibiotics has been observed.[115,116] Sequestration from the surrounding environment has the added effect of restricting nutrient levels within the biofilm, slowing bacterial growth and inducing physiological stress responses that further decrease susceptibility to exogenous factors.[117,118] Bacteria fixed within a biofilm, by virtue of greatly enhanced proximity between cells, also display enhanced lateral gene transfer, increasing the rate at which antibiotic resistance mechanisms are disseminated within the colony.[119] The recalcitrant nature of biofilm-embedded bacterial colonies, combined with their ability to shed cells into the aqueous environment and maintain systemic infection, makes them particularly challenging to control. It is estimated that up to 65% of serious nosocomial (hospital-acquired) infections are biofilm-mediated,[120] underscoring anti-biofilm agents as an area of unmet medical need. Biofilm formation is a particularly dire issue in the field of prosthetic implantation, prompting a regimen of very high doses of one or more antibiotics before and after the installation of internal prosthetics.[121]

Early in the course of our investigation into GAS-SK inhibitors, a gene expression array suggested that our lead compounds reduced transcription levels of several key virulence factors, including those associated with host substrate colonization and the initiation of biofilm formation.[45] Although GAS can form biofilms during systemic infection,[122] we sought to assess the broad-spectrum utility of our compounds by assaying for biofilm inhibition in more clinically relevant bacterial species. *Staphylococcus aureus* and *Staphylococcus epidermidis* have been identified as two of the most important species involved in biofilm-mediated systemic infection.[123,124] *S. epidermidis* is able to effectively colonize hydrophobic synthetic surfaces, and as a result is the most common pathogen associated with prosthetic-acquired systemic infections.[125,126] Genome sequencing has shown that outside of exotoxin β-hemolysin, *S. epidermidis* relies almost exclusively on biofilm-associated mechanisms for virulence.[127] *S. aureus* is recognized as one of the most serious threats to human health,[128] with its multiple vectors of virulence and a propensity to quickly develop antibiotic resistance.[129] *S. aureus* is also known to cause serious prosthesis-acquired infections, especially when introduced to the bloodstream via blood vessel catheters.[130] We have chosen to focus our medicinal chemistry

study on developing biofilm inhibitors effective in these species based on the unmet medical need associated with prosthesis-acquired infection.

Biofilm Inhibition Assay

Assaying for biofilm inhibition is based on an established protocol with a straightforward readout of inhibitor effectiveness (OD).[131] Briefly, bacterial colonies are grown in polystyrene 96-well plates in the presence of various test compounds or DMSO (negative control). The plate is incubated at 37°C for 16 hours, then an optical density measurement (OD_{600}) is made to gauge the effect of test compounds on general bacterial growth. Planktonic cells are removed by gentle washing, leaving only surface-associated bacteria behind. The biofilm is stained with crystal violet, and excess dye is washed away before anchored colonies are re-solubilized with detergent. Reading OD_{595} of the solubilized and stained biofilm colonies allows for the quantification of biofilm formation in test wells relative to controls treated only with DMSO. In keeping with our focus on developing antibiotics that minimize the induction of evolved resistance, we were interested in identifying compounds that potently inhibit biofilm formation without significantly affecting colony growth. The ease of testing compounds for anti-biofilm activity represents a significant improvement over the time consuming, inconsistent, and somewhat indirect nature of the GAS-SK activity assay.

Scheme 4.1. Structure of 6 active compounds identified from the original 100 µM screen of GAS-SK inhibitors for anti-biofilm activity.

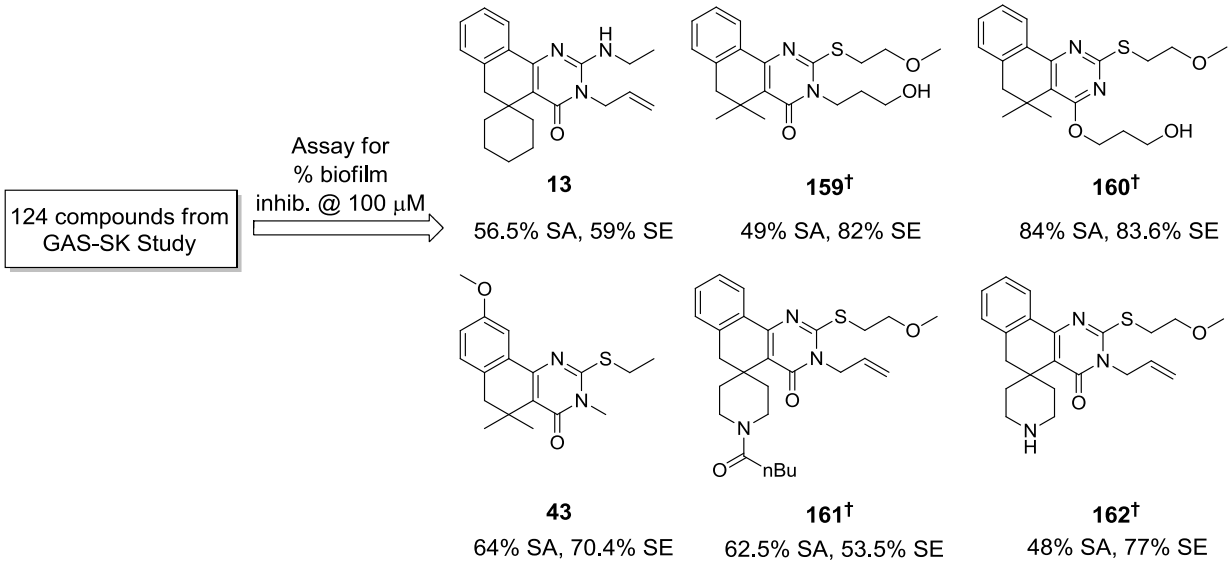

†Compound originally synthesized by W.G. Rajeswaran.

Initial Biofilm Inhibitor Screen

An initial screen for inhibitors of *Staphylococcus* biofilm formation was performed using the 124 compound SAR set based on the structure of **1**. All compounds were originally tested at a concentration of 100 μM to speed up the identification of hits. We were particularly interested in finding compounds potent in both *Staphylococcus* strains in order to maximize our chances of eventually developing a broadly active anti-biofilm compound. This initial screen revealed that 21 compounds (17%) were able to inhibit biofilm in *S. aureus* >50% at this concentration, while 8 (7%) were over 50% active in *S. epidermidis.* A total of 6 compounds overlapped between these data sets (Scheme 4.1): spiropiperidine analogs **159** and **160**, *n*-propanol-substituted amides **161** and **162**, and compound **43** identified during the metabolic attenuation study (Chapter 2). Although aminoethyl compound **13** also showed good activity in *S. epidermidis*, it was unacceptably toxic (35% growth inhib.) in *S. aureus* and was not followed up on in the biofilm study. We were gratified to see the activity of *O*-alkylated compound **160** in both strains, given the increased metabolic competence of this substitution pattern. This subset of active compounds is considerably more narrow than what is observed in the GAS-SK study, in which 68 compounds (55%) were capable of inhibition greater than 50% at the highest concentration tested (50 μM). We hypothesized that this smaller subset of active compounds should allow us to make more informed decisions regarding the efficient expansion of the SAR effort.

Figure 4.1. Inhibition of *S. aureus* biofilm formation on silicone wafers in the presence of increasing concentrations of CCG-203592 (31), as reported by Ma, *et al. PLoS One 2012*, e47255.

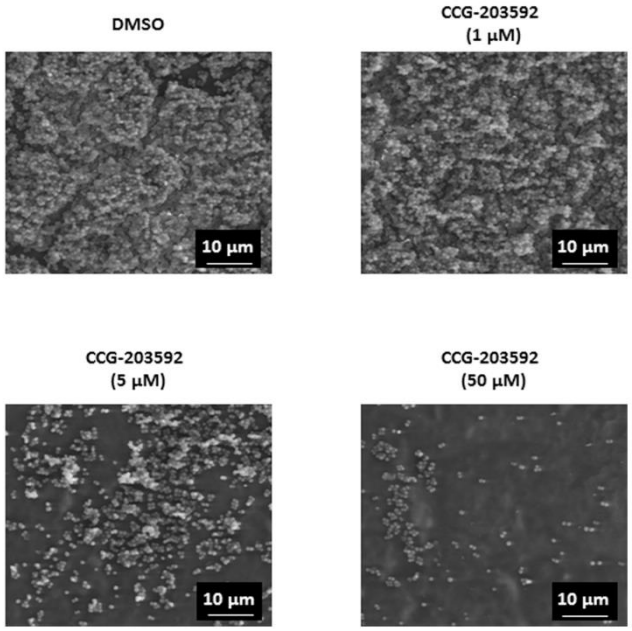

During the course of the biofilm activity re-screen, analog CCG-203592 (**31**) was identified as one of the most consistently potent compounds in *S. aureus*. A more in-depth study of **31**'s effects in *S. aureus* performed by Hongmin Sun and coworkers demonstrated the ability of this compound to inhibit biofilm formation with an IC_{50} of 2.4 ± 0.1 μM in virulent lab strain RN6390.[132] Other experiments performed during this study also indicated its ability to inhibit biofilm formation in clinically-important *S. aureus* strains, both in polystyrene test wells and on medical-grade silicone (Figure 4.1). Furthermore, **31** was shown to induce the down-regulation of several genes important for *S. aureus* biofilm formation and virulence, including fibronectin-, laminin-, and collagen-binding proteins that assist in anchoring GAS to host tissues. This finding reinforces the hypothesis that the target of these compounds is an upstream regulator of bacterial virulence. Although this compound exhibited no anti-biofilm effect in *S. epidermidis*, its structural features were taken into account during the SAR expansion study.

The promising results of these initial efforts prompted both the undertaking of a new synthetic SAR effort and a push to refine the initial 100 μM screening data. Although activity data at a single, high-concentration data point was helpful to suggest direction to the SAR campaign at first, knowledge of how the compounds behave at lower concentrations was critical

for determining their relative potencies. The limited solubility of most compounds in this series certainly excludes the possibility of each attaining an effective aqueous concentration of 100 µM, muddling the original dataset somewhat. In light of the limitations of a single-point activity determination, it was decided that each compound that was able to inhibit biofilm formation in either bacterial strain by more than 30% at 100 µM would be retested at 5 and 50 µM concentrations to more accurately assess their relative activity levels. Since this study was performed concurrently to SAR expansion, several key structural features of active compounds that have not yet been explored in new analogs.

According to the activity cutoff, 46 compounds were submitted for lower-concentration retesting against *S. aureus*, with a 10-compound subset also retested for activity in *S. epidermidis*. Of these, 19 were found to inhibit *S. aureus* biofilm by 50% or greater at a concentration of 50 µM, while only one, **31**, achieved >50% inhibition at 5 µM. None of the compounds tested were able to inhibit *S. epidermidis* biofilm >50% at 5 or 50 µM. A summary of the more-potent *S. aureus* biofilm inhibitors is included in Table 4.1. The aryl methyl ether analogs **31-33**, among the best compounds identified in the GAS-SK study, also showed good activity against *S. aureus* biofilms. Interestingly, analogs with polar pyrimidinone substitution (e.g. **20**, **42**, **159**, **160**, **163-165**) or more polar appendages adorning the phenyl ring (**166-169**), displayed relatively good potency against biofilm despite low activity in GAS. Compounds **159**, **160**, and **43** identified as active in both species in the 100 µM screen retained activity at lower concentrations in *S. aureus*, while **13**, **161**, and **162** did not. The moderate activity of **160** and **164** bolstered our hopes of synthesizing potent and metabolically stable *O*-alkyl amides. Compound **51** stands out as a good inhibitor of *S. aureus* biofilm with somewhat increased metabolic stability. Interestingly, compound **30** appears to be only weakly active in this assay, despite differing from potent compound **31** by only one carbon (*S*-allyl vs. *S*-ethyl).

Table 4.1. Activity of GAS-SK inhibitor analogs found to be particularly potent against *S. aureus* biofilm formation.

A **B** **C**

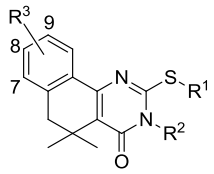
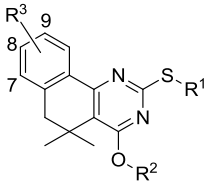
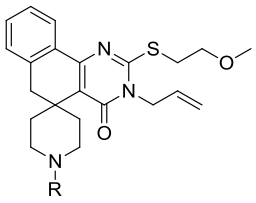

#	Scaffold	R^1	R^2	R^3	SA 5 μM[a]	SA 50 μM[a]	IC_{50} (μM)[b]
20[1]	A	$HOCH_2CH_2$	Allyl	H	0.97 ± 0.03	0.32 ± 0.07	>50
21	A	$NCCH_2$	Allyl	H	1.08 ± 0.00	0.69 ± 0.09	nd
30[2]	A	Allyl	Allyl	8-MeO	0.72 ± 0.13	0.56 ± 0.15	>50
31	A	Et	Allyl	8-MeO	0.37 ± 0.03	0.26 ± 0.03	1.4 ± 0.4
32	A	Et	Allyl	9-MeO	0.72 ± 0.09	0.21 ± 0.08	5.2 ± 0.4
33	A	Et	Allyl	7-MeO	0.61 ± 0.06	0.31 ± 0.01	2.7 ± 0.4
41	A	$CH_3OCH_2CH_2$	Et	H	0.99 ± 0.01	0.44 ± 0.22	nd
42	A	Et	$CH_3OCH_2CH_2$	H	0.84 ± 0.01	0.31 ± 0.08	8.7 ± 0.9
43	A	Et	Me	9-MeO	0.81 ± 0.10	0.28 ± 0.14	4.3 ± 0.6
51	A	F_3CCH_2	Allyl	9-MeO	0.80 ± 0.04	0.33 ± 0.04	2.9 ± 0.4
63	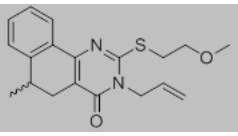				0.94 ± 0.00	0.39 ± 0.01	35.0 ± 7.4
159[3]	A	$CH_3OCH_2CH_2$	$HO(CH_2)_3$	H	0.90 ± 0.00	0.49 ± 0.14	41.6 ± 4.5
160[3]	B	$CH_3OCH_2CH_2$	$HO(CH_2)_3$	H	0.83 ± 0.05	0.18 ± 0.12	14.1± 2.5
161[3]	C	R = CONHBu			1.04 ± 0.13	0.74 ± 0.01	nd
162[3]	C	R = H			0.99 ± 0.10	0.87 ± 0.07	nd
163[3]	A	$CH_3OCH_2CH_2$	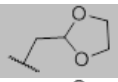	H	0.85 ± 0.07	0.41 ± 0.09	42 ± 8.5
164[3]	B	$CH_3OCH_2CH_2$	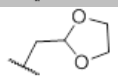	H	0.76 ± 0.15	0.52 ± 0.11	nd
165[3]	A	$CH_3OCH_2CH_2$	$NC(CH_2)_3$	H	0.92 ± 0.00	0.43 ± 0.04	>50
166[2]	A	Et	Allyl	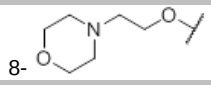	0.75 ± 0.16	0.36 ± 0.06	9.2 ± 1.3
167[2]	A	Et	Allyl	8-HO_2CCH_2O	1.04 ± 0.01	0.50 ± 0.01	43.7 ± 1.4
168[4]	A	$CH_3OCH_2CH_2$	Allyl	8-MeO_2C	0.64 ± 0.29	0.45 ± 0.13	7.4 ± 5.0
169[4]	A	$CH_3OCH_2CH_2$	Allyl	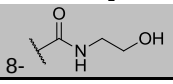	0.86 ± 0.09	0.39 ± 0.02	13.4 ± 5.3

[1]Synthesized by Meghan Breen. [2]Synthesized by Roderick Sorenson. [3]Synthesized by Dr. Walajapet Rajeswaran. [4]Synthesized by Michael Wilson. [a]Ratio of *S. aureus* biofilm formation by *S. aureus* cultures in the presence of the indicated concentration of test compound compared to DMSO control. [b]Half-maximal inhibitory concentrations against biofilm formation in the presence of the indicated compound, calculated from 6-point dose-response curve from 0.15 μM to 50 μM. nd = not determined.

Alternative Scaffold Screening

In addition to the scaffold based on compound **1**, our collaborators in the Sun group also screened the compounds originally purchased for the Broad Institute HTS follow-up in the GAS-SK study (Chapter 2). Compounds were screened at 100 µM, and only compounds potently inhibiting both *S. aureus* and *S. epidermidis* were considered. Of the 53 total compounds screened, 20 compounds inhibited biofilm by more than 30% in *S. aureus*, 4 of which by 50% or more. In contrast, only chromenone **170** (Scheme 4.2) was active in *S. epidermidis*, inhibiting biofilm formation by 40%. Luckily, this compound was also found to be active in *S. aureus* (46% inhibition at 50 µM). With only one compound meeting our criteria from the alternative scaffold screen, we purchased 17 analogs of **170** from commercial sources conforming to the general methylpiperidine-chromenone scaffold **171**. Unfortunately, none of the compounds were found to be active at 5 and 50 uM concentrations, including **170** itself. The lack of strong activity at low concentrations led us to abandon the alternative scaffold development aspect of the anti-biofilm study.

Scheme 4.2. Structure of alternative scaffold hit 170 and 17 related analogs of general structure 171.

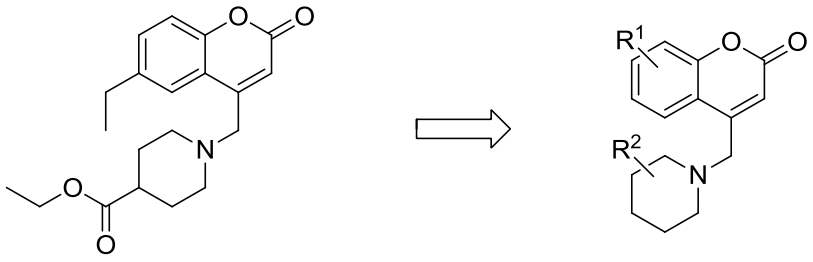

170 **171**

SAR Logic

The failure of the alternative scaffold screen led us to propose a number of new analogs of **1** optimized for anti-biofilm activity. We envisioned combining the salient features of several of the active compounds in the hope of generating compounds with synergistic gains in activity and/or pharmacokinetic competence. Specifically, we planned the incorporation of more polar substitution at the pyrimidinone (*n*-propanol, acetonitrile) and phenyl positions (larger aryl ethers), and installing a spiropiperidine ring in place of the gem-dimethyl group on the central

ring. Although **161** and **162** (Table 4.1) did not show particularly potent activity at less than 100 μM, the amine functionality of piperidine was incorporated to add an easily derivatized polar group in an otherwise lipophilic and difficult to functionalize region of the scaffold, allowing us to survey a wider range of substitutions and chemical space with our analogs.

Synthesis

Compared to the SAR effort in the GAS-SK project, the chemistry involved to generate analogs for the biofilm study was more streamlined. *N*-Boc-protected spiropiperidine analogs **177-189** were accessed through Scheme 4.3. Synthesis began with the Horner-Wadsworth-Emmons method of forming the α,β unsaturated ester **173** from 4-oxo-*N*-Boc piperidine **172**. This ester was employed as the Michael acceptor for the LDA and zinc iodide-mediated cyclization reaction with the methoxytolunitrile **26c**, generating β-aminoesters **174**.[55] Stepwise cyclization with benzoyl isothiocyanate followed by KOH afforded the unsubstituted 2-thioxopyrimidinone **175**.[57] Finally, stepwise chemoselective alkylation of sulfur followed by the *N*- or *O*- position of the amide was accomplished to generate Boc-substituted final compounds **177-189**.

Scheme 4.3. Synthesis of *N*-Boc spiropiperidine analogs 177-189.[a]

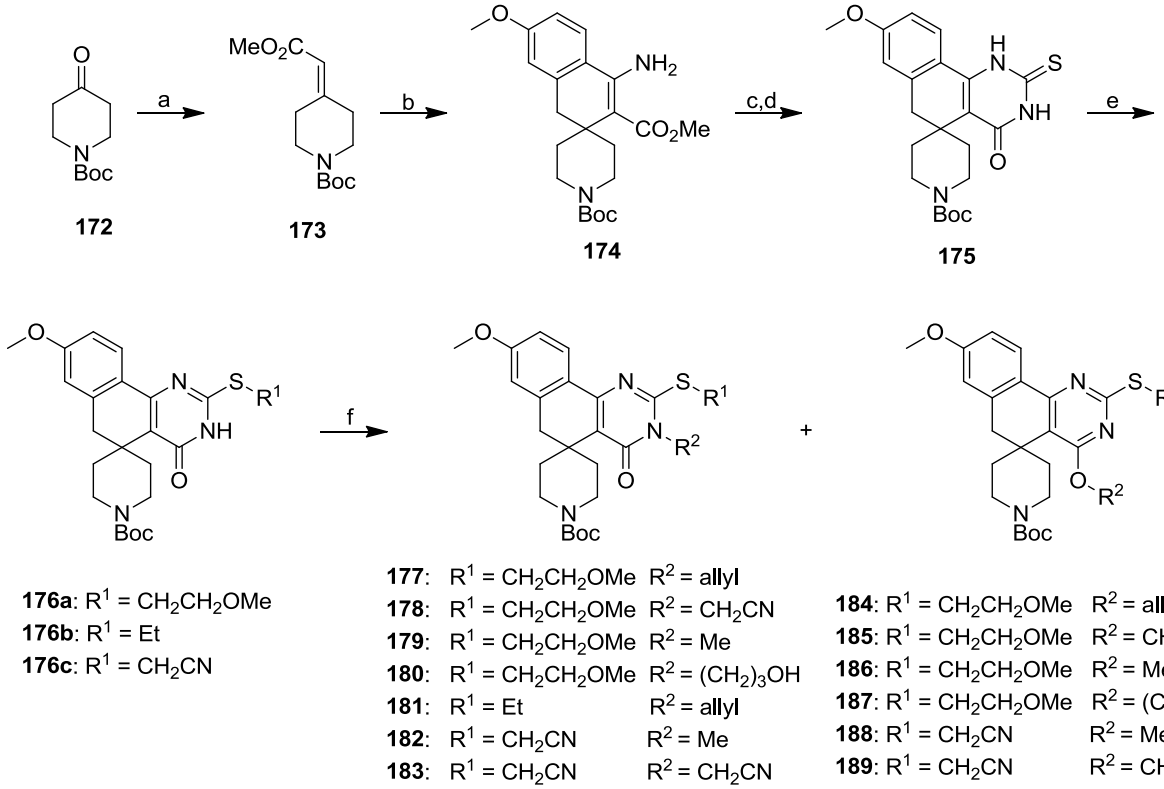

[a]Reagents and conditions: a) NaH, trimethyl phosphonoacetate, DMF, 0°C, 30 min; then **172**, 0°C-RT, 3h, 99%; b) LDA, **26c**, -78°C, diglyme, 1h, then **173**, ZnI_2, -78°C-RT, 2h, 74%; c) benzoyl isothiocyanate, EtOH, reflux, 6h, 65%; d) KOH, EtOH:H_2O (2:1), 70°C, 2h, 83%; e) R^1-X, $NaHCO_3$, DMF, 50-70°C, 16h, 63-81%; f) R^2-X, base, DMF, 50-70°C, 3-16h, 11-51%.

Derivatization of the piperidine portion of the molecule was originally attempted with compounds **177**, **181**, and **184** (Scheme 4.4). Boc deprotection was effected using 4M HCl in dioxane, which led to the near-instant precipitation of crystalline products **190-192** from the organic solution. To mimic the structure of active compound **161**, functionalization of the secondary amines with valeryl chloride yielded tertiary amides **193-195**. All of these compounds were submitted for biological testing with the exception of **192**, which rapidly decomposed in polar solvents via loss of allyl substitution at the *O*-position. The preparation of this compound as a hydrochloride salt may have allowed the chloride ion to nucleophilically cleave the *O*-allyl group under sufficiently polar conditions. However, the general instability of several similar compounds in this series bearing basic amines, even when prepared in the absence of other

nucleophiles or acid catalysis, may suggest the innate instability of these compounds mediated by the amine itself. This hypothesis is supported by the observation that the amidation of **192** without isolation proceeded smoothly, and resulting compound **195** showed no signs of instability.

Scheme 4.4. Synthesis of free amines 190-192 and pentanoyl amide derivatives 193-195.[a]

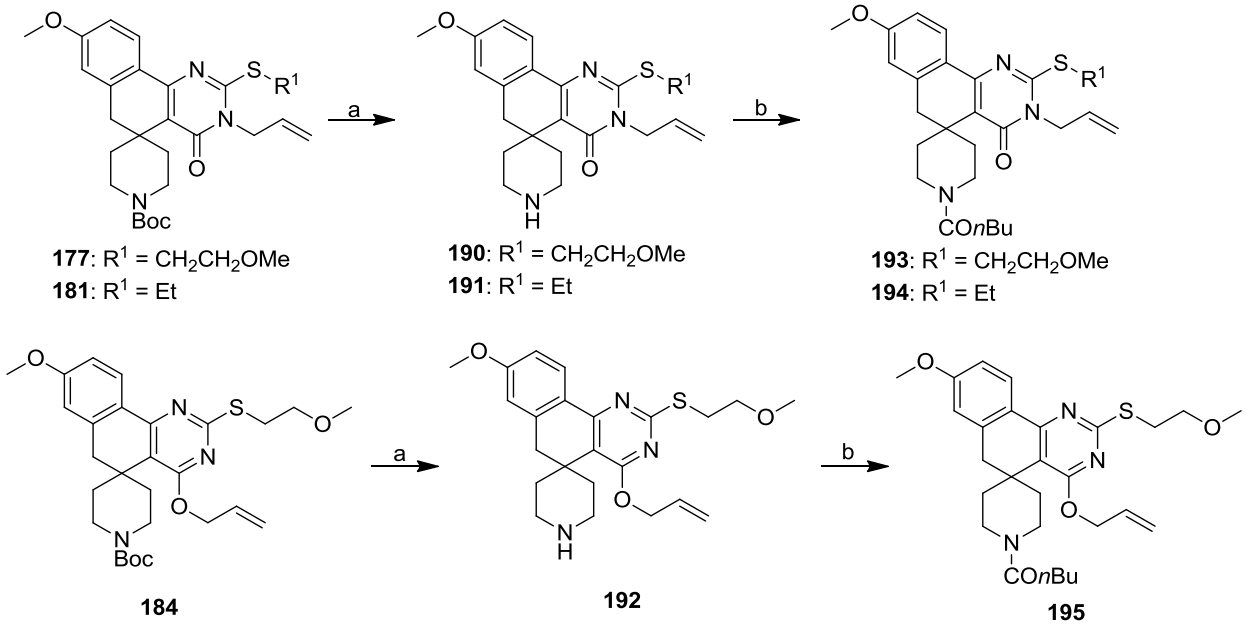

[a]Reagents and conditions: a) 4M HCl-dioxane, 0°C-RT, 2h, 78-100%; b) valeryl chloride, DIPEA, DCM, 0°C-RT, 3h, 63-74%.

Free amine **190** was further derivatized into several other nitrogen-containing functional groups using one of three one-step procedures (Scheme 4.5). Tertiary amines **196** and **197** were synthesized by reductive amination using sodium cyanoborohydride and the corresponding aldehyde.[133,134] Urea-containing compounds **198**-**200** were obtained via treatment with the corresponding carbamates under basic conditions. Finally, chiral amides **201**-**202** were synthesized using amide coupling conditions (HOBt, EDC, tertiary amine base).

Scheme 4.5. Synthesis of spiropiperidine derivatives 196-202. [a]

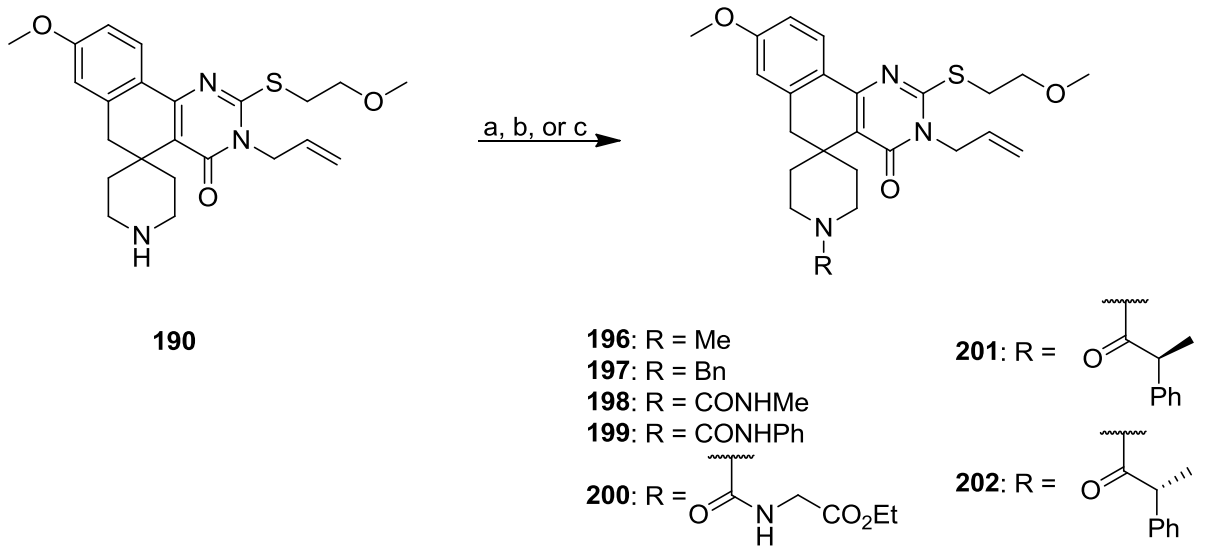

[a]Reagents and conditions: a) HCHO or PhCHO, AcOH, $NaBH(OAc)_3$, DCE, 16h, RT, 57-63%; b) R-NCO or R-NHCO-OSu, DIPEA, DCM, RT, 6h, 65-83%; c) (*R*)- or (*S*)-2-phenyl propanoic acid, DIPEA, HOBt, EDC, DCM, RT, 16h, 67-78%.

Based on the successful derivatization of **190**, we sought to generate the secondary amine analogs of the remaining 10 *N*-Boc final compounds. 4M HCl-dioxane was used to generate the original free amines **190-192** as easily handled, crystalline HCl salts, but stability issues were encountered under these conditions with a number of other compounds. We theorized this instability could be attributed to the acid-sensitivity of the nitrile group and formation of imino chlorides. In these cases, a switch to 15-33% TFA:DCM solutions for deprotection conferred greater stability due to the non-nucleophilic nature of the TFA conjugate base. In the cases where TFA deprotection failed, a mildly basic method employing TMS-OTf and triethylamine offered an alternative mechanism of deprotection[135] at the cost of necessitating purification by flash chromatography. Even so, only five of the 10 possible free NH compounds (**203-207**, Scheme 4.6) were sufficiently stable for characterization and use in the biofilm assay.

Scheme 4.6. Synthesis of free secondary amines 203-207.[a]

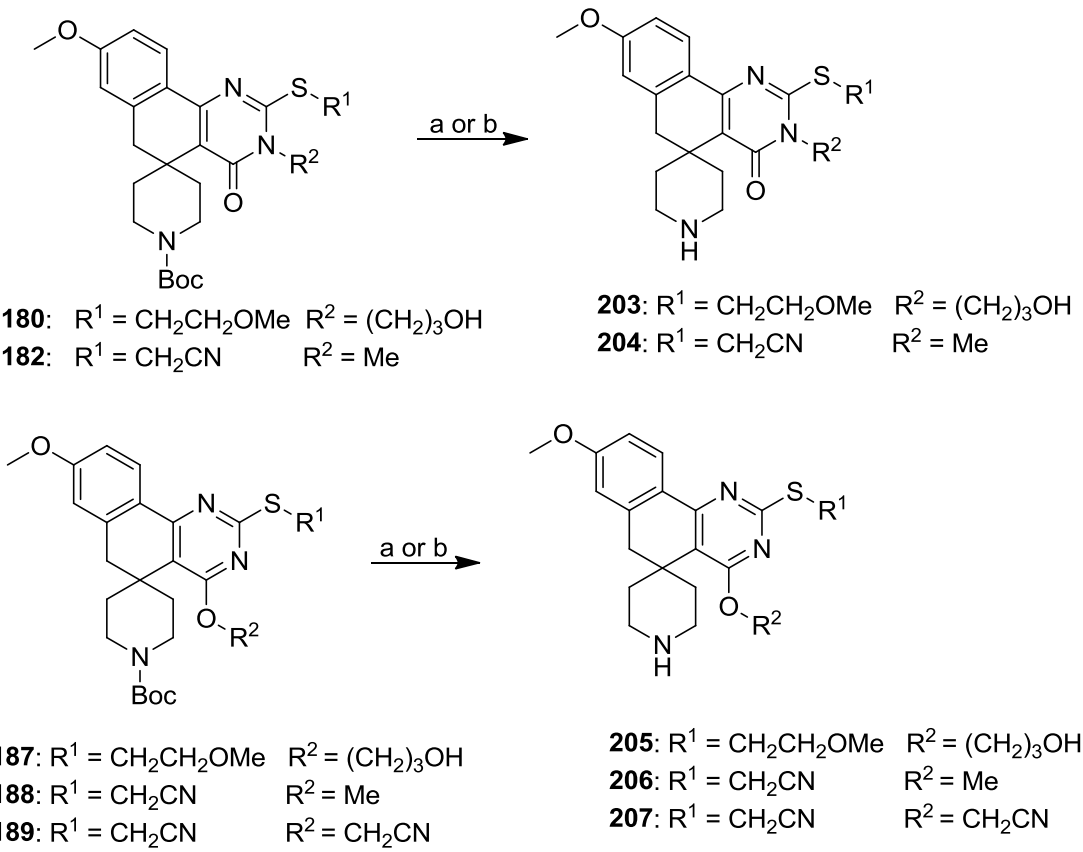

180: $R^1 = CH_2CH_2OMe$ $R^2 = (CH_2)_3OH$
182: $R^1 = CH_2CN$ $R^2 = Me$

203: $R^1 = CH_2CH_2OMe$ $R^2 = (CH_2)_3OH$
204: $R^1 = CH_2CN$ $R^2 = Me$

187: $R^1 = CH_2CH_2OMe$ $R^2 = (CH_2)_3OH$
188: $R^1 = CH_2CN$ $R^2 = Me$
189: $R^1 = CH_2CN$ $R^2 = CH_2CN$

205: $R^1 = CH_2CH_2OMe$ $R^2 = (CH_2)_3OH$
206: $R^1 = CH_2CN$ $R^2 = Me$
207: $R^1 = CH_2CN$ $R^2 = CH_2CN$

[a]Reagents and conditions: a) DCM:TFA (2-4:1), 0°C-RT, 4h, 63-90%; b) TMS-OTf, 2,6-lutidine, DCM, 0°C, 30 min, 56-100%.

The ongoing collection and refinement of SAR data prompted us to revisit the synthesis of several new gem-dimethyl analogs as well (Scheme 4.7). These compounds were synthesized in the same manner as the *N*- and *O*- alkylated amides **46**-**50** discussed in Chapter 2, beginning from unsubstituted 2-thioxopyrimidinone **44b**.

Scheme 4.7. Synthesis of additional gem-dimethyl analogs with decreased lipophilicity 209-215.[a]

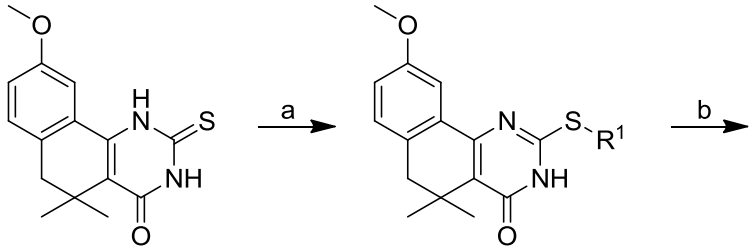

44b

45b: R^1 = Et
208a: R^1 = CH_2CF_3
208b: R^1 = CH_2CN

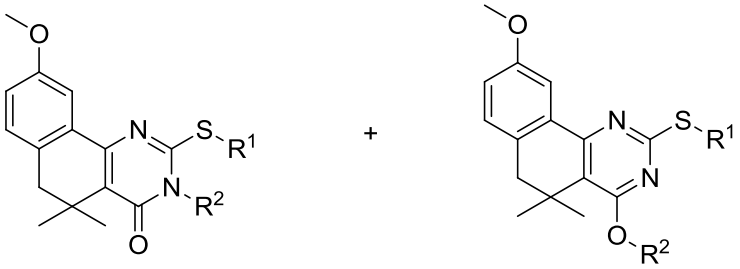

209: R^1 = Et, R^2 = CH_2CN
210: R^1 = CH_2CF_3, R^2 = Me
211: R^1 = R^2 = CH_2CN

212: R^1 = Et, R^2 = CH_2CN
213: R^1 = Et, R^2 = Me
214: R^1 = R^2 = CH_2CN
215: R^1 = CH_2CN, R^2 = allyl

[a]Reagents and conditions: a) R^1-X, $NaHCO_3$, DMF, 50-70°C, 16h, 73-93%; b) R^2-X, base, DMF, 50-70°C, 3-16h, 22-57%.

A synthetic effort to access chirally-substituted compounds was undertaken in order to assess the extent of chiral bias evident in the target-analog interaction. Spiropyrrolidine compounds **221-224** were originally synthesized as racemates to assess their activity before progressing to synthesis of enantiomerically enriched derivatives. The racemic synthesis proceeded adequately as described in Scheme 4.8, using chemistry already established in the generation of spiropiperidines **177-189**. Ultimately, Boc-protected analogs **221** and **222**, as well as their deprotected secondary amine counterparts **223** and **224**, were submitted for biological testing.

Scheme 4.8. Synthesis of racemic spiropyrrolidine compounds 221-224.[a]

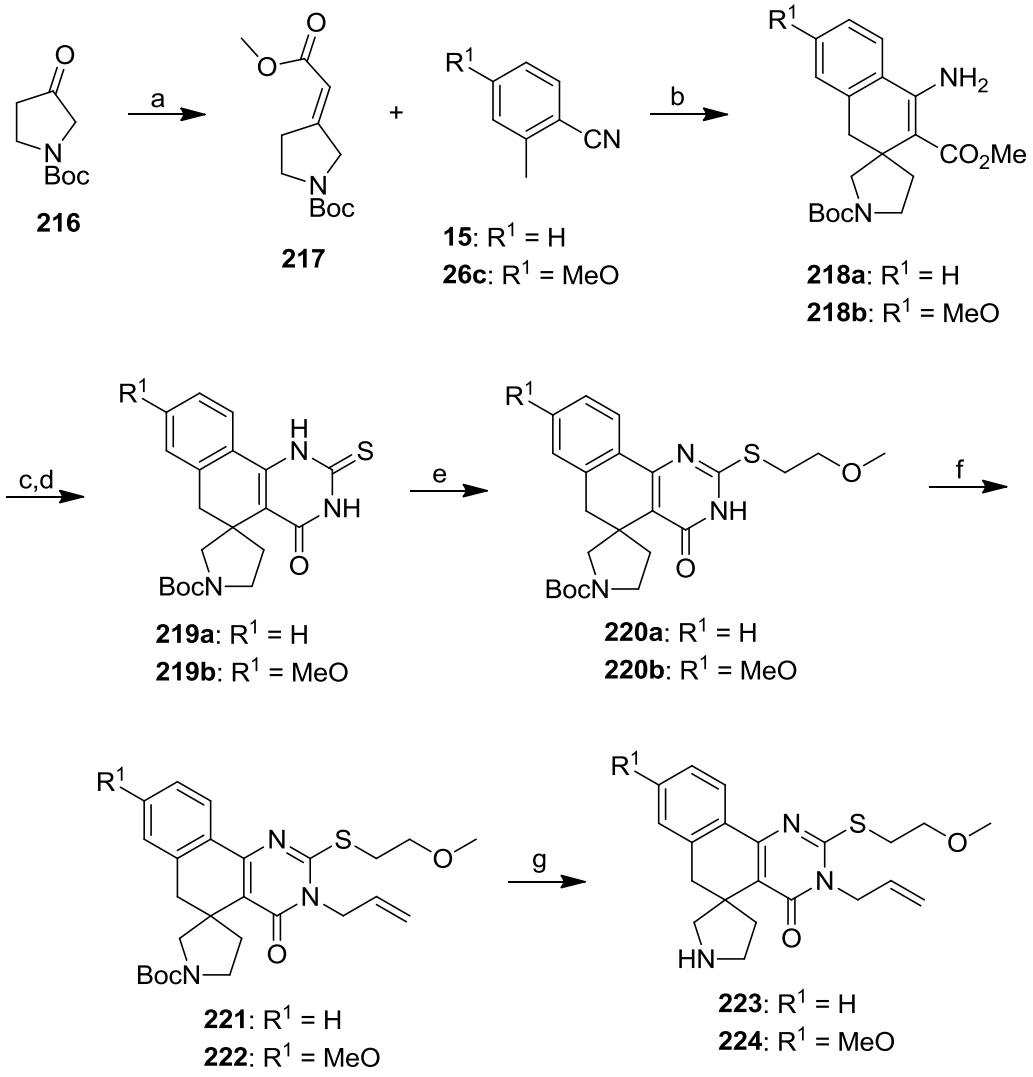

[a]Reagents and conditions: a) NaH, trimethyl phosphonoacetate, DMF, 0°C; then **216**, 0°C-RT, 3h, 82%; b) LDA, **217**, diglyme, -78°C, 1h; then **15** or **26c**, ZnI_2, -78°C-RT, 2h, 20-25%; c) benzoyl isothiocyanate, EtOH, reflux, 6h; d) KOH, EtOH:H_2O (2:1), reflux, 2h, 49-68% over 2 steps; e) $MeOCH_2CH_2OTs$, $NaHCO_3$, DMF, 70°C, 16h, 50-91%; f) allyl bromide, NaOMe, EtOH, 70°C, 16h, 32-42%; g) 4M HCl-dioxane, 0°C-RT, 2h, 77-94%.

The synthesis of the corresponding enantiopure pyrrolidines **231** met with much more synthetic adversity (Scheme 4.9). Since the LDA cyclization is not likely to induce asymmetry at the quaternary carbon, we pursued the functionalization of the pyrrolidine nitrogen with a chiral auxiliary. This chiral auxiliary would have ideally allowed for the separation of diastereomers at some stage of the synthesis, either by flash chromatography or HPLC, then be selectively removed to allow derivatization of the enantiopure compounds. We decided that

chiral α-methylbenzyl amine derivatives could function in this role since they can be removed via treatment with chloroformates.[136] Chiral succinimide **226** was successfully synthesized from DL-malic acid and α-methylbenzylamine, mediated by stepwise additions of acetyl chloride.[137] Pan-reduction of the acetyl group and the succinimide with LAH generated the pyrollidinol, which was oxidized to the ketone under Swern conditions.[138] Horner-Emmons olefination furnished the targeted chiral Michael acceptor. The LDA/ZnI_2 cyclization successfully afforded β-aminoester intermediate **229** as a 3:2 mixture of diastereomers, albeit in low yields. Unfortunately, the diastereomers were not separable at this stage, and it was found that no set of conditions led to the successful installation of the pyrimidinone ring. The synthesis of this class of compounds was shelved at this point to explore more easily accessible chiral analogs.

Scheme 4.9. Attempted synthesis of chiral spiropyrrolidine analogs 231 via diasteromeric functionalization.[a]

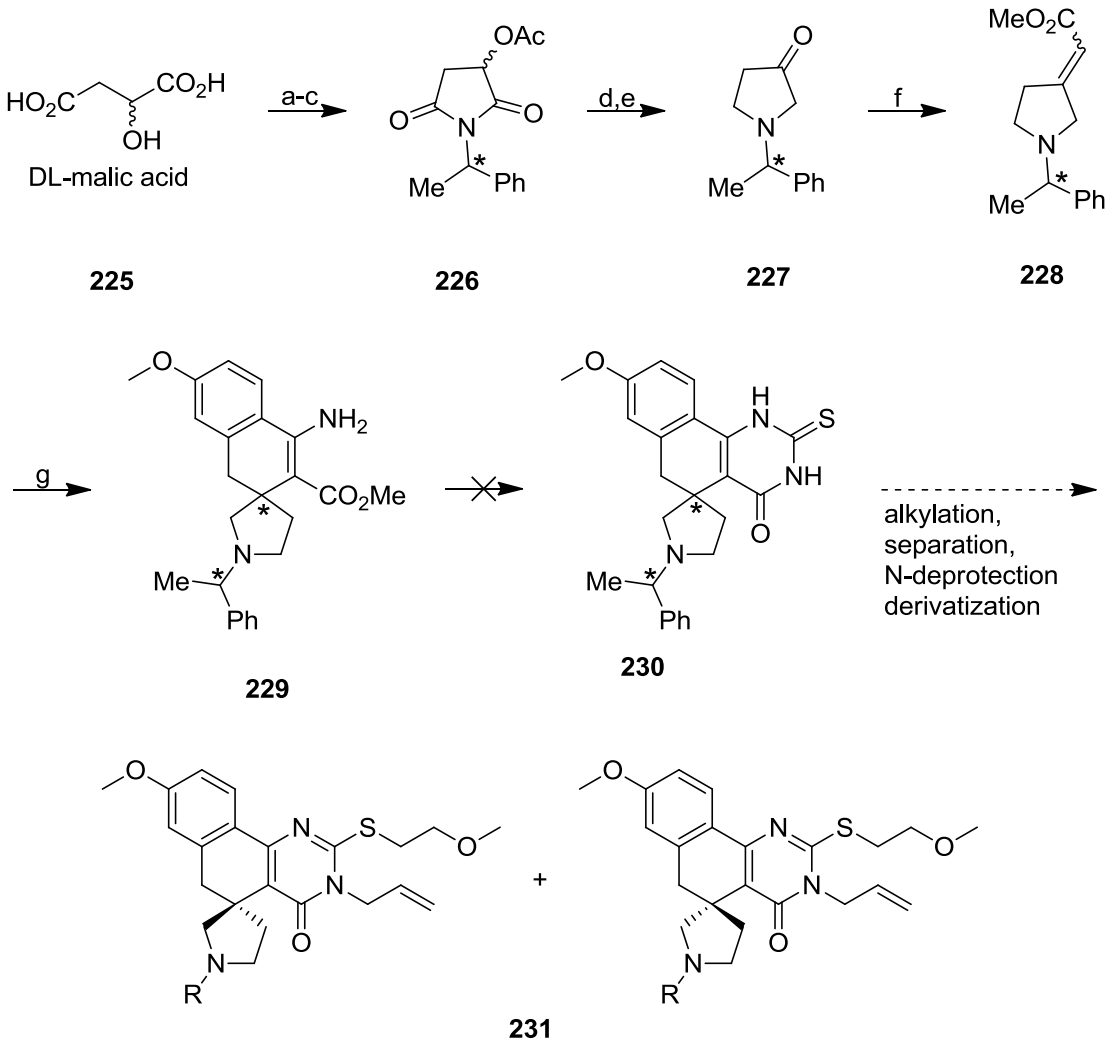

[a]Reagents and conditions: a) AcCl, reflux, 3h; b) (*S*)-α-methylbenzylamine, THF, RT, 4h; c) AcCl, reflux, 12h, 90% over 3 steps; d) LAH (6.5 eq), THF, 0°C-RT, 6h, 93%; e) oxalyl chloride, DMSO, DCM, -78°C, 10 min; then Et_3N, -78°C, 1h, 55%; f) NaH, trimethyl phosphonoacetate, 0°C; then **227**, 0°C-RT, 3h, 100%; g) LDA, **228**, diglyme, -78°C, 1h; then **26c**, ZnI_2, -78°C-RT, 2h, 25%.

Due to the failure of the chiral pyrrolidine series, new chiral analogs were proposed that take advantage of later-stage chiral derivatization and routes that did not rely on diasteromeric separation for stereoenrichment. The chiral amides (**201** and **202**) were easily accessed by coupling enantiomerically pure 2-phenyl-1-propionic acids to free amine **190** under standard EDC-mediated conditions, as shown in Scheme 4.5.

Scheme 4.10. Synthesis of pentacyclic enantiomer pairs 234-237.[a]

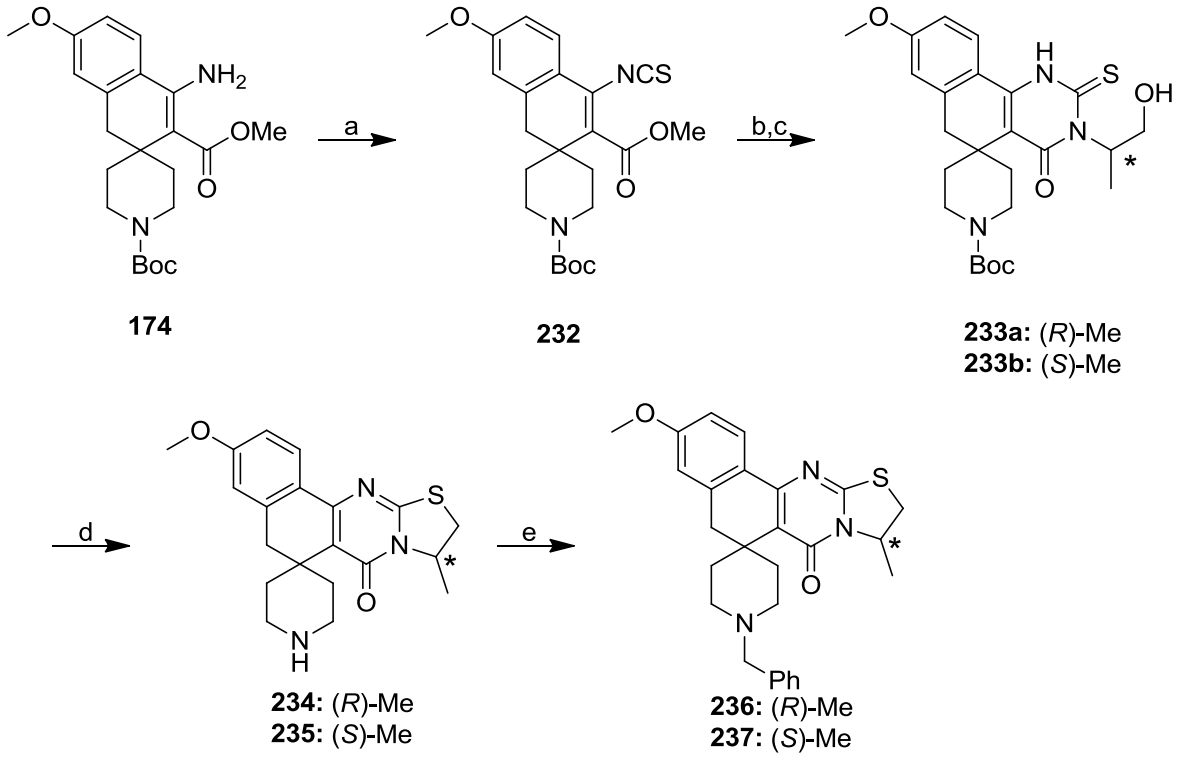

[a]Reagents and conditions: a) thiophosgene, $NaHCO_3$, DCM:H_2O (1.4:1) RT, 3.5h 79%; b) (*R*)- or (*S*)-2-amino-1-propanol, Et_2O, RT, 1h, 91%; c) NaOMe, MeOH, RT, 30 min 92%; d) TFA, DCM, 0°C-RT, 4h, 72-96%; e) Ph-CHO, AcOH, $NaBH(OAc)_3$, DCE, RT, 16h, 48-62%.

The generation of chiral pentacyclic analogs **234-237** (Scheme 4.10) required one significant alteration to the standard scheme. The amine functionality of **174** (Scheme 4.3) was efficiently converted to the isothiocyanate under the action of thiophosgene in DCM, with a layer of aqueous sodium carbonate used as an HCl sink.[139] The resulting β-isothiocyanato ester **232** was found to readily react with amines under neutral conditions. This reactivity was exploited using L- and D-alaninol to form chiral acyclic thiourea adducts that could be isolated via vacuum filtration and cyclized under basic conditions to intermediate **233a** or **233b** in the presence of sodium methoxide. An acid-mediated intramolecular S_N2 reaction assembled the fifth ring with concomitant removal of the Boc group, yielding chiral compounds **234** and **235**.[140] Further derivatization of the piperidine via reductive amination afforded tertiary benzylamine analogs **236** and **237** as well.

The drastically improved efficiency of synthesizing 2-thioxopyrimidinone rings beginning from the β-isothiocyanato ester led us to alter the synthetic strategy used to access chiral diversity at the phenyl ring (Scheme 4.11). Previously synthesized intermediates **140** and **173** were coupled together under standard LDA/ZnI_2 conditions, then the resultant amine **238** was converted to isothiocyanate **239**. Treatment with allylamine followed by sodium methoxide in methanol cleanly afforded the *N*-allyl 2-thioxo-pyrimidinone **240** in excellent yields, and subsequent sulfur alkylation with 2-methoxyethyl tosylate yielded **241**. This intermediate was treated with TBAF to reveal the phenol, which could be chirally substituted via Mitsunobu reaction with 1-phenylethanol in the presence of PPh_3 and DIAD, yielding enantiomer pair **242** and **243**.[141] Unfortunately, removal of the Boc group with TFA caused the concomitant loss of the chiral ether. We suspect that other methods of Boc removal (HCl-dioxane, TMS-OTF + base) would also result in loss of the ether. The resulting phenol **244** was submitted for activity assay nonetheless.

Scheme 4.11. Synthesis of aryl ether enantiomer pair 242 and 243, as well as phenol 244.[a]

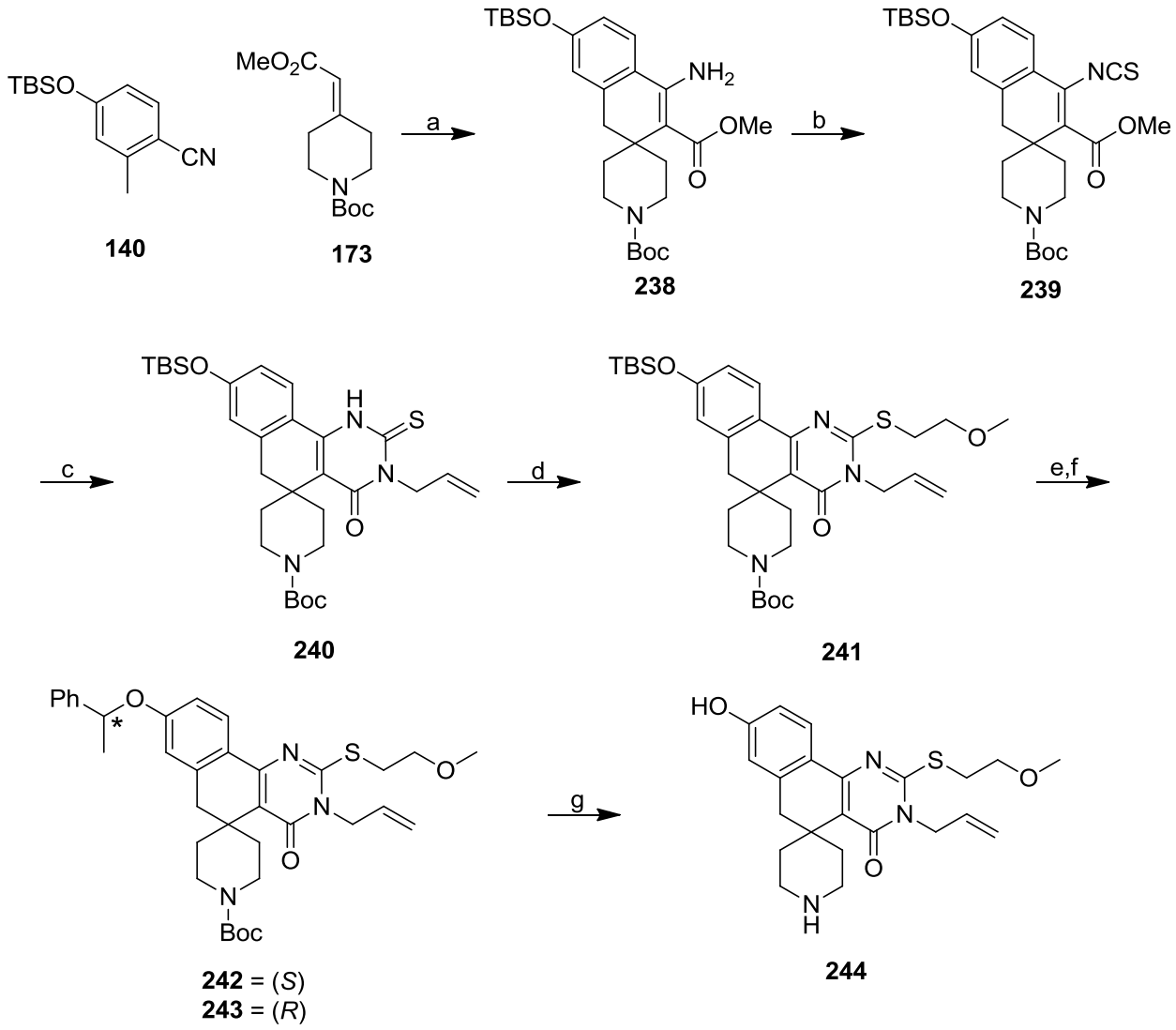

[a]Reagents and conditions: a) LDA, **140**, diglyme, -78°C, 1h; then **173**, ZnI_2, -78°C-RT, 2h, 40%; b) thiophosgene, $NaHCO_3$, DCM:H_2O (1.4:1), RT, 3.5h, 77%; c) allylamine, Et_2O, RT, 1h; then NaOMe, MeOH, RT, 3h, 96%; d) $MeOCH_2CH_2OTs$, Cs_2CO_3, DMF, 70°C, 16h, 49%; e) TBAF, THF, 0°C-RT, 4h, 87%; f) PPh_3, DIAD, (*R*)- or (*S*)-α-methylbenzyl alcohol, 0°C, 2h; then RT, 16h, 43-52%; g) TFA (4 eq.) DCM, 0°C-RT, 3h, 96%.

SAR Discussion

All new analogs for the SAR study were first assessed for their ability to inhibit biofilm in *S. aureus* and *S. epidermidis* relative to control at concentrations of 5 and 50 μM. Compounds that showed satisfactory anti-biofilm activity (>50% inhibition at 50 μM) were selected for full dose-response curve and IC_{50} determination. It is important to note that IC_{50} data was collected

after the completion of the entire 2-point concentration data set, and was thus not available to make SAR decisions until after nearly all of the analogs were synthesized. Therefore, the following section discusses the SAR study in the context of the 2-point concentration data, with interpretation of the IC_{50} data discussed more thoroughly in a later section of this chapter.

The feasibility of incorporating a spiropiperidine into the scaffold was explored with the first set of compounds synthesized, which drew inspiration from aryl ether **31** and spiropiperidines **161** and **162**. The activity data from this set of compounds (Table 4.2) identified several seemingly small changes that had significant effects on their ability to inhibit biofilm. Compounds based on **161** with pentanamide substitution (**193-195)** showed low or no activity in both bacterial strains. Interestingly, Boc-substituted compounds **177** and **181** possess similar and potent activity in *S. aureus*, but only weak activity in *S. epidermidis*. In contrast, piperidine HCl salt **190** was found to be active in both strains at 50 μM, while **191** was acutely bacteriotoxic (>90% growth inhibition at 50 μM). **162** possessed low activity. Considering that these three compounds essentially differ only in the positioning of one or two methoxy groups, this wide variation in activity was quite surprising. *O*-alkylated amides **184** and **195** exhibited little to no activity in either strain. Based on this dataset, we concluded that the pursuit of additional spiropiperidine compounds (both free NH and Boc-substituted) was warranted. Aryl methyl ether substitution was also included in most new analogs given the potency increase observed for **190** vs. **162**.

Table 4.2. Activity of spiropiperidine analogs with varied substitution patterns.

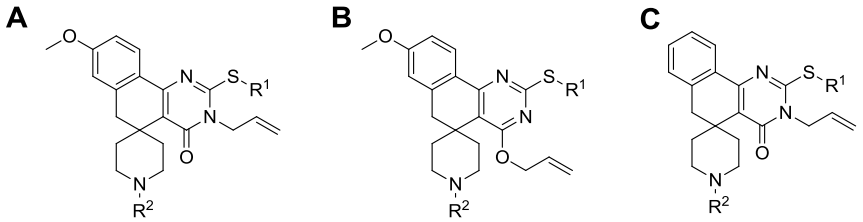

#	Scaffold	R^1	R^2	SA 5 μM[a]	SA 50 μM[a]	SA IC_{50} (μM)[b]	SE 5 μM[c]	SE 50 μM[c]
177	A	$CH_3OCH_2CH_2$	Boc	0.44 ± 0.06	0.72 ± 0.14	>50	0.75 ± 0.05	0.82 ± 0.16
181	A	Et	Boc	0.58 ± 0.07	0.58 ± 0.09	1.8 ± 0.7[3]	0.70 ± 0.04	0.78 ± 0.02
184	B	$CH_3OCH_2CH_2$	Boc	0.91 ± 0.21	1.03 ± 0.31		0.98 ± 0.10	0.90 ± 0.19
190	A	$CH_3OCH_2CH_2$	H	0.94 ± 0.06	0.41 ± 0.20	>50	1.01 ± 0.05	0.17 ± 0.05
191[1]	A	Et	H	0.97 ± 0.12	0.04 ± 0.01		0.87 ± 0.01	0.07 ± 0.04
193	A	$CH_3OCH_2CH_2$	CO*n*Bu	0.94 ± 0.15	1.24 ± 0.34		0.95 ± 0.13	1.07 ± 0.09
194	A	Et	CO*n*Bu	0.98 ± 0.02	1.04 ± 0.15		0.91 ± 0.02	1.12 ± 0.10
195	B	$CH_3OCH_2CH_2$	CO*n*Bu	0.85 ± 0.22	0.78 ± 0.16		1.01 ± 0.18	0.93 ± 0.20
161[2]	C	$CH_3OCH_2CH_2$	CO*n*Bu	1.04 ± 0.13	0.74 ± 0.01		0.78 ± 0.01	0.87 ± 0.01
162[2]	C	$CH_3OCH_2CH_2$	H	0.99 ± 0.10	0.87 ± 0.07		0.81 ± 0.08	0.62 ± 0.42

[a] Ratio of *S. aureus* biofilm formation by *S. aureus* cultures in the presence of the indicated concentration of test compound compared to DMSO control. [b] Half-maximal inhibitory concentrations against biofilm formation in the presence of the indicated compound, calculated from 6-point dose-response curve from 0.15 μM to 50 μM. [c] Ratio of *S. epidermidis* biofilm formation by *S. aureus* cultures in the presence of the indicated concentration of test compound compared to DMSO control. [1]Compound **191** induced acute bacteriotoxicity in both strains (>90% growth inhibition at 50 μM). [2]Synthesized by W.G. Rajeswaran. [3]IC_{50} curve indicates high potency but low efficacy (~35% max biofilm inhibition) for **181**.

Based on structural insights gleaned from the first set of biofilm analogs, we assessed diversity at the piperidine nitrogen using **190** as our reference compound (Table 4.3). Tertiary benzylamine **197** was equipotent to **190** against *S. aureus*, but significant variability in *S. epidermidis* implied that a considerable amount of activity had been lost. In response to the loss of activity exhibited by amide compounds (**193-195**), we generated three ureas of varying bulk and polarity. While the methyl (**198**) and phenyl (**199**) ureas were both found to be only weakly active, ethyl ester compound **200** was able to demonstrate modest activity against *S. aureus* biofilm. Compound **244**, an analog of **190** with an unmasked phenol, showed moderate but variable activity against *S. aureus*.

Table 4.3. Activity data for compounds with varied piperidine *N*-substitutions and phenol compound 244.

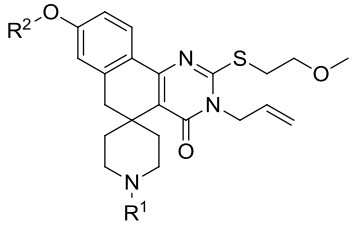

#	R^1	R^2	SA 5 μM[a]	SA 50 μM[a]	SA IC_{50} (μM)[b]	SE 5 μM[c]	SE 50 μM[c]
196	Me	Me	0.95 ± 0.13	0.83 ± 0.32	>50	0.93 ± 0.11	0.86 ± 0.15
197	Bn	Me	0.92 ± 0.27	0.37 ± 0.11	>50	0.96 ± 0.16	0.57 ± 0.29
198	CONHMe	Me	1.16 ± 0.05	0.68 ± 0.06		1.14 ± 0.23	1.02 ± 0.23
199	CONHPh	Me	1.11 ± 0.07	0.92 ± 0.07		0.93 ± 0.08	0.83 ± 0.10
200	$CONHCH_2CO_2Et$	Me	1.06 ± 0.09	0.48 ± 0.13		0.98 ± 0.14	0.81 ± 0.18
244	H	H	0.99 ± 0.03	0.59 ± 0.20		nd	nd
190	H	Me	0.94 ± 0.06	0.41 ± 0.20	>50	1.01 ± 0.05	0.17 ± 0.05

[a] Ratio of *S. aureus* biofilm formation by *S. aureus* cultures in the presence of the indicated concentration of test compound compared to DMSO control. [b] Half-maximal inhibitory concentrations against biofilm formation in the presence of the indicated compound, calculated from 6-point dose-response curve from 0.15 μM to 50 μM. [c] Ratio of *S. epidermidis* biofilm formation by *S. aureus* cultures in the presence of the indicated concentration of test compound compared to DMSO control.

Although **190** showed good activity in both test strains at 50 μM, the diversity of sulfur and amide substitutions in active compounds from the GAS-SK series suggested we may be able to install more polar functionality at these positions while retaining or improving activity. Higher polarity (lower cLogP) should enhance the aqueous solubility of this otherwise highly hydrophobic series and potentially decrease the scaffold's susceptibility to oxidation by P450s. Furthermore, as previously observed in the GAS-SK study, compounds alkylated at the *O*-position of the pyrimidinone amide were generally 4-15x more stable to metabolism when compared to their *N*-alkylated counterparts. Therefore, the identification of a reasonably active, more polar compound with an *O*-alkylated pyrimidinone amide was considered highly desirable. We focused on the replacement of the lipophilic allyl group with smaller methyl or more polar acetonitrile and *n*-propanol functionalities, while either retaining methoxyethyl substitution of the sulfur or again substituting with acetonitrile. A summary of the *N*-Boc substituted analogs is

presented in Table 4.4. Unfortunately, nearly all the compounds in this series displayed disappointingly low activity in both strains at 50 µM, with the exception of **180** in *S. aureus*. Although somewhat active at 50 µM, we had hoped that by combining the features of several distinct active compounds (N/O *n*-propanol, *N*-Boc or NH-piperidine, *S*-methoxyethyl) would result in drastic, synergistic gains in potency, but this was unfortunately not realized. Similarly, the five successfully synthesized and stable unsubstituted piperidines from this series (**203-207**) showed weak, highly variable, or no activity up to 50 µM (Table 4.5).

Table 4.4. Activity data for Boc-substituted spiropiperidines compounds with varied substitution on the pyrimidinone ring.

A

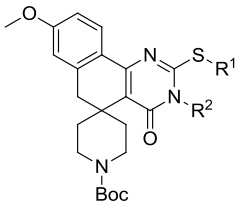

B

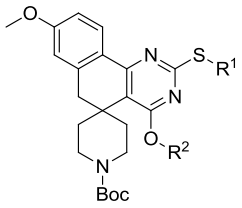

#	Scaffold	R^1	R^2	SA 5 µM[a]	SA 50 µM[a]	SA IC_{50} (µM)[b]	SE 5 µM[c]	SE 50 µM[c]
178	A	$CH_3OCH_2CH_2$	$NCCH_2$	0.74 ± 0.18	0.88 ± 0.15		1.00 ± 0.11	0.90 ± 0.06
179	A	$CH_3OCH_2CH_2$	Me	0.92 ± 0.01	1.01 ± 0.13		0.98 ± 0.14	0.92 ± 0.03
180	A	$CH_3OCH_2CH_2$	$HO(CH_2)_3$	0.81 ± 0.13	0.40 ± 0.10	16.7 ± 9.9	nd	nd
182	A	$NCCH_2$	Me	0.68 ± 0.02	0.70 ± 0.06		1.00 ± 0.16	0.95 ± 0.14
183	A	$NCCH_2$	$NCCH_2$	0.79 ± 0.18	0.80 ± 0.03		0.97 ± 0.09	0.95 ± 0.08
185	B	$CH_3OCH_2CH_2$	$NCCH_2$	0.82 ± 0.03	0.80 ± 0.02		0.88 ± 0.09	0.87 ± 0.02
186	B	$CH_3OCH_2CH_2$	Me	0.72 ± 0.09	1.03 ± 0.18		0.94 ± 0.09	0.85 ± 0.04
187	B	$CH_3OCH_2CH_2$	$HO(CH_2)_3$	0.81 ± 0.04	0.67 ± 0.25		nd	nd
188	B	$NCCH_2$	Me	0.68 ± 0.22	0.75 ± 0.12		0.98 ± 0.13	0.88 ± 0.05
189	B	$NCCH_2$	$NCCH_2$	0.75 ± 0.11	0.75 ± 0.11		0.94 ± 0.15	0.87 ± 0.08

[a] Ratio of *S. aureus* biofilm formation by *S. aureus* cultures in the presence of the indicated concentration of test compound compared to DMSO control. [b] Half-maximal inhibitory concentrations against biofilm formation in the presence of the indicated compound, calculated from 6-point dose-response curve from 0.15 µM to 50 µM. [c] Ratio of *S. epidermidis* biofilm formation by *S. aureus* cultures in the presence of the indicated concentration of test compound compared to DMSO control.

Table 4.5. Activity data for unsubstituted spiropiperidines compounds with varied substitution on the pyrimidinone ring.

A 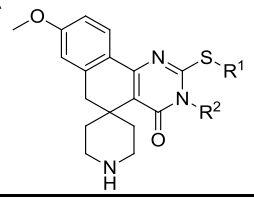

B 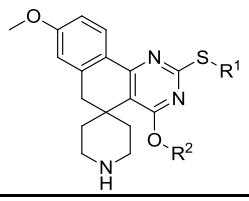

#	Scaffold	R^1	R^2	SA 5 μM[a]	SA 50 μM[a]	SA IC_{50} (μM)[b]	SE 5 μM[c]	SE 50 μM[c]
203	A	$CH_3OCH_2CH_2$	$HO(CH_2)_3$	0.97 ± 0.03	0.94 ± 0.02		nd	nd
204	A	$NCCH_2$	Me	1.01 ± 0.15	0.89 ± 0.11		1.03 ± 0.11	0.96 ± 0.30
205	B	$CH_3OCH_2CH_2$	$HO(CH_2)_3$	0.95 ± 0.01	0.61 ± 0.20		nd	nd
206	B	$NCCH_2$	Me	1.05 ± 0.34	0.82 ± 0.65		1.13 ± 0.10	0.92 ± 0.26
207	B	$NCCH_2$	$NCCH_2$	1.02 ± 0.21	0.69 ± 0.48		0.99 ± 0.91	0.91 ± 0.17
190	A	$CH_3OCH_2CH_2$	Allyl	0.94 ± 0.06	0.41 ± 0.20	>50	1.01 ± 0.05	0.17 ± 0.05

[a] Ratio of *S. aureus* biofilm formation by *S. aureus* cultures in the presence of the indicated concentration of test compound compared to DMSO control. [b] Half-maximal inhibitory concentrations against biofilm formation in the presence of the indicated compound, calculated from 6-point dose-response curve from 0.15 μM to 50 μM. [c] Ratio of *S. epidermidis* biofilm formation by *S. aureus* cultures in the presence of the indicated concentration of test compound compared to DMSO control.

In light of the limited success garnered from optimizing the spiropiperidine-based compounds for activity, we postulated that it may be useful to synthesize additional gem-dimethyl substituted compounds using the same guiding principles as above. Activity data for these compounds is summarized in Table 4.6. Although the majority of these compounds are not very active, **210** was observed to be equipotent to compound **31** in *S. aureus*. In contrast to our efforts to optimize the spiropiperidine series, **210** represents the successful realization of synergistic gains by combining the features of moderately potent analogs **51** and **43**. The enhanced microsomal stability and lower cLogP of this compound compared to **31** may distinguish **210** as being better suited for *in vivo* administration. *O*-methyl compound **213** continues the trend of being less active than its *N*-methylated counterpart **43**.

Table 4.6. Activity data for additional gem-dimethyl compounds 209-215 in comparison to compounds 43 and 51.

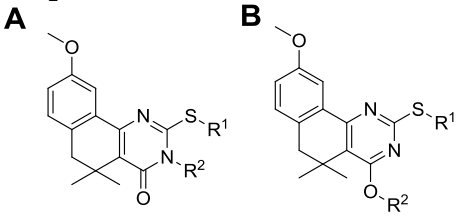

#	Scaffold	R^1	R^2	SA 5 μM[a]	SA 50 μM[a]	SA IC_{50} (μM)[b]	SE 5 μM[c]	SE 50 μM[c]
209	A	Et	$NCCH_2$	1.18 ± 0.09	1.12 ± 0.03		1.01 ± 0.23	0.94 ± 0.14
210	A	F_3CCH_2	Me	0.38 ± 0.05	0.33 ± 0.00	3.7 ± 0.9	0.94 ± 0.16	0.87 ± 0.06
211	A	$NCCH_2$	$NCCH_2$	1.13 ± 0.15	0.61 ± 0.02		1.03 ± 0.12	0.92 ± 0.22
212	B	Et	$NCCH_2$	1.09 ± 0.16	0.97 ± 0.07		0.88 ± 0.13	0.89 ± 0.15
213	B	Et	Me	1.22 ± 0.35	0.72 ± 0.06		0.94 ± 0.14	0.83 ± 0.02
214	B	$NCCH_2$	$NCCH_2$	1.03 ± 0.10	0.80 ± 0.00		1.01 ± 0.19	0.91 ± 0.18
215	B	$NCCH_2$	Allyl	0.84 ± 0.00	0.54 ± 0.09		0.92 ± 0.09	0.82 ± 0.12
43	A	Et	Me	0.81 ± 0.10	0.28 ± 0.14	4.3 ± 0.6	0.90 ± 0.07	0.57 ± 0.45
51	A	F_3CCH_2	Allyl	0.80 ± 0.04	0.33 ± 0.04	2.9 ± 0.4	nd	nd

[a] Ratio of *S. aureus* biofilm formation by *S. aureus* cultures in the presence of the indicated concentration of test compound compared to DMSO control. [b] Half-maximal inhibitory concentrations against biofilm formation in the presence of the indicated compound, calculated from 6-point dose-response curve from 0.15 μM to 50 μM. [c] Ratio of *S. epidermidis* biofilm formation by *S. aureus* cultures in the presence of the indicated concentration of test compound compared to DMSO control.

At this point in the SAR optimization process, we tentatively concluded that little progress had been made on the optimization of activity against *Staphylococcus* biofilms. Compounds **190** and **210**, the most active compounds against *S. aureus* from this series, were merely equipotent to GAS-SK compound **31**, albeit with potentially enhanced physicochemical properties. The picture was considerably more dire for the *S. epidermidis* arm of the SAR study. While progress had indeed been made in terms of identifying analogs with enhanced activity against *S. epidermidis* compared to GAS-SK compounds, **190** had proven to be the only compound with reproducible, non-toxic biofilm inhibition >50% at 50 μM. Based on this troubling data, we decided to focus our efforts more directly on optimization against *S. aureus*. The wider range of activities exhibited by our compounds in this strain gave us more data from which structural conclusions could be derived.

Chiral Derivative Discussion

The generation of several enantiomeric pairs of chiral analogs was undertaken as a complementary strategy to more traditional structural analog development for SAR optimization. Since macromolecules are chiral in nature, chiral ligands allow for potentially greater interaction with the macromolecular environment compared to achiral molecules. Furthermore, if a given chiral compound is effective in increasing activity, its enantiomer is unlikely to accommodate the same pose in the chiral protein environment, decreasing its binding affinity. This phenomenon can be very significant, and is generally proportional to the potency of the ligand.[142] The ratio of the affinity of the more active enantiomer ("eutomer") to that of the less active enantiomer ("distomer") is defined as the eudismic ratio. The phenomenon of chiral differentiation in binding affinity, on top of being an important tool for SAR optimization, can be a strong indicator that a given compound is making a specific interaction with one or a few target macromolecules rather than evoking its characteristic phenotype through nonspecific means (membrane effects, protein expression pan-inhibition, self-aggregation, etc.). It should be noted that although a high eudismic ratio implies a specific target-ligand interaction,[143] the opposite is not true when no significant eudismic ratio is observed. If, for example, the chiral portion of the molecule is situated in a region of the binding site that it does not meaningfully interact with, such as a solvent-exposed area, a significant eudismic ratio will not be observed. Therefore, when generating enantiomer pairs to assess chiral differentiation, it is important to vary the site of chiral substitution as much as possible. In light of this, we identified three distinct portions of the scaffold amenable to chiral derivatization.

A total of 12 compounds were synthesized for the chiral discrimination study. Spiropyrrolidine compounds **221-224** (Table 4.7) were originally synthesized as racemates to be compared with their chiral counterparts. While synthetic issues hampered the synthesis of the chiral versions, the racemates were submitted for activity assessment on their own. Similarly to spiropiperidine compounds **177** and **181**, Boc-substituted compounds **221** and **222** were found to be active, with methoxy-substituted **22** achieving slightly higher potency at 5 μM. The analogous free NH analogs **223** and **224** were nearly inactive.

Table 4.7. Activity data for racemic spiropyrrolidine compounds 221-224.

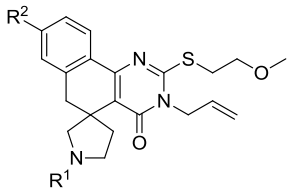

#	R^1	R^2	SA 5 μM[a]	SA 50 μM[a]	SA IC_{50} (μM)[b]	SE 5 μM[c]	SE 50 μM[c]
221	Boc	H	0.77 ± 0.12	0.48 ± 0.18	3.2 ± 0.7	0.98 ± 0.02	0.78 ± 0.05
222	Boc	MeO	0.58 ± 0.17	0.52 ± 0.06	1.4 ± 0.2	0.84 ± 0.06	0.75 ± 0.18
223	H	H	0.96 ± 0.14	1.03 ± 0.27		1.14 ± 0.07	1.13 ± 0.29
224	H	MeO	0.85 ± 0.11	0.72 ± 0.19	>50	0.99 ± 0.29	0.91 ± 0.29

[a] Ratio of *S. aureus* biofilm formation by *S. aureus* cultures in the presence of the indicated concentration of test compound compared to DMSO control. [b] Half-maximal inhibitory concentrations against biofilm formation in the presence of the indicated compound, calculated from 6-point dose-response curve from 0.15 μM to 50 μM. [c] Ratio of *S. epidermidis* biofilm formation by *S. aureus* cultures in the presence of the indicated concentration of test compound compared to DMSO control.

The first enantiomeric pairs synthesized for this study were the alaninol-derived pentacycles **234-237** (Table 4.8). Based on previous results, both the free secondary amine and tertiary benzylamine analogs were prepared. This decision would prove fortuitous, as secondary amines **234** and **235** showed very weak activity at 50 μM. Interestingly, there appears to be a slight degree of chiral differentiation between tertiary benzylamines **236** and **237** at 50 μM, though an activity ratio of 1.5 is not particularly conclusive. Furthermore, the calculation of the IC_{50} value for the more potent (*S*)-enantiomer **237** reveals a disappointingly low value of 46 μM. Since this value nearly reaches the functional concentration limit of the assay, the calculation of a true eudismic ratio between **236** and **237** would not be informative.

Table 4.8. Activity data for chiral alaninol-derived pentacycles 234-237.

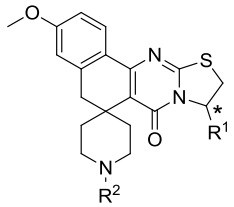

#	R^1	R^2	SA 5 μM[a]	SA 50 μM[a]	SA IC_{50} (μM)[b]	SE 5 μM[c]	SE 50 μM[c]
234	(*R*)-Me	H	0.97 ± 0.23	0.65 ± 0.31		nd	nd
235	(*S*)-Me	H	0.96 ± 0.16	0.68 ± 0.35		nd	nd
236	(*R*)-Me	Bn	0.86 ± 0.17	0.75 ± 0.09		nd	nd
237	(*S*)-Me	Bn	0.89 ± 0.15	0.50 ± 0.00	46 ± 1	nd	nd

[a] Ratio of *S. aureus* biofilm formation by *S. aureus* cultures in the presence of the indicated concentration of test compound compared to DMSO control. [b] Half-maximal inhibitory concentrations against biofilm formation in the presence of the indicated compound, calculated from 6-point dose-response curve from 0.15 μM to 50 μM. [c] Ratio of *S. epidermidis* biofilm formation by *S. aureus* cultures in the presence of the indicated concentration of test compound compared to DMSO control.

The final two enantiomeric pairs assessed the extent of chiral differentiation at two other points on the scaffold (Table 4.9). Unfortunately, the somewhat bulky substitutions at both the piperidine nitrogen and 8-position of the phenyl ring led to precipitous drops in activity. Compound **201** appears somewhat active, but its inter-assay variability is too high to make any meaningful comparison with **202**. It has been previously observed in this SAR study that only a few compounds with large substituents appended to the phenyl have retained activity. In its current state, the chiral differentiation study hints at possible dissimilarity between enantiomeric pairs, but not convincingly so based on this small number of analogs and their relatively low levels of biofilm activity.

Table 4.9. Activity data for chiral aryl ethers 242-243 and chiral amides 201 and 202.

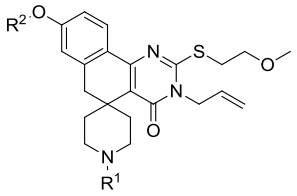

#	R^1	R^2	SA 5 μM[a]	SA 50 μM[a]	SE 5 μM[b]	SE 50 μM[b]
242	Boc	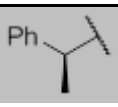	0.88 ± 0.17	0.90 ± 0.14	nd	nd
243	Boc	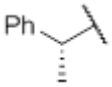	0.91 ± 0.14	0.83 ± 0.19	nd	nd
201	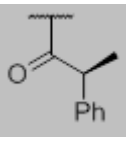	Me	0.70 ± 0.23	0.68 ± 0.24	nd	nd
202	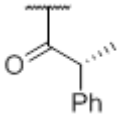	Me	0.87 ± 0.06	0.88 ± 0.02	nd	nd

[a] Ratio of *S. aureus* biofilm formation by *S. aureus* cultures in the presence of the indicated concentration of test compound compared to DMSO control. [b]Ratio of *S. epidermidis* biofilm formation by *S. aureus* cultures in the presence of the indicated concentration of test compound compared to DMSO control.

IC_{50} Data

As previously mentioned, our group decided to first examine the activity of each compound at 5 and 50 μM concentrations before progressing to IC_{50} determination. This decision delayed the determination of IC_{50} values for virtually all analogs produced in this series until the end of the campaign. Disappointingly, we found the *S. aureus* IC_{50} data for several compounds incongruous with the existing 2-point activity data we used to design our SAR strategy. For example, Compounds **177**, **190**, and **197**, identified as good performers in the original activity data, returned IC_{50} values greater than 50 μM, the highest concentration tested in our dose-response curves. The decision to employ the *S*-methoxyethyl appendage in a majority of later compounds, as well as our focus on preserving basic amine functionality, are counter to the conclusions one would draw from the IC_{50} data alone. The IC_{50} values for the three most potent compounds in *S. epidermidis*, **190**, **43**, and **197**, were all greater than 50 μM and highly variable, reinforcing our decision to focus more on *S. aureus* inhibition.

Although at first puzzling, a key difference between the 2-point activity data and IC_{50} data helps to partially explain the conflict. While the activity data measures the ratio of activity compared to control from 0.00 to 1.00, IC_{50}s by definition describe the point of half-maximal inhibitory concentration, calculated as the inflection point of a dose response curve. None of the compounds in this series achieve 100% biofilm inhibition (i.e. a ratio of 0.00) at any concentration, but instead hit a ceiling of inhibition that could be due to either physicochemical or mechanistic reasons. This phenomenon led to lower than expected IC_{50} values for compounds that reach a maximal point at relatively high values. Compound **181** (Table 4.2) is an excellent example of this phenomenon. Likewise, higher than expected values are reported for compounds that do not reach an activity plateau over the concentration range tested (0.15 µM – 50 µM), like compounds **190** and **197**. Essentially, the two-point concentration data is a gauge of the efficacy of compounds in this series, while the IC_{50} values are measuring the concentration to achieve half of this maximal effect (potency). It should also be noted that the most active compounds identified by the 2-point concentration data in SA, including **31**, **51**, and **210**, have IC_{50} values that are highly consistent with the 2-point data, presumably because they are able to inhibit biofilm to a greater maximal degree than other compounds. Thus, the IC_{50} values, when taken together with the original activity data, serve as an additional point of differentiation between compounds that allowed for the finer discrimination between our best analogs.

***In Vivo* Efficacy Assays**

Our collaborators in Hongmin Sun's group have also performed whole-animal studies to complement the cell-based activity determination studies. Catheters or silicone wafers inoculated with 10^7–10^8 CFU *S. aureus* or *S. epidermidis* were subcutaneously implanted into Balb/c mice, then treated IP with 100 µL of 2 mg/mL (8-10 mg/kg) test compound suspensions once a day for four days. Test compounds included some of the most potent compounds identified in the series, including **31** and **51**. The survival of test and control (PBS-treated) populations was compared over the course of seven days. Data gleaned from this study suggests that although displaying potent activity in plate-based assays, compounds **31** and **51** are not able to achieve protection at statistically significant levels. This is likely due to the previously identified issues of metabolic stability and solubility observed with these compounds (Chapter 2). Compound **21** was also chosen for *in vivo* study based on its increased aqueous solubility (~35 µM) and metabolic stability (MLM $t_{1/2}$ = 21 minutes). Interestingly, despite its fairly low

observed efficacy in plate-based assays (Table 4.1), **21** displays significant protective effects in mice (p = 0.004), underscoring the importance of solubility and stability to metabolism to *in vivo* efficacy.

Figure 4.2. Survival data for Balb/c mice infected via subcutaneously-implanted silicone wafers inoculated with *S. aureus* in the presence of test compounds vs. negative control.

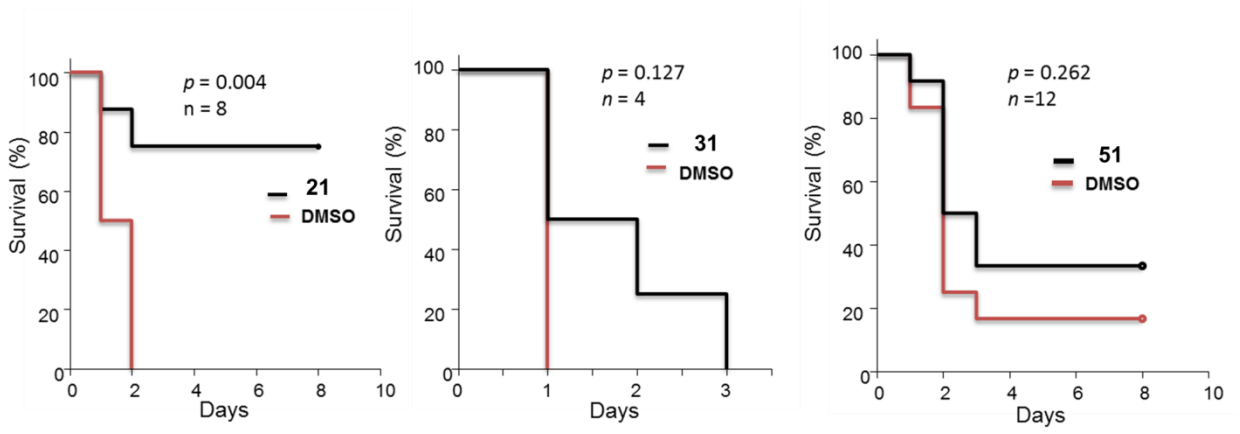

Metabolic Stability

After the completion of the SAR dataset, we submitted potent compounds **210** and **222** to Duxin Sun's group to assess their propensity for oxidation by mouse liver microsomal extract. Compound **222** (MLM $t_{1/2}$ = 5.7 min, Table 4.10) was found to have mediocre metabolic stability, but was still greater than potent compounds **31** and **43**. We were pleased to find that compound **210**, although slightly less potent than lead compound **31** (IC_{50} = 3.4 µM vs. 1.4 µM for **31**), is nearly 25-fold more metabolically stable (MLM $t_{1/2}$ = 19.7 min vs. 0.8 min for **31**). This result was somewhat unexpected, given our previous observation that *S*-trifluoroethyl (**51**) or amide *N*-methyl substitution (**43**) alone was not sufficient to confer a significant increase in metabolic stability. Thus, **31** represents the first potent and potential metabolically competent compound developed for the *S. aureus* anti-biofilm SAR study.

Table 4.10. Microsomal stability and IC_{50} data for selected compounds potent against *S. aureus* biofilm production.

#	Structure	SA IC_{50} (μM)[a]	MLM $t_{1/2}$ (min)[b]
21	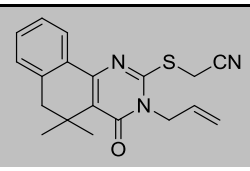	nd[c]	20.6
31	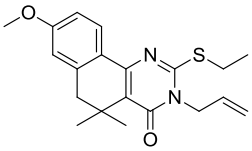	1.4 ± 0.4	0.8
32	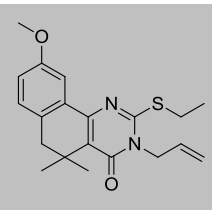	5.2 ± 0.4	2.3
51	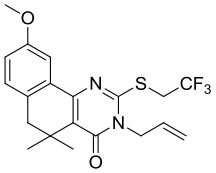	2.9 ± 0.4	4.8
43	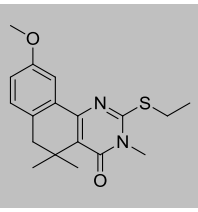	4.3 ± 0.6	1.7
210	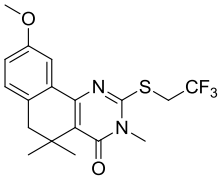	3.7 ± 0.9	19.6
222	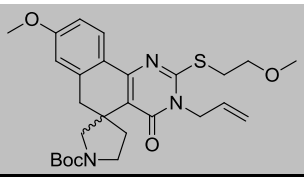	1.4 ± 0.2	5.7

[a]Half-maximal inhibitory concentrations against biofilm formation in the presence of the indicated compound, calculated from 6-point dose-response curve from 0.15 μM to 50 μM. [b]Half-life of parent compound during incubation with mouse liver microsomes. [c]Compound did not meet efficacy threshold to warrant IC_{50} determination. **21** achieved 31% biofilm inhibition vs. control at 50 μM in *S. aureus.*

Conclusions

Despite our efforts to improve activity through carefully planned SAR expansion, none of the additional 47 compounds synthesized for this effort achieved a level of potency against *S. aureus* biofilm production greater than previously identified compound **31**. The most active compounds in this series seem to inhabit a very narrow range of chemical space, characterized by small aryl methyl ethers and gem-dimethyl substitution on the central ring. While this was difficult to predict based on the initial 100 µM compound screen, it became increasingly clear over the course of data refinement studies performed simultaneously to the SAR effort. We were at first encouraged by several compounds which appeared efficacious (**190**, **180**, **197**, etc.) in both strains, but their weak and variable potencies observed during IC_{50} curve generation refuted the original 2-concentration activity data. While unfortunate, these findings underscore the absolute importance of fully defining testing criteria, assay parameters, and generating robust initial data (in this case, the determination of IC_{50} values from several experiments with proper controls) before designing follow-up SAR. While most of our compounds were weakly to moderately effective in inhibiting *S. aureus* biofilm production, no compounds possessing an IC_{50} less than 50 µM against *S. epidermidis* were identified. Nonetheless, we were able to demonstrate the potent inhibition of biofilm formation in *S. aureus* with compounds **210**, **221**, and **222**, which should serve as a starting point for the next round of SAR optimization. The unexpected efficacy of **21** in mouse trials serves to further reinforce the necessity of good aqueous solubility and metabolic stability in achieving adequate protection *in vivo*. The enhanced metabolic stability of **210**, combined with potency on par with **31**, implies it may be particularly well suited to achieving antibacterial efficacy in mouse models.

Chapter 5: Future Directions

GAS-SK SAR Studies

Chapter 2, as well as our publication in *Bioorganic Medicinal Chemistry*,[144] delineated our efforts toward optimizing the scaffold of **1** for activity against GAS-SK expression. Although we realized a 35-fold increase in the potency of the scaffold with analog **32** and identified amide alkylation at the *O*-position as protective against metabolic oxidation (compounds **48**-**50**), we were never able to combine these desirable traits into a single compound. By the time we discovered metabolically stable derivatives of **1**, we had already been discussing the feasibility of repurposing these compounds for other virulence targets, most notably biofilm formation.[132] The apparent intractability of potency optimization with retention of metabolic stability, combined with the increasingly promising potential of these compounds as biofilm inhibitors, led to the indefinite suspension of the SAR effort against GAS. It is unlikely that this project will be restarted unless major breakthroughs are made in the target identification effort.

If a target was indeed identified, this development would re-energize the GAS-SK SAR study. A validated target could lead to the development of a target-based biochemical assay, which would be an excellent supplement to the existing cell-based GAS-SK assay. A biochemical assay would represent a drastic simplification of the test system with far fewer sources of variability. Decreased variability would in turn increase data resolution between compounds and provide much clearer SAR guidance. Combining this enzymatic data with periodic cell assays to ensure we are retaining adequate cell permeability for activity would essentially give us the advantages of both phenotypic and target-based compound optimization. A third high-throughput screening effort, this time using the target in the primary screen and the cell-based GAS-SK assay as a means of hit validation, would have the potential to locate additional chemical matter useful against GAS virulence.

Going forward, if a co-crystal structure of the target protein with an analog of **1** could be obtained, this would be of great importance to designing new analogs using the power of

structure-based drug design (SBDD). Structural data derived from x-ray crystallography would allow us to identify which portions of the molecule are most important for interacting with the target, which would in turn guide the SAR effort and lead to analogs with potentially enhanced affinity. In light of the as yet unresolved issues of solubility and metabolic stability with this compound series, other target-based technologies could be used to identify new leads, such as fragment-based virtual screening or molecular docking.

Target Identification Studies

Chapter 3's discussion of the target identification effort ends on a rather unfinished note, with all three generations of probe molecules failing to specifically identify any potential target and displaying a significant degree of apparent nonspecific binding in the cellular milieu. As mentioned in the chapter, target identification with chemical probes using traditional affinity chromatography or fluorescence-based approaches is quite difficult, and only has a high chance of success in situations where the target is abundant and/or the target-ligand interaction is especially potent. Given that bacterial transcription factors are among the lowest-abundance proteins in cells, it is likely that the target of our compounds is also relatively low-copy. Furthermore, the high lipophilicity and corresponding low aqueous solubility of our probe molecules and competitors works against our target identification efforts, both by encouraging a higher level of nonspecific association and crosslinking with lipophilic proteins, and also by limiting the effective concentration of soluble competitor compounds. For example, in the benzophenone study, competitor concentrations were intended to be 500 µM and 1 mM, when in reality the effective concentration had to be far lower, given the aqueous solubility of compound **17** is around 15 µM. Essentially, to competitively block protein tagging at a level discernible by visual inspection of an SDS-PAGE gel, our assays should have had effective probe:competitor ratios of 1:100, instead of the level we more likely achieved, which is far from ideal for visualizing any strong competitive effect.

Although the issues with the probe compounds are not trivial, they are also not insurmountable. In recent years, several new strategies for target identification using chemical probes have arisen. Our collaborators in the Ginsburg group have proposed using genomic phage display libraries to screen for proteins interacting with probe molecules, a strategy that has previously been employed successfully to identify the targets of natural products (Figure 5.1).[107] Briefly, this technique is built around bacteriophages that are genetically altered to present

proteins or fragments of proteins on their outer protein coat. Bacterial DNA is inserted into the phage genome and transfected into bacteria, inducing the production of fully-constructed phages with bacterial protein fragments on the outer portion of the viral capsid. Depending on the conditions used to generate phage-bacteria hybrid genomes ("phagemids"), these phages may represent one, many, or all the proteins coded by the bacterial genome. The resulting phages are subjected to affinity chromatography using an immobilized photoprobe, UV-crosslinking, and subsequent washing away of non-bound phages. Similar to previous studies, complementary competition assays would assist in identifying hits attributable to nonspecific binding. The retained bacteriophage capsids are eluted from the matrix, then used to reinfect a new bacterial colony to amplify the enriched phage population. These phages can then be lysed and submitted for gene sequencing, or be cycled through the affinity matrix process again to further enrich based on target-ligand interaction. The ability to amplify and re-purify binding partners represents a significant advantage over traditional affinity screening methods. Identifying targets using this methodology also carries the major advantage of having every protein represented in relatively equal amounts, so identification is not biased against proteins with low cellular abundance.

Figure 5.1. Using phage display libraries and affinity chromatography to identify specific target-probe interactions. Adapted from Sche, Austin, *et al.*, *Chemistry and Biology* 1999, *6*, 707-716.

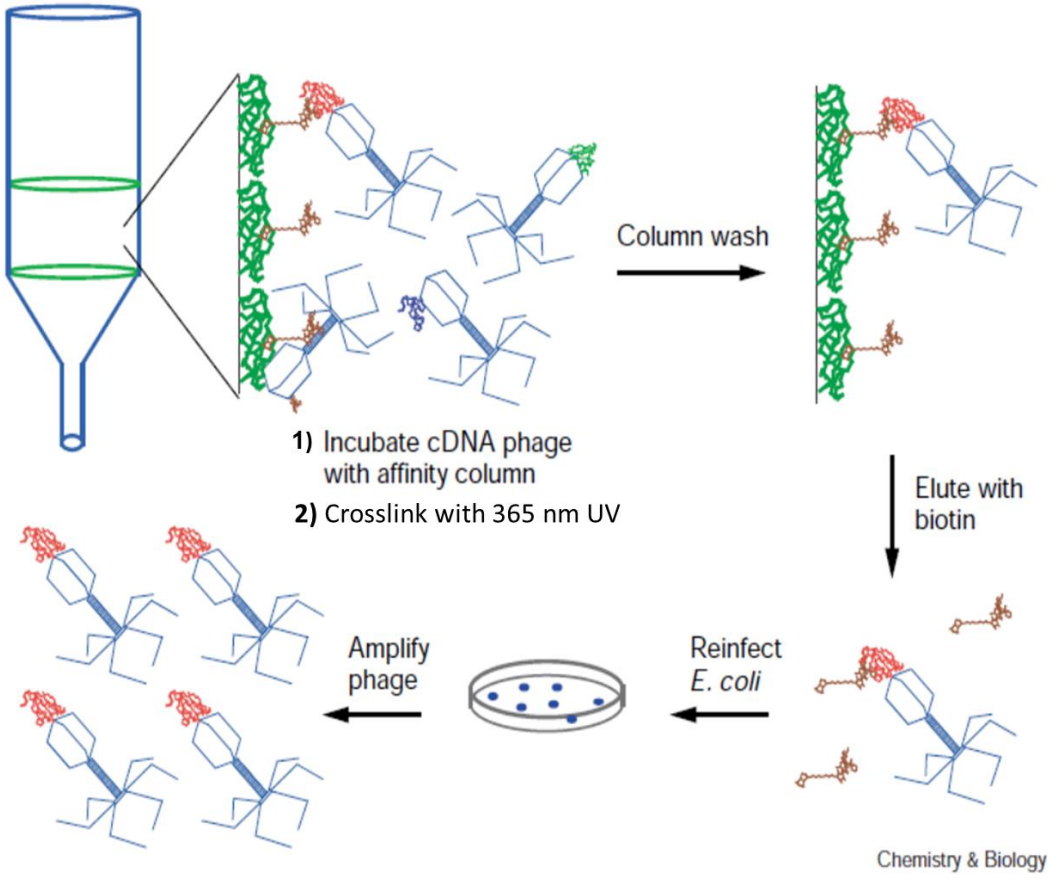

Members of the Ginsburg lab are developing a "shotgun" phage display library[145] for *S. aureus* that demonstrates fully redundant coverage of the *S. aureus* genome, with GAS soon to follow. However, the nature of the shotgun method of phage display library generation, in which bacterial genomic DNA is broken in random locations through the use of sonication before insertion into the phage genome, generates phage coding sequences with no regard for preservation of full proteins, correct reading frames, or the orientation of the gene insertion. Thus, a majority of the protein sequences presented by these phages are not informative, and a still smaller proportion of them will represent full proteins. Although this will likely muddle target data that arises from this study, the skillful employment of competition assays and affinity chromatography-phage amplification cycling should enhance our chances of finding a target

using this methodology. If the main issue with successful target ID to this point has been the low relative abundance of the target protein, this method should work to alleviate this problem.

A more quantitative approach to target identification was pioneered by the Schreiber group in a 2009 publication,[106] borne out of a desire to more easily resolve weak binding interactions between small molecules and proteins, and to give a more informative view of a given small compound's interaction with the entire proteome. This proteomic approach to target identification relies on stable isotopic labeling of amino acids in cell culture (SILAC)[146] to produce two nearly identical copies of the cellular proteome, differentiated by heavy carbon and nitrogen isotopes included in the growth medium of one of the populations. By purposing these two proteomes into a test and control population, one can employ highly sensitive mass spectrometry techniques for quantification and identification of proteins. Under optimal conditions, SILAC proteomic studies can detect differences in protein levels between the two populations as small as 1.3-fold.

Figure 5.2. Example of a successful competition-based target ID assay using SILAC.

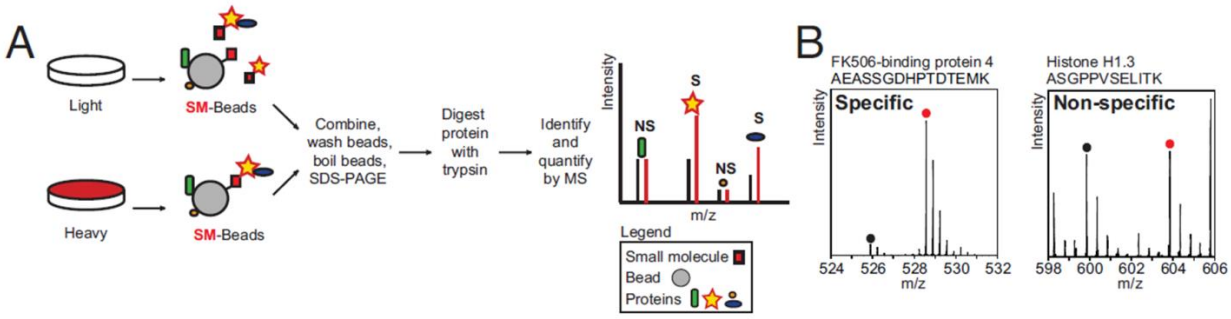

Panel A: Summary of of cell culture and affinity chromatography conditions used to generate "heavy" proteins enriched via specific interaction with immobilized probe. **Panel B:** Tandem mass spectrometry fingerprinting signatures consistent with specific and nonspecific protein-ligand interactions. Figure adapted from Ong, Carr, *et al.*¸ *PNAS* **2009**, *106* (12), 4617-4622.

SILAC methodology is easily adapted to target identification studies (Figure 5.2). In the case of our study, both bacteria populations would be treated with an active photoprobe, and one of the populations would be simultaneously treated with a soluble competitor (e.g. **17**, **21**, **32)**. UV-induced crosslinking would proceed as normal, then the cells would be lysed and both populations combined. Click chemistry to azido-biotin would be performed, then protein purification and enrichment via streptavidin affinity column would leave a crude mixture of "light" and "heavy" proteins for mass spectrometry analysis. Identifying the relative ratio of light and heavy proteins would rely on mass fingerprinting using tandem mass spectrometry. For

light/heavy pairs with a ratio around 1, this would imply that affinity for the probe molecule was unaffected by soluble competitor, and is thus a nonspecific interaction. A decrease in the protein population corresponding to the culture treated with soluble competitor, and thus a ratio significantly greater or less than 1, would imply a specific interaction and a potential target. The vastly increased sensitivity, differentiation of specific and nonspecific binding events, and automatic identification of the sequence of each protein via MS/MS analysis inherent to SILAC target ID would represent powerful enhancements to the methodology we initially employed for target identification.

The major caveat associated with SILAC is its reliance on near-quantitative replacement of targeted $^{12}C/^{14}N$ amino acids, normally lysine (K) and arginine (R), with their $^{13}C/^{15}N$ counterparts. Given the sensitivity of the mass spectrometric assays involved, a situation where even 10% of R and K positions are wild-type in the heavy population would lead to extra peaks on the mass spectrum, muddling the interpretation of protein ratios. In mammalian cell culture this is not an issue, as mammalian cells are completely unable to produce R and K *de novo*. The mammalian reliance on outside sources of these amino acids, known as auxotrophy, was central to the development of SILAC as a proteomic technique. Unfortunately, most bacteria possess the cellular machinery to produce all 20 natural amino acids, significantly complicating the use of SILAC in bacteria. In cases where auxotrophy cannot be relied on, raising cell colonies in tagged media is the most viable strategy. Unfortunately, this requires that a chemically defined medium for growth be established, rather than a medium based on biological extracts. Furthermore, even when defined media conditions are established, the $^{13}C/^{15}N$-tagged versions of the reagents needed are often extremely expensive. Several important lab strains, such as *E. coli*[147] and *S. aureus*,[148] have established chemically defined medium conditions; GAS does not.

In light of these issues, we attempted to modify our GAS-SK assay conditions to be compatible with *E. coli*. The Sun group screened the active tag-free photoprobes for activity in an *E. coli* strain transfected with the *ska-kan* plasmid used during the high throughput screening effort. Unfortunately, no kanamycin sensitization was observed with the diazirine or azide probes. This result suggests our probes either lack permeability across the Gram-negative cell membrane architecture, or that *E. coli* lacks virulence machinery sufficiently similar to GAS-SK to allow our probes to function as intended.

Given the challenges outlined above for SILAC-based target identification in GAS, the most promising way forward for the target ID portion of this study is to characterize probes built specifically for potency in *S. aureus*. Although several active compounds have been identified with anti-biofilm activity in *S. aureus*, few have been as potent as the best compounds from the GAS-SK series. In order to maximize the chances of a successful target ID, probe development for *S. aureus* will be postponed until the SAR effort identifies more potent (IC_{50} < 1 μM) compounds to use as templates for future probe molecules.

Biofilm Inhibitor Studies

Although initially showing promise, the optimization of this compound series in *S. aureus* and *S. epidermidis* strains has been difficult. The initial screen identified several compounds that showed acceptable inhibitory percentages at 100 μM, but this activity was found not to extend to lower concentrations, especially in *S. epidermidis*. The 47 compounds synthesized with the knowledge gained from screening the original 124 analogs developed against GAS-SK, while retaining modest potency in some cases, were not able to increase potency beyond that of **31** (IC_{50} = 1.4 μM). Compounds **180**, **187**, **203**, and **205**, designed to incorporate features from active compounds **159-161**, **43**, **177**, and **190**, generally showed poor activity.

Even though significant potency gains have yet to be realized against biofilm formation, compounds **210** and **222** possess a similar level of potency to **31**, while also exhibiting 7- to 25-fold increased stability in the presence of microsomal extract. Since Hongmin Sun's group was able to demonstrate *in vivo* efficacy with a metabolically stable and soluble, but weakly potent compound (**21**, Figure 4.2 and Table 4.10), **210** is a logical candidate for further murine trials. The observation of a significant protective effect in blocking biofilm formation (similar to **21**) would merit a follow-up study assaying the ability of **210** to reduce existing biofilm cultures, at first *in vitro*, then on prosthetic implants in mice. A compound able to destroy mature biofilms, rather than simply prevent initial attachment and nascent biofilm production, would have increased potential as an agent to be used in response to an established infection. In contrast, compounds that simply block initial biofilm establishment might only be useful as protective agents during prosthesis installation.

Scheme 5.1. General structure of potential SAR expansion compounds for the biofilm study.

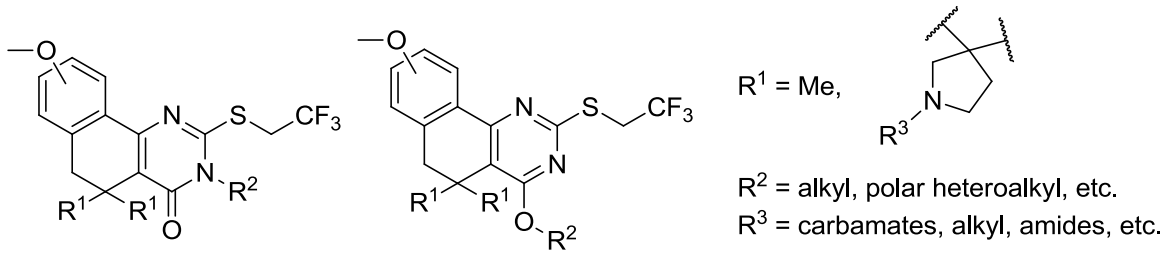

245 **246**

Based on the dearth of analogs displaying potency in *S. epidermidis*, we have decided to de-prioritize the requirement for activity in both strains when assessing the desirability of new compounds. When viewed solely in the context of compound efficacy in *S. aureus*, one can see a marked preference for gem-dimethyl and spiropyrrolidine compounds vs. the spiropiperidine series. Additionally, the increased activity of *S*-trifluoroethyl compounds **51** and **210** suggests the synthesis of more analogs with this substitution pattern. A reasonable follow-up to these findings would be the synthesis of additional *S*-trifluoroethyl compounds with varied substitution at the *N* and *O* positions, and either gem-dimethyl or spiropyrrolidine substitution of the central ring (Scheme 5.1). The substitution at the *N*- position of the pyrrolidine also warrants further investigation. To this point, Boc substitution has been the most consistently efficacious substitution, suggesting that more carbamates should be investigated. Carbamates are easily accessed through the reaction of the amine with chloroformates or dicarbonates.

Figure 5.3. Comparison of (*S*)- and (*R*)-enantiomers of model spiropyrrolidine analogs and the orientation of pyrrolidine *N*-substitution (green) as 2-D schematics and 3-D energy-minimized[a] structures.

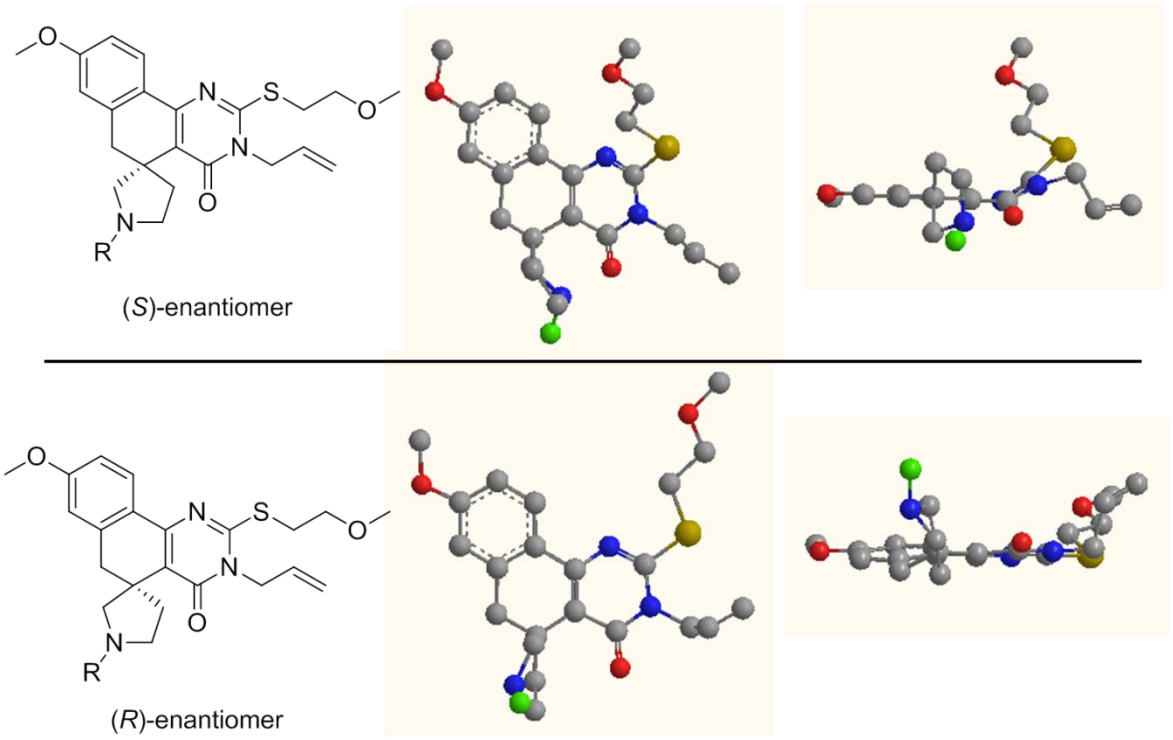

[a]Energy-minimized 3-D structures generated using MMFF94 algorithm, ChemBio3D Ultra version 12.0.

The synthesis of additional spiropyrrolidines warrants a re-examination of methods to synthesize enantiopure versions. The orientation of the spiropyrrolidine ring would allow each enantiomer to project its *N*-substitutuent (green) in opposite directions relative to the plane of the molecule (Figure 5.3), increasing the likelihood of differential potency. The failure of the original chiral spiropyrrolidine synthesis came during the installation of the thioxopyrimidinone ring. Since the original attempt was abandoned, we made great strides in achieving the mild construction of this ring by first converting the β-aminoester intermediate into the corresponding β-isothiocyanate. If this chemistry can be successfully applied to the previously synthesized aminoester, the following cyclization with a primary amine should be straightforward, leaving only an *S*-alkylation step to generate final compounds (Scheme 5.2). Each intermediate produced would be explored as a possible point for separating diastereomers and the pure enantiomers would be produced at the end through pyrrolidine deprotection with ethyl chloroformate. The

only drawback to this scheme is its current inability to produce *O*-alkylated amides, since the alkyl group at R^2 is already attached to nitrogen. One could potentially synthesize the unsubstituted amide using ammonia or a protected ammonia surrogate such as tosylamide, but no prior work in our group has explored this possibility to date.

Scheme 5.2. Proposed synthesis of chiral spiropyrrolidine analogs of general structure (*R*)- and (*S*)-250.[a]

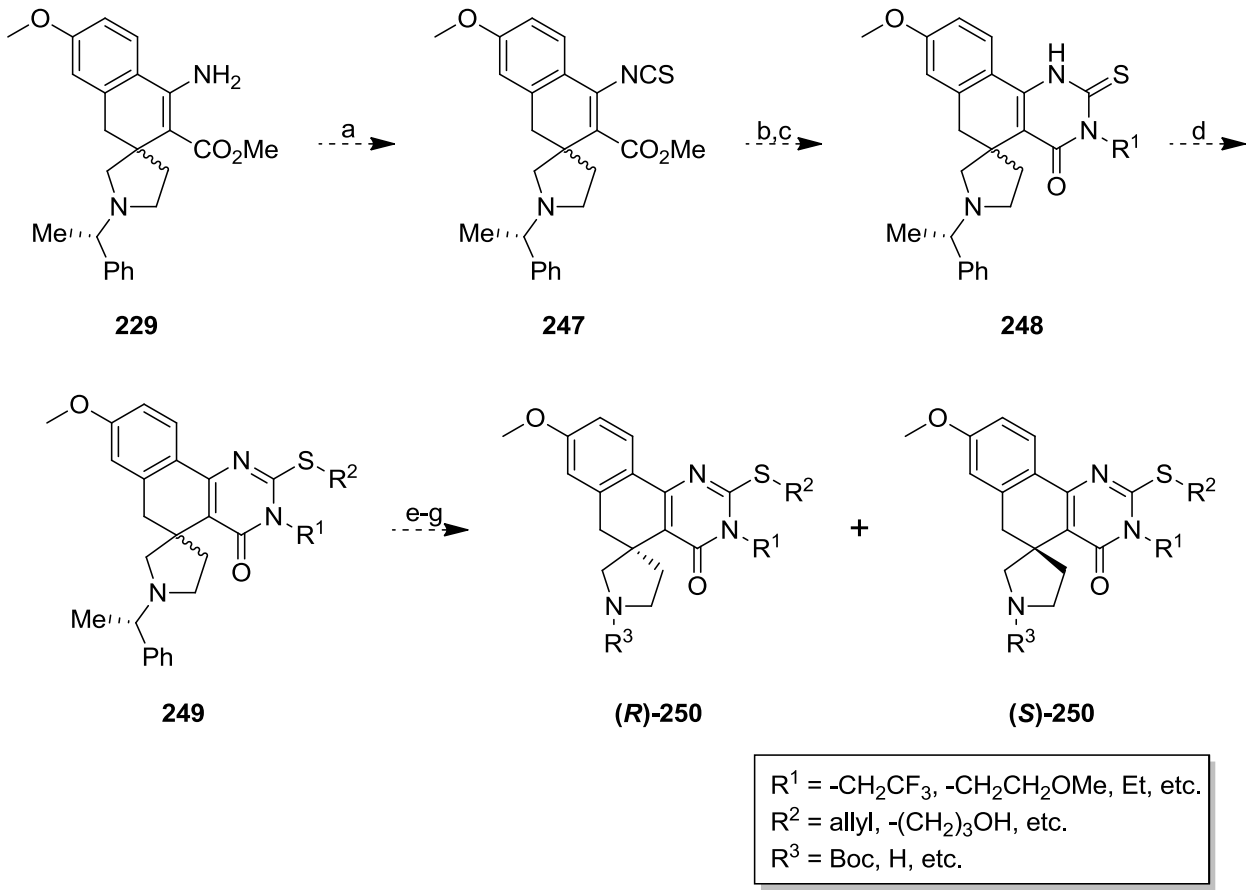

[a]Reagents and conditions: a) thiophosgene, $NaHCO_3$, DCM:H_2O (1:1), RT, 6h; b) R^1-NH_2, Et_2O, RT, 2h; c) NaOMe, MeOH, RT, 2h; d) R^2-X, Cs_2CO_3, DMF, 50-70°C, 16h; e) separation of diastereomers*; f) ethyl chloroformate, then KOH, EtOH, H_2O, RT; g) R^3-CHO, $(R^3)_2O$, R^3-Cl, etc. *separation may take place at any point after step c.

In addition to continuing efforts to generate chiral spiropyrrolidine analogs, the expansion of the enantiomer-pair study described in Chapter 4 is also warranted. The previous poor track record observed with bulky aryl substitution was continued with analogs **242** and **243**, and should not be further pursued. The inactivity of chiral piperidine amides **201** and **202** was more unexpected, given that several analogs with relatively bulky Boc groups were moderately active.

Furthermore, pentacycles **236** and **237** suggest a small amount of differentiation between enantiomers, even with variation in the configuration of only a methyl group; one would expect larger substitutions to make a bigger difference. Based on the limited number of compounds tested from these two classes, we propose the synthesis of additional analogs of each (Scheme 5.3). Both of these compound classes are amenable to the rapid generation of enantiomer pairs thanks to the readily availability of natural and unnatural amino acids. Chiral piperidine amides simply require a standard EDC-promoted coupling to any number of *N*-acetylated D- and L-amino acids, while further pentacycles of general structure **253** are derived from amino acids reduced to the corresponding amino alcohols.

Scheme 5.3. Proposed synthesis of chiral analogs 251 and 252 using previously established methodology.[a]

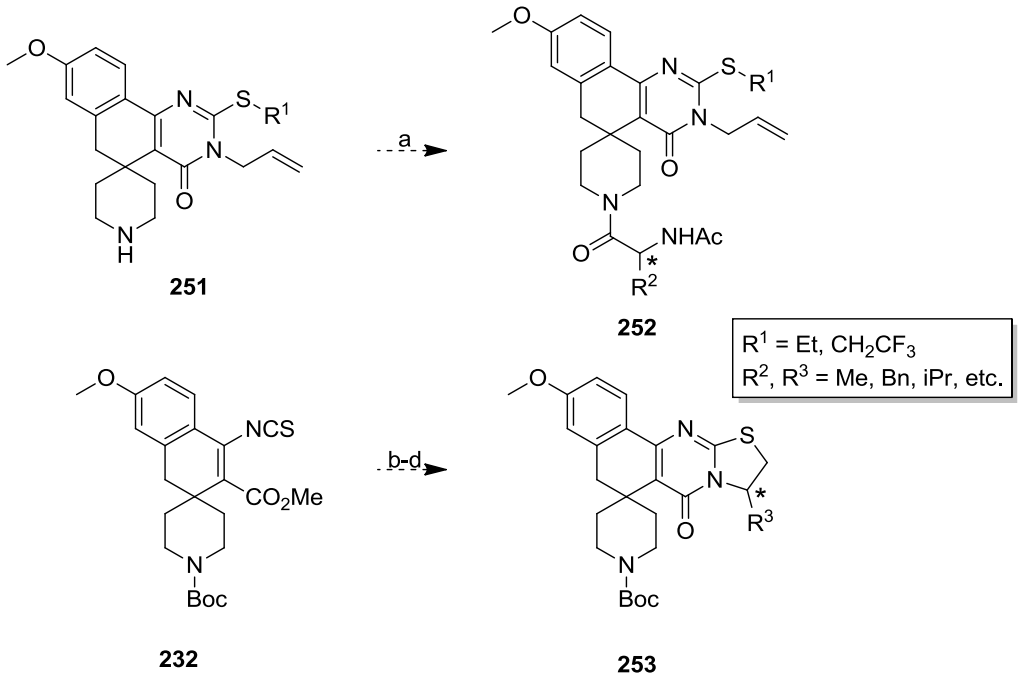

251 **252** **232** **253**

[a]Reagents and conditions: a) *N*-acetyl D- or L-amino acid, EDC, HOBt, DIPEA, DCM, RT; b) D- or L-amino alcohol, Et_2O, RT, 2h; c) NaOMe, MeOH, RT, 2h; d) TFA, DCM, 0°C-RT, 6h.

Chapter 6: Experimental Section

General information: Chemical names follow CAS nomenclature. Starting materials were purchased from Fisher, Sigma–Aldrich Lancaster, Fluka or TCI-America and were used as supplied unless otherwise indicated. All reaction solvents were purchased from Fisher and used as received. Reactions were monitored by TLC using precoated silica gel 60 F254 plates. All anhydrous reactions were run under an atmosphere of dry nitrogen. Silica gel chromatography was performed with silica gel (220–240 mesh) obtained from Silicycle. Solvent abbreviations used: $CDCl_3$, deutero-chloroform; DCM, dichloromethane; DMF, *N*,*N*-dimethylformamide; DMSO, dimethyl sulfoxide; EtOH, ethanol; EtOAc, ethyl acetate; hex, hexanes; MEK, methyl ethyl ketone; THF, tetrahydrofuran. Reagent abbreviations used: Cs_2CO_3, cesium carbonate; Na_2SO_4, sodium sulfate; $MgSO_4$, magnesium sulfate; *m*CPBA, meta-chloro peroxybenzoic acid; KOH, potassium hydroxide; LDA, lithium diisopropylamide; $NaHCO_3$, sodium bicarbonate; NaOMe, sodium methoxide; TMS, trimethylsilyl; HOBt 1-hydroxybenzotriazole; EDC, 1-(3-dimethylaminopropyl)-3-ethylcarbodiimide; ZnI_2, zinc iodide.

NMR spectra were recorded on a Bruker 400 MHz, Bruker 500 MHz, Varian 400 MHz, or Varian 500 MHz spectrometer. Chemical shifts are reported in d (parts per million), by reference to the hydrogen residues of deuterated solvent as internal standard CDCl3: d = 7.28 (1H NMR), or in reference to the hydrogen peaks of tetramethylsilane, d = 0.00 (1H NMR). Mass spectra were recorded on a Micromass LCT time-of-flight instrument utilizing electrospray ionization operating in positive-ion (ESI+) or negative-ion (ESI) modes where indicated. Melting points were measured on a MEL-TEMP melting point apparatus and are uncorrected. The purity of the compounds was assessed via analytical rpHPLC with one of three gradient methods. 'Method A': 10% B to 90% B over 6 min, hold at 90% B for 7 additional minutes; 'Method B': 50% B to 90% B, hold at 90% B for 7 additional minutes; 'Method C': 90% B over 12 min (solvent A = H_2O, solvent B = acetonitrile, C_{18} column, 3.5 µm, 4.6 100 mm, 254 nm l).

Compounds synthesized by other Vahlteich Medicinal Chemistry Core chemists that have appeared in our previous publications are cited where appropriate. All compounds synthesized by Bryan Yestrepsky appear here in full detail.

General Method A for generating methoxy-substituted *o*-tolunitriles:

To anhydrous THF (6.4 mL) in a dry round-bottom flask was added nickel(II) bromide (279 mg, 1.28 mmol), zinc powder (250 mg, 3.83 mmol), and triphenylphosphine (1.68 g, 6.39 mmol). The mixture was heated to 50°C and stirred for 30 minutes. The selected *o*-chlorotoluene (**25a** or **25b**, 12.78 mmol) was added, the temperature raised to 60°C, and the reaction was tightly capped and allowed to stir 30 minutes, then potassium cyanide (1.66g, 25.5 mmol) was added over the course of 5 hours in 2 equal portions. The mixture was allowed to stir an additional 16 hours. Water was added to quench the reaction, and the suspension extracted 3x with ether. The resulting organic layer was washed with H_2O and brine, dried over $MgSO_4$, filtered, and concentrated to a heterogeneous mixture of white crystals and clear oil. The residue was diluted with 10 mL of toluene, then methyl iodide (997 mg, 7.02 mmol) was added and allowed to stir 16 hours at room temperature. The resulting white crystals were removed via vacuum filtration. The filtrate was concentrated *in vacuo* to a clear oil. Flash chromatography with 2% EtOAc:hex delivered the pure product in 68-90% yield.

General Method B for generating β-aminoesters from *o*-tolunitriles:

A dry round bottom flask was charged with anhydrous diglyme (24 mL) and diisopropylamine (2.91 mL, 20.4 mmol), then cooled to -78°C in a dry ice/acetone bath. To this solution was added *n*-butyllithium (2.5M in hexanes, 8.15 mL, 20.4 mmol). The reaction was removed from the dry ice/acetone bath for 10 minutes, then re-cooled to -78°C. The desired *o*-tolunitrile (6.79 mmol), dissolved in anhydrous diglyme (2 mL), was then added slowly dropwise then allowed to stir at -78°C for 45 minutes.

A separate dry flask was charged with anhydrous diglyme (8.0 mL) and zinc powder (1.11 g, 17.0 mmol). Molecular iodine (3.45 g, 13.6 mmol) was added portionwise over the course of 10 minutes. The suspension was subsequently heated via heat gun in 30-second intervals until a silver precipitate of ZnI_2 had formed and all iodine color had disappeared (caution: exothermic).

The selected acrylate ester (1-2.5 eq) was added to the first flask dropwise over 10 minutes. The flask containing the ZnI_2 suspension was then added to the reaction vessel and the resulting suspension allowed to stir for an additional 2 hours, slowly warming to room temperature. The reaction was quenched by the addition of saturated ammonium chloride solution and the resulting biphasic suspension was extracted with diethyl ether (3 x 30 mL), then washed with water (4 x 50 mL) and brine (1 x 50 mL). The organic extract was dried over $MgSO_4$, vacuum filtered, and concentrated *in vacuo*. Further purification via flash chromatography (silica gel, 5% EtOAc:hex) delivered the desired products in 33-59% yields.

General Method C for synthesizing 2-thioxopyrimidinones:
Glacial acetic acid (147 μL, 2.56 mmol) and an alkyl isothiocyanate (2.56 mmol) were combined with the selected aminoester intermediate (1.28 mmol) in absolute ethanol (1.7 mL). The solution was allowed to stir at reflux under nitrogen atmosphere for 1 hour. Additional allyl isothiocyanate (373 μL, 3.84 mmol) was added in equal portions over the course of 3 hours. The reaction was allowed to stir at reflux 16 additional hours, then diluted with ethyl acetate. The organic mixture was washed with water and brine, dried over $MgSO_4$, filtered, and concentrated *in vacuo*. Trituration or flash chromatography delivered 2-thioxopyrimidinones in 21-59% yield.

General Method D for *S*-alkylating *N*-substituted 2-thioxopyrimidinones:
The selected 2-thioxopyrimidinone intermediate (0.101 mmol) was dissolved in MEK (0.591 mL), to which Cs_2CO_3 (66 mg, 0.201 mmol) and alkylating agent (0.151 mmol) were added. The reaction was heated to 70°C and allowed to stir 16 hours. The reaction mixture was diluted with H_2O and extracted 2x with EtOAc. The combined organic layers were washed with water and brine, then isolated, dried over $MgSO_4$, vacuum filtered, and concentrated *in vacuo*. Further purification via flash chromatography in an appropriate solvent system delivered the desired *S*-alkylated compounds in 24-88% yield.

General Method E for preparation of phenols from aryl methyl ethers. Boron tribromide solution (1M in dichloromethane, 4.42 mL) was added gradually to a stirred solution of the selected aryl ether intermediate (2.1 mmol) in dichloromethane (14 mL) at room temperature

under N_2. The mixture was heated to reflux for 6 hours, then cooled to room temperature. Water (10 mL) was then added dropwise and the mixture was partitioned between DCM and water. The layers were separated and the organic layer washed with water, saturated aqueous $NaHCO_3$, and saturated brine, then dried over $MgSO_4$. The solvent was removed under reduced pressure and the residue was triturated in ethyl acetate, filtered, and dried under high vacuum. The resulting crystalline phenols **16a-c** (43-62% isolated yield) were used without further purification.

General Method F to generate aryl ether compounds from phenols:
The selected phenol intermediate **34-36** (0.622 mmol) was dissolved in DMF (3.66 mL), to which Cs_2CO_3 (304 mg, 0.933 mmol) and an alkylating agent (0.716 mmol) were added. The resulting suspension was stirred at 70°C for 16 hours until the completion of the reaction. Compounds were purified as indicated in 35-92% yield.

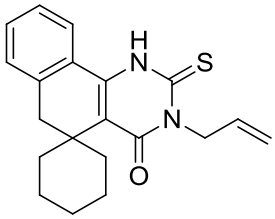

3-Allyl-2-thioxo-2,3-dihydro-1H-spiro[benzo[h]quinazoline-5,1′-cyclohexan]-4(6H)-one (6)
Synthesized by J. Ryu in 4 steps from cyclohexanone as previously reported._ENREF_145 TLC R_f = 0.25 (10% EtOAc:hex). ^{1}H NMR (500 MHz, $CDCl_3$) δ (ppm) 9.28 (s, 1H), 7.50 – 7.35 (m, 3H), 7.32 (d, *J* = 7.4 Hz, 1H), 6.00 (ddt, *J* = 16.2, 11.3, 5.8 Hz, 1H), 5.37 (dd, 1H), 5.27 (dd, 1H), 5.06 (d, *J* = 5.8 Hz, 2H), 3.03 (s, 2H), 2.48 (td, *J* = 13.3, 4.4 Hz, 2H), 1.72 (d, *J* = 13.3 Hz, 1H), 1.62 – 1.44 (m, 4H), 1.33 (d, *J* = 14.3 Hz, 3H).

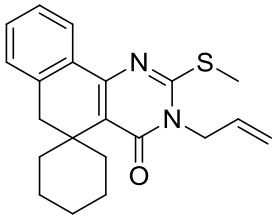

3-Allyl-2-(methylthio)-3H-spiro[benzo[h]quinazoline-5,1'-cyclohexan]-4(6H)-one (11) (CCG-102620). Compound **6** (150 mg, 0.443 mmol) was dissolved in absolute EtOH at 0°C (2.61 mL) to which KOH (37 mg, 0.665 mmol) and methyl iodide (33 μL, 0.532 mmol) were

added. The solution was allowed to stir for 10 minutes, resulting in the precipitation of white crystals. The suspension was diluted with H_2O and vacuum filtered to collect the precipitate. The precipitate was washed with water and dried *in vacuo*. Recovered 150 mg (95% yield). ^{1}H NMR (500 MHz, $CDCl_3$) δ (ppm) 8.14 (d, *J* = 7.4 Hz, 1H), 7.35 (t, *J* = 7.3 Hz, 1H), 7.31 (t, *J* = 6.8 Hz, 1H), 7.21 (d, *J* = 7.1 Hz, 1H), 5.94 (ddt, *J* = 15.9, 10.8, 5.6 Hz, 1H), 5.32 – 5.24 (m, 2H), 4.68 (d, *J* = 5.6 Hz, 2H), 3.04 (s, 2H), 2.68 (s, 3H), 2.64 – 2.54 (m, 2H), 1.71 (d, *J* = 12.8 Hz, 1H), 1.60 – 1.51 (m, 4H), 1.42 – 1.33 (m, 3H). ESI+MS *m/z* = 353.2 ($M + H^+$), 375.2 ($M + Na^+$). HPLC (Method C, t_R = 4.19 min), purity >95%.

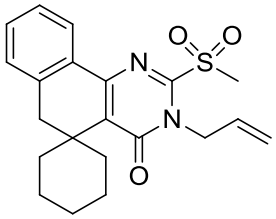

3-Allyl-2-(methylsulfonyl)-3H-spiro[benzo[h]quinazoline-5,1'-cyclohexan]-4(6H)-one (intermediate in synthesis of 13). Compound **11** (451 mg, 1.28 mmol) was dissolved in DCM (19.3 mL), then *m*CPBA (70 wt%, 787 mg, 3.19 mmol) was added and the reaction mixture allowed to stir over the course of 16 hours at room temperature. At this time the reaction mixture was diluted with DCM, washed with saturated aqueous $NaHCO_3$ solution, water, and brine. The organic layer was dried over $MgSO_4$, vacuum filtered, and concentrated *in vacuo*. Purification via flash chromatography isolated the sulfone intermediate (385 mg, 78% yield). ^{1}H NMR (500 MHz, Chloroform-*d*) δ 7.93 – 7.87 (m, 1H), 7.45 – 7.31 (m, 2H), 7.29 – 7.23 (m, 1H), 6.11 – 5.99 (m, 1H), 5.45 – 5.30 (m, 2H), 5.04 – 4.99 (m, 2H), 3.57 (s, 3H), 3.09 (s, 2H), 2.62 – 2.53 (m, 2H), 1.75 (d, *J* = 10.8 Hz, 1H), 1.67 – 1.51 (m, 5H), 1.41 (d, *J* = 12.6 Hz, 2H).

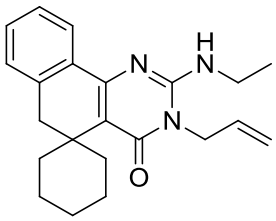

3-Allyl-2-(ethylamino)-3H-spiro[benzo[h]quinazoline-5,1'-cyclohexan]-4(6H)-one (13) (CCG-203043). The sulfone intermediate (385 mg, 1.00 mmol) was dissolved in a 1:1 mixture

of THF:DMF (2 mL). Potassium carbonate (165 mg, 1.19 mmol) and 2M ethylamine solution in THF (1.00 mL, 2.00 mmol) were added, then the reaction vessel was tightly capped and allowed to stir 5 hours at RT. The reaction mixture was diluted with diethyl ether, then washed with 3 portions of H_2O followed by brine. The organic layer was isolated, dried over $MgSO_4$, vacuum filtered, and concentrated *in vacuo*. The residue was further purified by flash chromatography (10-33% EtOAc:hex) and isolated as a white crystalline solid (237 mg, 53% yield over 2 steps). ^{1}H NMR (500 MHz, $CDCl_3$) δ (ppm) 8.13 (d, *J* = 7.4 Hz, 1H), 7.34 – 7.27 (m, 2H), 7.18 (d, *J* = 6.6 Hz, 1H), 5.92 (ddt, *J* = 17.3, 10.5, 5.3 Hz, 1H), 5.36 – 5.26 (m, 2H), 4.66 (d, *J* = 5.2 Hz, 2H), 4.56 (d, *J* = 5.0 Hz, 1H), 3.57 (qd, *J* = 7.2, 5.0 Hz, 2H), 3.01 (s, 2H), 2.64 – 2.54 (m, 2H), 1.70 (d, *J* = 12.6 Hz, 1H), 1.62 – 1.48 (m, 5H), 1.38 (d, *J* = 12.8 Hz, 3H), 1.28 (t, *J* = 7.2 Hz, 3H). ESI+MS *m/z* = 350.2 ($M + H^+$), 372.2 ($M + Na^+$). HPLC (Method B, t_R = 7.18 min), purity = 94%.

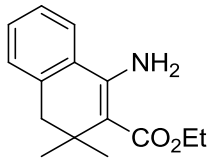

Ethyl 1-amino-3,3-dimethyl-3,4-dihydronaphthalene-2-carboxylate (15). Prepared according to General Method B from *o*-tolunitrile (**14**) and ethyl 3,3-dimethyl acrylate. Isolated as a pale yellow oil (860 mg, 41% yield). TLC R_f = 0.30 (10% EtOAc:hex). ^{1}H NMR (500 MHz, $CDCl_3$) δ (ppm) 7.42 (d, *J* = 8.6 Hz, 1H), 7.36 – 7.29 (m, 2H), 7.20 (d, *J* = 7.3 Hz, 1H), 6.35 (s, 1H), 4.28 (q, *J* = 7.1 Hz, 2H), 2.68 (s, 2H), 1.37 (t, *J* = 7.1 Hz, 3H), 1.22 (s, 6H).

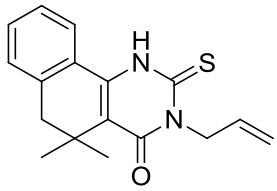

3-Allyl-5,5-dimethyl-2-thioxo-2,3,5,6-tetrahydrobenzo[h]quinazolin-4(1H)-one (16). Prepared according to General Method C from **15** and allyl isothiocyanate. Purified via trituration of the crude organic isolate with hexanes and diethyl ether; recovered in 24% yield (356 mg) as a white solid. R_f = 0.34 (10% EtOAc:hex). ^{1}H NMR (500 MHz, $CDCl_3$) δ (ppm) 9.28 (s, 1H), 7.50 – 7.37 (m, 3H), 7.29 (d, *J* = 7.4 Hz, 1H), 6.00 (ddt, *J* = 17.1, 10.3, 5.8 Hz, 1H),

5.37 (d, *J* = 17.1 Hz, 1H), 5.27 (d, *J* = 10.3 Hz, 1H), 5.07 (d, *J* = 5.8 Hz, 2H), 2.79 (s, 2H), 1.34 (s, 6H).

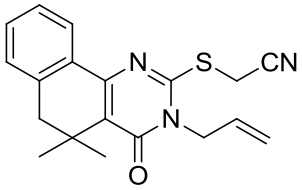

2-((3-Allyl-5,5-dimethyl-4-oxo-3,4,5,6-tetrahydrobenzo[h]quinazolin-2-yl)thio)acetonitrile (21) (CCG-205390). Prepared according to General Method D from intermediate **16**, using α-chloroacetonitrile as the alkylating agent. Isolated via flash chromatography (5% EtOAc:hex) as a white crystalline solid (92 mg, 81% yield). ^{1}H NMR (500 MHz, $CDCl_3$) δ (ppm) 8.16 (d, *J* = 7.0 Hz, 1H), 7.41 – 7.32 (m, 2H), 7.19 (d, *J* = 6.3 Hz, 1H), 5.91 (ddt, *J* = 16.1, 10.6, 5.6 Hz, 1H), 5.34 – 5.26 (m, 2H), 4.65 (d, *J* = 5.6 Hz, 2H), 4.06 (s, 2H), 2.80 (s, 2H), 1.39 (s, 6H). ESI+MS *m/z* = 338.1 ($M + H^+$), 360.1 ($M + Na^+$). HPLC (Method B, t_R = 5.57 min), purity >95%.

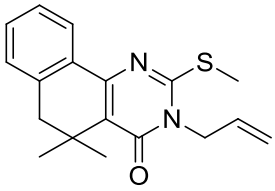

3-Allyl-5,5-dimethyl-2-(methylthio)-5,6-dihydrobenzo[h]quinazolin-4(3H)-one (22). Intermediate **16** (116 mg, 0.39 mmol) was dissolved in EtOH (2.3 mL), to which KOH (38 mg, 0.58 mmol) and methyl iodide (27 μL, 0.43 mmol) were added. The solution was stirred for 30 minutes, precipitating a crystalline white solid. The solution was diluted with ethyl acetate and water. The aqueous layer was extracted with additional EtOAc, then the combined organic layers were washed with water and brine. The organic layer was isolated, dried over $MgSO_4$, vacuum filtered, and concentrated *in vacuo*. The recovered crystalline material (116 mg, 96% yield) was found to be pure by NMR and used without further purification. ^{1}H NMR (400 MHz, $CDCl_3$) δ 8.15 (d, *J* = 7.3, 1H), 7.38-7.28 (m, 2H), 7.18 (d, *J* = 6.9, 1H), 6.01-5.75 (m, 1H), 5.33 – 5.23 (m, 2H), 4.69 (d, *J* = 5.5, 2H), 2.79 (s, 2H), 2.69 (s, 3H), 1.39 (s, 6H). HPLC (Method B, t_R = 7.57 min), purity >95%.

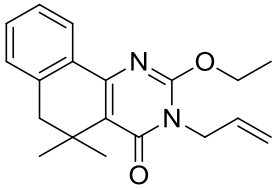

3-Allyl-2-ethoxy-5,5-dimethyl-5,6-dihydrobenzo[h]quinazolin-4(3H)-one (23) (CCG-203803). Metallic sodium was added to absolute ethanol and allowed to stir at room temperature for 30 minutes. Intermediate **22** was added, then the reaction was heated to 40°C and allowed to stir for 48 hours. The reaction was then diluted with water and extracted with ethyl acetate. The organic layer was dried over $MgSO_4$, filtered, and concentrated. Further purification via flash chromatography (15% EtOAc:hex) isolated **23** as a light yellow solid (22 mg, 69% yield). ^{1}H NMR (500 MHz, $CDCl_3$) δ (ppm) 8.09 (d, *J* = 7.3 Hz, 1H), 7.37 – 7.27 (m, 2H), 7.18 (d, *J* = 7.5 Hz, 1H), 5.92 (ddt, *J* = 16.0, 10.3, 5.8 Hz, 1H), 5.25 – 5.16 (m, 2H), 4.62 (d, *J* = 5.8 Hz, 2H), 4.57 (q, *J* = 7.1 Hz, 2H), 2.78 (s, 2H), 1.45 (t, *J* = 7.1 Hz, 3H), 1.37 (s, 6H). ESI+MS *m/z* = 311.1 ($M + H^+$), 333.1 ($M + Na^+$). HPLC (Method B, t_R = 7.94 min), purity >95%.

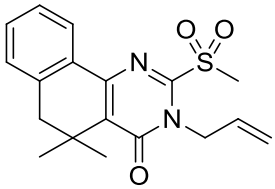

3-Allyl-5,5-dimethyl-2-(methylsulfonyl)-5,6-dihydrobenzo[h]quinazolin-4(3H)-one (intermediate in the synthesis of 24). The methyl sulfide intermediate **22** (116 mg, 0.371 mmol) and *m*CPBA (70 wt%, 229 mg, 0.928 mmol) were combined in DCM (5.6 mL) at 0°C. The reaction mixture was maintained at 0°C for 1 hour, then allowed to warm to RT over 16 hours. The reaction mixture was diluted with DCM and washed with saturated aqueous sodium bicarbonate solution, water, and brine, then isolated, dried over $MgSO_4$, filtered, and concentrated *in vacuo*. Purification of the crude material by FC (10g column, 5% -> 10% EtOAc:hex) afforded the desired product, confirmed by NMR, as a yellowish solid (70 mg, 55% yield). ^{1}H NMR (500 MHz, Chloroform-*d*) δ 7.92 (d, *J* = 7.6 Hz, 1H), 7.42 (t, *J* = 7.3 Hz, 1H), 7.35 (t, *J* = 7.3 Hz, 1H), 7.24 (d, *J* = 7.3 Hz, 1H), 6.10 – 6.00 (m, 1H), 5.42 (d, *J* = 17.2 Hz, 1H), 5.33 (d, *J* = 8.3 Hz, 1H), 5.03 (d, *J* = 5.8 Hz, 2H), 3.58 (s, 3H), 2.85 (s, 2H), 1.42 (s, 6H).

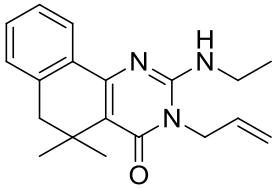

3-Allyl-2-(ethylamino)-5,5-dimethyl-5,6-dihydrobenzo[h]quinazolin-4(3H)-one (24) (CCG-203804). Prepared in a manner similar to **13** from the sulfone intermediate above (70 mg, 0.203 mmol). Isolated the desired compound as a white solid (48 mg, 77% yield; 41% overall yield from **22**). ^{1}H NMR (500 MHz, $CDCl_3$) δ (ppm) 8.15 (d, *J* = 7.3 Hz, 1H), 7.36 – 7.26 (m, 2H), 7.16 (d, *J* = 7.4 Hz, 1H), 5.92 (ddt, *J* = 17.3, 10.5, 5.3 Hz, 1H), 5.36 – 5.26 (m, 2H), 4.68 (d, *J* = 5.2 Hz, 2H), 4.58 (t, *J* = 4.9 Hz, 1H), 3.57 (qd, *J* = 7.2, 5.2 Hz, 2H), 2.77 (s, 2H), 1.37 (s, 6H), 1.28 (t, 3H). ESI+MS *m/z* = 310.1 ($M + H^+$), 332.1 ($M + Na^+$). HPLC (Method B, t_R = 5.47 min), purity >95%.

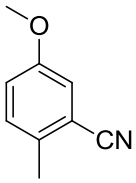

5-Methoxy-2-methylbenzonitrile (26a). Synthesized from **25a** according to General Method A. Isolated in 90% yield. ^{1}H NMR (400 MHz, $CDCl_3$) δ (ppm) 7.21 (d, *J* = 8.5 Hz, 1H), 7.08 (d, *J* = 2.8 Hz, 1H), 7.03 (dd, *J* = 8.5, 2.8 Hz, 1H), 3.81 (s, 3H), 2.47 (s, 3H).

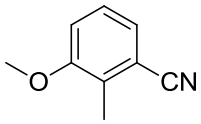

3-Methoxy-2-methylbenzonitrile (26b). Synthesized from **25b** according to General Method A. Isolated as a clear oil, 68% yield. ^{1}H NMR (500 MHz, $CDCl_3$) δ (ppm) 7.24 (t, *J* = 7.9 Hz, 1H), 7.19 (d, *J* = 7.7 Hz, 1H), 7.03 (d, *J* = 8.1 Hz, 1H), 3.86 (s, 3H), 2.42 (s, 3H).

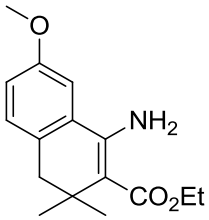

Ethyl 1-amino-7-methoxy-3,3-dimethyl-3,4-dihydronaphthalene-2-carboxylate (27a). Prepared according to General Method B from **26a** and ethyl 3,3-dimethyl acrylate. Isolated as a pale yellow oil (623 mg, 33% yield). ^{1}H NMR (500 MHz, $CDCl_3$) δ (ppm) 7.11 (d, *J* = 8.1 Hz, 1H), 6.96 (s, 1H), 6.88 (d, *J* = 8.1 Hz, 1H), 6.27 (s, 2H), 4.27 (q, *J* = 7.1 Hz, 2H), 3.85 (s, 3H), 2.60 (s, 2H), 1.37 (t, *J* = 7.1 Hz, 3H), 1.20 (s, 6H).

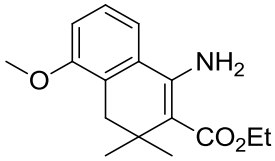

Ethyl 1-amino-5-methoxy-3,3-dimethyl-3,4-dihydronaphthalene-2-carboxylate (27b). Prepared according to General Method B from **26b** and ethyl 3,3-dimethyl acrylate. Isolated as a yellow oily solid (636 mg, 35% yield). ^{1}H NMR (500 MHz, $CDCl_3$) δ (ppm) 7.24 (t, *J* = 8.1 Hz, 2H), 7.04 (d, *J* = 8.1 Hz, 1H), 6.92 (d, *J* = 8.1 Hz, 1H), 6.31 (s, 2H), 4.25 (q, *J* = 7.1 Hz, 2H), 3.85 (s, 3H), 2.66 (s, 2H), 1.34 (t, *J* = 7.1 Hz, 3H), 1.20 (s, 6H).

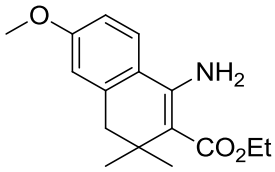

Ethyl 1-amino-6-methoxy-3,3-dimethyl-3,4-dihydronaphthalene-2-carboxylate (27c). Prepared according to General Method B from **26c** and ethyl 3,3-dimethyl acrylate. Isolated as pale yellow crystals (1.108 g, 59% yield). TLC R_f = 0.14 (10% EtOAc:hex). ^{1}H NMR (500 MHz, $CDCl_3$) δ (ppm) 7.35 (d, *J* = 8.5 Hz, 1H), 6.81 (dd, *J* = 8.5, 2.4 Hz, 1H), 6.73 (d, *J* = 2.4 Hz, 1H), 6.37 (s, 1H), 4.26 (q, *J* = 7.1 Hz, 2H), 3.86 (s, 3H), 2.64 (s, 2H), 1.36 (t, *J* = 7.1 Hz, 3H), 1.22 (s, 6H).

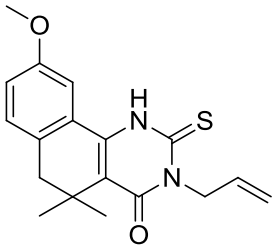

3-Allyl-9-methoxy-5,5-dimethyl-2-thioxo-2,3,5,6-tetrahydrobenzo[h]quinazolin-4(1H)-one (28a). Prepared according to General Method C from **27a** and allyl isothiocyanate. Purified via trituration with hexanes and diethyl ether (125 mg, 21% yield). ^{1}H NMR (400 MHz, $CDCl_3$) δ (ppm) 9.29 (s, 1H), 7.35 (d, *J* = 8.0 Hz, 1H), 7.06 (d, *J* = 8.0 Hz, 1H), 7.00 (s, 1H), 6.08 (ddt, *J* = 15.8, 10.9, 5.5 Hz, 1H), 5.45 – 5.30 (m, 2H), 5.18 (d, *J* = 5.5 Hz, 2H), 3.85 (s, 3H), 2.73 (s, 2H), 1.34 (s, 6H).

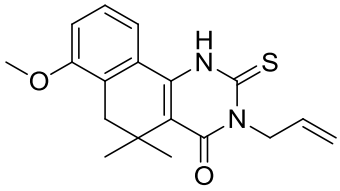

3-Allyl-7-methoxy-5,5-dimethyl-2-thioxo-2,3,5,6-tetrahydrobenzo[h]quinazolin-4(1H)-one (28b). Prepared according to General Method C from **27b** and allyl isothiocyanate. Purified via trituration of the crude organic isolate with hexanes and diethyl ether (133 mg, 24% yield). ^{1}H NMR (500 MHz, $CDCl_3$) δ (ppm) 9.29 (s, 1H), 7.35 (t, *J* = 8.0 Hz, 1H), 7.08 – 7.01 (m, 2H), 6.00 (ddt, *J* = 16.8, 10.8, 5.8 Hz, 1H), 5.37 (d, *J* = 16.8 Hz, 1H), 5.27 (d, *J* = 10.8 Hz, 1H), 5.06 (d, *J* = 5.8 Hz, 2H), 3.89 (s, 3H), 2.79 (s, 2H), 1.34 (s, 6H).

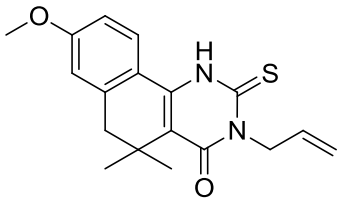

3-Allyl-8-methoxy-5,5-dimethyl-2-thioxo-2,3,5,6-tetrahydrobenzo[h]quinazolin-4(1H)-one (28c). Prepared according to General Method C from **27c** and allyl isothiocyanate. Purified via trituration of the crude organic isolate with hexanes and diethyl ether; isolated as tan crystals (252 mg, 59% yield). TLC R_f = 0.11 (10% EtOAc:hex). ^{1}H NMR (400 MHz, $CDCl_3$) δ (ppm)

9.27 (s, 1H), 7.38 (d, *J* = 8.6 Hz, 1H), 6.88 (dd, *J* = 8.6, 2.5 Hz, 1H), 6.80 (d, *J* = 2.5 Hz, 1H), 5.99 (ddt, *J* = 16.6, 10.4, 5.7 Hz, 1H), 5.36 (dd, *J* = 16.6, 1.3 Hz, 2H), 5.26 (dd, *J* = 10.4, 1.3 Hz, 1H), 5.06 (d, *J* = 5.7 Hz, 2H), 3.87 (s, 3H), 2.74 (s, 2H), 1.33 (s, 6H). ESI-MS *m/z* = 327 ($M-H^+$).

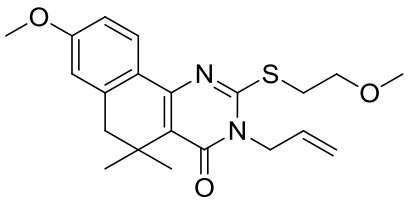

3-Allyl-8-methoxy-2-((2-methoxyethyl)thio)-5,5-dimethyl-5,6-dihydrobenzo[h]quinazolin-4(3H)-one (29) (CCG-203576). Prepared according to General Method D from intermediate **28c**, using 2-methoxyethyl *p*-toluenesulfonate as the alkylating agent. Isolated as a crystalline white solid after flash chromatography (67 mg, 76% yield). ^{1}H NMR (500 MHz, $CDCl_3$) δ (ppm) 8.01 (d, *J* = 8.6 Hz, 1H), 6.83 (d, *J* = 8.6 Hz, 1H), 6.71 (s, 1H), 5.92 (ddt, *J* = 16.1, 10.6, 5.5 Hz, 1H), 5.31 – 5.23 (m, 2H), 4.69 (d, *J* = 5.5 Hz, 2H), 3.86 (s, 3H), 3.75 (t, *J* = 6.3 Hz, 2H), 3.52 (t, *J* = 6.3 Hz, 2H), 3.42 (s, 3H), 2.75 (s, 2H), 1.38 (s, 6H). ESI+MS *m/z* = 387.2 ($M + H^+$), 409.2 ($M + Na^+$). HPLC (Method B, t_R = 7.05 min), purity >95%.

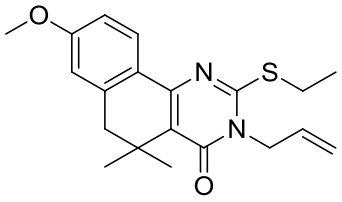

3-Allyl-2-(ethylthio)-8-methoxy-5,5-dimethyl-5,6-dihydrobenzo[h]quinazolin-4(3H)-one (31) (CCG-203592). Prepared according to General Method D from intermediate **28c**, using iodoethane as the alkylating agent. Isolated as white crystals via flash chromatography (105 mg, 88% yield). ^{1}H NMR (500 MHz, $CDCl_3$) δ (ppm) 8.05 (d, *J* = 8.6 Hz, 1H), 6.84 (dd, *J* = 8.6, 2.4 Hz, 1H), 6.71 (d, *J* = 2.1 Hz, 1H), 5.93 (ddt, *J* = 15.8, 10.8, 5.5 Hz, 1H), 5.30 – 5.22 (m, 2H), 4.67 (d, *J* = 5.4 Hz, 2H), 3.86 (s, 3H), 3.30 (q, *J* = 7.3 Hz, 2H), 2.75 (s, 2H), 1.47 (t, *J* = 7.3 Hz, 3H), 1.38 (s, 6H). ESI+MS *m/z* = 357.2 ($M + H^+$), 379.2 ($M + Na^+$). HPLC (Method B, t_R = 8.26 min), purity >95%.

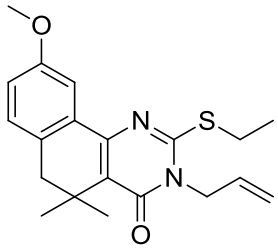

3-Allyl-2-(ethylthio)-9-methoxy-5,5-dimethyl-2,3,5,6-tetrahydrobenzo[h]quinazolin-4(1H)-one (32) (CCG-203625). Prepared according to General Method D from intermediate **28a**, using iodoethane as the alkylating agent. Isolated via flash chromatography as a white solid (74 mg, 71% yield). ^{1}H NMR (400 MHz, $CDCl_3$) δ (ppm) 7.70 (s, 1H), 7.10 (d, *J* = 8.2 Hz, 1H), 6.91 (d, *J* = 8.2 Hz, 1H), 5.93 (ddt, *J* = 15.8, 10.9, 5.5 Hz, 1H), 5.33 – 5.21 (m, 2H), 4.68 (d, *J* = 5.5 Hz, 2H), 3.85 (s, 3H), 3.31 (q, *J* = 7.3 Hz, 2H), 2.72 (s, 2H), 1.49 (t, *J* = 7.3 Hz, 3H), 1.37 (s, 6H). ESI+MS *m/z* = 357.2 ($M + H^+$), 379.2 ($M + Na^+$). HPLC (Method B, t_R = 8.53 min) purity >95%.

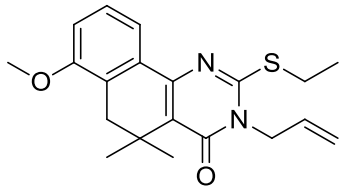

3-Allyl-2-(ethylthio)-7-methoxy-5,5-dimethyl-5,6-dihydrobenzo[h]quinazolin-4(3H)-one (33) (CCG-203629). Prepared according to General Method D from intermediate **28b**, using iodoethane as the alkylating agent. Isolated via flash chromatography (75 mg, 69% yield). ^{1}H NMR (500 MHz, $CDCl_3$) δ (ppm) 7.80 (d, *J* = 7.8 Hz, 1H), 7.30 (t, *J* = 8.0 Hz, 1H), 6.97 (d, *J* = 8.1 Hz, 1H), 5.95 (ddt, *J* = 16.0, 10.6, 5.6 Hz, 1H), 5.34 – 5.25 (m, 2H), 4.70 (d, *J* = 5.5 Hz, 2H), 3.90 (s, 3H), 3.33 (q, *J* = 7.3 Hz, 2H), 2.82 (s, 2H), 1.49 (t, *J* = 7.3 Hz, 3H), 1.41 (s, 6H). ESI+MS *m/z* = 357.2 ($M + H^+$), 379.1 ($M + Na^+$). HPLC (Method B, t_R = 8.52 min), purity >95%.

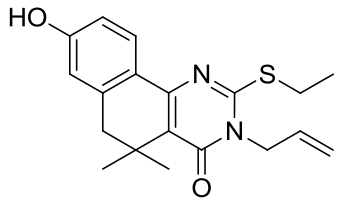

3-Allyl-2-(ethylthio)-8-hydroxy-5,5-dimethyl-5,6-dihydrobenzo[h]quinazolin-4(3H)-one (34) (CCG-203594). Prepared according to General Method E from compound **31.** Isolated as tan crystals (310 mg, 43% yield). ^{1}H NMR (500 MHz, $CDCl_3$) δ (ppm) 7.62 (d, *J* = 8.2 Hz, 1H), 6.85 – 6.79 (m, 2H), 5.88 (ddt, *J* = 16.3, 10.8, 5.9 Hz, 1H), 5.48 – 5.40 (m, 2H), 4.86 (d, *J* = 5.9 Hz, 2H), 4.22 (q, *J* = 7.3 Hz, 2H), 2.74 (s, 2H), 1.59 (t, *J* = 7.3 Hz, 3H), 1.31 (s, 6H).

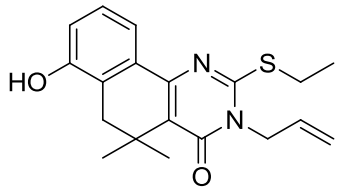

3-Allyl-2-(ethylthio)-7-hydroxy-5,5-dimethyl-5,6-dihydrobenzo[h]quinazolin-4(3H)-one (35) (CCG-203631). Prepared according to General Method E from compound **33.** Isolated as a tan solid (43 mg, 45% yield). ^{1}H NMR (500 MHz, $CDCl_3$) δ (ppm) 7.76 (d, *J* = 7.8 Hz, 1H), 7.18 (t, *J* = 7.8 Hz, 1H), 6.89 (d, *J* = 7.8 Hz, 1H), 5.99 – 5.87 (m, 1H), 5.31 – 5.24 (m, 2H), 5.18 (s, 1H), 4.68 (d, *J* = 5.5 Hz, 2H), 3.31 (q, *J* = 7.4 Hz, 2H), 2.78 (s, 2H), 1.47 (t, *J* = 7.4 Hz, 3H), 1.41 (s, 6H).

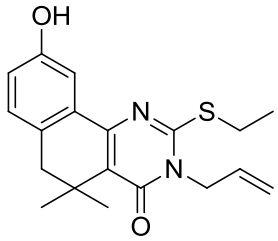

3-Allyl-2-(ethylthio)-9-hydroxy-5,5-dimethyl-5,6-dihydrobenzo[h]quinazolin-4(3H)-one (36). Prepared according to General Method E from compound **32.** Isolated as a tan solid (60 mg, 62% yield). ^{1}H NMR (500 MHz, $CDCl_3$) δ (ppm) 7.91 (s, 1H), 7.05 (d, *J* = 8.2 Hz, 1H), 6.98 (d, *J* = 8.2 Hz, 1H), 5.90 (ddt, *J* = 16.3, 10.7, 5.6 Hz, 1H), 5.44 – 5.36 (m, 2H), 4.83 (d, *J* = 5.6 Hz, 2H), 3.95 (q, *J* = 6.8 Hz, 2H), 2.75 (s, 2H), 1.52 (t, *J* = 6.8 Hz, 3H), 1.36 (s, 6H).

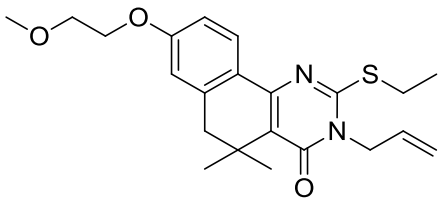

3-Allyl-2-(ethylthio)-8-(2-methoxyethoxy)-5,5-dimethyl-5,6-dihydrobenzo[h]quinazolin-4(3H)-one (37) (CCG-203596). Prepared using General Method F from phenol intermediate **34** and 2-methoxyethyl *p*-toluenesulfonic ester**,** heated to 70°C for 16 hours**.** Reaction mixture was partitioned between ethyl acetate and water, then the organic layer washed with water and brine. The organic layer was isolated, dried over $MgSO_4$, vacuum filtered, and concentrated *in vacuo.* Further purification via flash chromatography (0-10% EtOAc:hex) delivered the desired product (39 mg, 71% yield). ^{1}H NMR (500 MHz, $CDCl_3$) δ (ppm) 8.04 (d, *J* = 8.6 Hz, 1H), 6.86 (dd, *J* = 8.6, 2.4 Hz, 1H), 6.74 (d, *J* = 2.2 Hz, 1H), 5.92 (ddt, *J* = 15.9, 10.6, 5.4 Hz, 1H), 5.30 – 5.22 (m, 2H), 4.67 (d, *J* = 5.5 Hz, 2H), 4.18 (t, *J* = 5.0 Hz, 2H), 3.78 (t, *J* = 5.0 Hz, 2H), 3.47 (s, 3H), 3.30 (q, *J* = 7.4 Hz, 2H), 2.74 (s, 2H), 1.47 (t, *J* = 7.3 Hz, 3H), 1.37 (s, 6H). ESI+MS *m/z* = 401.1 (M + H^+), 423.1 (M + Na^+). HPLC (Method B, t_R = 7.56 min), purity >95%.

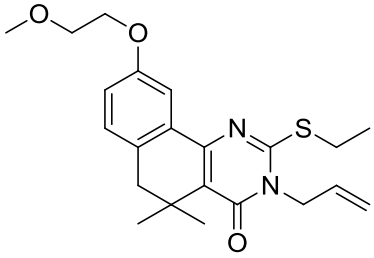

3-Allyl-2-(ethylthio)-9-(2-methoxyethoxy)-5,5-dimethyl-5,6-dihydrobenzo[h]quinazolin-4(3H)-one (38) (CCG-203627). Prepared using General Method F from **36** and 2-methoxyethyl *p*-toluenesulfonic ester**,** heated to 70°C for 16 hours**.** Reaction mixture was partitioned between ethyl acetate and water, then the organic layer washed with water and brine. The organic layer was isolated, dried over $MgSO_4$, vacuum filtered, and concentrated *in vacuo.* Further purification via flash chromatography (0-10% EtOAc:hex) delivered the desired product (38 mg, 65% yield). ^{1}H NMR (500 MHz, $CDCl_3$) δ (ppm) 7.71 (s, 1H), 7.09 (d, *J* = 8.2 Hz, 1H), 6.94 (d, *J* = 8.2 Hz, 1H), 5.93 (ddt, *J* = 16.0, 10.7, 5.6 Hz, 1H), 5.31 – 5.23 (m, 2H), 4.68 (d, *J* = 5.5 Hz, 2H), 3.81 – 3.75 (m, 2H), 3.61 – 3.55 (m, 2H), 3.47 (s, 3H), 3.31 (q, *J* = 7.3 Hz, 2H), 2.72 (s, 2H), 1.48 (t, *J*

= 7.3 Hz, 3H), 1.37 (s, 6H). ESI+MS *m/z* = 401.2 ($M + H^+$), 423.2 ($M + Na^+$). HPLC (Method B, t_R = 7.83 min), purity >95%.

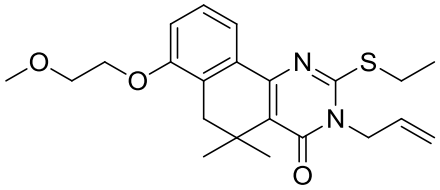

3-Allyl-2-(ethylthio)-7-(2-methoxyethoxy)-5,5-dimethyl-5,6-dihydrobenzo[h]quinazolin-4(3H)-one (39) (CCG-203633). Prepared using General Method F from phenol intermediate **35** and 2-methoxyethyl *p*-toluenesulfonic ester**,** heated to 70°C for 16 hours**.** Reaction mixture was partitioned between ethyl acetate and water, then the organic layer washed with water and brine. The organic layer was isolated, dried over $MgSO_4$, vacuum filtered, and concentrated *in vacuo.* Further purification via flash chromatography (0-10% EtOAc:hex) delivered the desired product (36 mg, 68% yield). ^{1}H NMR (500 MHz, $CDCl_3$) δ (ppm) 7.78 (d, *J* = 7.8 Hz, 1H), 7.25 (t, *J* = 8.0 Hz, 1H), 6.96 (d, *J* = 8.1 Hz, 1H), 5.99 – 5.87 (m, 1H), 5.31 – 5.23 (m, 2H), 4.68 (d, *J* = 5.5 Hz, 2H), 4.17 (dd, *J* = 5.5, 4.2 Hz, 2H), 3.80 (dd, *J* = 5.5, 4.2 Hz, 2H), 3.48 (s, 3H), 3.30 (q, *J* = 7.4 Hz, 2H), 2.83 (s, 2H), 1.47 (t, *J* = 7.4 Hz, 3H), 1.39 (s, 6H). ESI+MS *m/z* = 401.2 ($M + H^+$), 423.2 ($M + Na^+$). HPLC (Method B, t_R = 7.91 min), purity >95%.

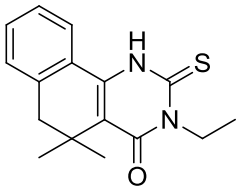

3-Ethyl-5,5-dimethyl-2-thioxo-2,3,5,6-tetrahydrobenzo[h]quinazolin-4(1H)-one (40a). Prepared according to General Method C from **15** and ethyl isothiocyanate. Purified via flash chromatography (0 to 10% EtOAc:hex); recovered in 31% yield. TLC R_f = 0.20 (10% EtOAc:hex). ^{1}H NMR (500 MHz, $CDCl_3$) δ (ppm) 9.24 (s, 1H), 7.49 – 7.35 (m, 3H), 7.29 (d, *J* = 7.4 Hz, 1H), 4.49 (q, *J* = 7.0 Hz, 2H), 2.79 (s, 2H), 1.35 (t, *J* = 7.0 Hz, 3H), 1.34 (s, 6H).

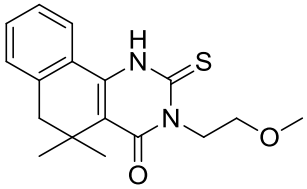

3-(2-Methoxyethyl)-5,5-dimethyl-2-thioxo-2,3,5,6-tetrahydrobenzo[h]quinazolin-4(1H)-one (40b). Prepared according to General Method C from **15** and 2-methoxyethyl isothiocyanate. Evaporation of the solvent, followed by trituration with ethyl acetate returned the desired product as a white crystalline solid (40 mg, 27% yield). ^{1}H NMR (300 MHz, $CDCl_3$) δ (ppm) 9.40 (s, 1H), 7.50-7-31 (m, 4H), 4.70 (t, *J* = 6.2 Hz, 2H), 3.80 (t, *J* = 6.2 Hz, 2H), 3.43 (s, 3H), 2.80 (s, 2H), 1.35 (s, 6H).

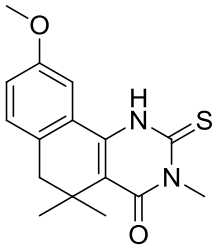

9-Methoxy-3,5,5-trimethyl-2-thioxo-2,3,5,6-tetrahydrobenzo[h]quinazolin-4(1H)-one (40c). Prepared according to General Method C from **27a** and methyl isothiocyanate. Purified via flash chromatography (0-10% EtOAc:hex) and recovered in 27% yield. ^{1}H NMR (400 MHz, $CDCl_3$) δ (ppm) 9.35 (s, 1H), 7.20 (d, *J* = 8.3 Hz, 1H), 6.99 (dd, *J* = 8.3, 2.3 Hz, 1H), 6.94 (d, *J* = 2.3 Hz, 1H), 3.87 (s, 3H), 3.74 (s, 3H), 2.71 (s, 2H), 1.33 (s, 6H).

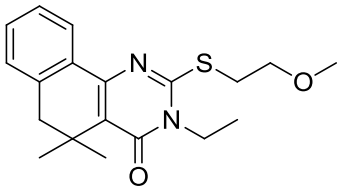

3-Ethyl-2-((2-methoxyethyl)thio)-5,5-dimethyl-5,6-dihydrobenzo[h]quinazolin-4(3H)-one (41) (CCG-203598). Prepared according to General Method D from intermediate **40a**, using 2-methoxyethyl *p*-toluenesulfonate as the alkylating agent. Isolated as a clear oil after flash chromatography (66 mg, 71% yield). ^{1}H NMR (500 MHz, $CDCl_3$) δ (ppm) 8.09 (dd, *J* = 7.5, 1.3 Hz, 1H), 7.37 (td, *J* = 7.3, 1.6 Hz, 1H), 7.33 (td, *J* = 7.5, 1.4 Hz, 1H), 7.21 (d, *J* = 6.9 Hz, 1H), 4.14 (q, *J* = 7.1 Hz, 2H), 3.80 (t, *J* = 6.2 Hz, 2H), 3.57 (t, *J* = 6.2 Hz, 2H), 3.46 (s, 3H), 2.81 (s,

2H), 1.43 – 1.36 (m, 9H). ESI+MS *m/z* = 345.2 ($M + H^+$), 367.2 ($M + Na^+$). HPLC (Method B, t_R = 7.53 min), purity >95%.

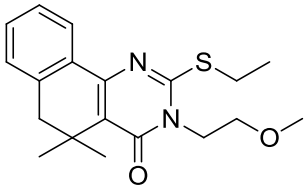

2-(Ethylthio)-3-(2-methoxyethyl)-5,5-dimethyl-5,6-dihydrobenzo[h]quinazolin-4(3H)-one (42) (CCG-203802). Prepared according to General Method D from intermediate **40b**, using iodoethane as the alkylating agent. Isolated as a clear oil after flash chromatography. ^{1}H NMR (500 MHz, $cdcl_3$) δ 8.11 (dd, *J* = 7.5, 1.5, 1H), 7.38 – 7.33 (td, J = 7.5, 1.5, 1H), 7.31 (td, *J* = 7.5, 1.5, 1H), 7.18 (d, *J* = 6.9, 1H), 4.26 (t, *J* = 6.4, 2H), 3.71 (t, *J* = 6.4, 2H), 3.40 (s, 3H), 3.32 (q, *J* = 7.4, 2H), 2.79 (s, 2H), 1.48 (t, *J* = 7.4, 3H), 1.38 (s, 6H). ESI+MS *m/z* = 345.2 ($M + H^+$), 367.2 ($M + Na^+$). HPLC (Method B, t_R = 7.95 min), purity >95%.

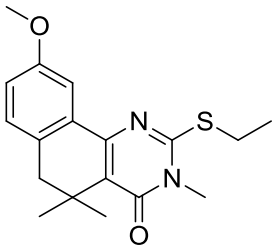

2-(Ethylthio)-9-methoxy-3,5,5-trimethyl-5,6-dihydrobenzo[h]quinazolin-4(3H)-one (43) (CCG-206353). Prepared according to General Method D from intermediate **40c**, using iodoethane as the alkylating agent. Isolated as a colorless oil (20 mg, 55% yield) after flash chromatography. ^{1}H NMR (400 MHz, $CDCl_3$) δ (ppm) 7.70 (s, 1H), 7.10 (d, *J* = 8.2 Hz, 1H), 6.90 (d, *J* = 8.2 Hz, 1H), 3.85 (s, 3H), 3.50 (s, 3H), 3.32 (q, *J* = 7.3 Hz, 2H), 2.72 (s, 2H), 1.50 (t, *J* = 7.3 Hz, 3H), 1.38 (s, 6H). ESI+MS *m/z* = 331.2 ($M + H^+$), 353.2 ($M + Na^+$). HPLC (Method A, t_R = 9.25 min), purity >95%.

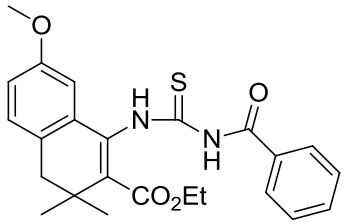

Ethyl 1-(3-benzoylthioureido)-7-methoxy-3,3-dimethyl-3,4-dihydronaphthalene-2-carboxylate (intermediate leading to 44b). To a solution of β-aminoester intermediate **27a** (3.47 g, 12.64 mmol) in absolute EtOH (15 mL) was added benzoyl isothiocyanate (1.7 mL, 12.64 mmol), and the reaction mixture was warmed to reflux for 30 minutes. Additional benzoyl isothiocyanate (400 μL, 2.7 mmol) was added in two equal portions over the course of 1 hour, then the reaction was allowed to cool. The thiourea adduct can be purified via crystallization from ethanol, but was generally used as a crude mixture in the next step with assumed 100% conversion. ^{1}H NMR (400 MHz, Chloroform-*d*) δ 11.70 (s, 1H), 9.17 (s, 1H), 7.91 (d, *J* = 7.4 Hz, 2H), 7.71 – 7.62 (m, 1H), 7.55 (t, *J* = 7.8 Hz, 2H), 7.10 (d, *J* = 8.2 Hz, 1H), 6.85 (d, *J* = 2.6 Hz, 1H), 6.80 (dd, *J* = 8.3, 2.3 Hz, 1H), 4.26 (q, *J* = 7.1 Hz, 2H), 3.77 (s, 3H), 2.76 (s, 2H), 1.29 (t, *J* = 7.1 Hz, 3H), 1.25 (s, 6H).

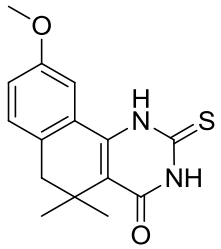

9-Methoxy-5,5-dimethyl-2-thioxo-2,3,5,6-tetrahydrobenzo[h]quinazolin-4(1H)-one (44b). The crude benzoyl thiourea adduct (12.64 mmol) was added to a solution of KOH (1.21 g, 21.57 mmol) in ethanol:water (2:1, 30 mL). The reaction mixture was warmed to reflux and allowed to stir for 1.5 hours. The reaction mixture was cooled, then acidified to pH 5-6 with 1N HCl. The resulting precipitate was isolated via vacuum filtration, washed with EtOH and water and dried under high vacuum. Isolated in 62% yield (2.26 g) over 2 steps as a white crystalline solid. ^{1}H NMR (400 MHz, $CDCl_3$) δ (ppm) 9.32 (s, 2H), 7.20 (d, *J* = 8.2 Hz, 1H), 7.00 (dd, *J* = 8.2, 2.4 Hz, 1H), 6.97 (d, *J* = 2.4 Hz, 1H), 3.87 (s, 3H), 2.71 (s, 2H), 1.32 (s, 6H).

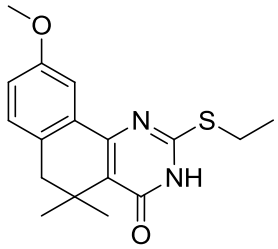

2-(Ethylthio)-9-methoxy-5,5-dimethyl-5,6-dihydrobenzo[h]quinazolin-4(3H)-one (45b). The 2-thioxo intermediate **44b** (118 mg, 0.409 mmol) was dissolved in EtOH (2.4 mL), to which KOH (23 mg, 0.409 mmol) and iodoethane (64 mg, 0.409 mmol) were added. The reaction was warmed to 75°C and allowed to stir for 3 hours. The reaction mixture was diluted with 1N HCl and the resulting precipitate was collected via sintered glass funnel, washed with water, and dried under high vacuum. Isolated the desired product as a white powder (91 mg, 71% yield). ^{1}H NMR (400 MHz, DMSO-d_6) δ 12.53 (s, 1H), 7.61 (d, J = 2.3 Hz, 1H), 7.17 (d, J = 8.2 Hz, 1H), 6.96 (dd, J = 8.3, 2.7 Hz, 1H), 3.78 (s, 3H), 3.22 (q, J = 7.3 Hz, 2H), 2.68 (s, 2H), 1.39 (t, J = 7.3 Hz, 3H), 1.27 (s, 6H).

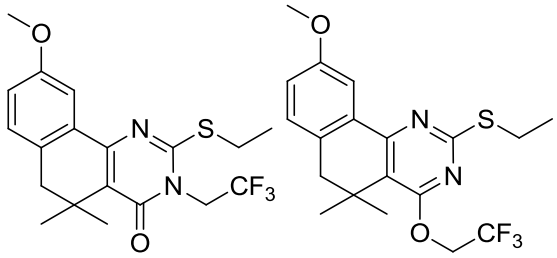

2-(Ethylthio)-9-methoxy-5,5-dimethyl-3-(2,2,2-trifluoroethyl)-5,6-dihydrobenzo[h]quinazolin-4(3H)-one (47) (CCG-206357) and 2-(Ethylthio)-9-methoxy-5,5-dimethyl-4-(2,2,2-trifluoroethoxy)-5,6-dihydrobenzo[h]quinazoline (49) (CCG-206356). A portion of the *S*-alkylated adduct (27 mg, 0.085 mmol) was combined with 1,1,1-trifluoro-2-iodoethane (27 mg, 0.128 mmol) and Cs_2CO_3 (33 mg, 0.102 mmol) in DMF (500 μL). The reaction was tightly capped and heated to 70°C for 16 hours. The reaction mixture was partitioned between ethyl acetate and water, then the organic layer was washed with water and brine. The organic layer was concentrated *in vacuo* and purified via flash chromatography (0-3% EtOAc:hex) to yield compounds **47** (6 mg, 13% yield over 2 steps) and **49** (17 mg, 36% yield over 2 steps) as crystalline white solids.

2-(Ethylthio)-9-methoxy-5,5-dimethyl-3-(2,2,2-trifluoroethyl)-5,6-dihydrobenzo[h]quinazolin-4(3H)-one (47) (CCG-206357). ^{1}H NMR (400 MHz, $CDCl_3$) δ (ppm) 7.68 (d, *J* = 2.8 Hz, 1H), 7.11 (d, *J* = 8.2 Hz, 1H), 6.93 (dd, *J* = 8.2, 2.8 Hz, 1H), 4.78 (q, *J* = 8.0 Hz, 2H), 3.85 (s, 3H), 3.35 (q, *J* = 7.3 Hz, 2H), 2.74 (s, 2H), 1.50 (t, *J* = 7.3 Hz, 3H), 1.36 (s, 6H). ESI+MS *m/z* = 399.2 ($M + H^+$), 421.2 ($M + Na^+$). HPLC (Method B, t_R = 8.49 min), purity >95%.

2-(Ethylthio)-9-methoxy-5,5-dimethyl-4-(2,2,2-trifluoroethoxy)-5,6-dihydrobenzo[h]quinazoline (49) (CCG-206356). ^{1}H NMR (400 MHz, $CDCl_3$) δ (ppm) 7.81 (d, *J* = 2.7 Hz, 1H), 7.10 (d, *J* = 8.2 Hz, 1H), 6.94 (dd, *J* = 8.2, 2.7 Hz, 1H), 4.80 (q, *J* = 8.5 Hz, 2H), 3.87 (s, 3H), 3.21 (q, *J* = 7.3 Hz, 2H), 2.76 (s, 2H), 1.47 (t, *J* = 7.3 Hz, 3H), 1.33 (s, 6H). ESI+MS *m/z* = 399.2 ($M + H^+$). HPLC (Method A, t_R = 9.84 min), purity >95%.

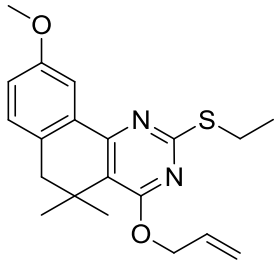

4-(Allyloxy)-2-(ethylthio)-9-methoxy-5,5-dimethyl-5,6-dihydrobenzo[h]quinazoline (50) (CCG-206358). A portion of the *S*-alkylated adduct (30 mg, 0.095 mmol) was combined with Cs_2CO_3 (37 mg, 0.114 mmol) and allyl bromide (17 mg, 0.142 mmol) in DMF (558 μL). The reaction mixture was tightly capped and warmed to 75°C, and allowed to stir for 16 hours. The reaction mixture was partitioned between ethyl acetate and water, then the organic layer was washed with water and brine. The organic layer was concentrated *in vacuo*, and the residue was purified via flash chromatography (0-5% EtOAc:hex) to yield **50** (14 mg, 30% yield over 2 steps). ^{1}H NMR (400 MHz, $CDCl_3$) δ (ppm) 7.81 (d, *J* = 2.5 Hz, 1H), 7.08 (d, *J* = 8.2 Hz, 1H), 6.91 (dd, *J* = 8.2, 2.5 Hz, 1H), 6.09 (ddt, *J* = 16.4, 10.6, 5.5 Hz, 1H), 5.40 (d, *J* = 16.4 Hz, 1H), 5.27 (d, *J* = 10.6 Hz, 1H), 4.94 (d, *J* = 5.5 Hz, 2H), 3.87 (s, 3H), 3.19 (q, *J* = 7.3 Hz, 2H), 2.74 (s, 2H), 1.47 (t, *J* = 7.3 Hz, 3H), 1.33 (s, 6H). ESI+MS *m/z* = 357.2 ($M + H^+$), 379.2 ($M + Na^+$). HPLC (Method B, t_R = 10.41 min), purity >95%. *N*-allyl compound **32** was also isolated (10 mg, 21% yield over 2 steps).

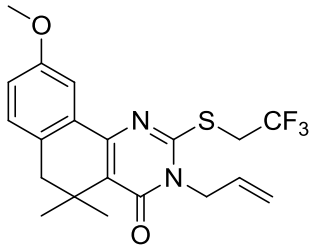

3-Allyl-9-methoxy-5,5-dimethyl-2-((2,2,2-trifluoroethyl)thio)-5,6-dihydrobenzo[h]quinazolin-4(3H)-one (51) (CCG-206352). Prepared according to General Method D from intermediate **28a**, using 2,2,2-trifluoro-1-iodoethane as the alkylating agent. Reaction was heated to 50°C to avoid evaporation of the alkylating agent. Flash chromatography (5-10% EtOAc:hex) delivered the product (7 mg, 24% yield). ^{1}H NMR (400 MHz, $CDCl_3$) δ (ppm) 7.61 (s, 1H), 7.10 (d, *J* = 8.1 Hz, 1H), 6.93 (d, *J* = 8.1 Hz, 1H), 5.93 (ddt, *J* = 16.5, 11.1, 5.6 Hz, 1H), 5.34 – 5.23 (m, 2H), 4.71 (d, *J* = 5.6 Hz, 2H), 4.16 (q, *J* = 9.7 Hz, 2H), 3.84 (s, 3H), 2.73 (s, 2H), 1.37 (s, 6H). ESI+MS *m/z* = 411.2 ($M + H^+$), HPLC (Method B, t_R = 7.98 min), purity = >95%.

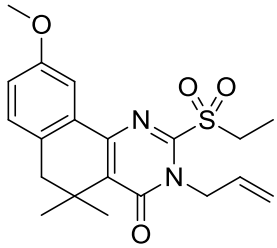

3-Allyl-2-(ethylsulfonyl)-9-methoxy-5,5-dimethyl-5,6-dihydrobenzo[h]quinazolin-4(3H)-one (52) (CCG-206354). Compound **32** (28 mg, 0.79 mmol) and *m*CPBA (70 wt%, 48 mg, 0.196 mmol) were combined in DCM (1.2mL) at 0°C. The reaction mixture was kept at 0°C for 1 hour, then allowed to warm to RT over the course of 16 hours. The reaction mixture was then diluted with more DCM and washed with saturated sodium bicarbonate solution, water, and brine. The organic layer was isolated, dried over $MgSO_4$, vacuum filtered, and concentrated *in vacuo*. Further purification via flash chromatography (5-10% EtOAc:hex) delivered the desired product as a light yellow solid (19 mg, 62% yield). ^{1}H NMR (400 MHz, $CDCl_3$) δ (ppm) 7.43 (s, 1H), 7.14 (d, *J* = 8.2 Hz, 1H), 6.94 (d, *J* = 8.2 Hz, 1H), 6.04 (ddt, *J* = 16.8, 10.3, 5.5 Hz, 1H), 5.40 (d, *J* = 16.8 Hz, 1H), 5.30 (d, *J* = 10.3 Hz, 1H), 5.02 (d, *J* = 5.5 Hz, 2H), 3.84 (s, 3H), 3.81

(q, *J* = 7.3 Hz, 2H), 2.75 (s, 2H), 1.62 (t, *J* = 7.3 Hz, 3H), 1.38 (s, 6H). ESI+MS *m/z* = 389.2 (M + H^+), 411.2 (M + Na^+). HPLC (Method A, t_R = 8.64 min), purity >95%.

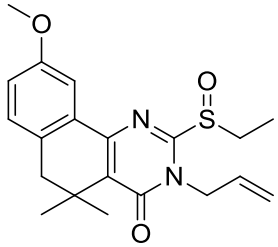

3-Allyl-2-(ethylsulfinyl)-9-methoxy-5,5-dimethyl-5,6-dihydrobenzo[h]quinazolin-4(3H)-one (53) (CCG-206355). Compound **32** (20 mg, 0.056 mmol) was added to a 3.5:1 THF:water mixture (0.617 mL), and the reaction then cooled to 0°C. A solution of Oxone (34 mg, 0.056 mmol) in water (0.411 mL) was added slowly dropwise, and the reaction was allowed to stir 3.5 hours at 0°C, then allowed to warm to room temperature over 16 hours. At this point the reaction was partitioned between EtOAc and water. The organic layer was washed with water and brine, then isolated, dried over $MgSO_4$, vacuum filtered, and concentrated under reduced pressure. The resulting residue was purified via flash chromatography (10-33% EtOAc:hex) to deliver the product as light yellow crystals (13 mg, 62% yield). ^{1}H NMR (400 MHz, $CDCl_3$) δ (ppm) 7.66 (d, *J* = 2.7 Hz, 1H), 7.12 (d, *J* = 8.2 Hz, 1H), 6.93 (dd, *J* = 8.2, 2.7 Hz, 1H), 6.56 – 5.61 (m, 1H), 5.30 (d, *J* = 10.3 Hz, 1H), 5.24 (d, *J* = 17.2 Hz, 1H), 5.13 (ab with 5.00; ddt, *J* = 1.6, 5.0, 15.8 Hz, 1H), 5.00 (ab with 5.13; dd, *J* = 5.0, 15.8 Hz, 1H), 3.86 (s, 3H), 3.46 – 3.27 (m, 2H), 2.75 (s, 2H), 1.43 (t, *J* = 7.5 Hz, 3H), 1.39 (s, 3H), 1.38 (s, 3H). ESI+MS *m/z* = 395.2 (M + H^+). HPLC (Method A, t_R = 7.39 min), purity >95%.

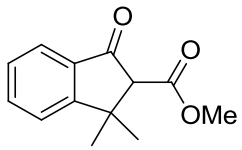

Methyl 1,1-dimethyl-3-oxo-2,3-dihydro-1H-indene-2-carboxylate (55). Sodium hydride (80 wt%, 280 mg, 9.36 mmol) was added to a dry flask containing anhydrous dimethyl carbonate (2.62 mL, 31.2 mmol). The resulting metallic suspension was heated to 80°C, then 3,3-dimethyl 1-indanone (**54**, 500 mg, 3.12 mmol) in anhydrous THF (4 mL) was added over 1 hour via syringe pump. The reaction was allowed to stir at 80°C for 3 additional hours, then halted by the

addition of water (~10 mL). The suspension was extracted into diethyl ether 2x, then the pooled organic extract was washed with water and brine, then dried over $MgSO_4$, vacuum filtered, and concentrated *in vacuo* to a reddish oil (664 mg, 97% yield), used without further purification. NMR indicates the compound is isolated as a 2:1 mixture of keto and enol tautomers (664 mg, 97% yield). ^{1}H NMR (keto form): (500 MHz, Chloroform-*d*) δ 7.79 (d, *J* = 7.8 Hz, 1H), 7.68 (t, *J* = 7.6 Hz, 1H), 7.52 (d, *J* = 7.8 Hz, 1H), 7.43 (t, *J* = 7.6 Hz, 1H), 3.77 (s, 3H), 3.51 (s, 1H), 1.58 (s, 3H), 1.38 (s, 3H).

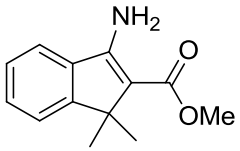

Methyl 3-amino-1,1-dimethyl-1H-indene-2-carboxylate (56). A solution of **55** (664 mg, 3.04 mmol) in methanol (9.2 mL) was warmed to reflux, then ammonium acetate (5.85 g, 76 mmol) was added. The solution was allowed to stir at reflux for 18 hours, at which point additional ammonium acetate (5.85 g, 76 mmol) was added. After an additional 5 hours at reflux, the solution was evaporated to dryness and the resulting residue was partitioned between ethyl acetate and saturated sodium bicarbonate solution. The organic layer was washed with water and brine, then isolated, dried over $MgSO_4$, vacuum filtered, and concentrated *in vacuo*. Further purification via column chromatography (10% ethyl acetate: hexanes) isolated 365 mg of a light tan crystalline solid found to be product by NMR (yield = 55%). ^{1}H NMR (500 MHz, Chloroform-*d*) δ 7.40 (m, 4H), 3.85 (s, 3H), 1.46 (s, 6H).

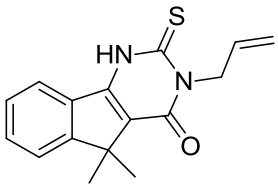

3-Allyl-5,5-dimethyl-2-thioxo-2,3-dihydro-1H-indeno[1,2-d]pyrimidin-4(5H)-one (57). Intermediate **56** (125 mg, 0.575 mmol) and allyl isothiocyanate (56 µL, 0.575 mmol) were combined in a high pressure reaction vessel with anhydrous pyridine (0.75 mL) and heated to reflux. Additional allyl isothiocyanate (168 µL, 1.73 mmol) was added in 3 equal portions over the next 5 hours, and the reaction was allowed to stir at reflux an additional 12 hours. At this

time, the reaction was allowed to cool to room temperature, then was diluted with aqueous 1N HCl and extracted with ethyl acetate. The organic layer was washed with additional aqueous 1N HCl, water, and brine, then isolated, dried over $MgSO_4$, vacuum filtered, and concentrated to a brown oil. Further purification via flash chromatography (0-10% EtOAc:hex) isolated the desired product as a white crystalline solid (46 mg, 23% yield). ^{1}H NMR (500 MHz, Chloroform-*d*) δ 11.33 (s, 1H), 7.97 – 7.81 (m, 1H), 7.64 – 7.50 (m, 2H), 7.46 (t, *J* = 7.3 Hz, 1H), 6.14 – 5.98 (m, 1H), 5.42 (dd, *J* = 17.2, 1.7 Hz, 1H), 5.30 (d, *J* = 10.2 Hz, 1H), 5.20 (d, *J* = 5.9 Hz, 2H), 1.56 (s, 6H).

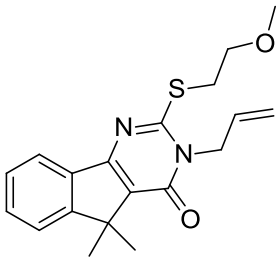

3-Allyl-2-((2-methoxyethyl)thio)-5,5-dimethyl-3H-indeno[1,2-d]pyrimidin-4(5H)-one (58) (CCG-203572). Intermediate **57** (37 mg, 0.130 mmol) was dissolved in 2-butanone (0.75 mL), to which cesium carbonate (63.5 mg, 0.195 mmol) and 2-methoxyethyl *p*-toluenesulfonic ester (60 mg, 0.260 mmol) were added. The solution was warmed to 80°C and allowed to stir for 16 hours, at which point the reaction was diluted with ethyl acetate and washed with water and brine. The organic layer was isolated, dried over $MgSO_4$, vacuum filtered, and concentrated *in vacuo*. Purification via flash chromatography (0-10 % ethyl acetate:hexane) yielded the desired compound as white crystals (27.5 mg, 62% yield). ^{1}H NMR (500 MHz, Chloroform-*d*) δ 7.85 (d, *J* = 7.5 Hz, 1H), 7.54 – 7.46 (m, 2H), 7.42 (t, *J* = 7.0 Hz, 1H), 5.97 (ddt, *J* = 16.3, 10.8, 5.4 Hz, 1H), 5.36 – 5.27 (m, 2H), 4.81 (d, *J* = 5.4 Hz, 2H), 3.81 (t, *J* = 6.2 Hz, 2H), 3.60 (t, *J* = 6.2 Hz, 2H), 3.47 (s, 3H), 1.57 (s, 6H). ESI+MS *m/z* = 343.1 ($M + H^+$). HPLC (Method B, t_R = 6.22 min), purity >95%.

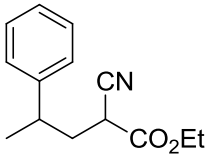

Ethyl 2-cyano-4-phenylpentanoate (60). Diisopropylazodicarboxylate (358 mg, 1.77 mmol) and triphenylphosphine (464 mg, 1.77 mmol) were combined in anhydrous THF (2.5 mL) and cooled to -20°C. The reaction mixture was allowed to stir at this temperature for 20 minutes, then 2-phenyl-1-propanol (200 mg, 1.47 mmol) and ethyl cyanoacetate (249 mg, 2.20 mmol) in THF (2.5 mL) were slowly added and the reaction was allowed to stir at -20°C for an additional 3 hours. The reaction vessel was transferred to a 4°C refrigerator to stand overnight (20h), then was subsequently concentrated to a crude brown oil *in vacuo*. Purification via FC (0 to 10% EA:hex) yielded the desired cyanoester product as a brown oil (280 mg, 82% yield). NMR indicates the product is a nearly 1:1 mixture of diastereomers. ^{1}H NMR (500 MHz, Chloroform-*d*) δ 7.41 – 7.32 (m, 2H), 7.32 – 7.20 (m, 3H), 4.23 (q, *J* = 7.1 Hz, 1H), 4.17 (qd, *J* = 7.1, 3.3 Hz, 1H), 3.41 (t, *J* = 7.3 Hz, 0.5H), 3.12 (dd, *J* = 9.7, 6.5 Hz, 0.5H), 3.09 – 2.95 (m, 1H), 2.33 – 2.18 (m, 2H), 1.37 (dd, *J* = 14.5, 6.9 Hz, 3H), 1.31 (td, *J* = 7.1, 2.5 Hz, 3H).

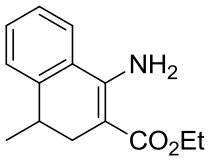

Ethyl 1-amino-4-methyl-3,4-dihydronaphthalene-2-carboxylate (61). Intermediate **60** (166 mg, 0.718 mmol) was dissolved in DCM (7 mL) under N_2, to which trifluoromethanesulfonic acid (1 mL) was added slowly dropwise. The reaction mixture was allowed to stir 24 hours at room temperature. The reaction was judged complete by TLC, and the mixture neutralized by the slow addition of saturated sodium bicarbonate to ~pH 7. The mixture was then extracted 2x with ethyl acetate, and the organic layer washed with water and brine. Organic layer dried over $MgSO_4$, vacuum filtered, and concentrated *in vacuo* to a white powder, confirmed to be the desired β-aminoester compound **61** (153 mg, 92% yield). ^{1}H NMR (500 MHz, Chloroform-*d*) δ 7.50 (d, *J* = 7.6 Hz, 1H), 7.39 (t, *J* = 7.4 Hz, 1H), 7.35 – 7.29 (m, 2H), 6.88 – 6.14 (m, 2H), 4.24 (q, *J* = 7.1 Hz, 2H), 2.96 – 2.85 (m, 1H), 2.67 (dd, *J* = 15.4, 5.2 Hz, 1H), 2.39 (dd, *J* = 15.4, 8.0 Hz, 1H), 1.35 (t, *J* = 7.1 Hz, 3H), 1.29 (d, *J* = 7.0 Hz, 3H).

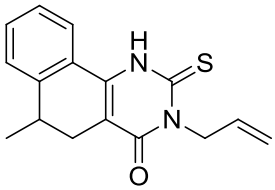

3-Allyl-6-methyl-2-thioxo-2,3,5,6-tetrahydrobenzo[h]quinazolin-4(1H)-one (62). Compound **61** (310 mg, 1.34 mmol) was dissolved in absolute ethanol (1.8 mL) under N_2, to which allyl isothiocyanate (268 μL, 2.68 mmol) and acetic acid (158 μL, 2.68 mmol) were added. The reaction was warmed to reflux and allowed to stir for 4h; over this time, additional allyl isothiocyanate (402 μL, 4.01mmol) was added in 3 portions. After complete addition of the allyl isothiocyanate, reaction allowed to stir at reflux an additional 12 hours. The reaction was diluted with ethyl acetate, washed with water and brine, then dried over $MgSO_4$ and concentrated *in vacuo*. The resulting orange oil was purified via flash chromatography (5-10% EA:hex), delivering the desired cyclic thiourea **62** as a white crystalline solid (135 mg, 35% yield). ^{1}H NMR (500 MHz, Chloroform-*d*) δ 9.35 (s, 1H), 7.53 – 7.44 (m, 2H), 7.39 (t, *J* = 8.1 Hz, 2H), 6.07 – 5.95 (m, 1H), 5.39 (d, *J* = 17.0 Hz, 1H), 5.28 (d, *J* = 10.2 Hz, 1H), 5.11 (d, *J* = 6.0 Hz, 2H), 3.09 (q, *J* = 6.9 Hz, 1H), 2.80 (dd, *J* = 16.6, 6.7 Hz, 1H), 2.59 (dd, *J* = 16.6, 6.7 Hz, 1H), 1.28 (d, *J* = 6.9 Hz, 3H).

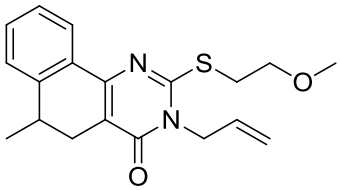

3-Allyl-2-((2-methoxyethyl)thio)-6-methyl-5,6-dihydrobenzo[h]quinazolin-4(3H)-one (63) (CCG-203574). Compound **62** (30 mg, 0.105 mmol), cesium carbonate (52 mg, 0.158 mmol), and *p*-toluenesulfonic acid 2-methoxyethyl ester (27 mg, 0.116 mmol) were combined in 2-butanone (618 μL) and warmed to 75°C. The reaction mixture was allowed to stir 16h, at which point the reaction was judged complete by TLC. The reaction mixture was diluted with ethyl acetate and the organic layer washed with water and brine. The organic layer was dried over $MgSO_4$, vacuum filtered, and concentrated *in vacuo*. The resulting crude oil was purified via flash chromatography (0-8% EA:hex) to deliver the desired compound as a clear brown oil (27 mg, 75% yield). ^{1}H NMR (500 MHz, $cdcl_3$) δ 8.13 (dd, *J* = 7.4, 1.4, 1H), 7.39 (td, *J* = 7.4, 1.4,

1H), 7.33 (td, *J* = 7.4, 1.4, 1H), 7.28 (d, *J* = 7.4, 1H), 5.94 (ddt, *J* = 17.1, 10.3, 5.7, 1H), 5.36 – 5.23 (m, 2H), 4.75 (qdt, *J* = 15.9, 5.7, 1.5, 2H), 3.78 (t, *J* = 6.3, 2H), 3.56 (t, *J* = 6.3, 2H), 3.43 (s, 3H), 3.09 (h, *J* = 6.7, 1H), 2.91 (dd, *J* = 16.6, 6.7, 1H), 2.70 (dd, *J* = 16.6, 6.7, 1H), 1.27 (d, *J* = 6.7, 3H). TOF ES+ MS: 343.1 (M+H), 365.1 (M+Na). HPLC (Method B, t_R = 5.81 min), purity >95%.

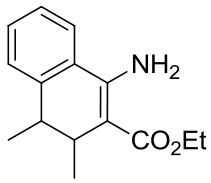

Ethyl 1-amino-3,4-dimethyl-3,4-dihydronaphthalene-2-carboxylate (65). Prepared according to General Method B from 2-ethylbenzonitrile **64** and ethyl 3-methyl acrylate. Isolated in 36% yield. ^{1}H NMR (400 MHz, Chloroform-*d*) δ 7.45 (d, *J* = 7.6, 1.3H), 7.39 (td, *J* = 7.5, 1.3 Hz, 0.3H), 7.33 (td, *J* = 7.4, 1.4 Hz, 1.0H), 7.30 – 7.24 (m, 1.6H), 7.19 (dd, *J* = 7.3, 1.5 Hz, 1H), 6.50 (bs, 2.6H), 4.30– 4.15 (m, 2.6H), 3.11 – 3.01 (m, 0.3H), 2.93 – 2.81 (m, 1.3H), 2.69 (qd, *J* = 7.1, 1.4 Hz, 1H), 1.38 (d, *J* = 7.0 Hz, 0.9H), 1.32 (td, *J* = 7.1, 1.1 Hz, 3.9H), 1.15 (d, *J* = 7.1 Hz, 3H), 0.90 (d, *J* = 6.9 Hz, 3H), 0.66 (d, *J* = 6.8 Hz, 0.9H).

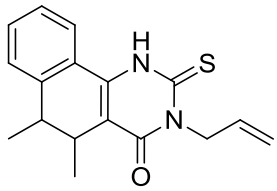

3-Allyl-5,6-dimethyl-2-thioxo-2,3,5,6-tetrahydrobenzo[h]quinazolin-4(1H)-one (66). Prepared according to General Method C from Ethyl 1-amino-3,4-dimethyl-3,4-dihydronaphthalene-2-carboxylate (**65)** and allyl isothiocyanate. Purified via flash chromatography (0-15% ethyl acetate:hexanes) to yield the product as a mixture of the cyclized 2-thioxopyrimidinone and the uncyclized thiourea-ester adduct, used together without further purification (36 mg, 30% yield).

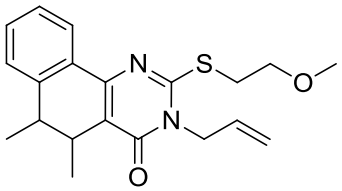

3-Allyl-2-((2-methoxyethyl)thio)-5,6-dimethyl-5,6-dihydrobenzo[h]quinazolin-4(3H)-one (67) (CCG-206601). Prepared according to General Method D from intermediate **66** (36 mg, 0.121 mmol), using 2-methoxyethyl *p*-toluenesulfonic ester (56 mg, 0.241 mmol) as the alkylating agent. Flash chromatography (5-10% EtOAc:hex) delivered the product as a clear oil (10:3 mixture of diastereomers, 29 mg, 67% yield). ^{1}H NMR (400 MHz, Chloroform-*d*) δ 8.16 – 8.06 (m, 1.3H), 7.46 – 7.28 (m, 2.9H), 7.22 (d, *J* = 7.3 Hz, 1.0H), 5.94 (ddt, *J* = 16.5, 10.9, 5.7 Hz, 1.3H), 5.35 – 5.24 (m, 2.6H), 4.84 – 4.66 (m, 2.6H), 3.78 (q, *J* = 5.4, 4.7 Hz, 2.6H), 3.63 – 3.50 (m, 2.6H), 3.43 (s, 3.9H), 3.22 – 3.09 (m, 1.6H), 2.85 (q, *J* = 7.0 Hz, 1.0H), 1.45 (d, *J* = 6.1 Hz, 0.9H), 1.12 (d, *J* = 7.0 Hz, 3.0H), 1.03 (d, *J* = 7.0 Hz, 3.0H), 0.82 (d, *J* = 6.1 Hz, 0.9H). ESI+MS *m/z* = 357.1 ($M + H^+$), 379.1 ($M + Na^+$). HPLC (Method B, t_R = 6.44 and 6.89 min), purity >95%.

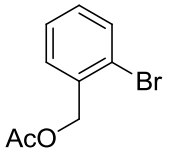

2-Bromobenzyl acetate (69). Anhydrous DMF (12 mL) was added to a dry reaction vessel under N_2, followed by 2-bromomethyl bromobenzene (**68**, 1.50 g, 6.00 mmol) and sodium acetate (1.48 g, 18.01 mmol). The reaction mixture was heated to 70°C and allowed to stir 16 hours. After this time, the reaction was diluted with water (100 mL) and extracted 3x with diethyl ether. The organic extract was washed 3x with water and 1x with brine, then isolated, dried over $MgSO_4$, vacuum filtered, and concentrated, leaving a very pale yellow oil (1.28 g, 93% yield) that was used without further purification. ^{1}H NMR (400 MHz, Chloroform-*d*) δ 7.58 (d, *J* = 7.8 Hz, 1H), 7.41 (d, *J* = 7.5 Hz, 1H), 7.32 (t, *J* = 7.5 Hz, 1H), 7.19 (t, *J* = 7.8 Hz, 1H), 5.20 (s, 2H), 2.14 (s, 3H).

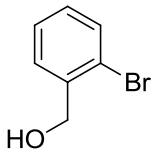

(2-Bromophenyl)methanol (70). The brominated benzyl acetate **69** (1.28 g, 5.59 mmol) was dissolved in methanol (11.2 mL), followed by potassium carbonate (927 mg, 6.71 mmol). The resulting suspension was allowed to stir 60 minutes at room temperature under N_2, then diluted with saturated aqueous sodium chloride solution and extracted three times with ethyl acetate. The combined organic extract was washed with brine, then dried over $MgSO_4$, vacuum filtered, and concentrated to a clear oil that eventually crystallized. The white crystalline product (1.01 g, 96% yield) was used without further purification. ^{1}H NMR (400 MHz, Chloroform-*d*) δ 7.55 (d, *J* = 8.0 Hz, 1H), 7.48 (d, *J* = 7.6 Hz, 1H), 7.34 (t, *J* = 7.5 Hz, 1H), 7.17 (t, *J* = 7.7 Hz, 1H), 4.76 (s, 2H), 2.00 (s, 1H).

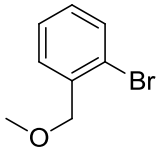

1-Bromo-2-(methoxymethyl)benzene (71) . 2-bromophenyl methanol **70** (880 mg, 4.71 mmol) and potassium hydroxide (1.30 g, 19.8 mmol) were dissolved in DMSO (11.2 mL), then the reaction mixture was allowed to stir at room temperature for 10 minutes. Methyl iodide (647 µL, 10.35 mmol) was added dropwise, then the reaction was stirred for an additional 90 minutes. The reaction was halted by the addition of water (~40 mL), then was extracted with diethyl ether 3 times. The combined organic extract was washed with saturated aqueous sodium bicarbonate solution (1x), water (3x), and brine (1x), then dried over $MgSO_4$, vacuum filtered, and concentrated to a clear oil (910 mg, 96% yield) that was used without further purification. ^{1}H NMR (400 MHz, Chloroform-*d*) δ 7.54 (d, *J* = 7.9 Hz, 1H), 7.46 (d, *J* = 7.6 Hz, 1H), 7.32 (t, *J* = 7.5 Hz, 1H), 7.15 (t, *J* = 7.5 Hz, 1H), 4.53 (s, 2H), 3.47 (s, 3H).

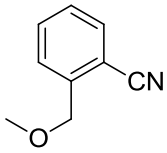

2-(Methoxymethyl)benzonitrile (72). Aryl bromide intermediate **71** (400 mg, 1.99 mmol) was dissolved in anhydrous DMF (15.3 mL) in a dry reaction vessel. Copper (I) cyanide (356 mg, 3.98 mmol) was added, then the solution was warmed to 120°C and allowed to stir for 16 h. The reaction was quenched via the addition of saturated aqueous sodium bicarbonate solution (80 mL), then the resulting suspension was extracted with diethyl ether (3x). The combined organic extract was combined and washed 3x with water and 1x with brine, then was isolated, dried over $MgSO_4$, vacuum filtered and concentrated to a light yellow oil (237 mg, 81% yield) that was used without further purification. ^{1}H NMR (400 MHz, Chloroform-*d*) δ 7.66 (d, *J* = 7.6 Hz, 1H), 7.63 – 7.54 (m, 2H), 7.40 (t, *J* = 7.2 Hz, 1H), 4.65 (s, 2H), 3.48 (s, 3H).

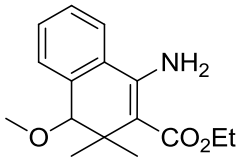

Ethyl 1-amino-4-methoxy-3,3-dimethyl-3,4-dihydronaphthalene-2-carboxylate (73). Prepared according to General Method B from 2-(methoxyethyl)benzonitrile (**72**) and ethyl 3,3-dimethyl acrylate. Isolated via flash chromatography (5-15% EtOAc:hex) as a yellow oil (238 mg, 54% yield) ^{1}H NMR (400 MHz, Chloroform-*d*) δ 7.57 – 7.28 (m, 4H), 6.32 (s, 2H), 4.32 – 4.18 (m, 2H), 3.67 (s, 1H), 3.35 (s, 3H), 1.34 (t, *J* = 7.0 Hz, 3H), 1.28 (s, 3H), 1.11 (s, 3H).

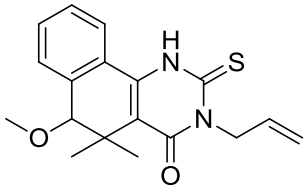

3-Allyl-6-methoxy-5,5-dimethyl-2-thioxo-2,3,5,6-tetrahydrobenzo[h]quinazolin-4(1H)-one (74). To a dry vessel containing absolute ethanol (1 mL), acetic acid (94 µL, 1.63 mmol), and intermediate **73** (225 mg, 0.817 mmol) was added allyl isothiocyanate (159 µL, 1.64 mmol). This reaction was securely capped and warmed to 75°C. Additional allyl isothiocyanate (238 µL, 2.45 mmol) was added in 3 equal portions over 3 hours, then the reaction was allowed to stir an additional 16 hours at 75°C. The reaction mixture was then diluted with ethyl acetate and washed with water and brine in a separatory funnel. The organic layer was isolated, dried over $MgSO_4$, vacuum filtered, and concentrated to an orange oil. This crude material was redissolved

in sodium ethoxide solution in ethanol (1.0 M, 1.5 mL) and allowed to stir for 30 minutes. The reaction was halted via the addition of water (20 mL) and extracted 3x with ethyl acetate. The pooled organic extract was washed with water and brine, then dried over $MgSO_4$, vacuum filtered, and concentrated. Flash chromatography (0->10% EtOAc:hex) isolated the desired product as a white crystalline solid (142 mg, 53% yield).[1]H NMR (400 MHz, Chloroform-*d*) δ 9.67 (s, 1H), 7.61 (d, *J* = 7.2 Hz, 1H), 7.58 – 7.48 (m, 2H), 7.42 (d, *J* = 7.0 Hz, 1H), 6.04 – 5.90 (m, 1H), 5.37 (d, *J* = 17.2 Hz, 1H), 5.25 (d, *J* = 10.3 Hz, 1H), 5.14 – 4.94 (m, 2H), 3.70 (s, 1H), 3.27 (s, 3H), 1.56 (s, 3H), 1.11 (s, 3H).

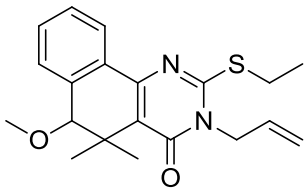

3-Allyl-2-(ethylthio)-6-methoxy-5,5-dimethyl-5,6-dihydrobenzo[h]quinazolin-4(3H)-one (75) (CCG-206602). Compound synthesized according to General Method D from intermediate **74** (100 mg, 0.304 mmol) using iodoethane (95 mg, 0.609 mmol) as the alkylating agent. Isolated after chromatography (5% EtOAc:hex) as a white crystalline solid (60 mg, 55% yield). [1]H NMR (400 MHz, Chloroform-*d*) δ 8.19 (dd, *J* = 7.4, 1.6 Hz, 1H), 7.50 – 7.38 (m, 2H), 7.35 – 7.28 (m, 1H), 5.99 – 5.84 (m, 1H), 5.35 – 5.22 (m, 2H), 4.73 – 4.57 (m, 2H), 3.69 (s, 1H), 3.37 – 3.27 (m, 2H), 3.25 (s, 3H), 1.65 (s, 3H), 1.47 (t, *J* = 7.4 Hz, 3H), 1.13 (s, 3H). ESI-MS+ *m/z* = 357.0 ($M + H^+$), 379.0 ($M + Na^+$). HPLC (Method B, t_R = 7.59 min), purity >95%.

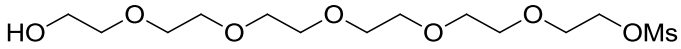

17-Hydroxy-3,6,9,12,15-pentaoxaheptadecyl methanesulfonate (106). PEG-6 (**105**, 1.00 g, 3.54 mmol) was dissolved in DCM (8 mL), to which silver oxide (862 mg, 3.72 mmol) was added. A solution of mesyl chloride (345 µL, 4.43 mmol) in DCM (1.4 mL) was added dropwise, then the reaction was allowed to stir for 48 hours. The reaction was diluted with additional DCM (20 mL), filtered through celite, then concentrated *in vacuo*. Further purification via flash chromatography (10% MeOH:EtOAc) furnished the desired product as a clear oil (330 mg, 26% yield). [1]H NMR (500 MHz, Chloroform-*d*) δ 4.43 – 4.38 (m, 2H), 3.81 – 3.77 (m, 2H), 3.77 – 3.72 (m, 2H), 3.71 – 3.65 (m, 16H), 3.65 – 3.61 (m, 2H), 3.11 (s, 3H), 2.71 (s, 1H).

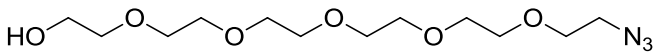

17-Azido-3,6,9,12,15-pentaoxaheptadecan-1-ol (107). Mesylated intermediate **106** (330 mg, 0.569 mmol) was dissolved in anhydrous DMF (1.3 mL). Sodium azide (119 mg, 1.83 mmol) was added and the solution heated to 90°C for 6 hours. The reaction was cooled and partitioned between brine and ethyl acetate. The organic layer was separated, dried over $MgSO_4$, filtered, and concentrated to a colorless oil (189 mg, 67% yield). ^{1}H NMR (500 MHz, Chloroform-*d*) δ 3.78 – 3.56 (m, 22H), 3.41 (td, *J* = 5.1, 2.0 Hz, 2H), 2.75 (s, 1H).

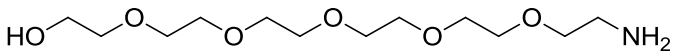

17-Amino-3,6,9,12,15-pentaoxaheptadecan-1-ol (108). Azide intermediate **107** was dissolved in THF (1.1 mL) and cooled to 0°C. Triphenylphosphine (126 mg, 0.480 mmol) was added and the solution was stirred for 12 hours while warming to room temperature. Water (50 µL, 2.78 mmol) was added and the reaction allowed to stir for 12 hours at room temperature. Volatiles were removed *in vacuo*, then the resulting crude oil was dissolved in water and washed 3 times with toluene. The aqueous layer was evaporated under reduced pressure to yield the desired product as a colorless oil (115 mg, 94% yield). ^{1}H NMR (500 MHz, Chloroform-*d*) δ 3.76 – 3.71 (m, 2H), 3.71 – 3.63 (m, 16H), 3.63 – 3.58 (m, 2H), 3.56 – 3.51 (m, 2H), 2.88 (t, *J* = 5.1 Hz, 2H), 2.44 (s, 3H).

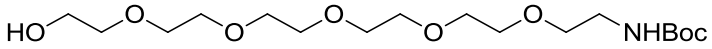

***tert*-Butyl (17-hydroxy-3,6,9,12,15-pentaoxaheptadecyl)carbamate (109)**. Monoamine **108** (115 mg, 0.409 mmol) was dissolved in 0.6 mL of 2:1 H_2O:dioxane solution and cooled to 0°C. Potassium hydroxide (25 mg, 0.450 mmol) was added and the mixture allowed to stir for 15 minutes, then di-*tert*-butyl dicarbamate (98 mg, 0.450 mmol) was added. The reaction was allowed to stir and warm to room temperature over 5 hours, then the reaction halted by the addition of dichloromethane and brine. The organic layer was washed with additional brine, isolated, dried over $MgSO_4$, and concentrated *in vacuo* to a clear oil (129 mg, 83% yield), used without further purification. (^{1}H NMR (500 MHz, Chloroform-*d*) δ 3.80 – 3.60 (m, 20H), 3.56 (t, *J* = 5.3 Hz, 2H), 3.34 (d, *J* = 5.2 Hz, 2H), 2.80 (s, 1H), 2.06 (s, 1H), 1.46 (s, 9H).

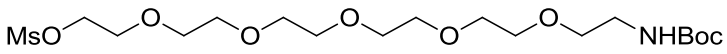

2,2-Dimethyl-4-oxo-3,8,11,14,17,20-hexaoxa-5-azadocosan-22-yl methanesulfonate (110). Boc-protected intermediate **109** (129 mg, 0.338 mmol) was dissolved in DCM (1.7 mL) and cooled to 0°C. Triethylamine (52 µL, 0.372 mmol) and mesyl chloride (29 µL, 0.372 mmol) were added, and the solution was allowed to stir at 16 h while warming to room temperature. The solvent was removed *in* vacuo and purified via flash chromatography (30-100% EtOAc:hex) to a clear oil (107 mg, 69% yield). (^{1}H NMR (500 MHz, Chloroform-*d*) δ 5.05 (s, 1H), 4.41 – 4.36 (m, 2H), 3.80 – 3.74 (m, 2H), 3.69 – 3.60 (m, 16H), 3.54 (t, *J* = 5.2 Hz, 2H), 3.32 (d, *J* = 5.5 Hz, 2H), 3.09 (s, 3H), 1.44 (s, 9H).

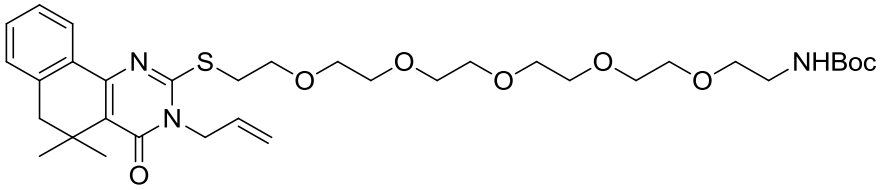

***tert*-Butyl (17-((3-allyl-5,5-dimethyl-4-oxo-3,4,5,6-tetrahydrobenzo[*h*]quinazolin-2-yl)thio)-3,6,9,12,15-pentaoxaheptadecyl)carbamate (111).** Synthesized according to General Method D from 2-thioxo intermediate **16** and alkylating agent **110**. Isolated in 62% yield. ^{1}H NMR (500 MHz, Chloroform-*d*) δ 8.09 (d, *J* = 7.5 Hz, 1H), 7.40 – 7.30 (m, 2H), 7.20 (d, *J* = 7.2 Hz, 1H), 5.95 (ddt, *J* = 16.2, 10.6, 5.6 Hz, 1H), 5.34 – 5.25 (m, 2H), 5.06 (s, 1H), 4.71 (d, *J* = 5.6 Hz, 2H), 3.87 (t, *J* = 6.4 Hz, 2H), 3.75 – 3.59 (m, 16H), 3.59 – 3.49 (m, 4H), 3.33 (d, *J* = 5.2 Hz, 2H), 2.81 (s, 2H), 1.46 (s, 9H), 1.40 (s, 6H).

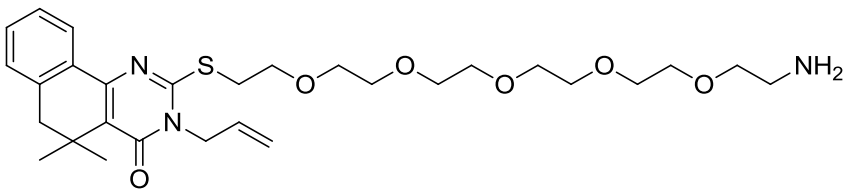

3-Allyl-2-((17-amino-3,6,9,12,15-pentaoxaheptadecyl)thio)-5,5-dimethyl-5,6-dihydrobenzo[*h*]quinazolin-4(3H)-one (112). The Boc-protected intermediate **111** was dissolved in a 2:1 solution of DCM:TFA and allowed to stir at room temperature for 3 hours. The reaction mixture was neutralized via the slow addition of aqueous sodium carbonate solution

until bubbling stopped. The organic layer was isolated and the aqueous layer was washed 3 times with additional DCM. The combined organic layers were concentrated *in vacuo* to a sticky oil that was used without further purification, isolated in 81% yield. ^{1}H NMR (500 MHz, Chloroform-*d*) δ 9.47 (s, 2H), 8.01 (d, *J* = 7.7 Hz, 1H), 7.39 (t, *J* = 7.3 Hz, 1H), 7.35 – 7.11 (m, 2H), 5.89 (ddt, *J* = 17.2, 10.8, 5.5 Hz, 1H), 5.33 – 5.19 (m, 2H), 4.81 – 4.65 (m, 2H), 3.88 (t, *J* = 6.3 Hz, 2H), 3.81 – 3.58 (m, 18H), 3.55 (t, *J* = 6.3 Hz, 2H), 3.19 (d, *J* = 5.0 Hz, 2H), 2.81 (s, 2H), 1.36 (s, 6H).

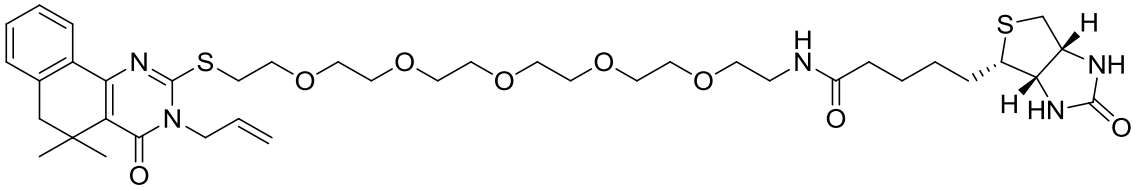

***N*-(17-((3-Allyl-5,5-dimethyl-4-oxo-3,4,5,6-tetrahydrobenzo[*h*]quinazolin-2-yl)thio)-3,6,9,12,15-pentaoxaheptadecyl)-5-((3a*S*,4*S*,6a*R*)-2-oxohexahydro-1*H*-thieno[3,4-*d*]imidazol-4-yl)pentanamide (113) (CCG-203618).** The PEG-6 functionalized intermediate **112** was dissolved in DCM, to which DIPEA and biotin-*O*-succinimide were added. The reaction was allowed to stir for 24 hours, then volatiles were removed *in vacuo*. Further purification via flash chromatography (0-10% MeOH:DCM) isolated the desired product (51% yield). ^{1}H NMR (500 MHz, Chloroform-*d*) δ 8.07 (d, *J* = 7.5 Hz, 1H), 7.38 – 7.27 (m, 2H), 7.18 (d, *J* = 6.4 Hz, 1H), 6.56 (s, 1H), 5.99 – 5.86 (m, 2H), 5.32 – 5.23 (m, 2H), 5.04 (s, 1H), 4.74 – 4.62 (m, 2H), 4.53 – 4.46 (m, 1H), 4.35 – 4.28 (m, 1H), 3.84 (td, *J* = 6.7, 3.0 Hz, 2H), 3.72 – 3.58 (m, 16H), 3.59 – 3.49 (m, 4H), 3.48 – 3.36 (m, 2H), 3.14 (td, *J* = 7.3, 3.9 Hz, 1H), 2.94 – 2.86 (m, 1H), 2.79 (s, 2H), 2.73 (d, *J* = 12.7 Hz, 1H), 2.28 – 2.17 (m, 2H), 1.79 – 1.61 (m, 4H), 1.48 – 1.41 (m, 2H), 1.38 (s, 6H).

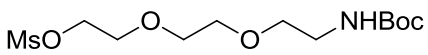

2,2-Dimethyl-4-oxo-3,8,11-trioxa-5-azatridecan-13-yl methanesulfonate (115). Compound supplied by Jessica Bell, used without further purification.

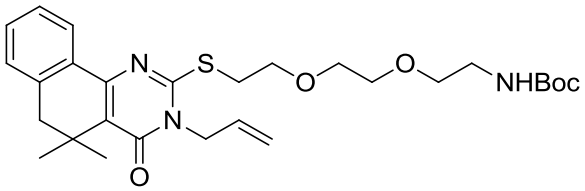

***tert*-Butyl (2-(2-(2-((3-allyl-5,5-dimethyl-4-oxo-3,4,5,6-tetrahydrobenzo[*h*]quinazolin-2-yl)thio)ethoxy)ethoxy)ethyl)carbamate (116).** The thiourea intermediate (85 mg, 0.284 mmol) and Boc protected PEG-3 mesylate (**115**) (111 mg, 0.340 mmol) were dissolved in DMF (1.7 mL), and cesium carbonate (139 mg, 0.425 mmol) was then added. The solution was heated to 75°C and allowed to stir for 3 hours, then quenched by the addition of water. The resulting suspension was extracted with ethyl acetate twice. The pooled organic extract was washed with water 2x and brine, then isolated, dried over $MgSO_4$, vacuum filtered, and concentrated. Isolated 156 mg (104% crude yield) as the desired product with a trace amount of the alkylating agent present. Used without further purification. ^{1}H NMR (500 MHz, Chloroform-*d*) δ 8.09 (d, *J* = 7.5 Hz, 1H), 7.37 (td, *J* = 7.3, 1.5 Hz, 1H), 7.32 (t, *J* = 7.5 Hz, 1H), 7.21 (d, *J* = 7.3 Hz, 1H), 6.01 – 5.89 (m, 1H), 5.34 – 5.26 (m, 2H), 5.01 (s, 1H), 4.71 (d, *J* = 5.6 Hz, 2H), 3.87 (t, *J* = 6.4 Hz, 2H), 3.72 – 3.63 (m, 4H), 3.60 – 3.54 (m, 4H), 3.38 – 3.28 (m, 2H), 2.81 (s, 2H), 1.45 (s, 9H), 1.40 (s, 6H).

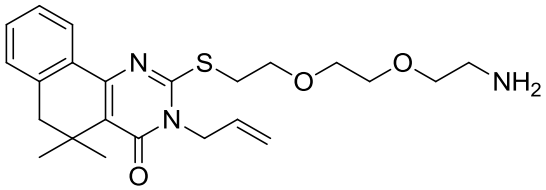

3-Allyl-2-((2-(2-(2-aminoethoxy)ethoxy)ethyl)thio)-5,5-dimethyl-5,6-dihydrobenzo[*h*]quinazolin-4(3*H*)-one (117). Boc-protected intermediate **116** (156 mg, 0.295 mmol) was dissolved in DCM (2.0 mL), then TFA (1.0 mL) was added slowly. The reaction mixture was allowed to stir under N_2 for 1 hour and 45 minutes, then concentrated *in vacuo*, and treated with saturated sodium bicarbonate solution. The aqueous mixture was extracted with ethyl acetate 3x, then the pooled organic extract was isolated, dried over $MgSO_4$, vacuum filtered, concentrated *in vacuo* to a clear oil (163 mg, 130% crude yield) and used directly in the next step. ^{1}H NMR (500 MHz, Chloroform-*d*) δ 10.29 (s, 3H), 7.92 (d, *J* = 7.8 Hz, 1H), 7.43 (td, *J* = 7.4, 1.3 Hz, 1H), 7.34 (td, *J* = 7.6, 1.3 Hz, 1H), 7.25 (d, *J* = 7.5 Hz, 1H), 5.94 – 5.82 (m, 1H),

5.36 – 5.25 (m, 2H), 4.76 (d, *J* = 5.7 Hz, 2H), 4.00 (t, *J* = 5.8 Hz, 2H), 3.77 – 3.66 (m, 6H), 3.61 (t, *J* = 5.8 Hz, 2H), 3.32 – 3.25 (m, 2H), 2.82 (s, 2H), 1.36 (s, 6H).

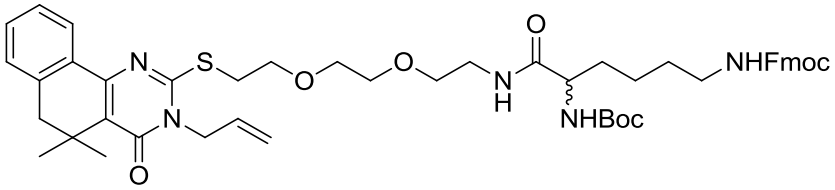

(9*H*-fluoren-9-yl)methyl tert-butyl (6-((2-(2-(2-((3-allyl-5,5-dimethyl-4-oxo-3,4,5,6-tetrahydrobenzo[*h*]quinazolin-2-yl)thio)ethoxy)ethoxy)ethyl)amino)-6-oxohexane-1,5-diyl)dicarbamate (118). Primary amine **117** (163 mg, 0.379 mmol) was combined with HOBT (87 mg, 0.569 mmol), EDC (109 mg, 0.569 mmol), DIPEA (166 µL, 0.949 mmol), and orthogonally protected DL-lysine (267 mg, 0.569 mmol) in DCM (3.8 mL) under N_2. The reaction mixture was allowed to stir at room temperature for 24 hours. The reaction mixture was diluted with additional DCM (20 mL) and washed with saturated aqueous sodium bicarbonate, sat. aq. ammonium chloride solution, water, and brine. The organic layer was then dried over $MgSO_4$, vacuum filtered, and concentrated *in vacuo*. The resulting residue was further purified via column chromatography (5% MeOH:DCM) to yield 194 mg of the desired amide as a gelatinous solid (145 mg, 58% yield over 3 steps). 10% MeOH:DCM rf = .35.

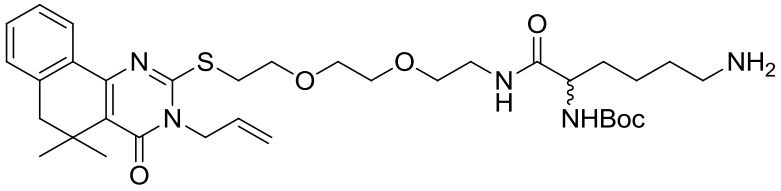

***tert*-Butyl (1-((2-(2-(2-((3-allyl-5,5-dimethyl-4-oxo-3,4,5,6-tetrahydrobenzo[*h*]quinazolin-2-yl)thio)ethoxy)ethoxy)ethyl)amino)-6-amino-1-oxohexan-2-yl)carbamate (119).** Orthogonally protected Lys intermediate **118** (194 mg, 0.220 mmol) was dissolved in DMF (1.7 mL), to which piperidine was added (440 mg, 5.17 mmol). This mixture was stirred at RT for 1 hour, then the solvent was removed under reduced pressure. Flash chromatography (10% MeOH:DCM, then 10% 7N NH_3-MeOH:DCM) was used to isolate the product. The fractions containing the desired product were evaporated under reduced pressure, then redissolved in dichloromethane, filtered via vacuum filtration, and concentrated, resulting in the isolation of the desired product as a yellow oil (109 mg, 75% yield). ^{1}H NMR (500 MHz, Chloroform-*d*) δ 8.07

(d, *J* = 7.5 Hz, 1H), 7.39 – 7.30 (m, 2H), 7.20 (d, *J* = 7.3 Hz, 1H), 6.01 – 5.89 (m, 1H), 5.53 – 5.42 (m, 1H), 5.33 – 5.25 (m, 2H), 4.71 (d, *J* = 5.9 Hz, 2H), 4.21 (s, 1H), 3.87 (t, *J* = 6.3 Hz, 2H), 3.68 (d, *J* = 11.3 Hz, 4H), 3.62 (t, *J* = 5.5 Hz, 2H), 3.57 (t, *J* = 6.5 Hz, 2H), 3.51 (s, 2H), 3.47 – 3.38 (m, 1H), 3.20 – 3.14 (m, 2H), 3.10 – 3.02 (m, 2H), 2.80 (s, 2H), 1.99 – 1.88 (m, 4H), 1.73 – 1.65 (m, 2H), 1.43 (s, 9H), 1.39 (s, 6H).

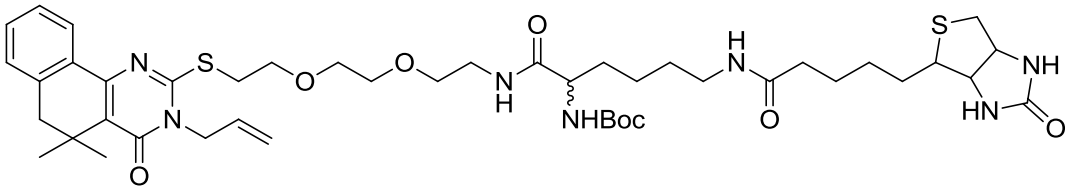

***tert*-Butyl (1-((3-allyl-5,5-dimethyl-4-oxo-3,4,5,6-tetrahydrobenzo[*h*]quinazolin-2-yl)thio)-10,17-dioxo-21-(2-oxohexahydro-1*H*-thieno[3,4-d]imidazol-4-yl)-3,6-dioxa-9,16-diazahenicosan-11-yl)carbamate (120).** Free amine intermediate **119** (112 mg, 0.170 mmol) was combined with biotin-*O*-succinimide (58 mg, 0.170 mmol) and DIPEA in DCM under N_2. The reaction was allowed to stir at RT for 16h, then the reaction mixture was diluted with additional DCM and washed with H_2O and brine. The organic layer was isolated, dried over $MgSO_4$, vacuum filtered, and concentrated. Column chromatography (10% MeOH:DCM) was used to further purify the product; isolated as a gelatinous solid (118 mg, 79% yield). ^{1}H NMR (500 MHz, Chloroform-*d*) δ 8.09 (d, *J* = 7.5 Hz, 1H), 7.41 – 7.31 (m, 2H), 7.21 (d, *J* = 7.2 Hz, 1H), 6.19 (s, 1H), 6.05 (s, 1H), 5.95 (ddd, *J* = 16.1, 10.6, 5.4 Hz, 1H), 5.73 (s, 1H), 5.45 (s, 1H), 5.40 – 5.26 (m, 3H), 5.04 (s, 1H), 4.72 (d, *J* = 5.5 Hz, 2H), 4.56 – 4.49 (m, 1H), 4.37 – 4.30 (m, 1H), 4.14 (s, 1H), 3.88 (t, *J* = 6.3 Hz, 2H), 3.72 – 3.64 (m, 4H), 3.63 – 3.54 (m, 4H), 3.52 – 3.44 (m, 2H), 3.33 – 3.21 (m, 2H), 3.17 (s, 1H), 2.81 (s, 2H), 2.29 – 2.16 (m, 2H), 1.69 (d, *J* = 31.2 Hz, 8H), 1.56 (d, *J* = 7.5 Hz, 2H), 1.53 – 1.30 (m, 18H).

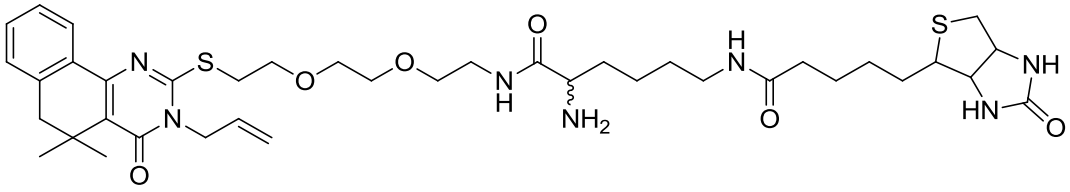

***N*-(2-(2-(2-((3-Allyl-5,5-dimethyl-4-oxo-3,4,5,6-tetrahydrobenzo[*h*]quinazolin-2-yl)thio)ethoxy)ethoxy)ethyl)-2-amino-6-(5-(2-oxohexahydro-1*H*-thieno[3,4-*d*]imidazol-4-yl)pentanamido)hexanamide (121).** Reaction was performed in a manner similar to that

employed for **112** using **120** (50 mg, 0.057 mmol) as the substrate. After neutralization with saturated aqueous sodium bicarbonate, extraction into dichloromethane, drying over $MgSO_4$, filtering, and concentration under reduced pressure, the desired amine product was isolated as a light brown oil (44 mg, 99% yield). ^{1}H NMR (500 MHz, Chloroform-*d*) δ 8.08 (d, *J* = 6.9 Hz, 1H), 7.39 – 7.26 (m, 2H), 7.19 (d, *J* = 7.2 Hz, 1H), 5.94 (ddt, *J* = 17.3, 10.6, 5.6 Hz, 1H), 5.33 – 5.24 (m, 2H), 4.70 (d, *J* = 5.5 Hz, 2H), 4.51 (q, *J* = 5.6 Hz, 1H), 4.35 – 4.28 (m, 1H), 3.90 – 3.83 (m, 2H), 3.71 – 3.63 (m, 4H), 3.61 – 3.52 (m, 4H), 3.51 – 3.41 (m, 2H), 3.28 – 3.12 (m, 3H), 2.80 (s, 2H), 2.78 – 2.71 (m, 1H), 2.26 – 2.12 (m, 7H), 1.79 – 1.64 (m, 5H), 1.61 – 1.21 (m, 16H).

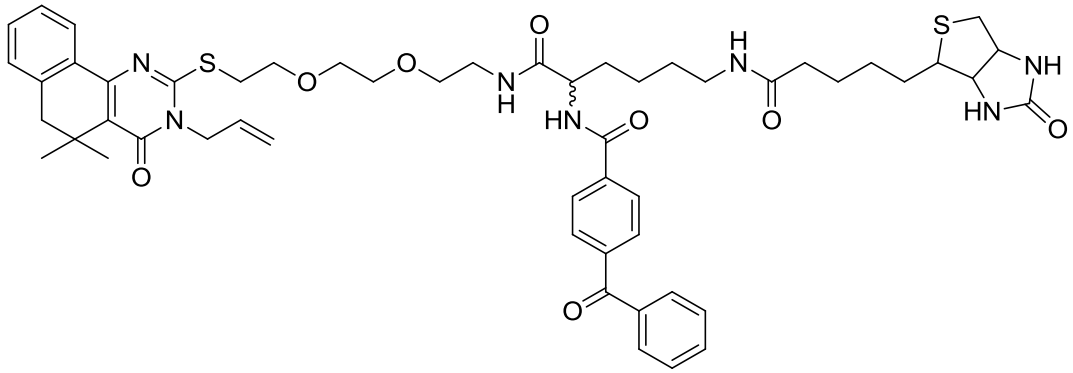

***N*-(1-((3-Allyl-5,5-dimethyl-4-oxo-3,4,5,6-tetrahydrobenzo[*h*]quinazolin-2-yl)thio)-10,17-dioxo-21-(2-oxohexahydro-1*H*-thieno[3,4-*d*]imidazol-4-yl)-3,6-dioxa-9,16-diazahenicosan-11-yl)-4-benzoylbenzamide (122) (CCG-203924).** Free amine **121** (50 mg, 0.064 mmol) was dissolved in DCM (0.64 mL), then DIPEA (56 µL, 0.319 mmol), HOBT (15 mg, 0.096 mmol), EDC (18 mg, 0.096 mmol) and 4-benzoyl benzoic acid (22 mg, 0.096) were added. The reaction was allowed to stir for 24 hours at room temperature, then the reaction was quenched by the addition of H_2O and additional DCM. The organic layer was washed with saturated aqueous sodium carbonate (10 mL), aqueous ammonium hydroxide (10 mL), water (20 mL), and brine (10 mL), then isolated, dried over $MgSO_4$, filtered, and concentrated *in vacuo*. Purification by flash chromatography (5% MeOH:DCM) furnished the product as a sticky light brown solid (26 mg, 41% yield). ^{1}H NMR (500 MHz, Chloroform-*d*) δ 8.08 (d, *J* = 7.6 Hz, 1H), 8.02 (dd, *J* = 8.3, 3.4 Hz, 2H), 7.91 – 7.82 (m, 2H), 7.82 – 7.77 (m, 2H), 7.63 (t, *J* = 7.4 Hz, 1H), 7.51 (t, *J* = 7.7 Hz, 2H), 7.47 – 7.30 (m, 2H), 7.20 (d, *J* = 7.0 Hz, 1H), 6.50 – 6.42 (m, 1H), 6.37 (t, *J* = 5.6 Hz, 0.5H), 6.19 (s, 0.5H), 5.99 – 5.87 (m, 1H), 5.67 (s, 0.5H), 5.40 (s, 0.5H), 5.35 – 5.24 (m, 2H),

4.78 – 4.64 (m, 3H), 4.50 (t, *J* = 6.3 Hz, 1H), 4.36 – 4.26 (m, 1H), 3.85 (t, *J* = 6.4 Hz, 2H), 3.66 (d, *J* = 4.8 Hz, 4H), 3.64 – 3.58 (m, 2H), 3.58 – 3.52 (m, 2H), 3.52 – 3.44 (m, 2H), 3.37 – 3.18 (m, 2H), 3.18 – 3.09 (m, 1H), 2.89 (dt, *J* = 12.8, 4.4 Hz, 1H), 2.80 (s, 2H), 2.72 (dd, *J* = 20.1, 12.8 Hz, 1H), 2.24 – 2.14 (m, 2H), 1.97 – 1.78 (m, 2H), 1.77 – 1.52 (m, 6H), 1.50 – 1.41 (m, 3H), 1.39 (s, 6H), 1.28 (m, 3H). ESI-MS+ *m/z* = 1014.2 ($M + Na^+$).

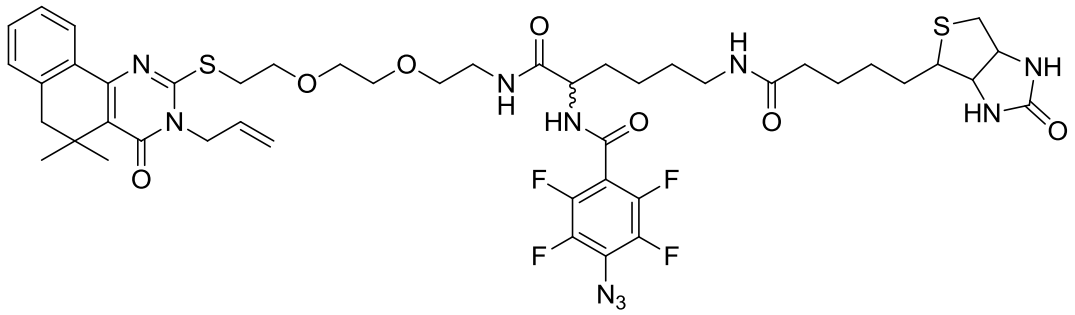

***N*-(1-((3-allyl-5,5-dimethyl-4-oxo-3,4,5,6-tetrahydrobenzo[*h*]quinazolin-2-yl)thio)-10,17-dioxo-21-(2-oxohexahydro-1*H*-thieno[3,4-*d*]imidazol-4-yl)-3,6-dioxa-9,16-diazahenicosan-11-yl)-4-azido-2,3,5,6-tetrafluorobenzamide (123).** The free amine starting material **121** (27 mg, 0.034 mmol) was dissolved in DCM (140 µL), to which the NHS-azidotetrafluorophenylazide ester (14 mg, 0.041 mg) and DIPEA (9 µL, 0.052 mmol) were added. The reaction vessel was covered in tinfoil and the solution was allowed to stir for 48 hours at room temperature, then the solvent was removed at reduced pressure. Flash chromatography (5% MeOH:EtOAc) delivered the final product as a light brown oil (12.5 mg, 36% yield). ^{1}H NMR (500 MHz, Chloroform-*d*) δ 8.05 (d, *J* = 7.7 Hz, 1H), 7.38 – 7.28 (m, 2H), 7.18 (d, *J* = 7.3 Hz, 1H), 6.50 (s, 0.5H), 6.36 (s, 0.5H), 6.16 (s, 0.5H), 6.07 (s, 0.5H), 5.99 – 5.86 (m, 1H), 5.35 – 5.21 (m, 2H), 4.74 – 4.66 (m, 2H), 4.65 – 4.55 (m, 1H), 4.52 – 4.42 (m, 1H), 4.34 – 4.23 (m, 1H), 3.85 (t, *J* = 6.3 Hz, 2H), 3.71 – 3.62 (m, 4H), 3.59 (q, *J* = 4.8 Hz, 2H), 3.54 (t, *J* = 6.5 Hz, 2H), 3.51 – 3.36 (m, 3H), 3.18 – 3.04 (m, 1H), 2.92 – 2.82 (m, 1H), 2.78 (s, 2H), 2.69 (dd, *J* = 31.6, 12.8 Hz, 1H), 2.21 – 2.15 (m, 1H), 1.86 (s, 5H), 1.68 – 1.62 (m, 2H), 1.54 (s, 2H), 1.44 (s, 2H), 1.37 (s, 6H), 1.30 – 1.23 (m, 4H).

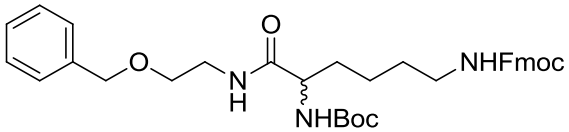

(9*H*-Fluoren-9-yl)methyl tert-butyl (6-((2-(benzyloxy)ethyl)amino)-6-oxohexane-1,5-diyl)dicarbamate (125). Boc-Fmoc-DL-lysine (200 mg, 0.427 mmol) was dissolved in anhydrous DMF (2.2 mL), to which HATU (195 mg, 0.512 mmol) and DIPEA (112 µL, 0.640 mmol) were added. After 10 minutes, 2-(benzyloxy)ethanamine (**124**, 77 mg, 0.512 mmol) was added. This mixture was allowed to stir at RT for 1.5 hours, then the reaction was diluted with water. The resulting suspension was extracted into ethyl acetate 2x, then the organic layer washed with saturated aqueous $NaHCO_3$, sat. aq. NH_4Cl, water, and brine. The organic layer was isolated, dried over $MgSO_4$, vacuum filtered, and concentrated. The crude product (257 mg, quant. yield) was carried on to the next reaction without further purification. ^{1}H NMR (500 MHz, Chloroform-*d*) δ 7.79 (d, *J* = 7.5 Hz, 2H), 7.62 (d, *J* = 7.5 Hz, 2H), 7.42 (t, *J* = 7.4 Hz, 2H), 7.39 – 7.30 (m, 7H), 6.52 – 6.44 (m, 1H), 5.16 (d, *J* = 8.1 Hz, 1H), 5.00 – 4.90 (m, 1H), 4.52 (s, 2H), 4.47 – 4.37 (m, 2H), 4.23 (t, *J* = 6.8 Hz, 1H), 4.14 – 4.03 (m, 1H), 3.55 (t, *J* = 5.3 Hz, 2H), 3.50 (q, *J* = 5.4 Hz, 2H), 3.23 – 3.12 (m, 2H), 1.82 (d, *J* = 7.0 Hz, 2H), 1.57 – 1.49 (m, 2H), 1.44 (s, 9H), 1.41 – 1.34 (m, 2H).

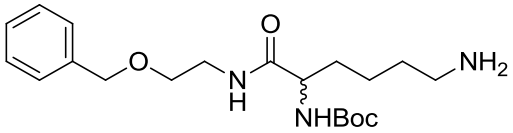

***tert*-Butyl (6-amino-1-((2-(benzyloxy)ethyl)amino)-1-oxohexan-2-yl)carbamate (126).** Boc (Fmoc) protected, amide functionalized lysine **125** (266 mg, 0.442 mmol) was dissolved in DCM (3.5 mL). Piperidine (0.9 mL) was added and the reaction was allowed to stir for 1 hour under N_2. The reaction mixture was concentrated *in vacuo* on a rotary evaporator, then under high vacuum. The resulting residue was purified by flash chromatography (1%MeOH:DCM to 10% methanolic ammonia:DCM) Compound successfully isolated and confirmed to be the desired material by NMR (167 mg, 100% yield). ^{1}H NMR (500 MHz, Chloroform-*d*) δ 7.42 – 7.30 (m, 5H), 6.71 (s, 1H), 5.17 (s, 1H), 4.53 (s, 2H), 4.18 – 4.02 (m, 1H), 3.57 (t, *J* = 5.2 Hz, 2H), 3.53 – 3.42 (m, 2H), 2.70 (t, *J* = 6.8 Hz, 2H), 2.01 (s, 3H), 1.88 – 1.78 (m, 1H), 1.69 – 1.55 (m, 2H), 1.55 – 1.32 (m, 12H).

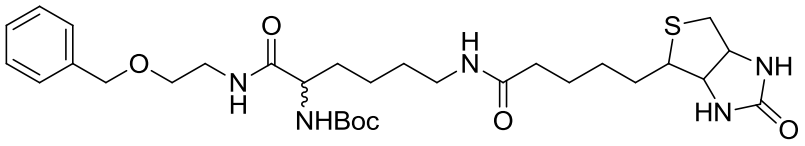

***tert*-Butyl (1-((2-(benzyloxy)ethyl)amino)-1-oxo-6-(5-(2-oxohexahydro-1*H*-thieno[3,4-*d*]imidazol-4-yl)pentanamido)hexan-2-yl)carbamate (127).** The free amine intermediate **126** (152 mg, 0.401 mmol) was combined with biotin-*O*-succinimide (137 mg, 0.401 mmol) and DIPEA (105 µL, 0.602 mmol) in DCM (2 mL) under N_2. The reaction was allowed to stir at RT for 16h, then was diluted with additional DCM and washed 1x with H_2O and brine. The organic layer was isolated, dried over $MgSO_4$, vacuum filtered, and concentrated. Column chromatography (10% MeOH:DCM) was used to further purify the product, isolated as a gelatinous solid in 76% yield (184 mg). ^{1}H NMR (500 MHz, Chloroform-*d*) δ 7.39 – 7.29 (m, 5H), 6.56 – 6.49 (m, 1H), 6.42 (s, 0.5H), 6.28 (s, 0.5H), 5.94 (s, 0.5H), 5.78 (s, 0.5H), 5.47 – 5.38 (m, 1H), 4.53 (s, 2H), 4.45 (dd, *J* = 7.8, 4.8 Hz, 0.5H), 4.33 – 4.26 (m, 1H), 4.15 – 4.08 (m, 1H), 3.64 – 3.58 (m, 2H), 3.56 – 3.45 (m, 2H), 3.35 – 3.23 (m, 1H), 3.19 – 3.12 (m, 2H), 2.90 – 2.79 (m, 1H), 2.75 – 2.67 (m, 2H), 2.61 (d, *J* = 12.8 Hz, 0.5H), 2.26 – 2.19 (m, 2H), 1.83 – 1.64 (m, 6H), 1.58 – 1.50 (m, 2H), 1.48 – 1.36 (m, 13H).

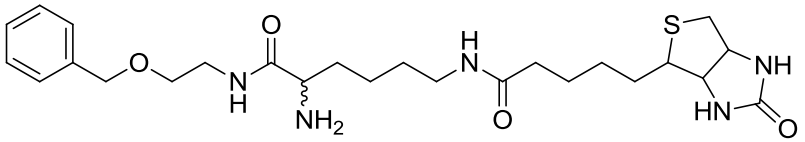

2-Amino-*N*-(2-(benzyloxy)ethyl)-6-(5-(2-oxohexahydro-1*H*-thieno[3,4-*d*]imidazol-4-yl)pentanamido)hexanamide (128). Boc-protected dummy probe intermediate **127** (51 mg, 0.084 mmol) was dissolved in a 2:1 mixture of DCM and TFA (850 µL) and allowed to stir for 2 hours. The solution was concentrated under reduced pressure, and the crude material was redissolved in water. The aqueous phase was washed with DCM, then isolated and evaporated under reduced pressure to afford the desired product (48 mg, 113% yield due to water contaminant), used without further purification.

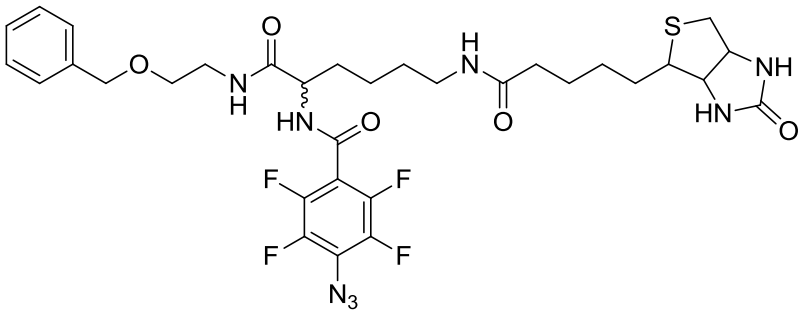

4-Azido-*N*-(1-((2-(benzyloxy)ethyl)amino)-1-oxo-6-(5-(2-oxohexahydro-1*H*-thieno[3,4-*d*]imidazol-4-yl)pentanamido)hexan-2-yl)-2,3,5,6-tetrafluorobenzamide (129) (CCG-204000). The free amine starting material **128** (43 mg, 0.085 mmol) was dissolved in DMF (1 mL), to which the NHS-azidotetrafluorophenylazide ester (34 mg, 0.102 mmol) and DIPEA (22 µL, 0.128 mmol) were added. The reaction vessel was covered in tin foil and was allowed to stir for 24 hours at room temperature. The reaction was diluted with H_2O then extracted 2x with EtOAc. Organic layer washed with sat. aq. $NaHCO_3$, 2x with water, and once with brine. The organic layer was isolated, dried over $MgSO_4$, filtered, and concentrated, leaving a brownish crude residue. Further purification via flash chromatography (0-10% MeOH:DCM) recovered the product as a sticky brown oil (22 mg, 36% yield).

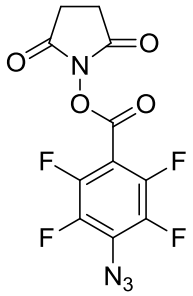

2,5-Dioxopyrrolidin-1-yl 4-azido-2,3,5,6-tetrafluorobenzoate (131). 4-azido tetrafluorobenzoic acid (**130**, 25 mg, 0.106 mmol), *N*-hydroxy succinimide (15 mg, 0.128 mmol), and EDC (24 mg, 0.128 mmol) were added to DCM (0.4 mL). The reaction vessel was covered in tinfoil and warmed to 35°C. Mixture allowed to stir for 16h. Additional EDC (12 mg, 0.064 mmol) was added and the reaction stirred for a further 3 hours. The reaction was quenched with H_2O and extracted 2x with DCM. The pooled organic layers were washed 2x with water and 1x with brine, isolated, dried over $MgSO_4$, vacuum filtered, and concentrated. The ^{1}H-NMR spectrum of the resulting white crystalline material was consistent with that of literature

precedent and was used without further purification. Isolated 28 mg (78% yield). ^{1}H NMR (500 MHz, Chloroform-*d*) δ 2.92 (s, 4H).

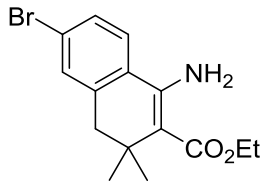

Ethyl 1-amino-6-bromo-3,3-dimethyl-3,4-dihydronaphthalene-2-carboxylate (133). To a dry flask containing anhydrous diglyme (18 mL) was added diisopropylamine (1.45 mL, 10.2 mmol). The solution was cooled to -78°C in a dry ice bath, then *n*-butyllithium (2.5 M in hexane, 4.1 mL, 10.2 mmol) was added slowly. A solution of 4-bromo-2-methylbenzonitrile (**132**, 1.00 g, 5.1 mmol) in anhydrous diglyme (~3 mL) was added slowly dropwise, then the solution allowed to stir for 45 minutes before the dropwise addition of ethyl-3,3-dimethyl acrylate (1.06 mL, 7.65 mmol) was added dropwise. The solution was allowed to stir for 1 hour at -78°C before addition of a freshly prepared solution of zinc iodide (3.26 g, 10.2 mmol) in anhydrous diglyme (6 mL) was added. The suspension was allowed slowly warm to room temperature and stir an additional 2 hours. Reaction was quenched with sat. aq. NH_4Cl, then extracted 3x with diethyl ether. Organic layer was washed 3x with H_2O, 1x with brine, then isolated, dried, filtered, and concentrated. Purification by FC (100% hex -> 5% EtOAc:hex) isolated the desired product as 867 mg of a yellow oil, 50.4% yield.^{1}H NMR (500 MHz, Chloroform-*d*) δ 7.41 (dd, *J* = 8.3, 2.1 Hz, 1H), 7.33 (d, *J* = 2.1 Hz, 1H), 7.25 (d, *J* = 8.3 Hz, 1H), 6.23 (s, 2H), 4.25 (q, *J* = 7.1 Hz, 2H), 2.62 (s, 2H), 1.34 (t, *J* = 7.1 Hz, 3H), 1.19 (s, 6H).

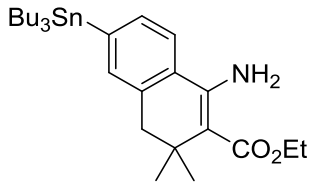

Ethyl 1-amino-3,3-dimethyl-6-(tributylstannyl)-3,4-dihydronaphthalene-2-carboxylate (intermediate in synthesis of 134). Brominated aminoester **133** (890 mg, 2.75 mmol) was added to dry toluene (27.5 mL) under N_2, followed by bis(tributyltin) (2.39 g, 4.12 mmol) and tetrakis(triphenylphosphine) palladium (0) (317 mg, 0.275 mmol). The flask was fitted with a reflux condenser and an N_2 needle and warmed to reflux for 16 hours. The reaction was cooled

and the solvent removed *in vacuo*. The crude isolate was purified via flash chromatography (0-5% ethyl acetate: hexanes) to yield the stannylated product as a clear oil (547 mg, 37% yield). ^{1}H NMR (500 MHz, Chloroform-*d*) δ 7.37 (d, *J* = 7.5 Hz, 1H), 7.31 (d, *J* = 7.5 Hz, 1H), 7.25 (d, *J* = 7.5 Hz, 1H), 6.33 (s, 2H), 4.25 (q, *J* = 7.1 Hz, 2H), 2.63 (s, 2H), 1.60 – 1.49 (m, 6H), 1.39 – 1.28 (m, 9H), 1.20 (s, 6H), 1.10 – 1.03 (m, 6H), 0.89 (t, *J* = 7.3 Hz, 9H).

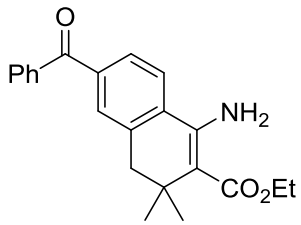

Ethyl 1-amino-6-benzoyl-3,3-dimethyl-3,4-dihydronaphthalene-2-carboxylate (134). The stannylated aminoester (553 mg, 1.035 mmol) was combined with anhydrous DMF (4.2 mL) in a dry round bottom flask. Iodobenzene (128 µL, 1.14 mmol) and bis-(triphenylphosphine) palladium (II) dichloride (73 mg, 0.103 mmol) were then added. Gaseous carbon monoxide was bubbled into the solution via needle for 5 minutes. The reaction securely capped and affixed with a CO-filled balloon. The reaction warmed to 90°C and allowed to stir for 4 hours. The reaction vessel was allowed to cool, then excess CO was purged via nitrogen for 15 minutes. Water was added to the reaction mixture, and the resulting suspension was extracted 2x with diethyl ether. The pooled organic extract was washed with water and saturated NaCl solution, then isolated, dried over $MgSO_4$, vacuum filtered, and concentrated, leaving a bright yellow residue. Flash chromatography (5% EtOAc:hex) isolated 210 mg of the product as a bright yellow solid (58% yield). ^{1}H NMR (400 MHz, Chloroform-*d*) δ 7.81 (d, *J* = 8.2 Hz, 2H), 7.74 – 7.56 (m, 3H), 7.50 (t, *J* = 8.2 Hz, 3H), 6.26 (s, 2H), 4.28 (q, *J* = 7.1 Hz, 2H), 2.72 (s, 2H), 1.36 (t, *J* = 7.1 Hz, 3H), 1.22 (s, 6H).

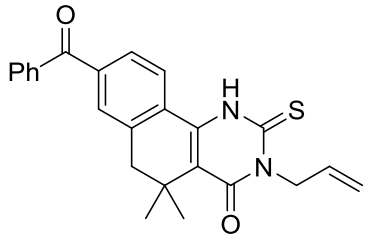

3-Allyl-8-benzoyl-5,5-dimethyl-2-thioxo-2,3,5,6-tetrahydrobenzo[*h*]quinazolin-4(1*H*)-one (135). Allyl isothiocyanate (117 µL, 1.2 mmol) was added to a solution of aminoester **134** (210 mg, 0.60 mmol) and acetic acid (69 µL, 1.20 mmol) in absolute ethanol (0.8 mL). The solution was warmed to 78°C and allowed to stir in a capped vial. Additional allyl isothiocyanate (175 µL, 1.80 mmol) was added in equal portions over 3 hours, then allowed to stir for an additional 12h at 78°C. The solution was diluted with ethyl acetate and the organic layer washed with saturated sodium bicarbonate solution, water, and brine. The organic extract was then dried over $MgSO_4$, vacuum filtered, and concentrated *in vacuo*. Trituration of the crude extract with hexanes caused the precipitation of a light yellow solid, confirmed to be the desired product by NMR. Recovered 64 mg (27% yield). ^{1}H NMR (400 MHz, Chloroform-*d*) δ 9.36 (s, 1H), 7.84 – 7.80 (m, 2H), 7.78 – 7.72 (m, 2H), 7.66 – 7.62 (m, 1H), 7.57 (d, *J* = 8.0 Hz, 1H), 7.53 (t, *J* = 7.7 Hz, 2H), 6.00 (ddt, *J* = 17.0, 10.7, 5.8 Hz, 1H), 5.39 (d, *J* = 17.0 Hz, 1H), 5.28 (d, *J* = 10.7 Hz, 1H), 5.07 (d, *J* = 5.8 Hz, 2H), 2.87 (s, 2H), 1.37 (s, 6H).

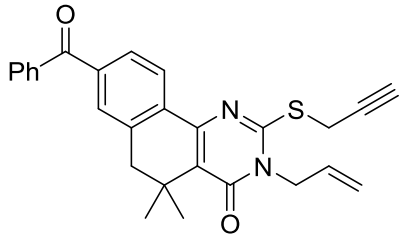

3-Allyl-8-benzoyl-5,5-dimethyl-2-(prop-2-yn-1-ylthio)-5,6-dihydrobenzo[*h*]quinazolin-4(3*H*)-one (136) (CCG-204080). Thiourea **135** (30 mg, 0.075 mmol) was dissolved in 2-butanone (0.44 mL), to which cesium carbonate (27 mg, 0.082 mmol) and propargyl bromide (10 mg, 0.082 mmol) were added. The reaction was warmed to 75°C and allowed to stir for 16 hours. The reaction was quenched via the addition of water, and the suspension was extracted with ethyl acetate. The organic layer was washed with water 2x and brine 1x, isolated, dried over $MgSO_4$, vacuum filtered, and concentrated *in vacuo*. Flash chromatography isolated the desired product as white crystals (23 mg, 70% yield). ^{1}H NMR (500 MHz, Chloroform-*d*) δ 8.27

(d, *J* = 8.0 Hz, 1H), 7.83 (d, *J* = 7.6 Hz, 2H), 7.73 (d, *J* = 8.0 Hz, 1H), 7.66 (s, 1H), 7.61 (t, *J* = 7.6 Hz, 1H), 7.51 (t, *J* = 7.6 Hz, 2H), 5.97 – 5.87 (m, 1H), 5.35 – 5.27 (m, 2H), 4.68 (d, *J* = 5.5 Hz, 2H), 4.07 (d, *J* = 2.6 Hz, 2H), 2.87 (s, 2H), 2.27 (t, *J* = 2.6 Hz, 1H), 1.41 (s, 6H). ESI-MS+ *m/z* = 441.2 ($M + H^+$), 463.2 ($M + Na^+$).

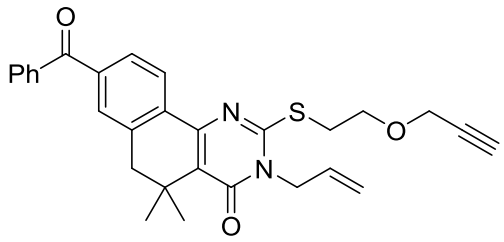

3-Allyl-8-benzoyl-5,5-dimethyl-2-((2-(prop-2-yn-1-yloxy)ethyl)thio)-5,6-dihydrobenzo[*h*]quinazolin-4(3*H*)-one (137) (CCG-205365). Prepared in the same manner as **136**, using 2-(prop-2-yn-1-yloxy)ethyl 4-methylbenzenesulfonate (**139**) as the alkylating agent. Product isolated after column chromatography (0-10% ethyl acetate: hexanes) as a white solid (53 mg, 69% yield). ^{1}H NMR (500 MHz, Chloroform-*d*) δ 8.18 (d, *J* = 8.1 Hz, 1H), 7.84 (d, *J* = 75.0 Hz, 2H), 7.73 (d, *J* = 8.1 Hz, 1H), 7.66 (s, 1H), 7.62 (t, *J* = 7.5 Hz, 1H), 7.51 (t, *J* = 7.5 Hz, 2H), 5.94 (ddt, *J* = 16.6, 10.7, 5.7 Hz, 1H), 5.35 – 5.26 (m, 2H), 4.71 (d, *J* = 5.7 Hz, 2H), 4.23 (d, *J* = 2.4 Hz, 2H), 3.91 (t, *J* = 6.4 Hz, 2H), 3.57 (t, *J* = 6.4 Hz, 2H), 2.86 (s, 2H), 2.44 (t, *J* = 2.4 Hz, 1H), 1.41 (s, 6H). ESI-MS+ *m/z* = 485.0 ($M + H^+$), 507.0 ($M + Na^+$). HPLC (Method B, T_R = 8.15 min), 86% purity.

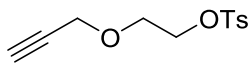

2-(Prop-2-yn-1-yloxy)ethyl 4-methylbenzenesulfonate (139). Prepared in a manner similar to compound **149** from propynol ethoxylate (**138**, 500 mg, 4.99 mmol). Isolated the desired compound as a light yellow oil (914 mg, 72% yield).^{1}H NMR (400 MHz, Chloroform-*d*) δ 7.81 (d, *J* = 8.2 Hz, 2H), 7.34 (d, *J* = 8.2 Hz, 2H), 4.23 – 4.16 (m, 2H), 4.12 (d, *J* = 2.4 Hz, 2H), 3.75 – 3.71 (m, 2H), 2.45 (s, 3H), 2.42 (t, *J* = 2.4 Hz, 1H).

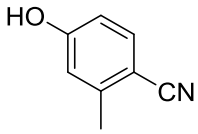

4-Hydroxy-2-methylbenzonitrile (intermediate in synthesis of 140). To a dry flask of dichloromethane (34 mL) was added 4-methoxy-2-methylbenzonitrile **26c** (1.5 g, 10.2 mmol). Boron trifluoride dimethyl sulfide complex (10.7 mL, 102 mmol) was then added slowly to the reaction mixture over 5 minutes. The reaction was allowed to stir 16 hours at room temperature. The reaction was quenched by the addition of water, and was allowed to stir for 15 minutes until fuming stopped. The reaction was diluted with ethyl acetate (~100 mL) and partitioned via separatory funnel. The aqueous layer was extracted 2 more times with EtOAc, then the combined organic extract was washed with water 2x and brine. The organic layer was isolated, dried over $MgSO_4$, vacuum filtered and concentrated *in vacuo* to a light pink solid (1.31 g, 96% yield), used without further purification ^{1}H NMR (500 MHz, DMSO-d_6) δ 10.49 (s, 1H), 7.56 (d, J = 8.5 Hz, 1H), 6.79 (d, J = 2.4 Hz, 1H), 6.72 (dd, J = 8.5, 2.4 Hz, 1H), 2.38 (s, 3H).

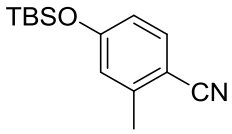

4-((*tert*-Butyldimethylsilyl)oxy)-2-methylbenzonitrile (140). The phenol intermediate (1.305 g, 9.80 mmol) was combined with dry DMF (1.7 mL) in a flask at room temperature. Imidazole (1.67 g, 24.5 mmol) and TBS-Cl (1.77 g, 11.8 mmol) were added and the reaction was allowed to stir for 16h. The reaction became biphasic over the course of reaction. After 16h, the reaction mixture was poured into diethyl ether and washed 3x with water and 1x with brine. The organic layer was isolated, dried over $MgSO_4$, vacuum filtered, and concentrated *in vacuo* to a transparent red oil. After further solvent removal via vacuum pump, the resulting oil (2.41 g, quant) was carried on without further purification. ^{1}H NMR (500 MHz, Chloroform-d) δ 7.47 (d, J = 8.4 Hz, 1H), 6.74 (d, J = 2.3 Hz, 1H), 6.70 (dd, J = 8.4, 2.3 Hz, 1H), 2.48 (s, 3H), 0.98 (s, 9H), 0.22 (s, 6H).

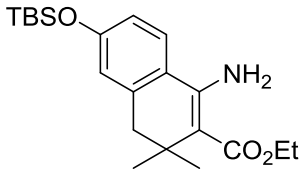

Ethyl 1-amino-6-((tert-butyldimethylsilyl)oxy)-3,3-dimethyl-3,4-dihydronaphthalene-2-carboxylate (141). To a dry flask under N_2 atmosphere was added anhydrous diglyme (46 mL) and diisopropylamine (5.5 mL, 38.8 mmol). The solution was cooled to -78°C in a dry ice bath, then *n*-butyllithium (2.5M in hexanes, 5.53 mL) was added slowly. Benzonitrile intermediate **140** (2.4 g, 9.7 mmol) was dissolved in ~3mL dry diglyme and added slowly dropwise to the reaction and was allowed to stir at -78°C for 60 minutes. Ethyl-3,3-dimethyl acrylate (4.05 mL, 29.1 mmol) was added dropwise and allowed to stir an additional 1 hour at -78°C. Concurrently, ZnI_2 was generated in situ in a separate flame-dried flask containing dry diglyme (15 mL). After addition of zinc powder (1.59 g, 24.3 mmol) to the flask, iodine (4.92 g, 19.4 mmol) was added portionwise over 20 minutes to the reaction (warning: exothermic). The reaction vessel was warmed in 30 second bursts with a heat gun until the color of iodine was replaced with a metallic silver color. The suspension was allowed to cool to room temperature, then added to the first reaction mixture after its 2nd hour of stirring at -78°C, and then allowed to slowly warm to room temperature over the course of 2 hours. The reaction was quenched with sat. aq. NH_4Cl solution then extracted 3x with diethyl ether. The combined organic extract was washed 3x with water and 1x with brine, then isolated, dried over $MgSO_4$, vacuum filtered, and concentrated *in vacuo*. Purification via FC (0-15% EtOAc:hex) isolated 1.9 g of the desired product; a second FC purification of impure fractions resulted in an additional 400 mg to combine for 2.3 g of a light yellow solid (63% yield).^{1}H NMR (500 MHz, Chloroform-*d*) δ 7.28 (d, *J* = 8.4 Hz, 1H), 6.74 (dd, *J* = 8.4, 2.5 Hz, 1H), 6.67 (d, *J* = 2.4 Hz, 1H), 6.35 (s, 2H), 4.26 (q, *J* = 7.1 Hz, 2H), 2.60 (s, 2H), 1.36 (t, *J* = 7.1 Hz, 3H), 1.21 (s, 6H), 1.01 (s, 9H), 0.24 (s, 6H).

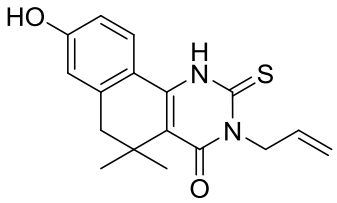

3-Allyl-8-hydroxy-5,5-dimethyl-2-thioxo-2,3,5,6-tetrahydrobenzo[h]quinazolin-4(1H)-one (142). TBS-protected aminoester **141** (1.9 g, 5.06 mmol) was dissolved in absolute ethanol (7

mL). Cesium carbonate (3.30 g, 10.12 mmol) was added, along with allyl isothiocyanate (983 µL, 10.1 mmol). The reaction mixture was warmed to 75°C and tightly capped. Additional allyl isothiocyanate (1.48 mL, 15.2 mmol) was added in equal portions over the course of the next 3 hours, then the reaction mixture was allowed to stir 12 additional hours at 75°C. Reaction diluted with water and extracted into EtOAc 3x. The pooled organic layers were washed with water and brine, then concentrated *in vacuo*. Trituration of the resulting orange residue caused the precipitation of white crystals. The crystals were collected via vacuum filtration and washed with cold hexanes and diethyl ether. The desired product was recovered as a white powder (900 mg, 57% yield). Used without further purification. ^{1}H NMR (400 MHz, DMSO-d_6) δ 12.16 (s, 1H), 10.15 (s, 1H), 7.78 (d, J = 8.3 Hz, 1H), 6.73 – 6.66 (m, 2H), 5.89 (ddd, J = 23.0, 10.6, 5.4 Hz, 1H), 5.20 – 5.11 (m, 2H), 4.96 (d, J = 5.4 Hz, 2H), 2.65 (s, 2H), 1.21 (s, 6H).

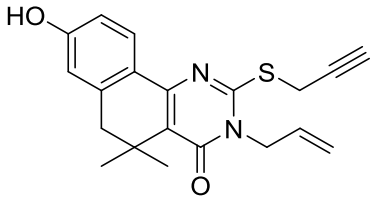

3-Allyl-8-hydroxy-5,5-dimethyl-2-(prop-2-yn-1-ylthio)-5,6-dihydrobenzo[h]quinazolin-4(3H)-one (intermediate leading to 143). Deprotected thiourea **142** (50 mg, 0.159 mmol) was dissolved in dry DMF (1.0 mL) and cooled to 0°C in an ice bath. Sodium bicarbonate (27 mg, 0.318 mmol) was added, followed by propargyl bromide (21 µL, 0.239 mmol). The reaction was allowed to stir for 16 hours while warming to room temperature. The reaction was diluted with sat. aq. ammonium chloride solution. The resulting suspension was extracted 3x with ethyl acetate, then the combined organic layers were washed 3x with water and 1x with brine. The organic layer was dried over $MgSO_4$, vacuum filtered, and concentrated *in vacuo.* Further purification via column chromatography (100 hex -> 10% EtOAc:hex -> 20% EtOAc:hex) isolated the compound as a yellow solid (40 mg, 71% yield). ^{1}H NMR (500 MHz, DMSO-d_6) δ 9.91 (s, 1H), 8.02 (d, J = 8.5 Hz, 1H), 6.76 – 6.61 (m, 2H), 5.95 – 5.80 (m, 1H), 5.28 – 5.13 (m, 2H), 4.57 (d, J = 5.2 Hz, 2H), 4.14 (s, 2H), 3.23 (s, 1H), 2.69 (s, 2H), 1.28 (s, 6H).

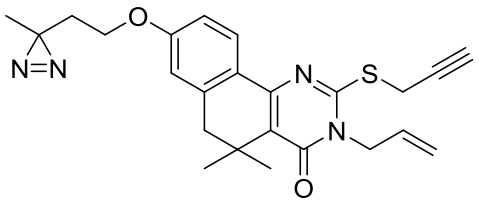

3-Allyl-5,5-dimethyl-8-(2-(3-methyl-3H-diazirin-3-yl)ethoxy)-2-(prop-2-yn-1-ylthio)-5,6-dihydrobenzo[h]quinazolin-4(3H)-one (143) (CCG-205457). The *S*-propargyl phenol intermediate (30 mg, 0.085 mmol), alkylating agent **149** (16 mg, 0.063 mmol), and cesium carbonate (37 mg, 0.113 mmol) were combined in dry DMF (0.3 mL). The reaction was capped and heated to 70°C for 1 hour. The reaction mixture was diluted with water, and extracted 2x with diethyl ether. The organic layer was then washed with water and brine, dried over $MgSO_4$, vacuum filtered, and concentrated. The resulting residue was purified via FC (0-10% EtOAc:hex) to furnish the product as a white solid (4 mg, 16% yield). ^{1}H NMR (400 MHz, Chloroform-*d*) δ 8.08 (d, *J* = 8.6 Hz, 1H), 6.83 (dd, *J* = 8.6, 2.4 Hz, 1H), 6.75 – 6.64 (m, 2H), 5.92 (ddt, *J* = 15.9, 10.7, 5.5 Hz, 1H), 5.37 – 5.22 (m, 2H), 5.16 (d, *J* = 6.5 Hz, 2H), 4.65 (d, *J* = 5.5 Hz, 2H), 3.93 (t, *J* = 6.3 Hz, 2H), 2.74 (s, 2H), 1.84 (t, *J* = 6.3 Hz, 2H), 1.37 (s, 6H), 1.14 (s, 3H). ESI+MS *m/z* = 435.2 ($M + H^+$), 457.2 ($M + Na^+$).

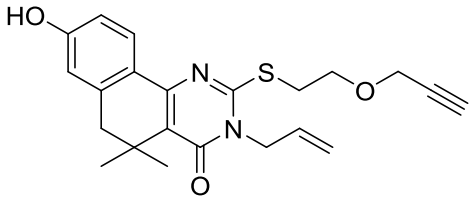

3-Allyl-8-hydroxy-5,5-dimethyl-2-((2-(prop-2-yn-1-yloxy)ethyl)thio)-5,6-dihydrobenzo[h]quinazolin-4(3H)-one (intermediate leading to 144). Thiourea **142** (300 mg, 0.954 mmol) was dissolved in DMF (5.6 mL), to which sodium bicarbonate (120 mg, 1.43 mmol) and propargyloxyethyl tosylate **139** (291 mg, 1.145 mmol) were added. The reaction was warmed to 75°C, capped, and allowed to stir for 16 h. Water was added to quench the reaction, and the resulting suspension was extracted 2x with ethyl acetate. The organic layer washed with water 2x and brine 1x, then dried over $MgSO_4$, vacuum filtered, and concentrated. The partially crystalline residue was further purified via flash chromatography (5-25% EtOAc:hex) to deliver 248 mg of the desired product (66% yield). ^{1}H NMR (400 MHz, DMSO-d_6) δ 9.91 (s, 1H), 7.90 (d, *J* = 8.5 Hz, 1H), 6.72 (d, *J* = 8.5 Hz, 1H), 6.64 (s, 1H), 5.91 – 5.79 (m, 1H), 5.21 (d, *J* = 10.4

Hz, 1H), 5.12 (d, *J* = 17.3 Hz, 1H), 4.59 (d, *J* = 5.2 Hz, 2H), 4.20 (d, *J* = 2.3 Hz, 2H), 3.78 (t, *J* = 6.2 Hz, 2H), 3.50 (t, *J* = 6.2 Hz, 2H), 3.46 (t, *J* = 2.3 Hz, 1H), 2.67 (s, 2H), 1.27 (s, 6H).

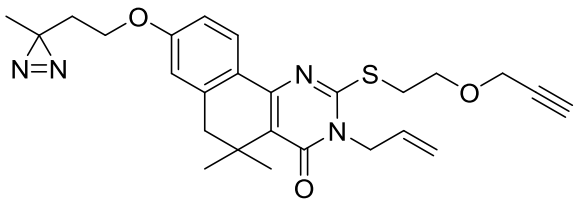

3-Allyl-5,5-dimethyl-8-(2-(3-methyl-3*H*-diazirin-3-yl)ethoxy)-2-((2-(prop-2-yn-1-yloxy)ethyl)thio)-5,6-dihydrobenzo[h]quinazolin-4(3*H*)-one (144) (CCG-205458). The *S*-ethyloxypropargyl phenol intermediate (248 mg, 0.622 mmol) was dissolved in DMF (3.7 mL), to which cesium carbonate (304 mg, 0.933 mmol) and alkylating agent **149** (182 g, 0.716 mmol) were added. The reaction was warmed to 75°C and tightly capped. The reaction was allowed to stir for 4 hours, at which point water was added to quench the reaction, and the suspension was extracted with ethyl acetate. The resulting organic layer was washed with water 2x and brine 1x, then isolated, dried over $MgSO_4$, filtered, and concentrated. Further purification via flash chromatography (0-15% EtOAc:hex) isolated the desired product as 190 mg of a white crystalline solid (64% yield). ^{1}H NMR (400 MHz, Chloroform-*d*) δ 8.00 (d, *J* = 8.5 Hz, 1H), 6.81 (d, *J* = 8.5 Hz, 1H), 6.70 (s, 1H), 5.91 (ddt, *J* = 16.1, 10.5, 5.6 Hz, 1H), 5.31 – 5.21 (m, 2H), 4.67 (d, *J* = 5.6 Hz, 2H), 4.21 (d, *J* = 2.4 Hz, 2H), 3.95 – 3.84 (m, 4H), 3.53 (t, *J* = 6.4 Hz, 2H), 2.73 (s, 2H), 2.43 (t, *J* = 2.4 Hz, 1H), 1.83 (t, *J* = 6.4 Hz, 2H), 1.36 (s, 6H), 1.13 (s, 3H). ESI+MS *m/z* = 479.2 ($M + H^+$), 501.2 ($M + Na^+$). HPLC (Method B, T_R = 8.17 min), >95% purity.

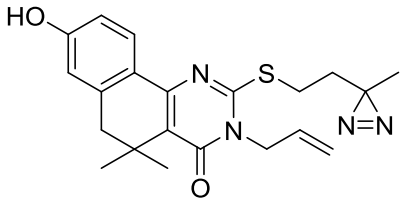

3-Allyl-8-hydroxy-5,5-dimethyl-2-((2-(3-methyl-3H-diazirin-3-yl)ethyl)thio)-5,6-dihydrobenzo[h]quinazolin-4(3H)-one (intermediate leading to 145 and 146). Thiourea **142** (100 mg, 0.318 mmol) was dissolved in dry DMF (1.9 mL) and heated to 50°C. Sodium bicarbonate (53 mg, 0.636 mmol) was added, followed by alkylating agent **149** (121 mg, 0.477

mmol). Reaction was allowed to stir for 16h at 50°C. Reaction mixture was diluted with sat. aq. NH_4Cl, causing a white precipitate to form. The suspension was extracted with EtOAc 3x, then the organic layer was washed 2x with water and 1x with brine. The organic extract was dried over $MgSO_4$, vacuum filtered, and concentrated, leaving an impure white solid. Trituration with diethyl ether furnished the desired product as 57 mg of a white solid (45% yield). ^{1}H NMR (400 MHz, DMSO-d_6) δ 9.93 (s, 1H), 7.85 (d, J = 8.5 Hz, 1H), 6.72 (dd, J = 8.5, 2.4 Hz, 1H), 6.64 (d, J = 2.4 Hz, 1H), 5.86 (ddt, J = 16.6, 10.4, 5.1 Hz, 1H), 5.21 (d, J = 10.4 Hz, 1H), 5.11 (d, J = 16.6 Hz, 2H), 4.57 (d, J = 5.1 Hz, 2H), 3.21 (t, J = 7.6 Hz, 2H), 2.67 (s, 2H), 1.80 (t, J = 7.6 Hz, 2H), 1.26 (s, 6H), 1.09 (s, 3H).

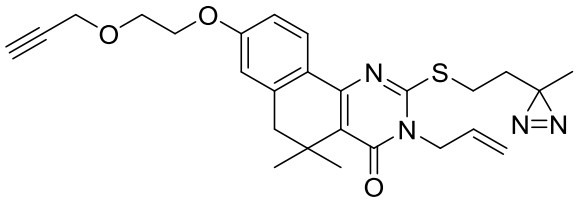

3-Allyl-5,5-dimethyl-2-((2-(3-methyl-3*H*-diazirin-3-yl)ethyl)thio)-8-(2-(prop-2-yn-1-yloxy)ethoxy)-5,6-dihydrobenzo[*h*]quinazolin-4(3*H*)-one (145) (CCG-205459). The *S*-2,2-diazirinylbutane phenol (37 mg, 0.093 mmol) and alkylating agent **139** (36 mg, 0.140 mmol) were combined in dry DMF (549 µL) along with of cesium carbonate (61 mg, 0.187 mmol). The reaction heated to 70°C and stirred for 16h. The reaction was quenched via dilution with water, causing a white suspension to form. The solution was extracted with ether 3x, then the organic layer was washed 2x with water and 1x with brine. The organic layer was isolated, dried over $MgSO_4$, vacuum filtered, and concentrated. Very conservative flash chromatography conditions (0-5% ethyl acetate:hexanes) was required to separate unreacted alkylating agent from the desired product, which was eventually isolated as a clear oil (18 mg, 41% yield). ^{1}H NMR (400 MHz, Chloroform-*d*) δ 7.98 (d, J = 8.6 Hz, 1H), 6.88 (dd, J = 8.6, 2.2 Hz, 1H), 6.75 (d, J = 2.2 Hz, 1H), 5.91 (ddt, J = 15.7, 10.3, 5.5 Hz, 1H), 5.33 – 5.18 (m, 2H), 4.65 (d, J = 5.5 Hz, 2H), 4.29 (d, J = 2.3 Hz, 2H), 4.25 – 4.18 (m, 2H), 3.95 – 3.87 (m, 2H), 3.23 – 3.08 (m, 2H), 2.73 (s, 2H), 2.48 (t, J = 2.3 Hz, 1H), 1.96 – 1.81 (m, 2H), 1.37 (s, 6H), 1.12 (s, 3H). ESI+MS *m/z* = 479.2 ($M + H^+$), 501.2 ($M + Na^+$).

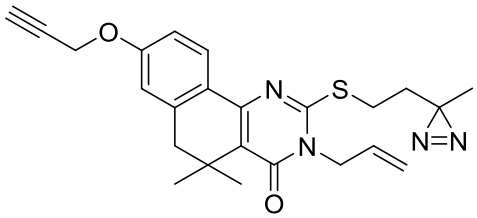

3-Allyl-5,5-dimethyl-2-((2-(3-methyl-3*H*-diazirin-3-yl)ethyl)thio)-8-(prop-2-yn-1-yloxy)-5,6-dihydrobenzo[*h*]quinazolin-4(3*H*)-one (146) (CCG-205460): The *S*-2,2-diazirinylbutane phenol intermediate (30 mg, 0.076 mmol)and propargyl bromide (14 mg, 0.113 mmol) were combined in dry DMF (0.5 mL) with cesium carbonate (49 mg, 0.151 mmol). The reaction heated to 70°C for 16 hours. The reaction was diluted with water, causing a white suspension to form. The solution was extracted with ether 3x, then the organic layer washed 2x with water and 1x with brine. The organic layer was isolated, dried over $MgSO_4$, filtered, and concentrated. Flash purification (100% hex to 5% EtOAc:hex) isolated the compound as a white crystalline solid (8 mg, 24% yield). ^{1}H NMR (400 MHz, Chloroform-*d*) δ 8.01 (d, *J* = 8.6 Hz, 1H), 6.94 (dd, *J* = 8.6, 2.4 Hz, 1H), 6.79 (d, *J* = 2.4 Hz, 1H), 5.91 (ddt, *J* = 15.6, 10.7, 5.5 Hz, 1H), 5.35 – 5.18 (m, 2H), 4.75 (d, *J* = 2.3 Hz, 2H), 4.66 (d, *J* = 5.5 Hz, 2H), 3.24 – 3.08 (m, 2H), 2.76 (s, 2H), 2.56 (t, *J* = 2.3 Hz, 1H), 1.96 – 1.80 (m, 2H), 1.37 (s, 6H), 1.12 (s, 3H). ESI+MS *m/z* = 435.2 (M + H^+), 457.2 (M + Na^+).

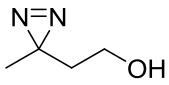

2-(3-Methyl-3*H*-diazirin-3-yl)ethan-1-ol (148). 4-hydroxy-2-butanone (**147**, 1.00 grams, 11.35 mmol) was pipetted into a dry RBF and cooled down to 0°C under N_2. 7N methanolic ammonia was added via syringe (11.2 mL, 79 mmol), and the solution was allowed to stir at 0°C for 3 hours. A solution of hydroxylamine-*O*-sulfonic acid (1.476 g, 13.05 mmol) in methanol (9.7 mL)was added dropwise, then was allowed to stir for an additional 16 hours while slowly warming to room temperature. The reaction was filtered through a sintered glass funnel, then transferred to a reaction vessel and re-cooled to 0°C. Triethylamine (1.58 mL, 11.35 mmol) was added, then molecular iodine (2.88 g, 11.35 mmol) was added slowly in 10 equal portions until the purple/brown color of iodine persisted in the reaction vessel. The solvent was removed under reduced pressure. Purification of the crude isolate via Kugelrohr distillation (60°C, 1-3 torr)

delivered the desired product as a clear oil (304 mg, 27% yield).[1]H NMR (500 MHz, Chloroform-*d*) δ 3.55 (t, *J* = 6.3 Hz, 2H), 1.65 (t, *J* = 6.3 Hz, 2H), 1.50 (bs, 1H), 1.08 (s, 3H).

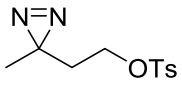

2-(3-Methyl-3*H*-diazirin-3-yl)ethyl 4-methylbenzenesulfonate (149). 3,3-diazirinyl butan-1-ol **148** (300 mg, 3.00 mmol) was dissolved in dry pyridine (6 mL) and cooled to 0°C in an ice bath. To this solution was added *p*-toluenesulfonyl chloride (628 mg, 3.30 mmol). The reaction mixture was allowed to stir for 24 hours at 0-4°C, then was poured into a mixture of 37% w/v HCl (15 mL) and ice (80 mL). The resulting suspension was extracted 3x with ether, then the pooled organic layers were washed with 1N HCl solution, 1N NaOH solution, water, and brine. The organic extract was dried over $MgSO_4$, vacuum filtered, and concentrated to a clear oil (428 mg, 56.2% yield) used without further purification. TLC Rf (2:1 hex:EtOAc) = 0.6.[1]H NMR (500 MHz, Chloroform-*d*) δ 7.82 (d, *J* = 7.9 Hz, 2H), 7.37 (d, *J* = 7.9 Hz, 2H), 3.96 (t, *J* = 6.4 Hz, 2H), 2.46 (s, 3H), 1.68 (t, *J* = 6.4 Hz, 2H), 1.01 (s, 2H).

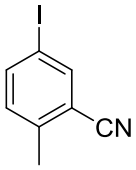

5-Iodo-2-methylbenzonitrile (intermediate used in synthesizing 151). Water (30 mL) and concentrated hydrogen chloride solution (37% w/v, 9 mL) were cooled to 0°C in an ice bath. Aniline intermediate **150** (3.00 g, 22.7 mmol) was added, followed by a solution of sodium nitrite (1.72 g, 25.0 mmol) in water (7.5 mL). The solution was allowed to stir at 0°C until all of the starting material dissolved (30 minutes). A solution of potassium iodide (5.65 g, 34.0 mmol) in water (7.5 mL) was added and allowed to stir for an additional 30 minutes at 0°C. Diethyl ether (20 mL) was added before stirring an additional 30 min. The reaction mixture was loaded into a separatory funnel, and the organic layer was isolated. The aqueous layer was extracted with additional diethyl ether, then the pooled organic extracts were washed with saturated aqueous sodium thiosulfate solution, saturated $NaHCO_3$, water, and brine. The organic layer was dried over $MgSO_4$, filtered, and concentrated, leaving an orange crystalline residue. Flash purification via 3-5% EtOAc:hex delivered the title compound as a white solid (3.86 g, 70%

yield). TLC Rf (10% EtOAc:hex) = 0.7, ^{1}H NMR (400 MHz, Chloroform-*d*) δ 7.90 (d, *J* = 1.9 Hz, 1H), 7.79 (dd, *J* = 8.2, 1.9 Hz, 1H), 7.07 (d, *J* = 8.2 Hz, 1H), 2.50 (s, 3H).

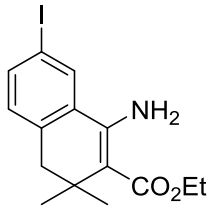

Ethyl 1-amino-7-iodo-3,3-dimethyl-3,4-dihydronaphthalene-2-carboxylate (151). Prepared according to General Method B from the previously described iodotolunitrile (3.5 g, 14.4 mmol). Recovered the desired product as light yellow crystals (1.23 g, 23% yield). ^{1}H NMR (400 MHz, Chloroform-*d*) δ 7.70 (d, *J* = 1.6 Hz, 1H), 7.61 (dd, *J* = 7.8, 1.6 Hz, 1H), 6.92 (d, *J* = 7.9 Hz, 1H), 6.18 (s, 2H), 4.26 (q, *J* = 7.1 Hz, 2H), 2.58 (s, 2H), 1.34 (t, *J* = 7.1 Hz, 3H), 1.18 (s, 6H).

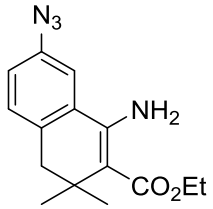

Ethyl 1-amino-7-azido-3,3-dimethyl-3,4-dihydronaphthalene-2-carboxylate (152). Iodo-aminoester **151** (1.00 g, 2.69 mmol) was added to a 5:1 DMSO:water solution (5.4 mL) under argon atmosphere. Sodium ascorbate (107 mg, 0.539 mmol), *N*,*N*-dimethyl-ethylenediamine (43 µL, 0.404 mmol) and sodium azide (350 mg, 5.39 mmol) were added and allowed to fully dissolve. The mixture was purged with argon via immersion of an argon needle below the surface for 2 minutes, then copper(I)iodide (51 mg, 0.269 mmol) was added and the reaction vessel sealed under argon atmosphere. The reaction vessel was lightly heated with a heat gun to promote reaction components to fully dissolve. The reaction vessel was covered in tin foil and allowed to stir at RT for 30 minutes. Reaction quenched via addition of more water, then was extracted with diethyl ether. The organic layer was washed 2x with water and 1x with brine, then dried over $MgSO_4$, vacuum filtered and concentrated *in vacuo*, delivering the title compound as a light brown oil (658 mg, 85% yield).^{1}H NMR (400 MHz, Chloroform-*d*) δ 7.17 (d, *J* = 7.8 Hz, 1H), 7.04 – 6.94 (m, 2H), 6.19 (s, 2H), 4.26 (q, *J* = 7.0 Hz, 2H), 2.62 (s, 2H), 1.35 (t, *J* = 7.0 Hz, 3H), 1.19 (s, 6H).

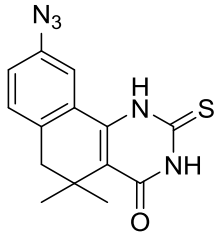

9-Azido-5,5-dimethyl-2-thioxo-2,3,5,6-tetrahydrobenzo[*h*]quinazolin-4(1*H*)-one (153). Aminoester intermediate **152** (658 mg, 2.30 mmol) was combined with benzoyl isothiocyanate (488 mg, 2.99 mmol) in absolute ethanol (2.7 mL). The reaction was warmed to 75°C and allowed to stir 3 hours. Additional benzoyl isothiocyanate (244 mg, 1.50 mmol) was added, and the reaction was allowed to stir at 75°C for an additional 12 hours. At this point the reaction mixture was dissolved in DCM, and the organic layer washed with water and brine. The organic layer was isolated, dried over $MgSO_4$, filtered, and concentrated, resulting in a yellow-orange oil. Column chromatography isolated the uncyclized *N*-benzoyl thiourea (690 mg) as a white solid. This intermediate was dissolved in EtOH (3 mL) and warmed to 75°C. A solution of KOH (172 mg, 3.07 mmol) in water (1.5 mL) was added to the flask allowed to stir for 1.5 hours. Reaction was quenched via the addition of ~5mL 1N HCl, causing the precipitation of a white solid. Solid was collected via vacuum filtration and washed with saturated aqueous sodium bicarbonate and water. Drying under high vacuum yielded the desired product as a white powder (372 mg, 54% yield over 2 steps). ^{1}H NMR (400 MHz, DMSO-d_6) δ 12.43 (s, 1H), 12.28 (s, 1H), 7.78 (d, J = 2.1 Hz, 1H), 7.33 (d, J = 8.0 Hz, 1H), 7.13 (dd, J = 8.0, 2.1 Hz, 1H), 2.71 (s, 2H), 1.21 (s, 6H).

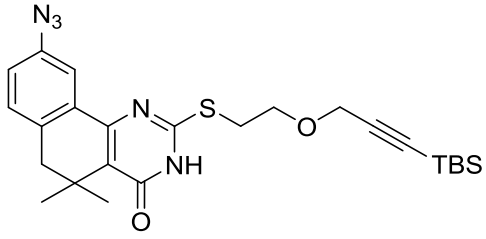

9-Azido-2-((2-((3-(tert-butyldimethylsilyl)prop-2-yn-1-yl)oxy)ethyl)thio)-5,5-dimethyl-5,6-dihydrobenzo[*h*]quinazolin-4(3*H*)-one (intermediate used in synthesis of 154). Azido 2-thioxopyrimidinone intermediate **153** (320 mg, 1.07 mmol) was dissolved in DMF (6.3 mL), to which the TBS-protected alkyne alkylating agent **156** (414 mg, 1.12 mmol) was added. Sodium bicarbonate (135 mg, 1.60 mmol) was added and the mixture was stirred at 50°C for 6 hours. The reaction was quenched by the addition of water, causing the precipitation of a white solid

from the aqueous layer. Vacuum filtration isolated 530 mg of solid (92% crude yield) found to be the title compound with a minor (~10%) impurity of alkylating agent. Carried on without further purification. ^{1}H NMR (400 MHz, Chloroform-*d*) δ 12.14 (s, 1H), 7.82 (d, *J* = 2.4 Hz, 1H), 7.17 (d, *J* = 8.0 Hz, 1H), 7.00 (dd, *J* = 8.0, 2.4 Hz, 1H), 4.26 (s, 2H), 3.92 (t, *J* = 6.1 Hz, 2H), 3.50 (t, *J* = 6.1 Hz, 2H), 2.76 (s, 2H), 1.41 (s, 6H), 0.88 (s, 9H), 0.06 (s, 6H).

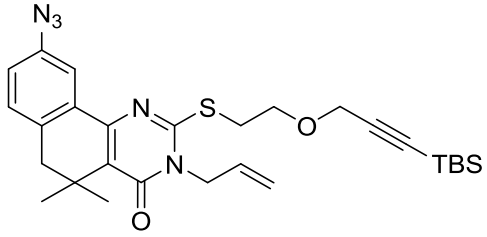

3-Allyl-9-azido-2-((2-((3-(tert-butyldimethylsilyl)prop-2-yn-1-yl)oxy)ethyl)thio)-5,5-dimethyl-5,6-dihydrobenzo[*h*]quinazolin-4(3*H*)-one (154). The *S*-alkylated intermediate described above (490 mg, 0.988 mmol) was dissolved in absolute EtOH (5.8 mL), to which sodium methoxide (107 mg, 1.98 mmol) was added. The mixture was allowed to stir for 20 minutes, then allyl bromide (598 mg, 4.94 mmol) was added. Reaction was heated to 75°C and allowed to stir for 16 hours. The reaction was halted by the addition of H_2O. The aqueous mixture was extracted into ethyl acetate 3 times, then the pooled organic extracts were washed twice with water and once with brine. The organic layer was isolated, dried over $MgSO_4$, filtered, and concentrated *in vacuo*. Further purification via FC (5% EtOAc:hex) returned the compound as a clear oil (254 mg, 48% yield). ^{1}H NMR (400 MHz, Chloroform-*d*) δ 7.78 (d, *J* = 2.4 Hz, 1H), 7.17 (d, *J* = 8.0 Hz, 1H), 6.99 (dd, *J* = 8.0, 2.4 Hz, 1H), 5.92 (ddt, *J* = 15.9, 10.9, 5.6 Hz, 1H), 5.34 – 5.23 (m, 2H), 4.69 (d, *J* = 5.6 Hz, 2H), 4.24 (s, 2H), 3.92 (t, *J* = 6.0 Hz, 2H), 3.54 (t, *J* = 6.0 Hz, 2H), 2.76 (s, 2H), 1.38 (s, 6H), 0.87 (s, 9H), 0.05 (s, 6H).

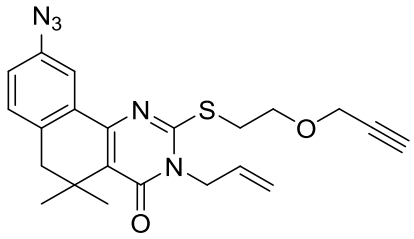

3-Allyl-9-azido-5,5-dimethyl-2-((2-(prop-2-yn-1-yloxy)ethyl)thio)-5,6-dihydrobenzo[*h*]quinazolin-4(3*H*)-one (155) (CCG-206603). The TBS-protected intermediate

154 (254 mg, 0.474 mmol) was dissolved in anhydrous THF (4 mL) and cooled to 0°C. TBAF (1M solution in THF, 1.00 mL) was then added dropwise to the reaction and monitored for 3 hours. After 3 hours, the spot corresponding to starting material had completely disappeared, being replaced by a more polar spot that still turned brown upon UV exposure. The reaction was quenched with water and diluted with diethyl ether. The organic layer was washed with water and brine, then dried, filtered, and concentrated. Further purification by FC (0-15% EtOAc:hex) delivered the desired product as a white crystalline solid (130 mg, 65% yield).^{1}H NMR (400 MHz, Chloroform-*d*) δ 7.77 (d, *J* = 2.2 Hz, 1H), 7.18 (d, *J* = 8.0 Hz, 1H), 7.00 (dd, *J* = 8.0, 2.2 Hz, 1H), 5.93 (ddt, *J* = 16.3, 10.8, 5.6 Hz, 1H), 5.34 – 5.24 (m, 2H), 4.70 (d, *J* = 5.6 Hz, 2H), 4.23 (d, *J* = 2.1 Hz, 2H), 3.92 (t, *J* = 6.2 Hz, 2H), 3.55 (t, *J* = 6.2 Hz, 2H), 2.76 (s, 2H), 2.43 (t, *J* = 2.1 Hz, 1H), 1.38 (s, 6H). ESI+MS *m/z* = 444.1 ($M + Na^{+}$). HPLC (Method B, t_R = 8.74 min), purity >95%.

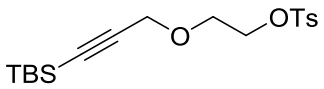

2-((3-(*tert*-Butyldimethylsilyl)prop-2-yn-1-yl)oxy)ethyl 4-methylbenzenesulfonate (156). A dry flask was charged with anhydrous THF (5.2 mL) and tosylated alkyne **139** (200 mg, 0.786 mmol) was cooled to -78°C. A hexane solution of *n*-butyllithium (2.5 M, 0.5 mL) was added slowly dropwise, and the mixture was allowed to stir for 2 hours before the dropwise addition of TBS-OTf (271 µL, 1.18 mmol). The reaction was stirred for an additional 30 minutes, then quenched via the addition of saturated aqueous NH_4Cl solution. The resulting suspension was extracted 3x into ether, then washed with saturated aqueous $NaHCO_3$ and brine, isolated, dried over $MgSO_4$, vacuum filtered, and concentrated. Flash chromatography (5% EtOAc:hex) isolated the title compound as a clear oil (182 mg, 63% yield). ^{1}H NMR (400 MHz, Chloroform-*d*) δ 7.80 (d, *J* = 8.2 Hz, 2H), 7.34 (d, *J* = 8.2 Hz, 2H), 4.23 – 4.15 (m, 2H), 4.13 (s, 2H), 3.76 – 3.69 (m, 2H), 2.45 (s, 3H), 0.92 (s, 9H), 0.10 (s, 6H).

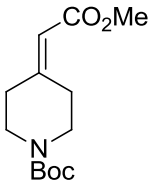

***tert*-Butyl 4-(2-methoxy-2-oxoethylidene)piperidine-1-carboxylate (173).** Sodium hydride (60 wt%, 1.31 g, 32.6 mmol) was added to a dry reaction vessel and triturated 2x with hexanes. Anhydrous DMF (50 mL) was added to the reaction flask and the resulting suspension was cooled to 0°C. Trimethyl phosphonoacetate (5.71 g, 31.4 mmol) was added slowly over the course of 15 minutes, causing the evolution of hydrogen gas bubbles. The reaction was allowed to stir for an additional 15 minutes, then a solution of tert-butyl 4-oxopiperidine-1-carboxylate (**172**, 5.00 g, 25.1 mmol) in anhydrous DMF (10 mL) was added over the course of 10 minutes. The reaction was allowed to slowly warm to room temperature over 3 hours with stirring. The reaction was quenched via the addition of water (200 mL), and the resulting aqueous suspension was extracted 3x with diethyl ether. The pooled organic fractions were washed with water (3x) and brine, then dried over $MgSO_4$, vacuum filtered, and concentrated *in vacuo*. The resulting white crystalline solid (6.36g, 99% yield) was used without further purification. ^{1}H NMR (400 MHz, Chloroform-*d*) δ 5.70 (s, 1H), 3.68 (s, 3H), 3.53 – 3.42 (m, 4H), 2.92 (t, *J* = 5.8 Hz, 2H), 2.27 (t, *J* = 5.8 Hz, 2H), 1.46 (s, 9H).

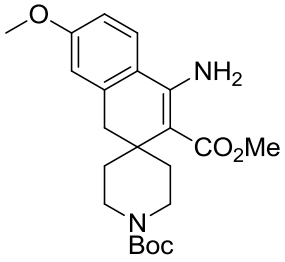

1'-*tert*-Butyl 3-methyl 4-amino-7-methoxy-1H-spiro[naphthalene-2,4'-piperidine]-1',3-dicarboxylate (174). Reaction performed according to General Method B from tolunitrile **26c** (2.31 g, 15.67 mmol) and Michael acceptor **173** (4.00 g, 15.67 mmol). Purification of the concentrated organic extract via flash chromatography (5-25% EtOAc:hex), followed by trituration of the resulting residue with cold diethyl ether furnished the desired product as a white powder (4.25 g, 74% yield). ^{1}H NMR (400 MHz, Chloroform-*d*) δ 7.33 (d, *J* = 8.6 Hz, 1H), 6.80

(dd, *J* = 8.6, 2.6 Hz, 1H), 6.73 (d, *J* = 2.6 Hz, 1H), 6.30 (s, 2H), 3.98 – 3.77 (m, 5H), 3.74 (s, 3H), 3.06 – 2.89 (m, 2H), 2.87 (s, 2H), 2.39 – 2.23 (m, 2H), 1.46 (s, 9H), 1.26 – 1.17 (m, 2H).

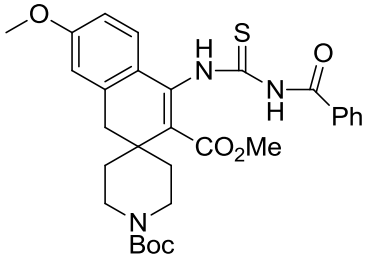

1'-*tert*-Butyl 3-methyl 4-(3-benzoylthioureido)-7-methoxy-1H-spiro[naphthalene-2,4'-piperidine]-1',3-dicarboxylate (intermediate in synthesis of 175). To a stirred solution of β-aminoester **174** (4.25 g, 10.6 mmol) in absolute ethanol (21.2 mL) was added benzoyl isothiocyanate (1.80 mL, 12.7 mmol). The reaction was warmed to reflux and allowed to stir for 2 hours. Additional benzoyl isothiocyanate (900 µL, 6.35 mmol) was added and the reaction was stirred at reflux for an additional 4 hours. The reaction was quenched via the addition of water (80 mL), and the resulting aqueous solution was extracted 3x with ethyl acetate. The organic extract was washed with water and brine, then dried over $MgSO_4$, vacuum filtered, and concentrated to an orange oil. Further purification via flash chromatography (10-40% EtOAc:hex) furnished the desired product as a pale yellow solid (3.88 g, 65% yield). ^{1}H NMR (400 MHz, Chloroform-*d*) δ 11.74 (s, 1H), 9.15 (s, 1H), 7.91 (d, *J* = 7.9 Hz, 2H), 7.67 (t, *J* = 7.4 Hz, 1H), 7.55 (t, *J* = 7.6 Hz, 2H), 7.22 (d, *J* = 8.4 Hz, 1H), 6.79 – 6.71 (m, 2H), 4.02 – 3.76 (m, 8H), 3.12 – 2.94 (m, 4H), 1.96 (td, *J* = 13.1, 4.8 Hz, 2H), 1.46 (d, *J* = 1.8 Hz, 11H).

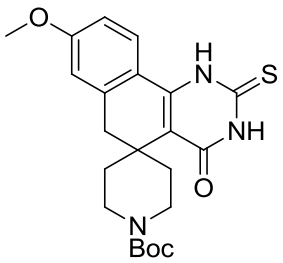

***tert*-Butyl 8-methoxy-4-oxo-2-thioxo-2,3,4,6-tetrahydro-1H-spiro[benzo[h]quinazoline-5,4'-piperidine]-1'-carboxylate (175).** The *N*-benzoyl thiourea intermediate (3.88 g, 6.86 mmol) was dissolved in absolute ethanol (18 mL) and warmed to 70°C. A solution of potassium hydroxide (85 wt%, 905 mg, 13.72 mmol) in water (9.2 mL) was added, and the resulting suspension was

stirred at 70°C for 2 hours. At this time the reaction was diluted with water (50 mL) and carefully acidified to pH ~7 with 1M HCl and cooled to 4°C. The resulting white precipitate was collected via vacuum filtration, washed with water and cold diethyl ether, and dried under high vacuum to yield the desired product (2.44 g, 83% yield) as an off-white solid used without further purification. ^{1}H NMR (400 MHz, DMSO-d_6) δ 12.12 (s, 2H), 7.83 (d, J = 8.7 Hz, 1H), 6.96 (d, J = 2.6 Hz, 1H), 6.90 – 6.82 (m, 1H), 3.82 – 3.69 (m, 5H), 3.11 – 2.84 (m, 4H), 2.59 – 2.30 (m, 2H), 1.37 (s, 9H), 1.11 (d, J = 12.8 Hz, 2H).

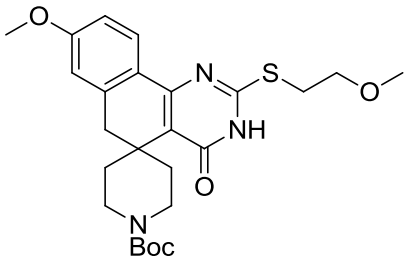

***tert*-Butyl 8-methoxy-2-((2-methoxyethyl)thio)-4-oxo-4,6-dihydro-3H-spiro[benzo[h]quinazoline-5,4'-piperidine]-1'-carboxylate (176a).** Cyclic thiourea intermediate **175** (500 mg, 1.16 mmol) was added to anhydrous DMF (6.8 mL), followed by sodium bicarbonate (108 mg, 1.28 mmol) and 2-methoxyethyl *p*-toluenesulfonic ester (281 mg, 1.22 mmol). The suspension was warmed to 70°C and allowed to stir for 16 hours. At this point the reaction was diluted with water (50 mL) and the resulting precipitate was collected via vacuum filtration. The precipitate was washed with water, followed by cold hexane:diethyl ether (1:1) and dried further under high vacuum to isolate the desired product as a white powder (360 mg, 63% yield). ^{1}H NMR (400 MHz, DMSO-d_6) δ 12.52 (s, 1H), 7.94 (d, J = 8.7 Hz, 1H), 6.94 – 6.83 (m, 2H), 3.81 – 3.69 (m, 5H), 3.60 (t, J = 6.3 Hz, 2H), 3.38 (t, J = 6.3 Hz, 2H), 3.26 (s, 3H), 3.02 (s, 4H), 2.67 – 2.38 (m, 2H), 1.38 (s, 9H), 1.19 (d, J = 13.3 Hz, 2H).

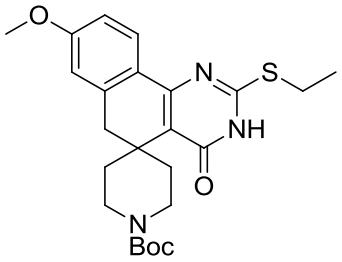

***tert*-Butyl 2-(ethylthio)-8-methoxy-4-oxo-4,6-dihydro-3H-spiro[benzo[h]quinazoline-5,4'-piperidine]-1'-carboxylate (176b).** The 2-thioxo pyrimidinone intermediate **175** (79 mg, 0.184 mmol) was dissolved in DMF (1.1 mL), to which sodium bicarbonate (23 mg, 0.276 mmol) and iodoethane (16 µL, 0.202 mmol) were added. The reaction was capped and heated to 50°C for 16 hours. The reaction was quenched via the addition of water, followed by extraction into ethyl acetate (3x). The pooled organic layers were then washed 3x with water and brine. The organic layer was isolated, dried over $MgSO_4$, vacuum filtered, and concentrated to a crystalline residue (68 mg, 81% yield), used without further purification. ^{1}H NMR (400 MHz, Chloroform-*d*) δ 10.59 (s, 1H), 8.06 (d, *J* = 8.6 Hz, 1H), 6.84 (dd, *J* = 8.6, 2.5 Hz, 1H), 6.72 (d, *J* = 2.5 Hz, 1H), 4.06 – 3.87 (m, 2H), 3.84 (s, 3H), 3.27 (q, *J* = 7.4 Hz, 2H), 3.15 – 2.92 (m, 4H), 2.90 – 2.77 (m, 1H), 2.71 – 2.56 (m, 1H), 1.45 (s, 12H), 1.42 – 1.34 (m, 2H).

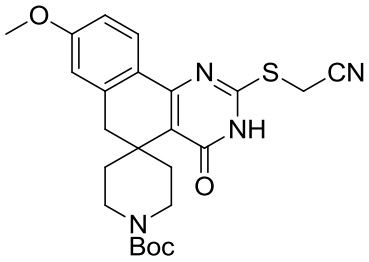

***tert*-Butyl 2-((cyanomethyl)thio)-8-methoxy-4-oxo-4,6-dihydro-3H-spiro[benzo[h]quinazoline-5,4'-piperidine]-1'-carboxylate (176c).** Synthesis performed in a manner similar to **176a** from **175** (250 mg, 0.582 mmol) using α-chloroacetonitrile (48 mg, 0.640 mmol) as the alkylating agent. The washed organic extract concentrated under high vacuum yielded a light yellow powder that was used without further purification (220 mg, 81% yield). ^{1}H NMR (400 MHz, DMSO-d_6) δ 12.79 (s, 1H), 8.13 (d, *J* = 8.8 Hz, 1H), 6.98 – 6.87 (m, 2H), 4.31 (s, 2H), 3.93 – 3.68 (m, 5H), 3.25 – 2.92 (m, 4H), 2.69 – 2.36 (m, 2H), 1.41 (s, 9H), 1.25 (d, *J* = 11.9 Hz, 2H).

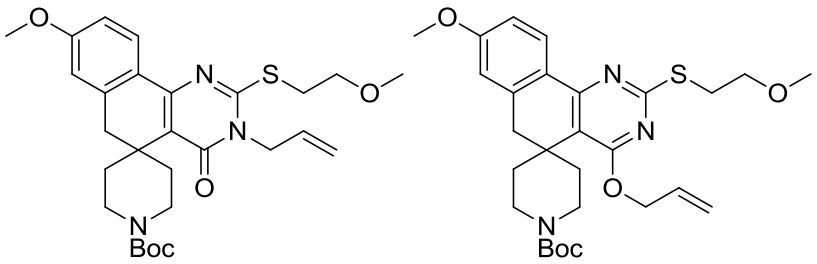

***tert*-Butyl 3-allyl-8-methoxy-2-((2-methoxyethyl)thio)-4-oxo-4,6-dihydro-3H-spiro[benzo[h]quinazoline-5,4'-piperidine]-1'-carboxylate (177) (CCG-206660)** and ***tert*-Butyl 4-(allyloxy)-8-methoxy-2-((2-methoxyethyl)thio)-6H-spiro[benzo[h]quinazoline-5,4'-piperidine]-1'-carboxylate (184) (CCG-208862).** The *S*-alkylated intermediate (790 mg, 1.62 mmol) was dissolved in absolute EtOH (9.5 mL), to which allyl bromide (210 µL, 2.43 mmol) and sodium methoxide (175 mg, 3.24 mmol) were added. Reaction was heated to 75°C and capped, allowed to stir for 2 hours. Additional allyl bromide (210 µL, 2.43 mmol) was added in 3 equal portions over the course of 3 hours, and the reaction mixture was then allowed to stir a further 12 hours. The reaction was cooled, then diluted with H_2O and extracted 3x with EtOAc. The organic extract was washed with water and brine, then isolated, dried over $MgSO_4$, vacuum filtered, and concentrated. Further purification via FC (5% EtOAc:hex) returned the pure *N*-alkylated **177** (210 mg, 25% yield) and *O*-alkylated **184** (94 mg, 11% yield).

***tert*-Butyl 3-allyl-8-methoxy-2-((2-methoxyethyl)thio)-4-oxo-4,6-dihydro-3H-spiro[benzo[h]quinazoline-5,4'-piperidine]-1'-carboxylate (177) (CCG-206660):** ^{1}H NMR (400 MHz, Chloroform-*d*) δ 8.02 (d, *J* = 8.6 Hz, 1H), 6.85 (dd, *J* = 8.6, 2.5 Hz, 1H), 6.74 (d, *J* = 2.4 Hz, 1H), 5.91 (ddt, *J* = 15.9, 10.4, 5.6 Hz, 1H), 5.29 – 5.23 (m, 2H), 4.67 (d, *J* = 4.9 Hz, 2H), 4.09 – 3.89 (m, 2H), 3.86 (s, 3H), 3.75 (t, *J* = 6.2 Hz, 2H), 3.52 (t, *J* = 6.2 Hz, 2H), 3.42 (s, 3H), 3.17 – 2.86 (m, 5H), 2.70 – 2.50 (m, 1H), 1.46 (s, 9H), 1.37 (d, *J* = 10.6 Hz, 2H). ESI+MS *m/z* = 528.2 ($M + H^+$), 550.2 ($M + Na^+$). HPLC (Method B, t_R = 8.14 min), purity >95%.

***tert*-Butyl 4-(allyloxy)-8-methoxy-2-((2-methoxyethyl)thio)-6H-spiro[benzo[h]quinazoline-5,4'-piperidine]-1'-carboxylate (184) (CCG-208862).** ^{1}H NMR (400 MHz, Chloroform-*d*) δ 8.13 (d, *J* = 8.6 Hz, 1H), 6.84 (dd, *J* = 8.6, 2.5 Hz, 1H), 6.70 (d, *J* = 2.5 Hz, 1H), 6.11 – 5.96 (m, 1H), 5.35 (d, *J* = 17.3 Hz, 1H), 5.24 (d, *J* = 10.5 Hz, 1H), 4.90 (d, *J* = 5.4 Hz, 2H), 4.05 – 3.86 (m, 2H), 3.84 (s, 3H), 3.70 (t, *J* = 6.9 Hz, 2H), 3.40 (s, 3H), 3.36 (t, *J* = 6.9 Hz, 2H), 3.16 – 2.94 (m, 4H), 2.48 (td, *J* = 13.1, 4.9 Hz, 2H), 1.48 – 1.38 (m, 11H). ESI+MS *m/z* = 528.2 ($M + H^+$), 550.2 ($M + Na^+$). HPLC (Method B, t_R = 9.07 min), purity 95%.

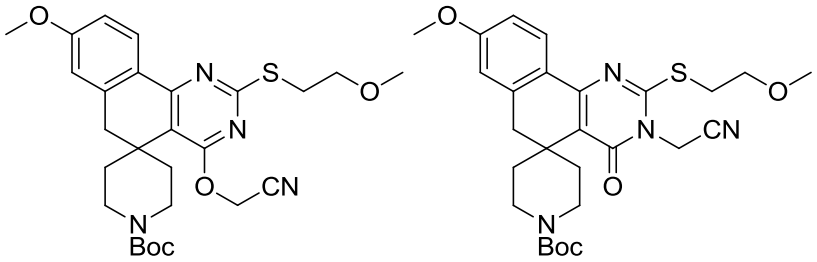

***tert*-Butyl 4-(cyanomethoxy)-8-methoxy-2-((2-methoxyethyl)thio)-6H-spiro[benzo[h]quinazoline-5,4'-piperidine]-1'-carboxylate (185) (CCG-211814)** and ***tert*-Butyl 3-(cyanomethyl)-8-methoxy-2-((2-methoxyethyl)thio)-4-oxo-4,6-dihydro-3H-spiro[benzo[h]quinazoline-5,4'-piperidine]-1'-carboxylate (178) (CCG-211815).** Prepared in a manner similar to **183** and **189** from intermediate **176a** (77 mg, 0.158 mmol) and alkylating agent α-chloroacetonitrile. Isolated the products via column chromatography (5-25% EtOAc:hex). ***tert*-Butyl 4-(cyanomethoxy)-8-methoxy-2-((2-methoxyethyl)thio)-6H-spiro[benzo[h]quinazoline-5,4'-piperidine]-1'-carboxylate (185) (CCG-211814)** 24 mg, 29% yield; ^{1}H NMR (500 MHz, Chloroform-*d*) δ 8.17 (d, *J* = 8.7 Hz, 1H), 6.88 (dd, *J* = 8.7, 2.4 Hz, 1H), 6.73 (d, *J* = 2.4 Hz, 1H), 5.21 – 4.93 (m, 2H), 4.08 – 3.88 (m, 2H), 3.87 (s, 3H), 3.75 (t, *J* = 6.7 Hz, 2H), 3.46 – 3.38 (m, 5H), 3.16 – 2.99 (m, 4H), 2.44 – 2.29 (m, 2H), 1.55 – 1.43 (m, 11H). ESI+MS *m/z* = 527.1 ($M + H^+$) 549.0 ($M + Na^+$). HPLC (Method B, t_R = 6.51 min), purity 84%.; ***tert*-Butyl 3-(cyanomethyl)-8-methoxy-2-((2-methoxyethyl)thio)-4-oxo-4,6-dihydro-3H-spiro[benzo[h]quinazoline-5,4'-piperidine]-1'-carboxylate (178) (CCG-211815)** 24 mg, 29% yield; ^{1}H NMR (500 MHz, Chloroform-*d*) δ 8.01 (d, *J* = 8.6 Hz, 1H), 6.87 (dd, *J* = 8.6, 2.5 Hz, 1H), 6.75 (d, *J* = 2.5 Hz, 1H), 5.09 – 4.78 (m, 2H), 4.07 – 3.90 (m, 2H), 3.87 (s, 3H), 3.78 (t, *J* = 6.1 Hz, 2H), 3.61 (t, *J* = 6.1 Hz, 2H), 3.43 (s, 3H), 3.16 – 2.92 (m, 4H), 2.91 – 2.75 (m, 1H), 2.69 – 2.46 (m, 1H), 1.47 (s, 9H), 1.44 – 1.32 (m, 2H). ESI+MS *m/z* = 527.1 ($M + H^+$) 549.0 ($M + Na^+$). HPLC (Method B, t_R = 6.53 min), purity >95%.

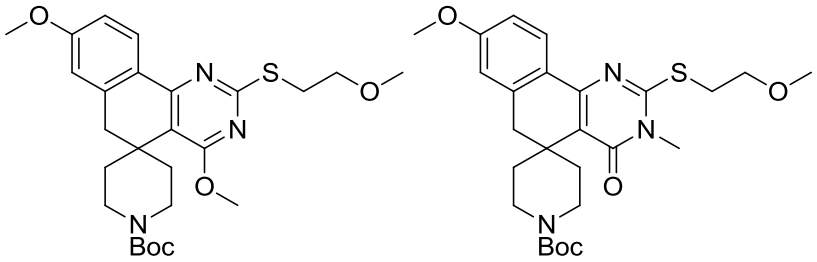

***tert*-Butyl 4,8-dimethoxy-2-((2-methoxyethyl)thio)-6H-spiro[benzo[h]quinazoline-5,4'-piperidine]-1'-carboxylate (186) (CCG-211816)** and ***tert*-Butyl 8-methoxy-2-((2-methoxyethyl)thio)-3-methyl-4-oxo-4,6-dihydro-3H-spiro[benzo[h]quinazoline-5,4'-piperidine]-1'-carboxylate (179) (CCG-211817).** Prepared in a manner similar to **182** and **188** from intermediate **176a** (150 mg, 0.308 mmol) and methyl tosylate. Isolated the products via column chromatography (5-25% EtOAc:hex). ***tert*-Butyl 4,8-dimethoxy-2-((2-methoxyethyl)thio)-6H-spiro[benzo[h]quinazoline-5,4'-piperidine]-1'-carboxylate (186) (CCG-211816)** 30 mg, 20% yield; ^{1}H NMR (500 MHz, Chloroform-*d*) δ 8.16 (d, *J* = 8.7 Hz, 1H), 6.86 (dd, *J* = 8.7, 2.5 Hz, 1H), 6.74 – 6.70 (m, 1H), 3.97 (s, 3H), 3.94 – 3.89 (m, 2H), 3.86 (s, 3H), 3.74 (t, *J* = 6.9 Hz, 2H), 3.47 – 3.36 (m, 5H), 3.14 – 3.05 (m, 2H), 3.04 (s, 2H), 2.54 – 2.37 (m, 2H), 1.49 (s, 9H), 1.44 (d, *J* = 12.0 Hz, 2H). ESI+MS *m/z* = 502.1 (M + H^+). HPLC (Method B, t_R = 8.44 min), purity >95%. ***tert*-Butyl 8-methoxy-2-((2-methoxyethyl)thio)-3-methyl-4-oxo-4,6-dihydro-3H-spiro[benzo[h]quinazoline-5,4'-piperidine]-1'-carboxylate (179) (CCG-211817)** 68 mg, 44% yield ^{1}H NMR (500 MHz, Chloroform-*d*) δ 8.02 (d, *J* = 8.6 Hz, 1H), 6.86 (dd, *J* = 8.6, 2.6 Hz, 1H), 6.74 (d, *J* = 2.6 Hz, 1H), 4.06 – 3.90 (m, 2H), 3.86 (s, 3H), 3.77 (t, *J* = 6.2 Hz, 2H), 3.54 (t, *J* = 6.2 Hz, 2H), 3.50 (s, 3H), 3.43 (s, 3H), 3.17 – 2.84 (m, 5H), 2.71 – 2.54 (m, 1H), 1.47 (s, 9H), 1.40 – 1.31 (m, 2H). ESI+MS *m/z* = 502.1 (M + H^+) 524.1 (M + Na^+). HPLC (Method B, t_R = 7.31 min), purity >95%.

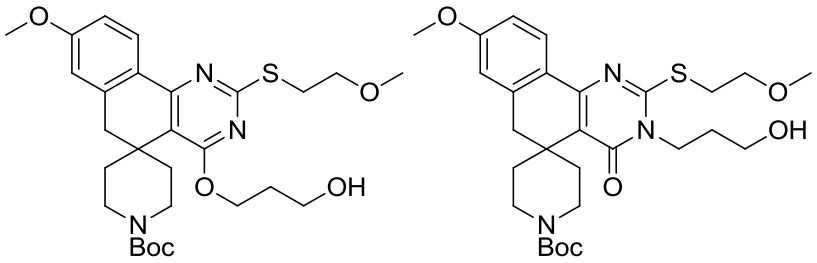

***tert*-Butyl 4-(3-hydroxypropoxy)-8-methoxy-2-((2-methoxyethyl)thio)-6H-spiro[benzo[h]quinazoline-5,4'-piperidine]-1'-carboxylate (187) (CCG-212346)** and ***tert*-**

Butyl 3-(3-hydroxypropyl)-8-methoxy-2-((2-methoxyethyl)thio)-4-oxo-4,6-dihydro-3H-spiro[benzo[h]quinazoline-5,4'-piperidine]-1'-carboxylate (180) (CCG-212347). Prepared in a manner similar to **182** and **188** from intermediate **176a** (300 mg, 0.615 mmol) and 3-bromopropan-1-ol (83 µL, 0.923 mmol). Separation of the crude mixture (180 mg, 54% crude yield) required the use of prep-scale HPLC, yielding 35 mg **180** and 20 mg **187**. ***tert*-Butyl 4-(3-hydroxypropoxy)-8-methoxy-2-((2-methoxyethyl)thio)-6H-spiro[benzo[h]quinazoline-5,4'-piperidine]-1'-carboxylate (187) (CCG-212346)** ^{1}H NMR (400 MHz, Chloroform-*d*) δ 8.15 (d, *J* = 8.6 Hz, 1H), 6.86 (dd, *J* = 8.6, 2.5 Hz, 1H), 6.72 (d, *J* = 2.5 Hz, 1H), 4.57 (t, *J* = 6.0 Hz, 2H), 4.13 – 3.89 (m, 2H), 3.86 (s, 3H), 3.81 – 3.62 (m, 4H), 3.42 (s, 3H), 3.39 (t, *J* = 7.0 Hz, 2H), 3.15 – 2.97 (m, 4H), 2.62 – 2.34 (m, 2H), 2.29 – 2.23 (m, 1H), 2.02 (p, *J* = 6.0 Hz, 2H), 1.48 (s, 9H), 1.44 (d, *J* = 13.6 Hz, 2H). ESI+MS *m/z* = 546.3 (M + H^+). HPLC (Method A, t_R = 8.56 min), purity >95%. ***tert*-Butyl 3-(3-hydroxypropyl)-8-methoxy-2-((2-methoxyethyl)thio)-4-oxo-4,6-dihydro-3H-spiro[benzo[h]quinazoline-5,4'-piperidine]-1'-carboxylate (180) (CCG-212347).** ^{1}H NMR (400 MHz, Chloroform-*d*) δ 7.99 (d, *J* = 8.6 Hz, 1H), 6.84 (dd, *J* = 8.6, 2.5 Hz, 1H), 6.73 (d, *J* = 2.5 Hz, 1H), 4.25 – 4.19 (m, 2H), 4.04 – 3.88 (m, 2H), 3.85 (s, 3H), 3.78 – 3.67 (m, 3H), 3.56 – 3.47 (m, 4H), 3.41 (s, 3H), 3.01 (d, *J* = 23.4 Hz, 4H), 2.90 – 2.73 (m, 1H), 2.70 – 2.50 (m, 1H), 1.97 (p, *J* = 5.9 Hz, 2H), 1.46 (s, 9H), 1.34 (d, *J* = 13.2 Hz, 2H). ESI+MS *m/z* = 546.3 (M + H^+) 568.3 (M + Na^+). HPLC (Method A, t_R = 8.24 min), purity 90%.

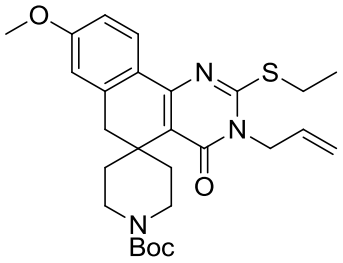

***tert*-Butyl 3-allyl-2-(ethylthio)-8-methoxy-4-oxo-4,6-dihydro-3H-spiro[benzo[h]quinazoline-5,4'-piperidine]-1'-carboxylate (181) (CCG-206663).** Compound synthesized in a manner similar to **177** beginning from *S*-ethyl intermediate **176b** (68 mg, 0.149 mmol). Isolated 38 mg of *N*-allyl product (51% yield) after column chromatography (5-15% EtOAc:hex). ^{1}H NMR (400 MHz, Chloroform-*d*) δ 8.05 (d, *J* = 8.6 Hz, 1H), 6.86 (dd, *J* = 8.6, 2.4 Hz, 1H), 6.74 (d, *J* = 2.4 Hz, 1H), 5.92 (ddt, *J* = 15.9, 10.8, 5.5 Hz, 1H), 5.30 – 5.22 (m, 2H), 4.65 (d, *J* = 5.5 Hz, 2H), 4.07 – 3.89 (m, 2H), 3.86 (s, 3H), 3.30 (q, *J* = 7.3 Hz, 2H), 3.19 – 2.86 (m, 5H), 2.69 – 2.52 (m,

1H), 1.51 – 1.42 (m, 12H), 1.42 – 1.32 (m, 2H). ESI+MS *m/z* = 520.2 ($M + Na^+$). HPLC (Method B, t_R = 9.16 min), purity >95%.

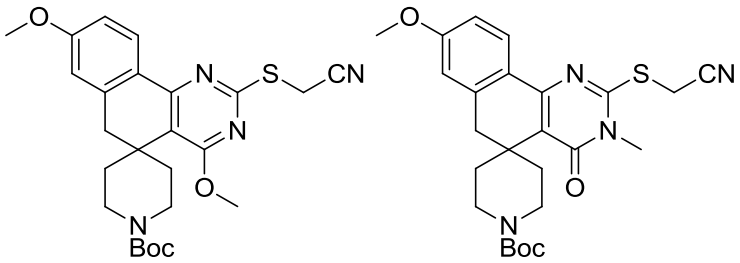

***tert*-Butyl 2-((cyanomethyl)thio)-4,8-dimethoxy-6H-spiro[benzo[h]quinazoline-5,4'-piperidine]-1'-carboxylate (188) (CCG-211810)** and ***tert*-Butyl 2-((cyanomethyl)thio)-8-methoxy-3-methyl-4-oxo-4,6-dihydro-3H-spiro[benzo[h]quinazoline-5,4'-piperidine]-1'-carboxylate (182) (CCG-211811).** *S*-alkylated intermediate **176c** (170 mg, 0.363 mmol) was dissolved in DMF (2.1 mL), to which cesium carbonate (142 mg, 0.435 mmol) and methyl tosylate (74 mg, 0.399 mmol) were added. Reaction was heated to 75°C and capped, allowed to stir for 16 hours. After this time, TLC indicated that the consumption of starting material was complete, and 2 new, less polar spots were evident. Reaction diluted with H_2O and extracted 3x with EtOAc. Organic layer washed with water and brine, then isolated, dried, filtered, and concentrated. Further purification via flash chromatography (5-25% EtOAc:hex) delivered the two products each in pure form; ***tert*-Butyl 2-((cyanomethyl)thio)-4,8-dimethoxy-6H-spiro[benzo[h]quinazoline-5,4'-piperidine]-1'-carboxylate (188) (CCG-211810)** 28 mg, 16% yield. ^{1}H NMR (500 MHz, Chloroform-*d*) δ 8.19 (d, *J* = 8.6 Hz, 1H), 6.89 (dd, *J* = 8.6, 2.6 Hz, 1H), 6.73 (d, *J* = 2.6 Hz, 1H), 4.03 (s, 3H), 4.07 – 3.82 (m, 2H), 3.92 (s, 2H), 3.86 (s, 3H), 3.13 – 3.00 (m, 4H), 2.56 – 2.34 (m, 2H), 1.49 (s, 9H), 1.47 – 1.41 (m, 2H). ESI+MS *m/z* = 483.1 ($M + H^+$) 505.0 ($M + Na^+$). HPLC (Method B, t_R = 7.23 min), purity 86%.

***tert*-Butyl 2-((cyanomethyl)thio)-8-methoxy-3-methyl-4-oxo-4,6-dihydro-3H-spiro[benzo[h]quinazoline-5,4'-piperidine]-1'-carboxylate (182) (CCG-211811)** 26 mg, 15% yield ^{1}H NMR (500 MHz, Chloroform-*d*) δ 8.11 (d, *J* = 8.6 Hz, 1H), 6.89 (dd, *J* = 8.6, 2.5 Hz, 1H), 6.74 (d, *J* = 2.5 Hz, 1H), 4.06 (s, 2H), 4.04 – 3.90 (m, 2H), 3.87 (s, 3H), 3.49 (s, 3H), 3.17 – 2.93 (m, 4H), 2.93 – 2.75 (m, 1H), 2.72 – 2.52 (m, 1H), 1.47 (s, 9H), 1.43 – 1.33 (m, 2H). ESI+MS *m/z* = 483.1 ($M + H^+$) 505.0 ($M + Na^+$). HPLC (Method B, t_R = 5.55 min), purity 84%.

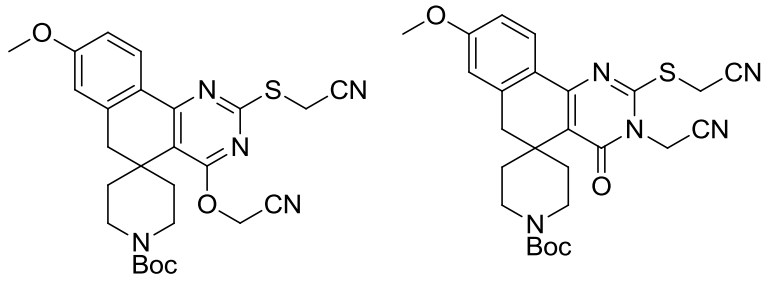

***tert*-Butyl 4-(cyanomethoxy)-2-((cyanomethyl)thio)-8-methoxy-6H-spiro[benzo[h]quinazoline-5,4'-piperidine]-1'-carboxylate (189) (CCG-211812)** and ***tert*-Butyl 3-(cyanomethyl)-2-((cyanomethyl)thio)-8-methoxy-4-oxo-4,6-dihydro-3H-spiro[benzo[h]quinazoline-5,4'-piperidine]-1'-carboxylate (183) (CCG-211813).** *S*-alkylated intermediate **176c** (170 mg, 0.363 mmol) was dissolved in DMF (2.1 mL), to which cesium carbonate (142 mg, 0.435 mmol) and α-chloroacetonitrile (25 µL, 0.399 mmol) were added. Reaction was heated to 50°C and capped, allowed to stir for 16 hours. After this time, TLC indicated that the consumption of starting material was complete, and 2 new, less polar spots were evident. Reaction diluted with H_2O and extracted 3x with EtOAc. Organic layer washed with water and brine, then isolated, dried, filtered, and concentrated. Further purification via flash chromatography (5-25% EtOAc:hex) delivered the two products each in pure form: ***tert*-Butyl 4-(cyanomethoxy)-2-((cyanomethyl)thio)-8-methoxy-6H-spiro[benzo[h]quinazoline-5,4'-piperidine]-1'-carboxylate (189) (CCG-211812)** 49 mg, 27% yield; ^{1}H NMR (500 MHz, Chloroform-*d*) δ 8.21 (d, *J* = 8.6 Hz, 1H), 6.90 (dd, *J* = 8.6, 2.5 Hz, 1H), 6.75 (d, *J* = 2.5 Hz, 1H), 5.11 (s, 2H), 4.09 – 3.96 (m, 2H), 3.93 (s, 2H), 3.88 (s, 3H), 3.15 – 3.01 (m, 4H), 2.46 – 2.27 (m, 2H), 1.56 – 1.45 (m, 11H). ESI+MS *m/z* = 508.0 (M + H^+) 530.0 (M + Na^+). HPLC (Method B, t_R = 6.31 min), purity >95%.; ***tert*-Butyl 3-(cyanomethyl)-2-((cyanomethyl)thio)-8-methoxy-4-oxo-4,6-dihydro-3H-spiro[benzo[h]quinazoline-5,4'-piperidine]-1'-carboxylate (183) (CCG-211813)** 27 mg, 14% yield; ^{1}H NMR (500 MHz, Chloroform-*d*) δ 8.11 (d, *J* = 8.6 Hz, 1H), 6.91 (dd, *J* = 8.7, 2.5 Hz, 1H), 6.76 (d, *J* = 2.5 Hz, 1H), 5.07 – 4.75 (m, 2H), 4.12 (s, 2H), 4.09 – 3.90 (m, 2H), 3.88 (s, 3H), 3.20 – 2.91 (m, 4H), 2.89 – 2.67 (m, 1H), 2.67 – 2.49 (m, 1H), 1.48 (s, 9H), 1.40 (d, *J* = 13.0 Hz, 2H). ESI+MS *m/z* = 530.0 (M + Na^+). HPLC (Method B, t_R = 5.25 min), purity >95%.

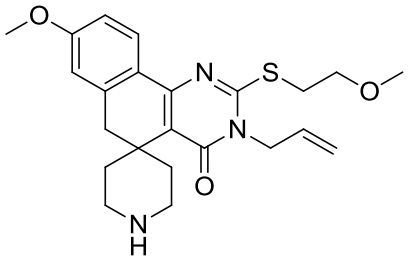

3-Allyl-8-methoxy-2-((2-methoxyethyl)thio)-3H-spiro[benzo[h]quinazoline-5,4'-piperidin]-4(6H)-one (190) (CCG-206661). 2-Thioxopyrimidinone intermediate **177** (1.071 g, 2.03 mmol) was suspended in DCM (10.2 mL) and cooled to 0°C. TFA (3.13 mL) was added dropwise and the suspension was allowed to stir 2 hours at 0°C, then an additional 2h at room temperature. Reaction was quenched via the slow addition of saturated aqueous sodium carbonate and then extraction of the aqueous layer with DCM (2x). The pooled organic layers were washed with water and brine, then isolated, dried over $MgSO_4$, vacuum filtered, and concentrated. Vacuum filtration followed by washing with diethyl ether furnished the desired product as a free-flowing white solid, (680 mg, 78% yield). ^{1}H NMR (400 MHz, Chloroform-*d*) δ 9.97 (s, 1H), 8.74 (s, 1H), 8.01 (d, *J* = 8.6 Hz, 1H), 6.87 (d, *J* = 8.6 Hz, 1H), 6.79 (s, 1H), 5.95 – 5.83 (m, 1H), 5.28 – 5.19 (m, 2H), 4.68 (d, *J* = 4.2 Hz, 2H), 3.87 (s, 3H), 3.75 (t, *J* = 6.1 Hz, 2H), 3.53 (t, *J* = 6.1 Hz, 2H), 3.50 – 3.43 (m, 2H), 3.42 (s, 3H), 3.36 – 3.21 (m, 2H), 3.02 (s, 2H), 2.99 – 2.84 (m, 2H), 1.69 (d, *J* = 13.7 Hz, 2H). ESI+MS *m/z* = 428.2 ($M + H^+$). HPLC (Method A, t_R = 5.73 min), purity >95%.

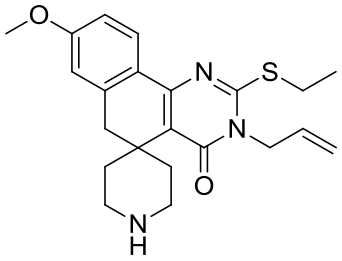

3-Allyl-2-(ethylthio)-8-methoxy-3H-spiro[benzo[h]quinazoline-5,4'-piperidin]-4(6H)-one (CCG-206664) (191). Boc intermediate **181** (24 mg, 0.048 mmol) was dissolved in 4M HCl solution in dioxane (0.5 mL). Reaction was allowed to stir at room temperature for 2 hours, then diluted with diethyl ether and the crystalline solid isolated via filtration and submitted without further purification. Isolated 17 mg (89% yield). ^{1}H NMR (400 MHz, Chloroform-*d*) δ 9.98 (s, 1H), 8.77 (s, 1H), 8.05 (d, *J* = 8.6 Hz, 1H), 6.87 (dd, *J* = 8.6, 1.9 Hz, 1H), 6.78 (s, 1H), 6.01 –

5.79 (m, 1H), 5.32 – 5.13 (m, 2H), 4.66 (d, *J* = 4.7 Hz, 2H), 3.87 (s, 3H), 3.55 – 3.41 (m, 2H), 3.35 – 3.22 (m, 4H), 3.02 (s, 2H), 2.98 – 2.85 (m, 2H), 1.69 (d, *J* = 14.2 Hz, 2H), 1.47 (t, *J* = 7.3 Hz, 3H). ESI+MS *m/z* = 398.2 ($M + H^+$) 420.2 ($M + Na^+$). HPLC (Method A, t_R = 6.13 min), purity >95%.

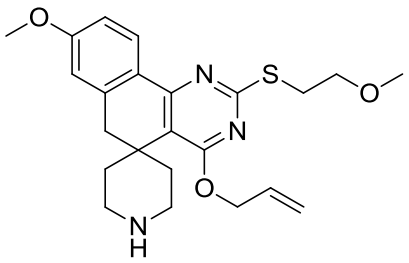

4-(Allyloxy)-8-methoxy-2-((2-methoxyethyl)thio)-6H-spiro[benzo[h]quinazoline-5,4'-piperidine] (192). Boc-protected intermediate **184** (94 mg, 0.178 mmol) was dissolved into a solution of HCl (4M in dioxane, 1.0 mL) cooled to 0°C. The reaction was allowed to stir for 2 hours while slowly warming to room temperature. At this time, the reaction mixture was diluted with diethyl ether (5 mL), causing the precipitation of a white solid that was collected via vacuum filtration. Drying under high vacuum delivers the desired product (82 mg, quant. yield) as a white solid that is unstable to dissolution in polar solvents. ^{1}H NMR (400 MHz, DMSO-d_6) δ 9.08 – 8.95 (m, 1H), 8.63 (s, 1H), 8.00 (d, *J* = 8.6 Hz, 1H), 6.98 (d, *J* = 2.5 Hz, 1H), 6.92 (dd, *J* = 8.5, 2.5 Hz, 1H), 6.14 (ddt, *J* = 16.1, 10.6, 5.3 Hz, 1H), 5.35 (dd, *J* = 17.4, 1.7 Hz, 1H), 5.25 (dd, *J* = 10.6, 1.7 Hz, 1H), 4.94 (d, *J* = 5.3 Hz, 2H), 3.80 (s, 3H), 3.63 (s, 4H), 3.34 – 3.24 (m, 5H), 3.15 (s, 4H), 2.59 (td, *J* = 13.4, 13.0, 6.4 Hz, 2H), 1.53 (d, *J* = 14.0 Hz, 2H). ESI-MS *m/z* = 428.2 ($M + H^+$).

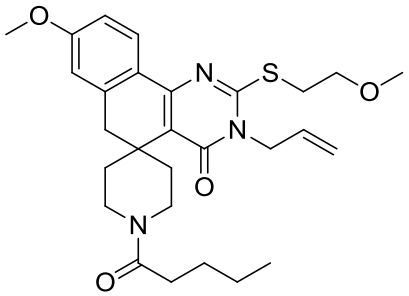

3-Allyl-8-methoxy-2-((2-methoxyethyl)thio)-1'-pentanoyl-3H-spiro[benzo[h]quinazoline-5,4'-piperidin]-4(6H)-one (193) (CCG-206662). *N*-deprotected intermediate **190** (12 mg, 0.028

mmol) was added to DCM (140 µL) in a dry 1 dram vial. *N*,*N*-diisopropylethylamine was added (9.8 µL, 0.056 mmol), then the mixture was cooled to 0°C. Pentanoyl chloride (4.0 µL, 0.034 mmol) was added, and the reaction allowed to stir while warming to RT over 3 hours. Reaction quenched via the addition of saturated NH_4Cl aqueous solution. The biphasic solution was partitioned between DCM and NH_4Cl, then the organic layer was washed with water and brine. The organic layer was isolated, dried over $MgSO_4$, vacuum filtered, and concentrated, then further purified via flash chromatography (10-40% EtOAc:hex) to yield the desired compound as a white solid (10 mg, 70% yield). ^{1}H NMR (400 MHz, Chloroform-*d*) δ 8.02 (d, *J* = 8.5 Hz, 1H), 6.86 (dd, *J* = 8.5, 2.4 Hz, 1H), 6.74 (d, *J* = 2.4 Hz, 1H), 5.95 – 5.83 (m, 1H), 5.32 – 5.22 (m, 2H), 4.66 (d, *J* = 5.6 Hz, 2H), 4.35 (d, *J* = 12.5 Hz, 1H), 3.86 (s, 3H), 3.84 – 3.71 (m, 3H), 3.52 (t, *J* = 6.3 Hz, 2H), 3.42 (s, 3H), 3.41 – 3.31 (m, 1H), 3.16 – 2.87 (m, 4H), 2.47 (dt, *J* = 13.5, 6.7 Hz, 1H), 2.38 – 2.29 (m, 2H), 1.68 – 1.53 (m, 2H), 1.49 – 1.31 (m, 4H), 0.93 (t, *J* = 7.3 Hz, 3H). ESI+MS *m/z* = 512.2 ($M + H^+$) 534.2 ($M + Na^+$). HPLC (Method B, t_R = 6.51 min), purity >95%.

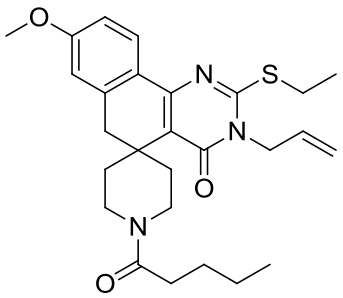

3-Allyl-2-(ethylthio)-8-methoxy-1'-pentanoyl-3H-spiro[benzo[h]quinazoline-5,4'-piperidin]-4(6H)-one (194) (CCG-206665). Compound was prepared in a manner similar to **193** from **191** (10.5 mg, 0.026 mmol). Isolated the desired compound after flash chromatography (10-40% EtOAc:hex) as a white powder (8 mg, 63% yield). ^{1}H NMR (400 MHz, Chloroform-*d*) δ 8.06 (d, *J* = 8.6 Hz, 1H), 6.87 (dd, *J* = 8.6, 2.5 Hz, 1H), 6.74 (d, *J* = 2.5 Hz, 1H), 5.98 – 5.84 (m, 1H), 5.30 – 5.22 (m, 2H), 4.65 (d, *J* = 5.6 Hz, 2H), 4.36 (d, *J* = 13.7 Hz, 1H), 3.87 (s, 3H), 3.80 (d, *J* = 13.7 Hz, 1H), 3.42 – 3.25 (m, 3H), 3.16 – 2.88 (m, 4H), 2.47 (td, *J* = 13.2, 4.8 Hz, 1H), 2.38 – 2.29 (m, 2H), 1.68 – 1.56 (m, 2H), 1.51 – 1.32 (m, 7H), 0.93 (t, *J* = 7.3 Hz, 3H). ESI+MS *m/z* = 482.2 ($M + H^+$) 504.2 ($M + Na^+$). HPLC (Method B, t_R = 7.63 min), purity >95%.

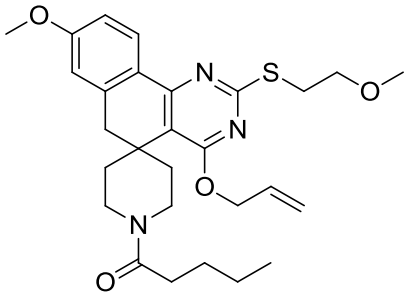

1-(4-(Allyloxy)-8-methoxy-2-((2-methoxyethyl)thio)-6H-spiro[benzo[h]quinazoline-5,4'-piperidin]-1'-yl)pentan-1-one (195) (CCG-208863). Reaction was performed in a manner similar to **193** beginning from intermediate **192** (30 mg, 0.070 mmol). Isolated the desired compound after flash chromatography (10-40% EtOAc:hex) as a white powder (27 mg, 74% yield). ^{1}H NMR (400 MHz, Chloroform-*d*) δ 8.16 (d, *J* = 8.6 Hz, 1H), 6.87 (dd, *J* = 8.6, 2.1 Hz, 1H), 6.73 (d, *J* = 2.1 Hz, 1H), 6.04 (ddt, *J* = 16.9, 10.6, 5.6 Hz, 1H), 5.35 (d, *J* = 16.9 Hz, 1H), 5.26 (d, *J* = 10.6 Hz, 1H), 4.91 (d, *J* = 5.6 Hz, 2H), 4.43 (d, *J* = 13.7 Hz, 1H), 3.86 (s, 3H), 3.72 (t, *J* = 6.8 Hz, 2H), 3.44 – 3.34 (m, 6H), 3.15 – 3.00 (m, 2H), 2.96 (t, *J* = 12.0 Hz, 1H), 2.57 (td, *J* = 13.3, 4.7 Hz, 1H), 2.44 (td, *J* = 13.3, 4.7 Hz, 1H), 2.35 (td, *J* = 7.3, 3.4 Hz, 2H), 1.70 – 1.58 (m, 3H), 1.58 – 1.46 (m, 2H), 1.46 – 1.33 (m, 2H), 0.94 (t, *J* = 7.3 Hz, 3H). ESI+MS *m/z* = 512.2 ($M + H^+$), 534.2 ($M + Na^+$). HPLC (Method B, t_R = 7.44 min), purity >95%.

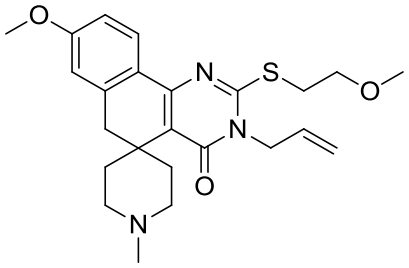

3-Allyl-8-methoxy-2-((2-methoxyethyl)thio)-1'-methyl-3H-spiro[benzo[h]quinazoline-5,4'-piperidin]-4(6H)-one (196) (CCG-208981). Intermediate **190** (30 mg, 0.065 mmol) was dissolved in dry 1,2-dichloroethane (300 µL), followed by acetic acid (4.5 µL, 0.078 mmol), paraformaldehyde (9.7 mg, 0.323 mmol), and sodium triacetoxyborohydride (21 mg, 0.097 mmol). The reaction was stirred at room temperature for 16 hours, then diluted with dichloromethane and washed with saturated aqueous sodium bicarbonate, water, and brine. The organic extract was dried over $MgSO_4$, vacuum filtered, and concentrated *in vacuo*. Further purification via flash chromatography (0-20% MeOH:DCM) furnished the desired product (18

mg, 63% yield) as a sticky yellow oil. ^{1}H NMR (400 MHz, Chloroform-*d*) δ 8.01 (d, *J* = 8.6 Hz, 1H), 6.84 (dd, *J* = 8.6, 2.3 Hz, 1H), 6.74 (d, *J* = 2.3 Hz, 1H), 5.91 (ddt, *J* = 16.2, 11.0, 5.7 Hz, 1H), 5.33 – 5.21 (m, 2H), 4.67 (d, *J* = 5.7 Hz, 2H), 3.86 (s, 3H), 3.75 (t, *J* = 6.3 Hz, 2H), 3.51 (t, *J* = 6.3 Hz, 2H), 3.42 (s, 3H), 3.00 (s, 2H), 2.98 – 2.89 (m, 2H), 2.74 (d, *J* = 11.6 Hz, 2H), 2.64 (s, 2H), 2.34 (s, 3H), 1.36 (d, *J* = 13.5 Hz, 2H). ESI+MS *m/z* = 442.1 (M + H^+). HPLC (Method A, t_R = 5.83 min), purity = 90%.

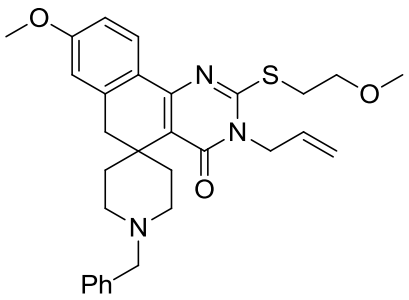

3-Allyl-1'-benzyl-8-methoxy-2-((2-methoxyethyl)thio)-3H-spiro[benzo[h]quinazoline-5,4'-piperidin]-4(6H)-one (197) (CCG-208982). Synthesized in a manner similar to **196** from **190** (36 mg, 0.078 mmol) and benzaldehyde (11 mg, 0.101 mmol). Product recovered after flash chromatography (0-20% MeOH:DCM) as a clear oil (23 mg, 57% yield). ^{1}H NMR (400 MHz, Chloroform-*d*) δ 7.99 (d, *J* = 8.8 Hz, 1H), 7.64 – 7.51 (m, 2H), 7.44 – 7.29 (m, 3H), 6.88 – 6.81 (m, 2H), 5.98 – 5.85 (m, 1H), 5.34 – 5.24 (m, 2H), 4.71 (d, *J* = 5.0 Hz, 2H), 3.85 (s, 3H), 3.75 (t, *J* = 6.2 Hz, 2H), 3.53 (t, *J* = 6.2 Hz, 2H), 3.42 (s, 3H), 3.31-3.04 (m, 4H), 3.06 – 2.93 (m, 3H), 1.90 – 1.61 (m, 5H). ESI+MS *m/z* = 518.2 (M + H^+) 540.2 (M + Na^+). HPLC (Method A, t_R = 6.83 min), purity >95%.

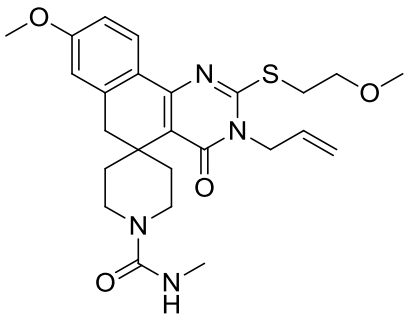

3-Allyl-8-methoxy-2-((2-methoxyethyl)thio)-N-methyl-4-oxo-4,6-dihydro-3H-spiro[benzo[h]quinazoline-5,4'-piperidine]-1'-carboxamide (198) (CCG-211970). The free

amine intermediate (30 mg, 0.070 mmol) was combined with *N*,*N*-diisopropylethylamine (18 µL, 0.105 mmol) and *N*-succinimidyl *N*-methylcarbamate (24 mg, 0.140 mmol) in DCM (350 µL). The reaction was stirred at room temperature for 6 hours, then partitioned between saturated aqueous sodium bicarbonate solution and additional DCM. The organic layer was washed with water and brine, then dried over $MgSO_4$ and concentrated *in vacuo*. The resulting crude residue was further purified via flash chromatography (0-10% MeOH:DCM) to yield the desired product as a white solid (22 mg, 65% yield). ^{1}H NMR (500 MHz, Chloroform-*d*) δ 8.02 (d, *J* = 8.6 Hz, 1H), 6.86 (dd, *J* = 8.6, 2.5 Hz, 1H), 6.74 (d, *J* = 2.5 Hz, 1H), 5.91 (ddt, *J* = 15.9, 10.7, 5.6 Hz, 1H), 5.31 – 5.23 (m, 2H), 4.67 (d, *J* = 5.6 Hz, 2H), 4.42 (d, *J* = 4.6 Hz, 1H), 3.86 (s, 3H), 3.82 – 3.72 (m, 4H), 3.52 (t, *J* = 6.3 Hz, 2H), 3.42 (s, 3H), 3.17 (td, *J* = 12.7, 3.0 Hz, 2H), 3.01 (s, 2H), 2.81 (d, *J* = 4.6 Hz, 3H), 2.74 (td, *J* = 13.2, 4.9 Hz, 2H), 1.43 (d, *J* = 13.6 Hz, 2H). ESI+MS *m/z* = 485.1 ($M + H^+$), 507.1 ($M + Na^+$). HPLC (Method B, t_R = 5.64 min), purity >95%.

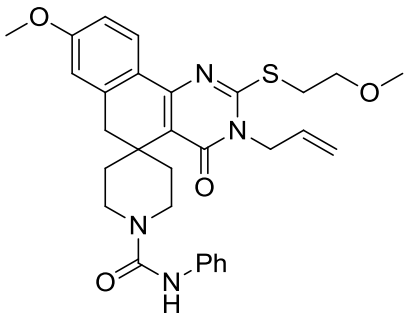

3-Allyl-8-methoxy-2-((2-methoxyethyl)thio)-4-oxo-N-phenyl-4,6-dihydro-3H-spiro[benzo[h]quinazoline-5,4'-piperidine]-1'-carboxamide (199) (CCG-211971). Prepared in the same manner as **198** from **190** (30 mg, 0.070 mmol) and phenyl isocyanate (15 µL, 0.140 mmol). Recovered the desired product after flash chromatography as a white powder (32 mg, 83% yield). ^{1}H NMR (500 MHz, Chloroform-*d*) δ 8.04 (d, *J* = 8.6 Hz, 1H), 7.37 (d, *J* = 7.7 Hz, 2H), 7.32 – 7.25 (m, 2H), 7.02 (t, *J* = 7.3 Hz, 1H), 6.88 (dd, *J* = 8.6, 2.5 Hz, 1H), 6.76 (d, *J* = 2.5 Hz, 1H), 6.39 (s, 1H), 5.92 (ddt, *J* = 15.9, 10.8, 5.6 Hz, 1H), 5.33 – 5.25 (m, 2H), 4.69 (d, *J* = 5.6 Hz, 2H), 3.94 (dt, *J* = 13.0, 4.1 Hz, 2H), 3.88 (s, 3H), 3.76 (t, *J* = 6.3 Hz, 2H), 3.54 (t, *J* = 6.3 Hz, 2H), 3.43 (s, 3H), 3.31 (td, *J* = 12.8, 3.0 Hz, 2H), 3.04 (s, 2H), 2.78 (td, *J* = 13.6, 4.7 Hz, 2H), 1.52 (d, *J* = 13.8 Hz, 2H). ESI+MS *m/z* = 547.1 ($M + H^+$), 569.1 ($M + Na^+$). HPLC (Method B, t_R = 5.83 min), purity >95%.

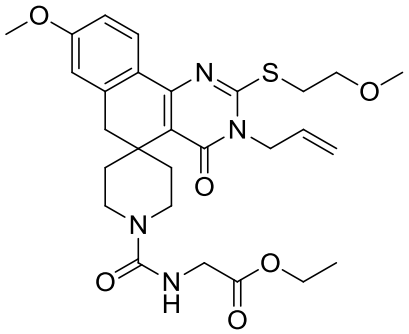

Ethyl 2-(3-allyl-8-methoxy-2-((2-methoxyethyl)thio)-4-oxo-4,6-dihydro-3H-spiro[benzo[h]quinazoline-5,4'-piperidin]-1'-ylcarboxamido)acetate (200) (CCG-211972). Prepared in a manner similar to **196** from intermediate **190** (30 mg, 0.070 mmol) and ethyl 2-isocyanatoacetate (16 µL, 0.140 mmol). The desired product was isolated via flash chromatography as a white powder (26 mg, 67% yield). ^{1}H NMR (500 MHz, Chloroform-*d*) δ 8.02 (d, *J* = 8.6 Hz, 1H), 6.86 (dd, *J* = 8.6, 2.5 Hz, 1H), 6.74 (d, *J* = 2.5 Hz, 1H), 5.91 (ddt, *J* = 15.9, 10.8, 5.6 Hz, 1H), 5.32 – 5.23 (m, 2H), 4.94 (t, *J* = 5.0 Hz, 1H), 4.67 (d, *J* = 5.6 Hz, 2H), 4.22 (q, *J* = 7.1 Hz, 2H), 4.02 (d, *J* = 5.0 Hz, 2H), 3.87 (s, 3H), 3.82 (dt, *J* = 12.9, 4.0 Hz, 2H), 3.75 (t, *J* = 6.3 Hz, 2H), 3.52 (t, *J* = 6.3 Hz, 2H), 3.42 (s, 3H), 3.23 (td, *J* = 12.7, 3.0 Hz, 2H), 3.01 (s, 2H), 2.75 (td, *J* = 13.3, 4.8 Hz, 2H), 1.45 (d, *J* = 13.6 Hz, 2H), 1.29 (t, *J* = 7.1 Hz, 3H). ESI+MS *m/z* = 557.1 ($M + H^+$), 579.1 ($M + Na^+$). HPLC (Method B, t_R = 4.12 min), purity >95%.

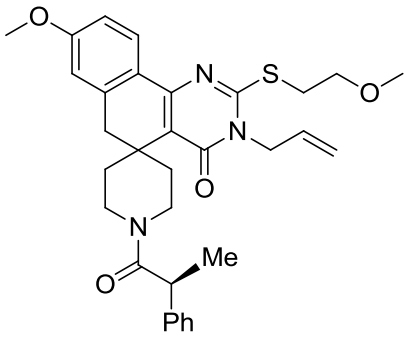

(*S*)-3-Allyl-8-methoxy-2-((2-methoxyethyl)thio)-1'-(2-phenylpropanoyl)-3H-spiro[benzo[h]quinazoline-5,4'-piperidin]-4(6H)-one (201) (CCG-212350). *S*-2-phenyl propanoic acid (26 mg, 0.175 mmol) was dissolved in DCM (1.2 mL), to which DIPEA (61 µL, 0.351 mmol), HOBt hydrate (27 mg, 0.175 mmol), and EDC (34 mg, 0.175 mmol) were added. The reaction mixture was allowed to stir at room temperature for 15 minutes, then intermediate

190 (50 mg, 0.117 mmol) was added and the mixture allowed to stir an additional 16 hours at room temperature. The reaction mixture was diluted with additional DCM (20 mL), then washed with saturated aqueous sodium carbonate and ammonium chloride solutions, followed by water and brine. The organic extract was isolated, dried over $MgSO_4$, vacuum filtered, and concentrated *in vacuo*. Further purification via flash chromatography (10-40% EtOAc:hex) furnished the product as a white solid (44 mg, 67% yield). ^{1}H NMR (400 MHz, Chloroform-*d*) δ 7.98 (t, *J* = 8.2 Hz, 1H), 7.37 – 7.21 (m, 5H), 6.83 (dd, *J* = 8.6, 2.4 Hz, 1H), 6.62 (d, *J* = 2.7 Hz, 1H), 5.97 – 5.82 (m, 1H), 5.32 – 5.20 (m, 2H), 4.69 – 4.60 (m, 2H), 4.40 – 4.28 (m, 1H), 3.94 – 3.68 (m, 6H), 3.56 – 3.45 (m, 2H), 3.41 (s, 3H), 3.37 – 3.27 (m, 1H), 3.16 – 2.91 (m, 4H), 2.82 – 2.73 (m, 1H), 2.55 – 2.44 (m, 1H), 2.10 – 2.00 (m, 1H), 1.49 – 1.35 (m, 3H), 1.26 (d, *J* = 11.2 Hz, 1H). ESI+MS *m/z* = 560.4 ($M + H^+$), 582.4 ($M + Na^+$). HPLC (Method B, t_R = 7.17 min), purity >95%.

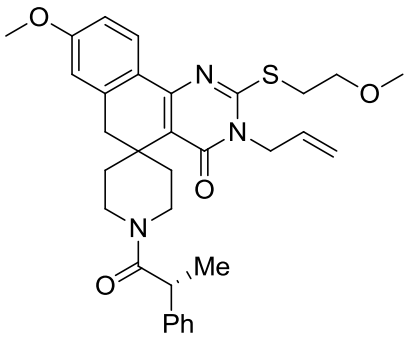

(*R*)-3-Allyl-8-methoxy-2-((2-methoxyethyl)thio)-1'-(2-phenylpropanoyl)-3H-spiro[benzo[h]quinazoline-5,4'-piperidin]-4(6H)-one (202) (CCG-212351). Prepared in a manner similar to **201** from intermediate **190** (50 mg, 0.117 mmol) and (*R*)-2-phenyl propanoic acid (26 mg, 0.175 mmol). Isolated after flash chromatography as a white solid (51 mg, 78% yield).^{1}H NMR (400 MHz, Chloroform-*d*) δ 7.98 (t, *J* = 8.2 Hz, 1H), 7.37 – 7.15 (m, 5H), 6.83 (dd, *J* = 8.6, 2.6 Hz, 1H), 6.62 (d, *J* = 2.5 Hz, 1H), 5.98 – 5.82 (m, 1H), 5.33 – 5.20 (m, 2H), 4.70 – 4.60 (m, 2H), 4.40 – 4.30 (m, 1H), 3.95 – 3.59 (m, 6H), 3.55 – 3.45 (m, 2H), 3.41 (s, 3H),3.37 – 3.26 (m, 1H), 3.18 – 2.89 (m, 4H), 2.78 (d, *J* = 15.8 Hz, 1H), 2.50 (td, *J* = 13.1, 4.9 Hz, 1H), 2.05 (t, *J* = 10.3 Hz, 1H), 1.49 – 1.36 (m, 3H), 1.26 (d, *J* = 12.2 Hz, 1H). ESI+MS *m/z* = 560.4 ($M + H^+$), 582.4 ($M + Na^+$). HPLC (Method B, t_R = 7.12 min), purity >95%.

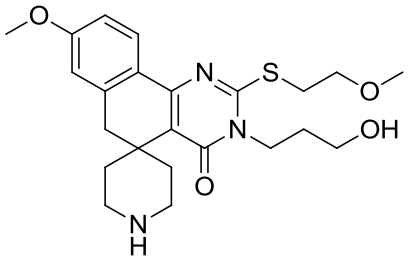

3-(3-Hydroxypropyl)-8-methoxy-2-((2-methoxyethyl)thio)-3H-spiro[benzo[h]quinazoline-5,4'-piperidin]-4(6H)-one (203) (CCG-212353). A 4:1 solution of DCM:TFA (0.55 mL) was cooled to 0°C in an ice bath to which compound **180** (30 mg, 0.055 mmol) was added. The reaction was stirred for 4 hours while gradually warming to room temperature. The reaction was quenched with saturated aqueous sodium carbonate, then extracted 3x with DCM. The organic layer was collected, dried over $MgSO_4$, vacuum filtered and concentrated. Resuspension of the crude organic extract in 3:2 diethyl ether:hexanes caused the precipitation of a white powder that was collected via vacuum filtration. Isolated 22 mg (90% yield). ^{1}H NMR (400 MHz, Methanol-d_4) δ 8.07 (d, J = 9.2 Hz, 1H), 6.96 – 6.89 (m, 2H), 4.21 – 4.13 (m, 2H), 3.86 (s, 3H), 3.75 (t, J = 6.3 Hz, 2H), 3.64 (t, J = 6.1 Hz, 2H), 3.56 (t, J = 6.3 Hz, 2H), 3.39 (s, 3H), 3.37 – 3.22 (m, J = 2.3, 1.9 Hz, 4H), 3.15 (s, 2H), 3.09 – 2.95 (m, 2H), 2.02 – 1.90 (m, 2H), 1.60 (d, J = 15.1 Hz, 2H). ESI+MS m/z = 446.3 ($M + H^+$), 468.3 ($M + Na^+$). HPLC (Method A, t_R = 4.93 min), purity >95%.

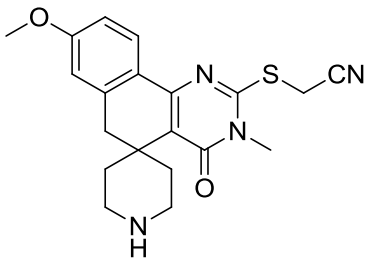

2-((8-Methoxy-3-methyl-4-oxo-4,6-dihydro-3H-spiro[benzo[h]quinazoline-5,4'-piperidin]-2-yl)thio)acetonitrile (204) (CCG-212013). Prepared in the same manner as **206** from intermediate **182**. Precipitation from 1:1 $CHCl_3$:diethyl ether and subsequent vacuum filtration yielded the product as a light yellow powder (10 mg, 63% yield). ^{1}H NMR (400 MHz, Methanol-d_4) δ 8.24 (d, J = 8.5 Hz, 1H), 7.01 – 6.82 (m, 2H), 4.29 (s, 2H), 3.85 (s, 3H), 3.50 (s, 3H), 3.41 –

3.22 (m, 4H), 3.15 (s, 2H), 3.01 (td, *J* = 13.4, 12.4, 6.0 Hz, 2H), 1.60 (d, *J* = 14.2 Hz, 2H). ESI-MS+ *m/z* = 383.0 (M + H^+). HPLC (Method A, t_R = 5.04 min), purity >95%.

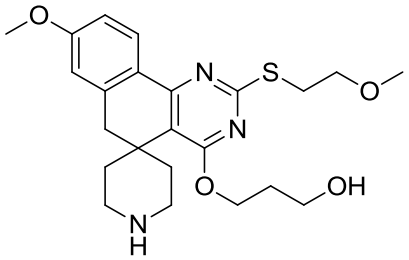

3-((8-Methoxy-2-((2-methoxyethyl)thio)-6H-spiro[benzo[h]quinazoline-5,4'-piperidin]-4-yl)oxy)propan-1-ol (205) (CCG-212354). Intermediate **187** (15 mg, 0.027 mmol) was dissolved in a 4:1 mixture of DCM:TFA (270 µL) at 0°C and allowed to stir for 2 hours while warming to room temperature. Reaction was quenched by the addition of saturated sodium carbonate. The organic layer was diluted with additional DCM, and the aqueous layer extracted 2x with additional DCM. Organic layer was isolated, dried over $MgSO_4$, filtered, and evaporated. Resuspension of the crude organic extract in 3:2 diethyl ether:hexanes caused the precipitation of a white powder that was collected via vacuum filtration. Isolated 9 mg (74% yield). ^{1}H NMR (400 MHz, Methanol-d_4) δ 8.10 (d, *J* = 9.4 Hz, 1H), 6.95 – 6.89 (m, 2H), 4.59 (t, *J* = 6.3 Hz, 2H), 3.86 (s, 3H), 3.74 (t, *J* = 6.3 Hz, 2H), 3.70 (t, *J* = 6.7 Hz, 2H), 3.41 – 3.38 (m, 3H), 3.38 – 3.22 (m, 6H), 3.17 (s, 2H), 2.74 (td, *J* = 13.9, 4.9 Hz, 2H), 2.07 (p, *J* = 6.3 Hz, 2H), 1.69 (d, *J* = 13.3 Hz, 2H). ESI+MS *m/z* = 446.3 (M + H^+), HPLC (Method A, t_R = 5.19 min), purity >95%.

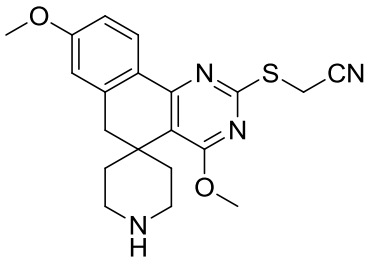

2-((4,8-Dimethoxy-6H-spiro[benzo[h]quinazoline-5,4'-piperidin]-2-yl)thio)acetonitrile (206) (CCG-212014). Boc-protected intermediate **188** (20 mg, 0.041 mmol) was dissolved in DCM (0.7 mL) and cooled to 0°C. 2,6-lutidine (19 µL, 0.166 mmol) was added, then TMS-OTf (22 µL, 0.124 mmol) was added slowly dropwise. The reaction was allowed to stir for 30 minutes at 0°C. TLC indicated the completion of the reaction. The reaction was quenched via the addition

of MeOH and allowed to stir 16h. The solvent was removed *in vacuo* and the crude residue was treated with a 1:1 mixture of chloroform and diethyl ether, causing the precipitation of a white solid, collected by vacuum filtration. Recovered the desired product as a white powder (16 mg, 100% yield). ^{1}H NMR (400 MHz, Methanol-d_4) δ 8.18 (d, J = 9.3 Hz, 1H), 6.98 – 6.91 (m, 2H), 4.12 (s, 2H), 4.10 (s, 3H), 3.86 (s, 3H), 3.43 – 3.25 (m, 4H), 3.20 (s, 2H), 2.75 (td, J = 14.2, 5.0 Hz, 2H), 1.72 (d, J = 15.2 Hz, 2H). ESI+MS *m/z* = 383.1 (M + H^+). HPLC (Method A, t_R = 5.32 min), purity >95%.

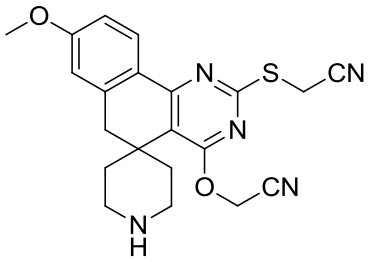

2-((4-(Cyanomethoxy)-8-methoxy-6H-spiro[benzo[h]quinazoline-5,4'-piperidin]-2-yl)thio)acetonitrile (207) (CCG-212015). Prepared in the same manner as **206** from intermediate **189**. Precipitation from 1:1 $CHCl_3$:diethyl ether and subsequent vacuum filtration yielded the product as a white powder (9 mg, 56% yield). ^{1}H NMR (400 MHz, Methanol-d_4) δ 8.24 (d, J = 8.7 Hz, 1H), 7.02 – 6.89 (m, 2H), 5.28 (s, 2H), 4.16 (s, 2H), 3.87 (s, 3H), 3.43 – 3.33 (m, 2H), 3.33 – 3.26 (m, 2H), 3.24 (s, 2H), 2.67 (td, J = 14.3, 13.8, 5.1 Hz, 2H), 1.80 (d, J = 15.1 Hz, 2H). ESI+MS *m/z* = 408.1 (M + H^+) 430.1 (M + Na^+). HPLC (Method A, t_R = 5.37 min), purity >95%.

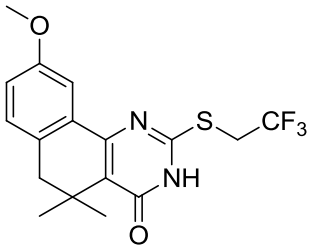

9-Methoxy-5,5-dimethyl-2-((2,2,2-trifluoroethyl)thio)-5,6-dihydrobenzo[h]quinazolin-4(3H)-one (208a). Prepared in a manner similar to **208b** from intermediate **44b** (175 mg, 0.607 mmol), using 1,1,1-trifluoro-2-iodoethane (150 µL, 1.517 mmol) as the alkylating agent. Concentration of the washed organic extract under high vacuum yielded a yellow solid that was

used without further purification (208 mg, 93% yield). ^{1}H NMR (400 MHz, Chloroform-*d*) δ 11.68 (s, 1H), 7.65 (d, *J* = 2.7 Hz, 1H), 7.11 (d, *J* = 8.2 Hz, 1H), 6.94 (dd, *J* = 8.2, 2.7 Hz, 1H), 4.10 (q, *J* = 9.6 Hz, 2H), 3.85 (s, 3H), 2.74 (s, 2H), 1.40 (s, 6H).

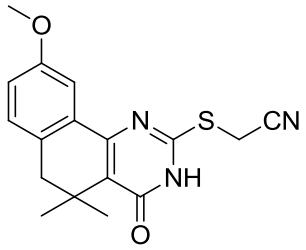

2-((9-Methoxy-5,5-dimethyl-4-oxo-3,4,5,6-tetrahydrobenzo[h]quinazolin-2-yl)thio)acetonitrile (208b). Intermediate **44b** (150 mg, 0.520 mmol) was combined with α-chloroacetonitrile (36 µL, 0.572 mmol) and sodium bicarbonate (66 mg, 0.780 mmol) in DMF (3 mL) and warmed to 50°C. The reaction was allowed to stir for 6 hours at 50°C, then was diluted with water and extracted twice with ethyl acetate. The organic extract was washed with water (3x) and brine (1x), then was dried over $MgSO_4$, vacuum filtered, and concentrated *in vacuo*. Further purification via flash chromatography (10-40% EtOAc:hex) returned the product as a yellow powdery solid (125 mg, 73% yield). ^{1}H NMR (400 MHz, DMSO-d_6) δ 12.85 (s, 1H), 7.80 (d, *J* = 2.4 Hz, 1H), 7.18 (d, *J* = 8.2 Hz, 1H), 6.97 (dd, *J* = 8.2, 2.4 Hz, 1H), 4.31 (s, 2H), 3.80 (s, 3H), 2.70 (s, 2H), 1.28 (s, 6H).

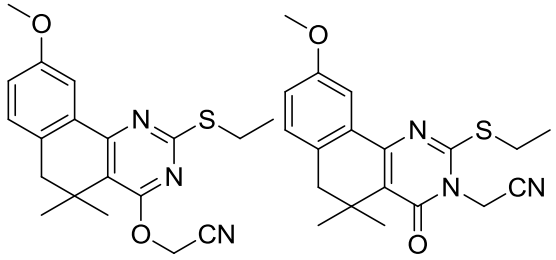

2-((2-(Ethylthio)-9-methoxy-5,5-dimethyl-5,6-dihydrobenzo[h]quinazolin-4-yl)oxy)acetonitrile (212) (CCG-211791) and **2-(2-(Ethylthio)-9-methoxy-5,5-dimethyl-4-oxo-5,6-dihydrobenzo[h]quinazolin-3(4H)-yl)acetonitrile (209) (CCG-211792).** Prepared in a manner similar to **215** from intermediate **45b** (60 mg, 0.190 mmol), using α-chloroacetonitrile (14 µL, 0.228 mmol) as the alkylating agent. Flash chromatography furnished both isomers in pure form. **2-((2-(Ethylthio)-9-methoxy-5,5-dimethyl-5,6-dihydrobenzo[h]quinazolin-4-**

yl)oxy)acetonitrile (212) (CCG-211791): 15 mg, 22% yield. ^{1}H NMR (400 MHz, Chloroform-*d*) δ 7.79 (d, *J* = 2.8 Hz, 1H), 7.09 (d, *J* = 8.2 Hz, 1H), 6.94 (dd, *J* = 8.2, 2.8 Hz, 1H), 5.08 (s, 2H), 3.86 (s, 3H), 3.22 (q, *J* = 7.3 Hz, 2H), 2.75 (s, 2H), 1.47 (t, *J* = 7.3 Hz, 3H), 1.31 (s, 6H). ESI+MS *m/z* = 356.1 (M + H^+) 378.0 (M + Na^+). HPLC (Method B, t_R = 7.54 min), purity >95%.

2-(2-(Ethylthio)-9-methoxy-5,5-dimethyl-4-oxo-5,6-dihydrobenzo[h]quinazolin-3(4H)-yl)acetonitrile (209) (CCG-211792): 31 mg, 46% yield. ^{1}H NMR (400 MHz, Chloroform-*d*) δ 7.66 (d, *J* = 2.7 Hz, 1H), 7.11 (d, *J* = 8.2 Hz, 1H), 6.93 (dd, *J* = 8.2, 2.7 Hz, 1H), 4.96 (s, 2H), 3.84 (s, 3H), 3.38 (q, *J* = 7.3 Hz, 2H), 2.72 (s, 2H), 1.52 (t, *J* = 7.4 Hz, 3H), 1.36 (s, 6H). ESI+MS *m/z* = 356.1 (M + H^+) 378.0 (M + Na^+). HPLC (Method B, t_R = 6.56 min), purity >95%.

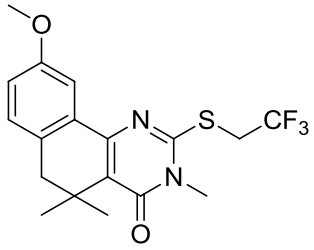

9-Methoxy-3,5,5-trimethyl-2-((2,2,2-trifluoroethyl)thio)-5,6-dihydrobenzo[h]quinazolin-4(3H)-one (210) (CCG-211790). Prepared in a manner similar to **215** from **208a** (54 mg, 0.146 mmol), using methyl iodide (23 mg, 0.160 mmol) as the alkylating agent. Flash chromatography isolated only the *N*-alkylated isomer (32 mg, 57% yield). ^{1}H NMR (500 MHz, Chloroform-*d*) δ 7.62 (d, *J* = 2.6 Hz, 1H), 7.10 (d, *J* = 8.2 Hz, 1H), 6.93 (dd, *J* = 8.2, 2.6 Hz, 1H), 4.18 (q, *J* = 9.7 Hz, 2H), 3.85 (s, 3H), 3.56 (s, 3H), 2.73 (s, 2H), 1.37 (s, 6H). ESI+MS *m/z* = 385.0 (M + H^+) 407.0 (M + Na^+). HPLC (Method B, t_R = 7.01 min), purity >95%.

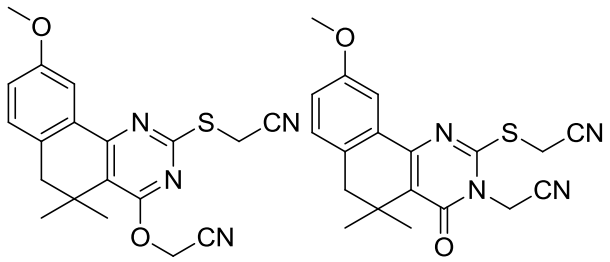

2-((4-(Cyanomethoxy)-9-methoxy-5,5-dimethyl-5,6-dihydrobenzo[h]quinazolin-2-yl)thio)acetonitrile (214) (CCG-202011) and **2-((3-(Cyanomethyl)-9-methoxy-5,5-dimethyl-4-oxo-3,4,5,6-tetrahydrobenzo[h]quinazolin-2-yl)thio)acetonitrile (211) (CCG-212012).**

Prepared in a manner similar to **215** from **208b** (60 mg, 0.183 mmol) using α-chloroacetonitrile as the alkylating agent. The crude mixture of *N*- and *O*-alkylated isomers was separated via flash chromatography (0-10% EtOAc:hex) to furnish **211** and **214**.

2-((4-(cyanomethoxy)-9-methoxy-5,5-dimethyl-5,6-dihydrobenzo[h]quinazolin-2-yl)thio)acetonitrile (214) (CCG-212011) 26 mg, 39% yield. ^{1}H NMR (400 MHz, Chloroform-*d*) δ 7.84 (d, *J* = 2.7 Hz, 1H), 7.12 (d, *J* = 8.3 Hz, 1H), 6.98 (dd, *J* = 8.3, 2.7 Hz, 1H), 5.12 (s, 2H), 3.92 (s, 2H), 3.89 (s, 3H), 2.78 (s, 2H), 1.34 (s, 6H). ESI+MS *m/z* = 367.1 (M + H^+) 389.1 (M + Na^+). HPLC (Method B, T_R = 5.85 min), purity >95%. **2-((3-(cyanomethyl)-9-methoxy-5,5-dimethyl-4-oxo-3,4,5,6-tetrahydrobenzo[h]quinazolin-2-yl)thio)acetonitrile (211) (CCG-212012).** 15 mg, 22% yield. ^{1}H NMR (400 MHz, Chloroform-*d*) δ 7.76 (d, *J* = 2.6 Hz, 1H), 7.12 (d, *J* = 8.2 Hz, 1H), 6.97 (dd, *J* = 8.2, 2.6 Hz, 1H), 4.96 (s, 2H), 4.10 (s, 2H), 3.88 (s, 3H), 2.75 (s, 2H), 1.37 (s, 6H). ESI+MS *m/z* = 367.1 (M + H^+) 389.1 (M + Na^+). HPLC (Method B, t_R = 4.59 min), purity >95%.

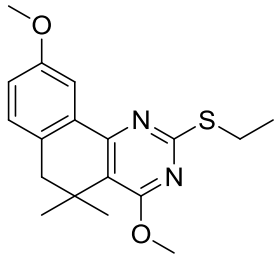

2-(Ethylthio)-4,9-dimethoxy-5,5-dimethyl-5,6-dihydrobenzo[h]quinazoline (213) (CCG-211793). Prepared in a manner similar to **215** from intermediate **45b** (55 mg, 0.174 mmol), using methyl *p*-toluenesulfonic ester (39 mg, 0.209 mmol) as the alkylating agent. Flash chromatography (2-15% EtOAc:hex) isolates the desired compound as a white powder (18 mg, 31% yield). *N*-alkylated regioisomer (**43**, CCG-206353) was also isolated (32 mg, 56% yield). ^{1}H NMR (500 MHz, Chloroform-*d*) δ 7.81 (d, *J* = 2.7 Hz, 1H), 7.08 (d, *J* = 8.2 Hz, 1H), 6.91 (dd, *J* = 8.2, 2.7 Hz, 1H), 4.00 (s, 3H), 3.87 (s, 3H), 3.21 (q, *J* = 7.3 Hz, 2H), 2.73 (s, 2H), 1.48 (t, *J* = 7.3 Hz, 3H), 1.30 (s, 6H). ESI+MS *m/z* = 331.0 (M + H^+) 353.0 (M + Na^+). HPLC (Method B, t_R = 9.35 min), purity 95%.

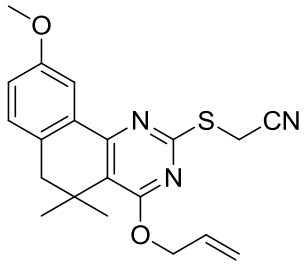

2-((4-(Allyloxy)-9-methoxy-5,5-dimethyl-5,6-dihydrobenzo[h]quinazolin-2-yl)thio)acetonitrile (215) (CCG-212010). *S*-alkylated intermediate **208b** (60 mg, 0.183 mmol) was dissolved in DMF (1 mL), to which allyl tosylate (43 mg, 0.202 mmol) and cesium carbonate (72 mg, 0.220 mmol) were added. Reaction was heated to 50°C and allowed to stir for 16 hours, then diluted with H_2O and extracted 3x with EtOAc. Organic layer washed with water and brine, then isolated, dried over $MgSO_4$, vacuum filtered, and concentrated. Further purification via FC (5% EtOAc:hex) returned the *O*-alkylated compound as a clear oil, (22 mg, 33% yield). The *N*-alkylated isomer was recovered in trace amounts and found to be significantly impure and was thus not further pursued. ^{1}H NMR (400 MHz, Chloroform-*d*) δ 7.83 (d, *J* = 2.7 Hz, 1H), 7.08 (d, *J* = 8.2 Hz, 1H), 6.93 (dd, *J* = 8.2, 2.7 Hz, 1H), 6.08 (ddt, *J* = 16.7, 10.6, 5.6 Hz, 1H), 5.41 (dd, *J* = 16.7, 1.4 Hz, 1H), 5.29 (dd, *J* = 10.6, 1.1 Hz, 1H), 4.96 (d, *J* = 5.6 Hz, 2H), 3.90 – 3.85 (m, 5H), 2.74 (s, 2H), 1.34 (s, 6H). ESI+MS *m/z* = 368.1 ($M + H^+$) 390.1 ($M + Na^+$). HPLC (Method B, T_R = 8.07 min) >95% purity.

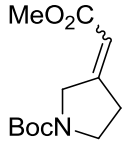

***tert*-Butyl 3-(2-methoxy-2-oxoethylidene)pyrrolidine-1-carboxylate (217).** Prepared in a manner similar to **173** beginning from tert-butyl 3-oxopyrrolidine-1-carboxylate (**216**, 2.00 g, 10.8 mmol). Isolated 2.14 g (82% yield) of a clear oil via flash chromatography (10-40% EtOAc:hex) as a separable mixture of E and Z isomers. ^{1}H NMR (400 MHz, Chloroform-*d*) δ 5.65 (isomer A, s, 1H), 5.61 (isomer B, s, 1H), 4.17 – 4.12 (isomer A, m, 4H), 4.12 – 4.08 (isomer B, m, 4H), 3.72 (isomer A, s, 3H), 3.70 (isomer B, s, 3H), 3.16 (isomer A+B, s, 4H), 1.48 (isomer A+B, d, *J* = 2.9 Hz, 18H).

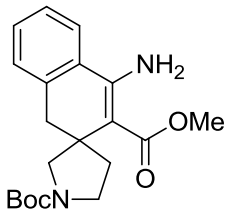

1'-*tert*-Butyl 3-methyl 4-amino-1H-spiro[naphthalene-2,3'-pyrrolidine]-1',3-dicarboxylate (218a). Prepared in a manner similar to **174** from *o*-tolunitrile **15** (631 mg, 5.39 mmol) and Michael acceptor **217** (1.00 g, 4.14 mmol). Isolated 297 mg (20% yield) after silica gel flash chromatography. ^{1}H NMR (400 MHz, Chloroform-*d*) δ 7.39 (d, *J* = 7.1 Hz, 1H), 7.36 – 7.26 (m, 2H), 7.18 (d, *J* = 6.5 Hz, 1H), 6.56 (s, 2H), 3.76 (s, 3H), 3.55 (d, *J* = 10.5 Hz, 1H), 3.51 – 3.30 (m, 2H), 3.22 – 3.04 (m, 1H), 2.89 – 2.70 (m, 2H), 2.49 – 2.33 (m, 1H), 1.61 – 1.52 (m, 1H), 1.44 (d, *J* = 18.5 Hz, 9H).

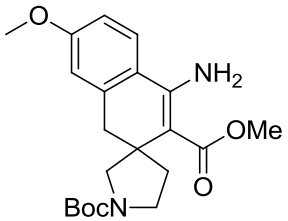

***tert*-Butyl 3-allyl-2-((2-methoxyethyl)thio)-4-oxo-4,6-dihydro-3H-spiro[benzo[h]quinazoline-5,3'-pyrrolidine]-1'-carboxylate (218b).** Prepared in a manner similar to **174** from Michael acceptor **217** (552 mg, 2.29 mmol) and tolunitrile **26c**. Isolated the desired product as a yellow oil (219 mg, 25% yield). ^{1}H NMR (400 MHz, Chloroform-*d*) δ 7.37 (d, *J* = 8.2 Hz, 1H), 6.82 (d, *J* = 6.4 Hz, 1H), 6.72 (s, 1H), 6.64 (s, 2H), 3.84 (s, 3H), 3.76 (s, 3H), 3.54 – 3.32 (m, 3H), 3.14 (dd, *J* = 36.6, 10.6 Hz, 1H), 2.88 – 2.68 (m, 2H), 2.52 – 2.33 (m, 1H), 1.63 – 1.52 (m, 1H), 1.46 (d, *J* = 15.8 Hz, 9H).

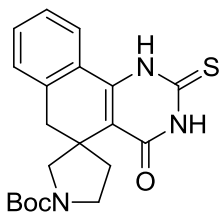

***tert*-Butyl 4-oxo-2-thioxo-2,3,4,6-tetrahydro-1H-spiro[benzo[h]quinazoline-5,3'-pyrrolidine]-1'-carboxylate (219a).** Aminoester intermediate **218a** (190 mg, 0.530 mmol) was

combined with benzoyl isothiocyanate (112 mg, 0.689 mmol) in absolute ethanol (0.63 mL). The reaction was capped, warmed to 75°C and stirred 3 hours. Additional benzoyl isothiocyanate (43 mg, 0.265 mmol) was added, and the reaction mixture was allowed to stir overnight at 75°C. The reaction mixture was cooled and the solvent evaporated under reduced temperature. The crude organic isolate was redissolved in a 2:1 ethanol:water solution (1.3 mL). Potassium hydroxide (49 mg, 0.870 mmol) was added, and the solution warmed to 75°C for 1.5 hours. The reaction was quenched via the addition of ~5mL saturated aqueous ammonium chloride, then extracted 3x into dichloromethane. The pooled organic layers were washed with sat. aq. $NaHCO_3$ and brine, then isolated, dried over $MgSO_4$, vacuum filtered and concentrated. Further purification via FC (10-30% EtOAc:hex) delivered the desired product as 114 mg of off-white crystals (68% yield). ESI-MS+ *m/z* = 408.0 ($M + Na^+$). ^{1}H NMR (400 MHz, Chloroform-*d*) δ 9.48 (s, 1H), 9.35 (s, 1H), 7.58 – 7.29 (m, 4H), 3.96 (d, *J* = 10.7 Hz, 0.5H), 3.83 (d, *J* = 10.9 Hz, 0.5H), 3.61 – 3.41 (m, 2H), 3.30 (d, *J* = 10.7 Hz, 0.5H), 3.19 (d, *J* = 10.7 Hz, 0.5H), 3.08 – 2.74 (m, 4H), 1.47 (s, 4.5H), 1.44 (s, 4.5H).

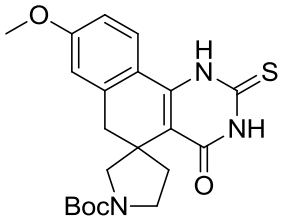

***tert*-Butyl 8-methoxy-4-oxo-2-thioxo-2,3,4,6-tetrahydro-1H-spiro[benzo[h]quinazoline-5,3'-pyrrolidine]-1'-carboxylate (219b).** Prepared in a manner similar to **175** from **218b** (520 mg, 1.34 mmol). Isolated the desired product as a crystalline white solid (275 mg, 49% yield over 2 steps). ^{1}H NMR (400 MHz, Chloroform-*d*) δ 9.41 (s, 2H), 7.46 (t, *J* = 7.7 Hz, 1H), 6.93 – 6.84 (m, 1H), 6.80 (d, *J* = 2.4 Hz, 1H), 3.95 (d, *J* = 10.8 Hz, 0.5H), 3.87 (s, 3H), 3.83 – 3.73 (m, 0.5H), 3.59 – 3.38 (m, 2.5H), 3.29 (d, *J* = 10.4 Hz, 0.5H), 3.17 (d, *J* = 10.4 Hz, 0.5H), 3.06 – 2.74 (m, 3.5H), 1.46 (s, 4.5H), 1.43 (s, 4.5H).

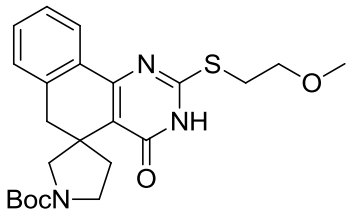

***tert*-Butyl 2-((2-methoxyethyl)thio)-4-oxo-4,6-dihydro-3H-spiro[benzo[h]quinazoline-5,3'-pyrrolidine]-1'-carboxylate (220a).** Prepared in a manner similar to **176a** from **219a** (111 mg, 0.288 mmol). Isolated the desired product as a white solid after vacuum filtration (116 mg, 91% yield).

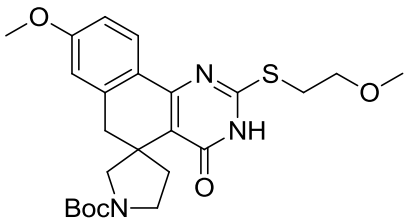

***tert*-Butyl 8-methoxy-2-((2-methoxyethyl)thio)-4-oxo-4,6-dihydro-3H-spiro[benzo[h]quinazoline-5,3'-pyrrolidine]-1'-carboxylate (220b)**. Prepared in a manner similar to **176a** from **219b** (275 mg, 0.728 mmol). Isolated the desired product after column chromatography (10-40% EtOAc:hex) as a white solid (155 mg, 50% yield). ^{1}H NMR (400 MHz, Chloroform-*d*) δ 10.85 (s, 1H), 8.05 (d, *J* = 8.4 Hz, 1H), 6.85 (d, *J* = 8.4 Hz, 1H), 6.70 (d, *J* = 2.5 Hz, 1H), 4.05 (d, *J* = 10.8 Hz, 0.5H), 3.94 (d, *J* = 10.6 Hz, 0H), 3.85 (s, 3H), 3.76 (t, *J* = 6.0 Hz, 2H), 3.65 – 3.47 (m, 2H), 3.45 (s, 3H), 3.41 (t, *J* = 6.0 Hz, 2H), 3.34 (d, *J* = 10.8 Hz, 0.5H), 3.22 (d, *J* = 10.6 Hz, 0.5H), 3.13 - 2.94 (m, 1H), 2.94 – 2.81 (m, 2H), 1.72 – 1.63 (m, 1H), 1.47 (s, 4.5H), 1.43 (s, 4.5H).

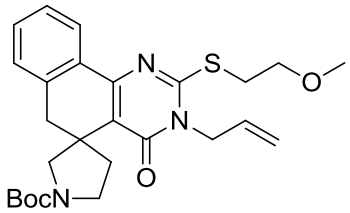

***tert*-Butyl 3-allyl-2-((2-methoxyethyl)thio)-4-oxo-4,6-dihydro-3H-spiro[benzo[h]quinazoline-5,3'-pyrrolidine]-1'-carboxylate (221) (CCG-208860).** Prepared in a manner similar to **177** from **220a** (116 mg, 0.262 mmol). Isolated as a clear oil (40 mg, 32%

yield) after column chromatography. ^{1}H NMR (400 MHz, Chloroform-d) δ 8.10 (t, *J* = 7.2 Hz, 1H), 7.41 – 7.30 (m, 2H), 7.19 (d, *J* = 7.2 Hz, 1H), 5.92 (d, *J* = 5.6 Hz, 1H), 5.30 (d, *J* = 18.7 Hz, 2H), 4.69 (d, *J* = 4.9 Hz, 2H), 3.99 (dd, *J* = 32.9, 10.8 Hz, 1H), 3.76 (t, *J* = 6.1 Hz, 2H), 3.63 – 3.45 (m, 4H), 3.42 (s, 3H), 3.27 (dd, *J* = 39.4, 10.4 Hz, 1H), 2.96 (q, *J* = 15.9 Hz, 3H), 1.70 – 1.62 (m, 1H), 1.45 (d, *J* = 15.7 Hz, 9H). ESI+MS *m/z* = 506.1 (M + Na^+). HPLC (Method B, t_R = 7.81 min), purity >95%.

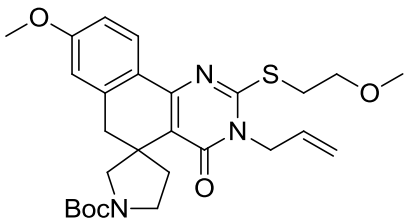

***tert*-Butyl 3-allyl-8-methoxy-2-((2-methoxyethyl)thio)-4-oxo-4,6-dihydro-3H-spiro[benzo[h]quinazoline-5,3'-pyrrolidine]-1'-carboxylate (222) (CCG-208864).** Prepared in a manner similar to **177** from intermediate **220b** (150 mg, 0.317 mmol). Isolated the desired product as a clear oil (68 mg, 42% yield). ^{1}H NMR (400 MHz, Chloroform-d) δ 8.03 (d, *J* = 8.4 Hz, 1H), 6.85 (d, *J* = 8.7 Hz, 1H), 6.70 (s, 1H), 5.89 (s, 1H), 5.28 (d, *J* = 19.5 Hz, 2H), 4.67 (d, *J* = 4.9 Hz, 2H), 3.97 (dd, *J* = 41.9, 10.2 Hz, 1H), 3.85 (s, 3H), 3.74 (t, *J* = 6.1 Hz, 2H), 3.62 – 3.43 (m, 4H), 3.41 (s, 3H), 3.25 (dd, *J* = 41.9, 10.6 Hz, 1H), 3.15 – 2.83 (m, 3H), 1.70 – 1.59 (m, 1H), 1.44 (d, *J* = 14.0 Hz, 9H). ESI+MS *m/z* = 536.1 (M + Na^+). HPLC (Method B, t_R = 7.61 min), purity >95%.

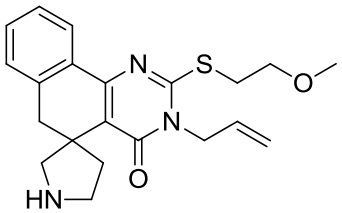

3-Allyl-2-((2-methoxyethyl)thio)-3H-spiro[benzo[h]quinazoline-5,3'-pyrrolidin]-4(6H)-one (223) (CCG-208861). Prepared in a manner similar to **190** from **221** (33 mg, 0.068 mmol). Isolated the desired product as a white powder after filtration (27 mg, 94% yield). ^{1}H NMR (400 MHz, Chloroform-*d*) δ 11.37 (s, 1H), 8.32 (s, 1H), 8.10 (d, *J* = 7.4 Hz, 1H), 7.48 – 7.36 (m, 2H), 7.31 (d, *J* = 7.0 Hz, 1H), 5.96 – 5.84 (m, 1H), 5.35 – 5.26 (m, 2H), 4.72 (d, *J* = 4.7 Hz, 2H), 4.00 – 3.86 (m, 1H), 3.76 (t, *J* = 6.0 Hz, 2H), 3.68 – 3.47 (m, 4H), 3.42 (s, 3H), 3.30 (d, *J* = 14.6 Hz,

2H), 2.96 (d, *J* = 14.8 Hz, 1H), 2.22 – 2.10 (m, 2H). ESI+MS *m/z* = 384.1 ($M + H^+$). HPLC (Method B, t_R = 1.25 min), purity 90%.

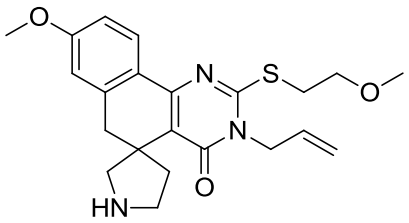

3-Allyl-8-methoxy-2-((2-methoxyethyl)thio)-3H-spiro[benzo[h]quinazoline-5,3'-pyrrolidin]-4(6H)-one (224) (CCG-208865). Prepared in a manner similar to **190** from **222** (30 mg, 0.058 mmol). Isolated the desired product as a white powder (20 mg, 77% yield). ^{1}H NMR (400 MHz, Chloroform-*d*) δ 11.62 (s, 1H), 8.16 (s, 1H), 8.03 (d, *J* = 8.4 Hz, 1H), 6.90 (d, *J* = 8.4 Hz, 1H), 6.81 (s, 1H), 5.97 – 5.80 (m, 1H), 5.38 – 5.20 (m, 2H), 4.78 – 4.59 (m, 2H), 4.05 – 3.92 (m, 1H), 3.88 (s, 3H), 3.75 (t, *J* = 6.0 Hz, 3H), 3.65 – 3.51 (m, 3H), 3.42 (s, 3H), 3.38 – 3.16 (m, 2H), 2.98 – 2.78 (m, 1H), 2.26 – 1.99 (m, 2H). ESI+MS *m/z* = 414.1 ($M + H^+$), 436.1 ($M + Na^+$). HPLC (Method B, t_R = 1.53 min), purity >95%.

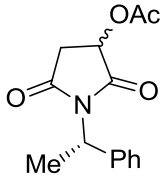

2,5-Dioxo-1-((*S*)-1-phenylethyl)pyrrolidin-3-yl acetate (226): DL-malic acid (1.00 g, 7.46 mmol) was dissolved in acetyl chloride (4 mL). The reaction vessel was affixed with a reflux condenser and warmed to reflux under N_2 atmosphere for 3 hours. The reaction was cooled and concentrated in vacuo, then under high vacuum. The resulting crude residue was dissolved in anhydrous THF (5 mL), then (*S*)-α-methylbenzylamine (961 µL, 7.46 mmol) was added. The reaction was allowed to stir at room temperature for 4 hours. The solvent was removed *in vacuo*, then additional acetyl chloride (4 mL) was added and the solution allowed to reflux for 12 hours. The reaction mixture was again concentrated *in vacuo*, and the crude organic residue was purified via flash chromatography (0-20% EtOAc:hex) to yield the desired product as a white solid (1.75 g, 90% yield). ^{1}H NMR (400 MHz, Chloroform-*d*) δ 7.45 (d, *J* = 7.4 Hz, 2H), 7.38 –

7.27 (m, 3H), 5.50 – 5.31 (m, 2H), 3.10 (ddd, *J* = 18.3, 8.8, 4.5 Hz, 1H), 2.63 (dt, *J* = 18.3, 5.2 Hz, 1H), 2.15 (d, *J* = 3.6 Hz, 3H), 1.83 (dd, *J* = 7.3, 3.3 Hz, 3H).

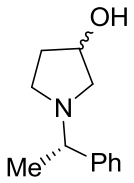

1-((*S*)-1-Phenylethyl)pyrrolidin-3-ol (intermediate in synthesis of 227). A suspension of lithium aluminum hydride (3.04 g, 80 mmol) was prepared at 0°C in anhydrous THF (24 mL). A solution of succinimide **226** (3.22 g, 12.32 mmol) was added slowly dropwise, then allowed to stir while coming to room temperature for 6 hours. Reaction was quenched by the dropwise, successive addition of 3 mL of water, 3 mL of 15% NaOH solution, and finally 9 mL of water. The resulting suspension was diluted with diethyl ether (40 mL) and filtered through Celite. The organic layer was dried over $MgSO_4$ and vacuum filtered, then concentrated under reduced pressure to a crude oil (2.20 g, 93% crude yield). Used in the next step without further purification. ^{1}H NMR (400 MHz, Chloroform-*d*) δ 7.36 – 7.20 (m, 5H), 4.38 – 4.24 (m, 1H), 3.25 (qd, *J* = 6.6, 4.1 Hz, 1H), 3.01 (td, *J* = 8.4, 7.6, 4.3 Hz, 0.5H), 2.81 (d, *J* = 9.9 Hz, 0.5H), 2.66 (td, *J* = 8.7, 5.1 Hz, 0.5H), 2.55 – 2.40 (m, 1.5H), 2.33 – 2.07 (m, 3H), 1.39 (dd, *J* = 6.6, 3.9 Hz, 3H).

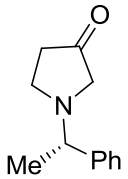

(*S*)-1-(1-Phenylethyl)pyrrolidin-3-one (227). A solution of oxalyl chloride (2.01 mL, 23.00 mmol) in dichloromethane (40 mL) was cooled to -78°C in a dry ice/acetone bath. Anhydrous DMSO (2.04 mL, 28.8 mmol) was added and the solution was allowed to stir for 10 minutes. A solution of the pyrrolidinol intermediate (2.2 g, 11.5 mmol) in DCM (3 mL) was added slowly dropwise, followed by the dropwise addition of triethylamine (8.02 mL, 57.5 mmol). The reaction was allowed to stir at -78°C for 1 hour. The reaction was quenched via the addition of saturated aqueous sodium bicarbonate solution and diethyl ether. The water layer was extracted 2x with ether, then the pooled organic fractions were washed with water and brine. The organic

layer was concentrated *in vacuo* and further purified by flash chromatography (10-33% EtOAc:hex) to furnish the product as a clear oil (1.20 g, 55% yield). ^{1}H NMR (400 MHz, Chloroform-*d*) δ 7.37 – 7.22 (m, 5H), 3.36 (q, *J* = 6.6 Hz, 1H), 3.02 (d, *J* = 17.1 Hz, 1H), 2.96 – 2.72 (m, 3H), 2.38 (t, *J* = 7.0 Hz, 2H), 1.42 (d, *J* = 6.6 Hz, 3H).

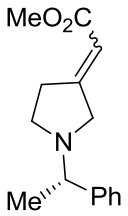

(*S*)-Methyl 2-(1-(1-phenylethyl)pyrrolidin-3-ylidene)acetate (228). Prepared in a manner similar to **217** from intermediate **227** (1.3 g, 8.93 mmol). Isolated the desired compound as a crude mixture of *Z*- and *E*-isomers, (1.7 g, 100% crude yield) which could be separated by column chromatography. *E*-isomer: ^{1}H NMR (400 MHz, Chloroform-*d*) δ 7.37 – 7.19 (m, 5H), 5.77 – 5.71 (m, 1H), 3.86 (d, *J* = 18.0 Hz, 1H), 3.66 (s, 3H), 3.49 (d, *J* = 18.0 Hz, 1H), 3.32 (q, *J* = 6.6 Hz, 1H), 2.66 – 2.50 (m, 4H), 1.43 (d, *J* = 6.6 Hz, 3H). *Z*-isomer: ^{1}H NMR (400 MHz, Chloroform-*d*) δ 7.35 – 7.29 (m, 4H), 7.28 – 7.23 (m, 1H), 5.76 – 5.70 (m, 1H), 3.68 (s, 3H), 3.32 – 3.13 (m, 3H), 2.94 (t, *J* = 6.4 Hz, 2H), 2.86 – 2.76 (m, 1H), 2.59 – 2.48 (m, 1H), 1.41 (d, *J* = 6.6 Hz, 3H).

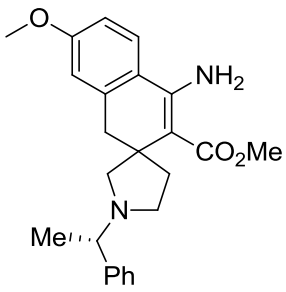

Methyl 4-amino-7-methoxy-1'-((*S*)-1-phenylethyl)-1H-spiro[naphthalene-2,3'-pyrrolidine]-3-carboxylate (229). Prepared in a manner similar to **218a** from tolunitrile **26c** and pyrollidine ester **228** (1.76 g, 7.17 mmol). Column chromatography resulted in the isolation of 754 mg of the desired product as a sticky brown oil (3:2 mixture of diastereomers, 25% yield). ^{1}H NMR (400 MHz, Chloroform-*d*) δ 7.40 – 7.06 (diastereomer a + b, m, 16H), 6.88 – 6.76 (diastereomer a+b, m, 2H), 6.73 – 6.67 (diastereomer a + b, m, 2H), 6.50 (diastereomer a, s, 2H), 6.45

(diastereomer b, s, 3H), 3.85 (diastereomer a, s, 3H), 3.80 (diastereomer b, s, 4.5H), 3.74 – 3.68 (diastereomer a+b, m, 7.5H), 3.68-3.52 (diastereomer a + b, m, 2.5H), 3.30 – 3.14 (diastereomer a + b, m, 4H), 3.11 – 2.98 (diastereomer a + b, m, 2H), 2.83 – 2.60 (diastereomer a + b, m, 4H), 2.49 – 2.18 (diastereomer a + b, m, 7H), 2.10 – 2.01 (diastereomer a + b, m, 2H), 1.75 – 1.61 (diastereomer b, m, 2H), 1.59 – 1.46 (diastereomer a, m, 1H), 1.34 (diastereomer b, d, *J* = 6.5 Hz, 4.5H), 1.24 (diastereomer a, d, *J* = 6.0 Hz, 3H).

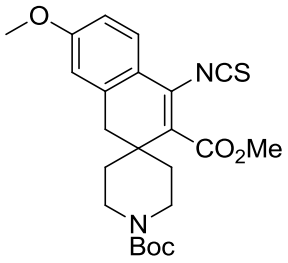

1'-*tert*-Butyl 3-methyl 4-isothiocyanato-7-methoxy-1H-spiro[naphthalene-2,4'-piperidine]-1',3-dicarboxylate (232). Thiophosgene (411 µL, 4.40 mmol) was dissolved in DCM (2.5 mL) and saturated aqueous sodium bicarbonate (2.5 mL) was added. β-aminoester **174** (1.18 g, 2.93 mmol) was dissolved in DCM (1 mL) with gentle heating and added dropwise to the biphasic thiophosgene mixture, causing a light refluxing of the organic layer. Allowed to stir for 1.5 hours, then additional thiophosgene (137 µL, 1.47 mmol) and sat. aq. $NaHCO_3$ (2 mL) was added and allowed to stir another 2 hours. The reaction mixture was diluted with additional DCM and partitioned. The aqueous layer was extracted twice with DCM, then the combined organic fractions were washed with sodium carbonate, water and brine. Organic layer dried over $MgSO_4$ and concentrated *in vacuo*. Further purification via column chromatography (15% EtOAc:hex) isolates the desired product as a sticky pale yellow solid (1.029g, 79% yield). ^{1}H NMR (400 MHz, Chloroform-*d*) δ 7.41 (d, *J* = 8.5 Hz, 1H), 6.81 (dd, *J* = 8.5, 2.6 Hz, 1H), 6.71 (d, *J* = 2.5 Hz, 1H), 4.00 – 3.85 (m, 5H), 3.82 (s, 3H), 3.05 – 2.83 (m, 4H), 1.89 (td, *J* = 13.0, 4.9 Hz, 2H), 1.52 – 1.39 (m, 11H).

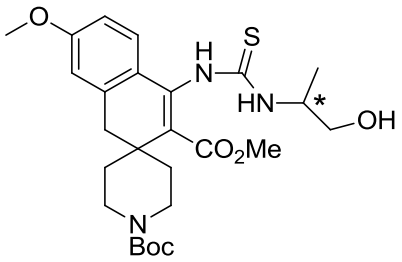

1'-*tert*-Butyl 3-methyl 4-(3-(1-hydroxypropan-2-yl)thioureido)-7-methoxy-1H-spiro[naphthalene-2,4'-piperidine]-1',3-dicarboxylate (intermediate in the synthesis of 233a, 233b). The isothiocyanate intermediate (200 mg, 0.450 mmol) was dissolved in anhydrous diethyl ether (1.6 mL). Enantiopure 2-amino-1-propanol (39 µL, 0.495 mmol) was added dropwise, then the reaction allowed to stir at room temperature for 1 hour, over which time a white precipitate accumulated. The reaction mixture was diluted with additional ether and the solid was collected via vacuum filtration. Isolated 220 mg (91% yield) as a white powder, used without further purification. ^{1}H NMR (500 MHz, Chloroform-*d*) δ 7.28 (d, *J* = 8.3 Hz, 1H), 6.91 (s, 1H), 6.81 – 6.74 (m, 2H), 5.96 (d, *J* = 8.4 Hz, 1H), 4.57 (s, 1H), 4.05 – 3.70 (m, 9H), 3.52 – 3.44 (m, 1H), 3.09 – 2.89 (m, 4H), 1.86 – 1.74 (m, 2H), 1.64 – 1.53 (m, 3H), 1.46 (s, 9H), 1.19 – 1.03 (m, 3H).

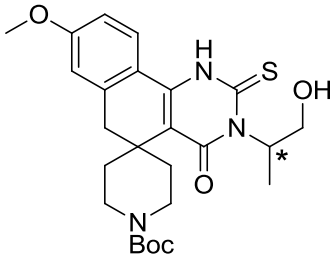

***tert*-Butyl 3-(1-hydroxypropan-2-yl)-8-methoxy-4-oxo-2-thioxo-2,3,4,6-tetrahydro-1H-spiro[benzo[h]quinazoline-5,4'-piperidine]-1'-carboxylate (233a and 233b).** The chiral amine-isothiocyanate adduct (234 mg, 0.450 mmol) was added to anhydrous methanol (1.60 mL), then sodium methoxide (49 mg, 0.901 mmol) was added and the solution allowed to stir for 30 minutes. Over this time the product slowly dissolves to leave a clear solution. Reaction quenched by the addition of sat. aq. NH_4Cl. The resulting aqueous suspension was extracted 2x with DCM, then the organic layers combined and washed with water and brine. The organic layer was dried over $MgSO_4$, vacuum filtered, and concentrated *in vacuo* to render the desired product as white crystals (203 mg, 92% yield). ^{1}H NMR (500 MHz, Chloroform-*d*) δ 9.31 (s,

1H), 7.39 (d, *J* = 8.6 Hz, 1H), 6.91 (dd, *J* = 8.6, 2.6 Hz, 1H), 6.83 (d, *J* = 2.5 Hz, 1H), 6.10 – 5.95 (m, 1H), 4.17 – 4.04 (m, 1H), 4.04 – 3.90 (m, 3H), 3.88 (s, 3H), 3.46 – 3.31 (m, 1H), 3.21 – 2.77 (m, 4H), 2.74 – 2.55 (m, 1H), 2.52 – 2.35 (m, 1H), 1.51 (d, *J* = 7.0 Hz, 3H), 1.48 (s, 9H), 1.30 (d, *J* = 13.5 Hz, 2H).

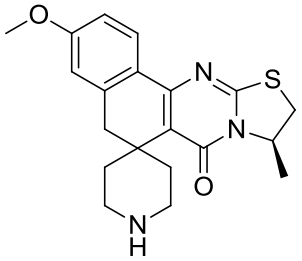

(*R*)-3-Methoxy-9-methyl-9,10-dihydrospiro[benzo[h]thiazolo[2,3-b]quinazoline-6,4'-piperidin]-7(5H)-one (234) (CCG-212230). The 2-thioxopyrimidinone intermediate **233a** (191 mg, 0.392 mmol) was suspended in DCM (2 mL) and cooled to 0°C. TFA (600 µL, 7.83 mmol) was added dropwise, then the solution allowed to stir for 4 hours, warming slowly to room temperature over this time. The reaction was quenched via the slow addition of saturated aqueous sodium carbonate, then the mixture was extracted with DCM. The pooled organic layers were washed with water and brine, then isolated, dried, filtered, and concentrated. Further purification via FC (0-20% MeOH-NH_3: DCM) furnished the desired product (139 mg) in 96% yield. ^{1}H NMR (500 MHz, Methanol-d_4) δ 7.97 (d, *J* = 9.0 Hz, 1H), 6.92 – 6.86 (m, 2H), 5.15 (p, *J* = 6.5 Hz, 1H), 3.85 (s, 3H), 3.81 (dd, *J* = 11.4, 7.8 Hz, 1H), 3.25 – 2.98 (m, 8H), 2.72 (td, *J* = 13.6, 5.2 Hz, 1H), 1.54 – 1.46 (m, 5H). ESI+MS *m/z* = 370.2 (M + H^+). HPLC (Method A, T_R = 5.22 min) >95% purity.

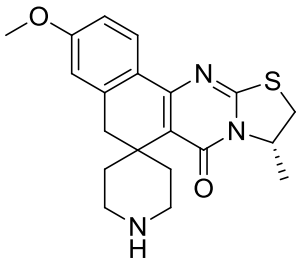

(*S*)-3-Methoxy-9-methyl-9,10-dihydrospiro[benzo[h]thiazolo[2,3-b]quinazoline-6,4'-piperidin]-7(5H)-one (235) (CCG-212231). Compound synthesized in a manner similar to that for **234** from intermediate **233b** (48 mg, 0.098 mmol). Isolated after column chromatography as

a white powder (26 mg, 72% yield). ^{1}H NMR (500 MHz, Methanol-d_4) δ 8.00 (d, J = 9.2 Hz, 1H), 6.95 – 6.89 (m, 2H), 5.21 – 5.12 (m, 1H), 3.86 (s, 3H), 3.83 (dd, J = 11.4, 7.8 Hz, 1H), 3.36 – 3.26 (m, 4H), 3.25 – 3.00 (m, 4H), 2.88 – 2.77 (m, 1H), 1.60 (d, J = 14.7 Hz, 2H), 1.52 (d, J = 6.4 Hz, 3H). ESI+MS m/z = 370.2 (M + H^+). HPLC (Method A, t_R = 5.15 min), purity >95%.

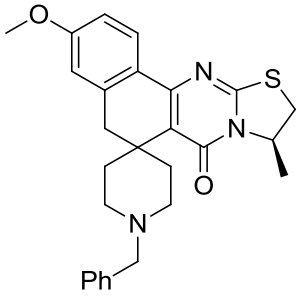

(*R*)-1'-Benzyl-3-methoxy-9-methyl-9,10-dihydrospiro[benzo[h]thiazolo[2,3-b]quinazoline-6,4'-piperidin]-7(5H)-one (CCG-212232) (236). Spiropiperidine intermediate **234** (40 mg, 0.108 mmol) was dissolved in DCE (0.55 mL). Benzaldehyde (14 µL, 0.141 mmol) and acetic acid (7.5 µL, 0.130 mmol) were added and the reaction allowed to stir for 30 minutes at room temperature. Sodium triacetoxyborohydride (34 mg, 0.162 mmol) was then added and the reaction mixture was allowed to stir at room temperature an additional 16 hours. At this time the reaction was quenched via the addition of sat. aq. sodium bicarbonate (5 mL). The biphasic mixture was extracted with diethyl ether (2x 10 mL), and the combined organic layers were pooled and washed with water and brine. The organic layer was dried over $MgSO_4$, vacuum filtered and concentrated *in vacuo*, then the solvent was removed under reduced pressure. Further purification via flash chromatography (0-10%) DCM:MeOH furnished the product as a white solid (31 mg, 62% yield). ^{1}H NMR (400 MHz, Chloroform-*d*) δ 8.01 (d, J = 8.6 Hz, 1H), 7.39 (s, 2H), 7.31 (t, J = 7.4 Hz, 2H), 7.27 – 7.20 (m, 1H), 6.82 (dd, J = 8.6, 2.6 Hz, 1H), 6.72 (d, J = 2.5 Hz, 1H), 5.18 (p, J = 6.7 Hz, 1H), 3.85 (s, 3H), 3.74 (dd, J = 11.2, 7.8 Hz, 1H), 3.67 – 3.48 (m, 2H), 3.19 – 3.05 (m, 2H), 2.97 (d, J = 11.1 Hz, 1H), 2.89 (d, J = 15.5 Hz, 1H), 2.83 – 2.68 (m, 2H), 2.45 – 2.20 (m, 2H), 1.87 – 1.69 (m, 2H), 1.57 (d, J = 6.4 Hz, 3H), 1.43 – 1.28 (m, 2H). ESI+MS m/z = 460.3 (M + H^+). HPLC (Method A, t_R = 5.98 min), purity >95%.

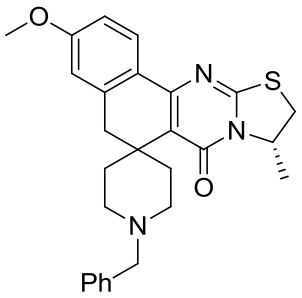

(*S*)-1'-Benzyl-3-methoxy-9-methyl-9,10-dihydrospiro[benzo[h]thiazolo[2,3-b]quinazoline-6,4'-piperidin]-7(5H)-one (CCG-212233) (237). Prepared in a manner similar to **236** from intermediate **235** (40 mg, 0.108 mmol). Isolated the desired product after chromatography as a white powder (24 mg, 48% yield). ^{1}H NMR (400 MHz, Chloroform-*d*) δ 8.00 (d, *J* = 8.6 Hz, 1H), 7.42 – 7.33 (m, 2H), 7.29 (t, *J* = 7.1 Hz, 2H), 7.25 – 7.20 (m, 1H), 6.81 (dd, *J* = 8.6, 2.2 Hz, 1H), 6.71 (d, *J* = 2.2 Hz, 1H), 5.16 (p, *J* = 6.9 Hz, 1H), 3.84 (s, 3H), 3.72 (dd, *J* = 11.2, 7.9 Hz, 1H), 3.63 – 3.48 (m, 2H), 3.17 – 3.04 (m, 2H), 2.95 (d, *J* = 11.1 Hz, 1H), 2.88 (d, *J* = 15.6 Hz, 1H), 2.80 – 2.65 (m, 2H), 2.40 – 2.21 (m, 2H), 1.80 – 1.66 (m, 2H), 1.55 (d, *J* = 6.4 Hz, 3H), 1.38 – 1.27 (m, 2H). ESI+MS *m/z* = 460.3 (M + H$^+$). HPLC (Method A, t_R = 6.02 min), purity >95%.

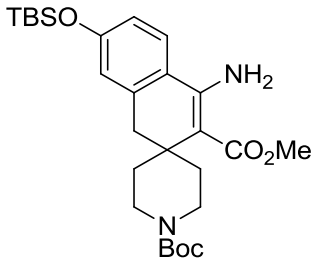

1'-*tert*-Butyl 3-methyl 4-amino-7-((tert-butyldimethylsilyl)oxy)-1H-spiro[naphthalene-2,4'-piperidine]-1',3-dicarboxylate (238). Prepared in a manner similar to compound xxx from tolunitrile **140** (1.94 g, 7.83 mmol) and α,β-unsaturated piperidine ester **173** (2.00 g, 7.83 mmol). After isolation of the crude organic extract, dissolution in a 3:2 mixture of diethyl ether:hexanes caused the precipitation of the desired product as a light yellow solid that was collected via vacuum filtration and used without further purification. Isolated 1.43 g (40% yield). ^{1}H NMR (400 MHz, Chloroform-*d*) δ 7.26 (d, *J* = 8.4 Hz, 1H), 6.73 (dd, *J* = 8.4, 2.5 Hz, 1H), 6.67 (d, *J* = 2.5 Hz, 1H), 6.29 (s, 2H), 3.98 – 3.76 (m, 2H), 3.74 (s, 3H), 3.05 – 2.86 (m, 2H), 2.83 (s, 2H), 2.40 – 2.22 (m, 2H), 1.46 (s, 9H), 1.26 – 1.16 (m, 2H), 0.98 (s, 9H), 0.21 (s, 6H).

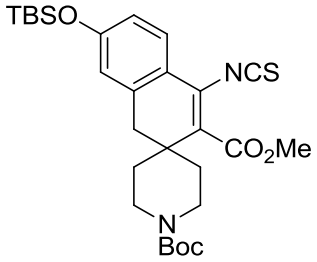

1'-*tert*-butyl 3-methyl 7-((tert-butyldimethylsilyl)oxy)-4-isothiocyanato-1H-spiro[naphthalene-2,4'-piperidine]-1',3-dicarboxylate (239). Prepared in a manner similar to **232** from intermediate **238** (1.42 g, 2.82 mmol). Isolated 1.18 g after chromatography of a yellow solid (77% yield), used without further purification. ^{1}H NMR (400 MHz, Chloroform-*d*) δ 7.35 (d, *J* = 8.4 Hz, 1H), 6.75 (dd, *J* = 8.4, 2.4 Hz, 1H), 6.65 (d, *J* = 2.4 Hz, 1H), 4.04 – 3.75 (m, 5H), 3.04 – 2.84 (m, 4H), 1.89 (td, *J* = 13.0, 4.9 Hz, 2H), 1.51 – 1.42 (m, 11H), 0.97 (s, 9H), 0.21 (s, 6H).

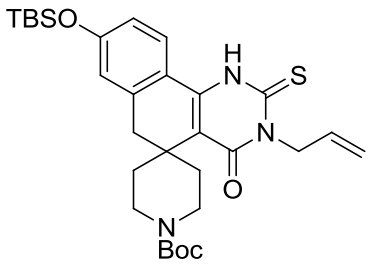

***tert*-Butyl 3-allyl-8-((tert-butyldimethylsilyl)oxy)-4-oxo-2-thioxo-2,3,4,6-tetrahydro-1H-spiro[benzo[h]quinazoline-5,4'-piperidine]-1'-carboxylate (240).** The β-isothiocyanato ester **239**(1.17 g, 2.15 mmol) was suspended in diethyl ether (3.8 mL), then allylamine (177 µL, 2.36 mmol) was added. The reaction mixture was allowed to stir 1 hour until a white precipitate formed. Anhydrous methanol (7 mL) was added, followed by sodium methoxide (174 mg, 3.22 mmol). The reaction was stirred for an additional 3 hours. At this time the hazy solution was diluted with saturated aqueous ammonium chloride solution (30 mL) and extracted 3x into diethyl ether. The organic layer was washed with water and brine, then concentrated *in vacuo* to the desired product as a white solid (1.18 g, 96% yield). ^{1}H NMR (400 MHz, Chloroform-*d*) δ 9.19 (s, 1H), 7.33 (d, *J* = 8.5 Hz, 1H), 6.83 (dd, *J* = 8.5, 2.4 Hz, 1H), 6.76 (d, *J* = 2.4 Hz, 1H), 5.97 (ddd, *J* = 17.3, 10.5, 5.6 Hz, 1H), 5.35 (dd, *J* = 17.3, 1.5 Hz, 1H), 5.25 (dd, *J* = 10.5, 1.4 Hz,

1H), 5.03 (d, *J* = 5.6 Hz, 2H), 4.07 – 3.87 (m, 2H), 3.12 – 2.86 (m, 4H), 2.84 – 2.70 (m, 1H), 2.63 – 2.43 (m, 1H), 1.45 (s, 9H), 1.29 (d, *J* = 12.9 Hz, 2H), 0.99 (s, 9H), 0.24 (s, 6H).

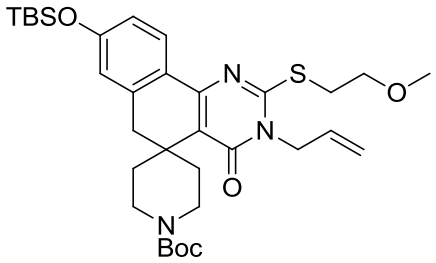

***tert*-Butyl 3-allyl-8-((tert-butyldimethylsilyl)oxy)-2-((2-methoxyethyl)thio)-4-oxo-4,6-dihydro-3H-spiro[benzo[h]quinazoline-5,4'-piperidine]-1'-carboxylate (241).** Intermediate **240** (1.17 g, 2.05 mmol) was combined with sodium bicarbonate (259 mg, 3.08 mmol) and 2-methoxyethyl tosylate (496 mg, 2.16 mmol) in anhydrous DMF (12 mL), and heated to 75°C. The reaction was allowed to stir for 16 hours, at which time the reaction was quenched by the addition of water. The aqueous suspension was extracted 3x into ethyl acetate, then the pooled organic extract was washed 2x with water and 1x with brine. The organic layer was dried over $MgSO_4$, vacuum filtered, and concentrated, then further purified via flash chromatography (0-20% EtOAc:hexanes) to furnish the product as a white solid (626 mg, 49% yield). ^{1}H NMR (500 MHz, Chloroform-*d*) δ 7.95 (d, *J* = 8.4 Hz, 1H), 6.79 (dd, *J* = 8.4, 2.4 Hz, 1H), 6.69 (d, *J* = 2.4 Hz, 1H), 5.91 (ddt, *J* = 16.2, 10.7, 5.6 Hz, 1H), 5.32 – 5.24 (m, 2H), 4.67 (d, *J* = 5.6 Hz, 2H), 4.06 – 3.87 (m, 2H), 3.76 (t, *J* = 6.2 Hz, 2H), 3.52 (t, *J* = 6.2 Hz, 2H), 3.43 (s, 3H), 3.16 – 2.84 (m, 5H), 2.67 – 2.52 (m, 1H), 1.46 (s, 9H), 1.41 – 1.32 (m, 2H), 1.00 (s, 9H), 0.24 (s, 6H).

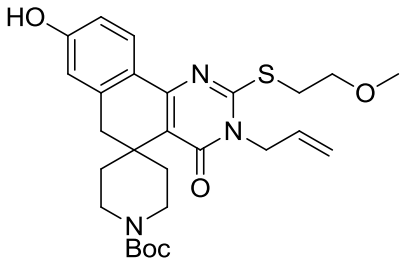

***tert*-Butyl 3-allyl-8-hydroxy-2-((2-methoxyethyl)thio)-4-oxo-4,6-dihydro-3H-spiro[benzo[h]quinazoline-5,4'-piperidine]-1'-carboxylate (intermediate in synthesis of 242, 243).** Silyl ether intermediate **241** (550 mg, 0.876 mmol) was dissolved in anhydrous THF (9 mL) and cooled to 0°C. TBAF (1M solution in THF, 1.05 mL) was added slowly dropwise. The

reaction was allowed to stir for 4 hours while slowly warming to room temperature. The reaction was quenched by the addition of water, and the resulting biphasic solution was extracted into ethyl acetate. The organic layer was washed 2x with water and 1x with brine, then isolated, dried over $MgSO_4$, filtered, and concentrated to a light yellow oil. Further purification by flash chromatography (5-25% EtOAc:hex) furnished the product as a white solid (390 mg, 87% yield). ^{1}H NMR (400 MHz, Chloroform-*d*) δ 7.95 (d, *J* = 8.5 Hz, 1H), 6.79 (dd, *J* = 8.5, 2.5 Hz, 1H), 6.69 (d, *J* = 2.5 Hz, 1H), 6.59 (s, 1H), 5.91 (ddt, *J* = 17.3, 10.7, 5.6 Hz, 1H), 5.32 – 5.22 (m, 2H), 4.67 (d, *J* = 4.9 Hz, 2H), 3.98 (d, *J* = 12.8 Hz, 2H), 3.75 (t, *J* = 6.2 Hz, 2H), 3.52 (t, *J* = 6.2 Hz, 2H), 3.42 (s, 3H), 3.23 – 2.82 (m, 5H), 2.51 – 2.35 (m, 1H), 1.47 (s, 9H), 1.37 (d, *J* = 12.8 Hz, 2H).

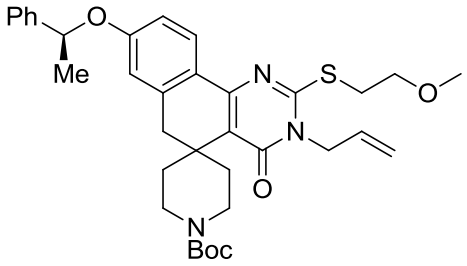

(*S*)-*tert*-Butyl 3-allyl-2-((2-methoxyethyl)thio)-4-oxo-8-(1-phenylethoxy)-4,6-dihydro-3H-spiro[benzo[h]quinazoline-5,4'-piperidine]-1'-carboxylate (242) (CCG-212348). Anhydrous THF (0.3 mL) was cooled to 0°C in an ice bath, then triphenylphosphine (28 mg, 0.107 mmol) and DIAD (22 mg, 0.107 mmol) were added. The solution was allowed to stir for 30 minutes, then (*R*)-α-methylbenzyl alcohol (13 µL, 0.107 mmol) was added and stirred for an additional 15 minutes. The deprotected phenol intermediate (50 mg, 0.097 mmol) was added and the reaction allowed to stir at 0°C for 2 hours, then an additional 16 hours at room temperature overnight. The reaction mixture was diluted with water and extracted into ethyl acetate 2x. The organic layer was washed with saturated aqueous ammonium chloride, water, and brine, then dried over $MgSO_4$, vacuum filtered, and concentrated under reduced pressure. The crude organic extract was purified via flash chromatography (5-40% EtOAc:hex) to furnish the desired product as a crystalline white solid (26 mg, 43% yield). ^{1}H NMR (400 MHz, Chloroform-*d*) δ 7.90 (d, *J* = 8.6 Hz, 1H), 7.42 – 7.31 (m, 4H), 7.31 – 7.21 (m, 1H), 6.78 (d, *J* = 8.6 Hz, 1H), 6.71 (s, 1H), 5.89 (ddt, *J* = 16.0, 10.7, 5.6 Hz, 1H), 5.37 (q, *J* = 6.4 Hz, 1H), 5.30 – 5.21 (m, 2H), 4.65 (d, *J* = 5.0 Hz, 2H), 4.05 – 3.81 (m, 2H), 3.71 (t, *J* = 6.2 Hz, 2H), 3.48 (t, *J* = 6.2 Hz, 2H), 3.39 (s, 3H), 3.13

– 2.79 (m, 5H), 2.66 – 2.43 (m, 1H), 1.66 (d, *J* = 6.4 Hz, 3H), 1.45 (s, 9H), 1.40 – 1.23 (m, 2H). ESI+MS *m/z* = 618.3 ($M + H^+$), 640.3 ($M + Na^+$). HPLC (Method B, t_R = 10.03 min), purity >95%.

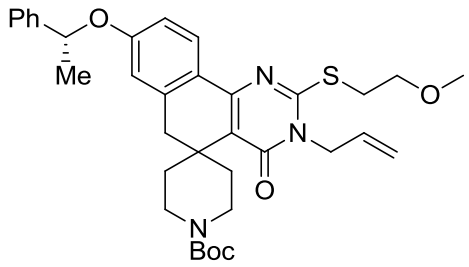

(*R*)-*tert*-Butyl 3-allyl-2-((2-methoxyethyl)thio)-4-oxo-8-(1-phenylethoxy)-4,6-dihydro-3H-spiro[benzo[h]quinazoline-5,4'-piperidine]-1'-carboxylate (243) (CCG-212349). Prepared in a manner similar to **242** from the deprotected phenol (50 mg, 0.097 mmol) and (*S*)-α-methylbenzyl alcohol (25 µL, 0.127 mmol). Isolated after column chromatography as a white powder (31 mg, 52% yield). ^{1}H NMR (400 MHz, Chloroform-*d*) δ 7.90 (d, *J* = 8.6 Hz, 1H), 7.42 – 7.30 (m, 4H), 7.31 – 7.23 (m, 1H), 6.78 (d, *J* = 8.7 Hz, 1H), 6.71 (s, 1H), 5.94 – 5.82 (m, 1H), 5.37 (q, *J* = 6.4 Hz, 1H), 5.30 – 5.21 (m, 2H), 4.65 (d, *J* = 5.3 Hz, 2H), 4.04 – 3.85 (m, 2H), 3.71 (t, *J* = 6.2 Hz, 2H), 3.48 (t, *J* = 6.2 Hz, 2H), 3.39 (s, 3H), 3.15 – 2.78 (m, 5H), 2.64 – 2.46 (m, 1H), 1.66 (d, *J* = 6.4 Hz, 3H), 1.45 (s, 9H), 1.39 – 1.22 (m, 2H).. ESI+MS *m/z* = 618.4 ($M + H^+$), 640.3 ($M + Na^+$). HPLC (Method B, t_R = 10.06 min), purity >95%.

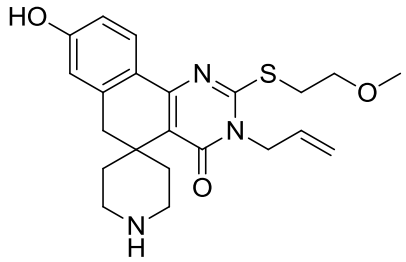

3-Allyl-8-hydroxy-2-((2-methoxyethyl)thio)-3H-spiro[benzo[h]quinazoline-5,4'-piperidin]-4(6H)-one (244) (CCG-212352). Chiral ether **242** (26 mg, 0.043 mmol) was dissolved in DCM (400 µL) and cooled to 0°C. TFA (14 µL, 0.171 mmol) was added and the reaction was allowed to stir and warm to room temperature over 3 hours. The reaction was quenched by the dropwise addition of saturated aqueous sodium carbonate, and the suspension extracted with additional DCM. The organic layer was washed with water and brine, then dried over $MgSO_4$, filtered, and

concentrated. Treatment of the organic extract with diethyl ether induced the precipitation of a white solid, found to be **244**, which was isolated by vacuum filtration (17 mg, 96% yield). ^{1}H NMR (400 MHz, Methanol-d_4) δ 7.96 (d, J = 8.4 Hz, 1H), 6.78 – 6.68 (m, 2H), 5.90 (ddd, J = 17.1, 10.5, 5.3 Hz, 1H), 5.27 – 5.15 (m, 2H), 4.69 (d, J = 5.4 Hz, 2H), 3.73 (t, J = 6.3 Hz, 2H), 3.53 (t, J = 6.3 Hz, 2H), 3.39 (s, 3H), 3.23 – 3.10 (m, 4H), 3.08 (s, 2H), 2.91 (td, J = 13.3, 5.8 Hz, 2H), 1.52 (d, J = 14.1 Hz, 2H). ESI-MS+ m/z = 414.0 ($M + H^+$). HPLC (Method A, t_R = 5.05 min), purity >95%.

References

1. World Health Organization, World Health Statistics Annual Report. **2013**.
2. Selwyn, S., Pioneer work on the 'penicillin phenomenon', 1870–1876. *J Antimicrob Chemoth* **1979,** *5* (3), 249-255.
3. Fleming, A., On the Antibacterial Action of Cultures of a Penicillium, with Special Reference to their Use in the Isolation of *B. Influenzae*. *British Journal of Experimental Pathology* **1929,** *X* (3), 226-236.
4. Chain, E.; Florey, H. W.; Gardner, A. D.; Heatley, N. G.; Jennings, M. A.; Orr-Ewing, J.; Sanders, A. G., Penicillin as a Chemotherapeutic Agent. *Lancet* **1940,** *236* (6104), 226-228.
5. Long, P. H.; Bliss, E. A., Observations Upon the Experimental and Clinical Use of Sulphanilamide in the Treatment of Certain Infections. *Can Med Assoc J* **1937,** *37* (5), 457-465.
6. Schatz, A.; Bugle, E.; Waksman, S. A., Streptomycin, a Substance Exhibiting Antibiotic Activity Against Gram-Positive and Gram-Negative Bacteria. *Exp Biol Med* **1944,** *55* (1), 66-69.
7. Duggar, B. M., Aureomycin: A product of the continuing search for new antibiotics. *Ann Ny Acad Sci* **1948,** *51* (2), 177-181.
8. Wolleswinkel-van den Bosch, J. H.; Looman, C. W.; Van Poppel, F. W.; Mackenbach, J. P., Cause-specific mortality trends in The Netherlands, 1875-1992: a formal analysis of the epidemiologic transition. *International Journal of Epidemiology* **1997,** *26* (4), 772-781.
9. Mackenbach, J. P.; Looman, C. W., Secular trends of infectious disease mortality in The Netherlands, 1911-1978: quantitative estimates of changes coinciding with the introduction of antibiotics. *International Journal of Epidemiology* **1988,** *17* (3), 618-624.
10. Guyer, B.; Freedman, M. A.; Strobino, D. M.; Sondik, E. J., Annual summary of vital statistics: trends in the health of Americans during the 20th century. *Pediatrics* **2000,** *106* (6), 1307-1317.
11. Petersdorf, R. G., The doctors' dilemma. *New Engl J Med* **1978,** *299* (12), 628-634.
12. Fauci, A. S., Infectious diseases: considerations for the 21st century. *Clinical Infectious Diseases* **2001,** *32* (5), 675-685.

13. NobelMedia-AB Sir Alexander Fleming - Nobel Lecture: Penicillin. . http://www.nobelprize.org/nobel_prizes/medicine/laureates/1945/fleming-lecture.html (accessed July 21, 2013).
14. Goldmann, D. A.; Huskins, W. C., Control of nosocomial antimicrobial-resistant bacteria: a strategic priority for hospitals worldwide. *Clinical Infectious Diseases* **1997,** *24 Suppl 1*, S139-S145.
15. Fischbach, M. A.; Walsh, C. T., Antibiotics for Emerging Pathogens. *Science* **2009,** *325* (5944), 1089-1093.
16. Tenover, F. C., Mechanisms of Antimicrobial Resistance in Bacteria. *Am J Med* **2006,** *119* (6, Supplement 1), S3-S10.
17. Nathan, C.; Goldberg, F. M., Outlook: the profit problem in antibiotic R&D. *Nat Rev Drug Discov* **2005,** *4* (11), 887-891.
18. Clatworthy, A. E.; Pierson, E.; Hung, D. T., Targeting virulence: a new paradigm for antimicrobial therapy. *Nat Chem Biol* **2007,** *3* (9), 541-548.
19. Karginov, V. A.; Nestorovich, E. M.; Yohannes, A.; Robinson, T. M.; Fahmi, N. E.; Schmidtmann, F.; Hecht, S. M.; Bezrukov, S. M., Search for cyclodextrin-based inhibitors of anthrax toxins: Synthesis, structural features, and relative activities. *Antimicrob Agents Ch* **2006,** *50* (11), 3740-3753.
20. Chorell, E.; Pinkner, J. S.; Bengtsson, C.; Banchelin, T. S. L.; Edvinsson, S.; Linusson, A.; Hultgren, S. J.; Almqvist, F., Mapping pilicide anti-virulence effect in Escherichia coli, a comprehensive structure-activity study. *Bioorgan Med Chem* **2012,** *20* (9), 3128-3142.
21. Borlee, B. R.; Geske, G. D.; Blackwell, H. E.; Handelsman, J., Identification of Synthetic Inducers and Inhibitors of the Quorum-Sensing Regulator LasR in Pseudomonas aeruginosa by High-Throughput Screening. *Appl Environ Microb* **2010,** *76* (24), 8255-8258.
22. Marsden, D. M.; Nicholson, R. L.; Skindersoe, M. E.; Galloway, W. R. J. D.; Sore, H. F.; Givskov, M.; Salmond, G. P. C.; Ladlow, M.; Welchd, M.; Spring, D. R., Discovery of a quorum sensing modulator pharmacophore by 3D small-molecule microarray screening. *Org Biomol Chem* **2010,** *8* (23), 5313-5323.
23. Rasko, D. A.; Moreira, C. G.; Li, D. R.; Reading, N. C.; Ritchie, J. M.; Waldor, M. K.; Williams, N.; Taussig, R.; Wei, S. G.; Roth, M.; Hughes, D. T.; Huntley, J. F.; Fina, M. W.; Falck, J. R.; Sperandio, V., Targeting QseC signaling and virulence for antibiotic development. *Science* **2008,** *321* (5892), 1078-1080.
24. Moayeri, M.; Robinson, T. A.; Leppla, S. H.; Karginov, V. A., In vivo efficacy of beta-cyclodextrin derivatives against anthrax lethal toxin. *Antimicrob Agents Ch* **2008,** *52* (6), 2239-2241.
25. Wu, H.; Song, Z.; Hentzer, M.; Andersen, J. B.; Molin, S.; Givskov, M.; Hoiby, N., Synthetic furanones inhibit quorum-sensing and enhance bacterial clearance in

Pseudomonas aeruginosa lung infection in mice. *J Antimicrob Chemoth* **2004,** *53* (6), 1054-1061.
26. Carapetis, J. R.; Steer, A. C.; Mulholland, E. K.; Weber, M., The global burden of group A streptococcal diseases. *Lancet Infect Dis* **2005,** *5* (11), 685-694.
27. World Health Organization. The current evidence for the burden of group A streptococcal diseases *World Health Organization Discussion Papers on Child Health.* [Online], 2005.
28. O'Loughlin, R. E.; Roberson, A.; Cieslak, P. R.; Lynfield, R.; Gershman, K.; Craig, A.; Albanese, B. A.; Farley, M. M.; Barrett, N. L.; Spina, N. L.; Beall, B.; Harrison, L. H.; Reingold, A.; Beneden, C. V.; Team, A. B. C. S., The Epidemiology of Invasive Group A Streptococcal Infection and Potential Vaccine Implications: United States, 2000–2004. *Clinical Infectious Diseases* **2007,** *45* (7), 853-862.
29. Stevens, D. L., Streptococcal Toxic-Shock Syndrome: Spectrum of Disease, Pathogenesis, and New Concepts in Treatment. *Emerg Infect Dis* **1995,** *1* (3), 69-78.
30. Bisno, A. L., Group A Streptococcal Infections and Acute Rheumatic Fever. *New Engl J Med* **1991,** *325* (11), 783-793.
31. Kaul, R.; McGeer, A.; Low, D. E.; Green, K.; Schwartz, B.; Simor, A. E., Population-Based Surveillance for Group A Streptococcal Necrotizing Fasciitis: Clinical Features, Prognostic Indicators, and Microbiologic Analysis of Seventy-Seven Cases. *The American Journal of Medicine* **1997,** *103* (1), 18-24.
32. Bisno, A. L.; Brito, M. O.; Collins, C. M., Molecular basis of group A streptococcal virulence. *The Lancet Infectious Diseases* **2003,** *3* (4), 191-200.
33. Phillips, G. N.; Flicker, P. F.; Cohen, C.; Manjula, B. N.; Fischetti, V. A., Streptococcal M protein: alpha-helical coiled-coil structure and arrangement on the cell surface. *PNAS USA* **1981,** *78* (8), 4689-4693.
34. Berggård, K.; Johnsson, E.; Morfeldt, E.; Persson, J.; Stålhammar-Carlemalm, M.; Lindahl, G., Binding of human C4BP to the hypervariable region of M protein: a molecular mechanism of phagocytosis resistance in Streptococcus pyogenes. *Mol Microbiol* **2001,** *42* (2), 539-551.
35. Bisno, A. L., Alternate complement pathway activation by group A streptococci: role of M-protein. *Infect Immun* **1979,** *26* (3), 1172-1176.
36. Dale, J. B.; Washburn, R. G.; Marques, M. B.; Wessels, M. R., Hyaluronate capsule and surface M protein in resistance to opsonization of group A streptococci. *Infect Immun* **1996,** *64* (5), 1495-1501.
37. Courtney, H. S.; Hasty, D. L.; Dale, J. B., Molecular mechanisms of adhesion, colonization, and invasion of group A streptococci. *Annals of Medicine* **2002,** *34* (2), 77-87.
38. Sierig, G.; Cywes, C.; Wessels, M. R.; Ashbaugh, C. D., Cytotoxic Effects of Streptolysin O and Streptolysin S Enhance the Virulence of Poorly Encapsulated Group A Streptococci. *Infect Immun* **2003,** *71* (1), 446-455.

39. Lukomski, S.; Sreevatsan, S.; Amberg, C.; Reichardt, W.; Woischnik, M.; Podbielski, A.; Musser, J. M., Inactivation of Streptococcus pyogenes extracellular cysteine protease significantly decreases mouse lethality of serotype M3 and M49 strains. *J Clin Invest* **1997,** *99* (11), 2574-2580.
40. Sun, H.; Ringdahl, U.; Homeister, J. W.; Fay, W. P.; Engleberg, N. C.; Yang, A. Y.; Rozek, L. S.; Wang, X.; Sjobring, U.; Ginsburg, D., Plasminogen is a critical host pathogenicity factor for group A streptococcal infection. *Science* **2004,** *305* (5688), 1283-1286.
41. Alkjaersig, N.; Fletcher, A. P.; Sherry, S., The mechanism of clot dissolution by plasmin. *J Clin Invest* **1959,** *38* (7), 1086-1095.
42. Lijnen, H. R., Elements of the Fibrinolytic System. *Ann Ny Acad Sci* **2001,** *936* (1), 226-236.
43. Law, Ruby H. P.; Caradoc-Davies, T.; Cowieson, N.; Horvath, Anita J.; Quek, Adam J.; Encarnacao, Joanna A.; Steer, D.; Cowan, A.; Zhang, Q.; Lu, Bernadine G. C.; Pike, Robert N.; Smith, A. I.; Coughlin, Paul B.; Whisstock, James C., The X-ray Crystal Structure of Full-Length Human Plasminogen. *Cell Reports* **2012,** *1* (3), 185-190.
44. Parry, M. A. A.; Zhang, X. C.; Bode, W., Molecular mechanisms of plasminogen activation: bacterial cofactors provide clues. *Trends Biochem Sci* **2000,** *25* (2), 53-59.
45. Sun, H.; Xu, Y.; Sitkiewicz, I.; Ma, Y.; Wang, X.; Yestrepsky, B. D.; Huang, Y.; Lapadatescu, M. C.; Larsen, M. J.; Larsen, S. D.; Musser, J. M.; Ginsburg, D., Inhibitor of streptokinase gene expression improves survival after group A streptococcus infection in mice. *PNAS USA* **2012,** *109* (9), 3469-3474.
46. Perez-Casal, J.; Caparon, M. G.; Scott, J. R., Mry, a trans-acting positive regulator of the M protein gene of Streptococcus pyogenes with similarity to the receptor proteins of two-component regulatory systems. *J Bacteriol* **1991,** *173* (8), 2617-2624.
47. Lipinski, C. A.; Lombardo, F.; Dominy, B. W.; Feeney, P. J., Experimental and computational approaches to estimate solubility and permeability in drug discovery and development settings. *Adv Drug Deliv Rev* **2001,** *46* (1-3), 3-26.
48. Lewis, D. F. V.; Jacobs, M. N.; Dickins, M., Compound lipophilicity for substrate binding to human P450s in drug metabolism. *Drug Discovery Today* **2004,** *9* (12), 530-537.
49. Craig, B. A., Modeling approach to diameter breakpoint determination. *Diagn Micr Infec Dis* **2000,** *36* (3), 193-202.
50. Ghaemmaghami, S.; Huh, W.; Bower, K.; Howson, R. W.; Belle, A.; Dephoure, N.; O'Shea, E. K.; Weissman, J. S., Global analysis of protein expression in yeast. *Nature* **2003,** *425* (6959), 737-741.
51. Markosyan, A. I.; Kuroyan, R. A.; Lilanyan, S. V., Synthesis and transformation of 4-amino-3-ethoxycarbonyl-1,2-dihydrospiro(naphthalene-2,1 '-cyclopentane). *Khim Geterotsikl Soed* **1998,** (6), 820-823.

52. Markosyan, A. I.; Kuroyan, R. A.; Karapetyan, K. V., Synthesis of 2-alkylthio-substituted 3-p-tolyl-4-oxo-3,4,5,6-tetrahydrospiro(benzo [h]quinazoline-5,1 '-cycloalkanes). *Khim Geterotsikl Soed* **1999,** (12), 1655-1658.
53. Boehm, T. L.; Christie, L. C.; Devadas, B.; Madsen, H. M.; Marrufo, L.; Selness, S. Substituted N-alkylpyrimidinones. WO2006040666, 2006.
54. Yestrepsky, B. D.; Xu, Y.; Breen, M. E.; Li, X.; Rajeswaran, W. G.; Ryu, J. G.; Sorenson, R. J.; Tsume, Y.; Wilson, M. W.; Zhang, W.; Sun, D.; Sun, H.; Larsen, S. D., Novel inhibitors of bacterial virulence: development of 5,6-dihydrobenzo[h]quinazolin-4(3H)-ones for the inhibition of group A streptococcal streptokinase expression. *Bioorg Med Chem* **2013,** *21* (7), 1880-97.
55. Kobayashi, K.; Uneda, T.; Takada, K.; Tanaka, H.; Kitamura, T.; Morikawa, O.; Konishi, H., Efficient synthesis of 1-amino-2-naphthalenecarboxylic acid derivatives via a sequential Michael addition enolate-nitrile coupling route and its application to facile preparation of 9-amino analogues of arylnaphthofuranone lignans. *J Org Chem* **1997,** *62* (3), 664-668.
56. Chong, J. A.; Abdesaken, F.; Wu, C. C. Process for synthesizing benzoic acids. US Patent No. 5,965,766, 1999.
57. Markosyan, A. I.; Kuroyan, R. A.; Dilanyan, S. V.; Aleksanyan, M. S.; Karapetyan, A. A.; Struchkov, Y. T., Synthesis and structure of 2-methyl-6-oxo-7,8-dihydrospiro(benzo[h]triazolo[3,4-b]quinazoline-7,1 '-cyclopentane). *Khim Geterotsikl Soed* **2000,** (5), 658-662.
58. Peifer, C.; Abadleh, M.; Bischof, J.; Hauser, D.; Schattel, V.; Hirner, H.; Knippschild, U.; Laufer, S., 3,4-Diaryl-isoxazoles and -imidazoles as Potent Dual Inhibitors of p38 alpha Mitogen Activated Protein Kinase and Casein Kinase 1 delta. *J Med Chem* **2009,** *52* (23), 7618-7630.
59. Roy, A.; Paul, T.; Mukherjee, D., A new total synthesis of (±)-isolongifolene involving an aryl participated diazoketone cyclisation strategy. *ARKIVOC* **2005,** *2005* (11), 218-225.
60. Guillon, J.; Dallemagne, P.; Leger, J. M.; Sopkova, J.; Bovy, P. R.; Jarry, C.; Rault, S., Synthesis of a novel class of non-peptide NK-2 receptor ligand, derived from 1-phenyl-3-pyrrol-1-ylindan-2-carboxamides. *Bioorgan Med Chem* **2002,** *10* (4), 1043-1050.
61. Chowdhury, A. Z.; Shibata, Y., Synthesis of new fused pyrimidines by isocyanate and isothiocyanate. *Chem Pharm Bull (Tokyo)* **2001,** *49* (4), 391-395.
62. Benincori, T.; Bruno, S.; Celentano, G.; Pilati, T.; Ponti, A.; Rizzo, S.; Sada, M.; Sannicolò, F., Process-Scale Total Synthesis of Nature-Identical (−)-(S,S)-7-Hydroxycalamenal in High Enantiomeric Purity through Catalytic Enantioselective Hydrogenation. *Helvetica Chimica Acta* **2005,** *88* (7), 1776-1789.
63. Nakamura, S.; Sugimoto, H.; Ohwada, T., Superacid-catalyzed intramolecular cyclization reaction of arylcyanopropionate: geminal substitution effect on superelectrophilicity. *J Org Chem* **2008,** *73* (11), 4219-4224.

64. Cho, W.-J.; Kim, I. J.; Park, S.-J., A Convenient Synthesis of 5-Methylbenzo[c]phenanthridin-6 (5H)-one. *Bulletin of the Korean Chemical Society* **2000,** *21* (10), 1035-1038.
65. Davis, F. A.; Mohanty, P. K.; Burns, D. M.; Andemichael, Y. W., Sulfinimine-mediated asymmetric synthesis of 1,3-disubstituted tetrahydroisoquinolines: a stereoselective synthesis of cis- and trans-6,8-dimethoxy-1,3-dimethyl-1,2,3,4-tetrahydroisoquinoline. *Org Lett* **2000,** *2* (24), 3901-3903.
66. Puupponen-Pimia, R.; Nohynek, L.; Meier, C.; Kahkonen, M.; Heinonen, M.; Hopia, A.; Oksman-Caldentey, K. M., Antimicrobial properties of phenolic compounds from berries. *J Appl Microbiol* **2001,** *90* (4), 494-507.
67. Lipinski, C. A., Drug-like properties and the causes of poor solubility and poor permeability. *J Pharmacol Toxicol* **2000,** *44* (1), 235-249.
68. Bevan, C. D.; Lloyd, R. S., A high-throughput screening method for the determination of aqueous drug solubility using laser nephelometry in microtiter plates. *Anal Chem* **2000,** *72* (8), 1781-1787.
69. Stockwell, B. R., Exploring biology with small organic molecules. *Nature* **2004,** *432* (7019), 846-854.
70. Payne, D. J.; Gwynn, M. N.; Holmes, D. J.; Pompliano, D. L., Drugs for bad bugs: confronting the challenges of antibacterial discovery. *Nat Rev Drug Discov* **2007,** *6* (1), 29-40.
71. Kreikemeyer, B.; McIver, K. S.; Podbielski, A., Virulence factor regulation and regulatory networks in Streptococcus pyogenes and their impact on pathogen–host interactions. *Trends in Microbiology* **2003,** *11* (5), 224-232.
72. McIver, K. S.; Scott, J. R., Role of mga in growth phase regulation of virulence genes of the group A streptococcus. *J Bacteriol* **1997,** *179* (16), 5178-5187.
73. Beckert, S.; Kreikemeyer, B.; Podbielski, A., Group A Streptococcal rofA Gene Is Involved in the Control of Several Virulence Genes and Eukaryotic Cell Attachment and Internalization. *Infect Immun* **2001,** *69* (1), 534-537.
74. Chaussee, M. S.; Ajdic, D.; Ferretti, J. J., The rgg Gene of Streptococcus pyogenes NZ131 Positively Influences Extracellular SPE B Production. *Infect Immun* **1999,** *67* (4), 1715-1722.
75. Chaussee, M. S.; Sylva, G. L.; Sturdevant, D. E.; Smoot, L. M.; Graham, M. R.; Watson, R. O.; Musser, J. M., Rgg Influences the Expression of Multiple Regulatory Loci To Coregulate Virulence Factor Expression in Streptococcus pyogenes. *Infect Immun* **2002,** *70* (2), 762-770.
76. Federle, M. J.; McIver, K. S.; Scott, J. R., A Response Regulator That Represses Transcription of Several Virulence Operons in the Group A Streptococcus. *J Bacteriol* **1999,** *181* (12), 3649-3657.
77. Voyich, J. M.; Sturdevant, D. E.; Braughton, K. R.; Kobayashi, S. D.; Lei, B.; Virtaneva, K.; Dorward, D. W.; Musser, J. M.; DeLeo, F. R., Genome-wide protective response used

by group A Streptococcus to evade destruction by human polymorphonuclear leukocytes. *PNAS USA* **2003,** *100* (4), 1996-2001.

78. Kreikemeyer, B.; Boyle, M. D. P.; Buttaro, B. A.; Heinemann, M.; Podbielski, A., Group A streptococcal growth phase-associated virulence factor regulation by a novel operon (Fas) with homologies to two-component-type regulators requires a small RNA molecule. *Mol Microbiol* **2001,** *39* (2), 392-406.
79. Ramirez-Peña, E.; Treviño, J.; Liu, Z.; Perez, N.; Sumby, P., The group A Streptococcus small regulatory RNA FasX enhances streptokinase activity by increasing the stability of the ska mRNA transcript. *Mol Microbiol* **2010,** *78* (6), 1332-1347.
80. Heath, A.; DiRita, V. J.; Barg, N. L.; Engleberg, N. C., A Two-Component Regulatory System, CsrR-CsrS, Represses Expression of Three Streptococcus pyogenesVirulence Factors, Hyaluronic Acid Capsule, Streptolysin S, and Pyrogenic Exotoxin B. *Infect Immun* **1999,** *67* (10), 5298-5305.
81. Agarwal, S.; Agarwal, S.; Pancholi, P.; Pancholi, V., Role of Serine/Threonine Phosphatase (SP-STP) in Streptococcus pyogenes Physiology and Virulence. *J Biol Chem* **2011,** *286* (48), 41368-41380.
82. Kang, S. O.; Caparon, M. G.; Cho, K. H., Virulence Gene Regulation by CvfA, a Putative RNase: the CvfA-Enolase Complex in Streptococcus pyogenes Links Nutritional Stress, Growth-Phase Control, and Virulence Gene Expression. *Infect Immun* **2010,** *78* (6), 2754-2767.
83. Jin, H.; Agarwal, S.; Agarwal, S.; Pancholi, V., Surface Export of GAPDH/SDH, a Glycolytic Enzyme, Is Essential for Streptococcus pyogenes Virulence. *Mbio* **2011,** *2* (3), e00068-11.
84. Beres, S. B.; Sylva, G. L.; Barbian, K. D.; Lei, B.; Hoff, J. S.; Mammarella, N. D.; Liu, M.-Y.; Smoot, J. C.; Porcella, S. F.; Parkins, L. D.; Campbell, D. S.; Smith, T. M.; McCormick, J. K.; Leung, D. Y. M.; Schlievert, P. M.; Musser, J. M., Genome sequence of a serotype M3 strain of group A Streptococcus: Phage-encoded toxins, the high-virulence phenotype, and clone emergence. *PNAS USA* **2002,** *99* (15), 10078-10083.
85. Leslie, B. J.; Hergenrother, P. J., Identification of the cellular targets of bioactive small organic molecules using affinity reagents. *Chem Soc Rev* **2008,** *37* (7), 1347-1360.
86. Harding, M. W.; Galat, A.; Uehling, D. E.; Schreiber, S. L., A receptor for the immuno-suppressant FK506 is a cis-trans peptidyl-prolyl isomerase. *Nature* **1989,** *341* (6244), 758-760.
87. Adam, G. C.; Vanderwal, C. D.; Sorensen, E. J.; Cravatt, B. F., (−)-FR182877 Is a Potent and Selective Inhibitor of Carboxylesterase-1. *Angewandte Chemie International Edition* **2003,** *42* (44), 5480-5484.
88. Bach, S.; Knockaert, M.; Reinhardt, J.; Lozach, O.; Schmitt, S.; Baratte, B.; Koken, M.; Coburn, S. P.; Tang, L.; Jiang, T.; Liang, D.-c.; Galons, H.; Dierick, J.-F.; Pinna, L. A.; Meggio, F.; Totzke, F.; Schächtele, C.; Lerman, A. S.; Carnero, A.; Wan, Y.; Gray, N.;

Meijer, L., Roscovitine Targets, Protein Kinases and Pyridoxal Kinase. *J Biol Chem* **2005,** *280* (35), 31208-31219.
89. Menger, F. M.; Zhang, H., Self-adhesion among phospholipid vesicles. *J Am Chem Soc* **2006,** *128* (5), 1414-1415.
90. Winssinger, N.; Ficarro, S.; Schultz, P. G.; Harris, J. L., Profiling protein function with small molecule microarrays. *PNAS USA* **2002,** *99* (17), 11139-11144.
91. Morales-Sanfrutos, J.; Lopez-Jaramillo, F. J.; Hernandez-Mateo, F.; Santoyo-Gonzalez, F., Vinyl Sulfone Bifunctional Tag Reagents for Single-Point Modification of Proteins. *J Org Chem* **2010,** *75* (12), 4039-4047.
92. Fleming, S. A., Chemical reagents in photoaffinity labeling. *Tetrahedron* **1995,** *51* (46), 12479-12520.
93. Keana, J. F. W.; Cai, S. X., New reagents for photoaffinity labeling: synthesis and photolysis of functionalized perfluorophenyl azides. *J Org Chem* **1990,** *55* (11), 3640-3647.
94. MacKinnon, A. L.; Garrison, J. L.; Hegde, R. S.; Taunton, J., Photo-leucine incorporation reveals the target of a cyclodepsipeptide inhibitor of cotranslational translocation. *J Am Chem Soc* **2007,** *129* (47), 14560-14561.
95. Mayer, T.; Maier, M. E., Design and synthesis of a tag-free chemical probe for Photoaffinity Labeling. *Eur J Org Chem* **2007,** (28), 4711-4720.
96. Fujii, T.; Manabe, Y.; Sugimoto, T.; Ueda, M., Detection of 210 kDa receptor protein for a leaf-movement factor by using novel photoaffinity probes. *Tetrahedron* **2005,** *61* (33), 7874-7893.
97. Salisbury, C. M.; Cravatt, B. F., Click chemistry-led advances in high content functional proteomics. *Qsar Comb Sci* **2007,** *26* (11-12), 1229-1238.
98. Carato, P.; Moussavi, Z.; Sabaouni, A.; Lebegue, N.; Berthelot, P.; Yous, S., Synthesis of 6- and 7-acyl-4H-benzothiazin-3-ones. *Tetrahedron* **2006,** *62* (38), 9054-9058.
99. Moriello, A. S.; Balas, L.; Ligresti, A.; Cascio, M. G.; Durand, T.; Morera, E.; Ortar, G.; Di Marzo, V., Development of the first potential covalent inhibitors of anandamide cellular uptake. *J Med Chem* **2006,** *49* (7), 2320-2332.
100. Bond, M. R.; Zhang, H. C.; Vu, P. D.; Kohler, J. J., Photocrosslinking of glycoconjugates using metabolically incorporated diazirine-containing sugars. *Nat Protoc* **2009,** *4* (7), 1044-1063.
101. Church, R. F. R.; Weiss, M. J., Diazirines .2. Synthesis and Properties of Small Functionalized Diazirine Molecules - Some Observations on Reaction of a Diaziridine with Iodine-Iodide Ion System. *J Org Chem* **1970,** *35* (8), 2465-&.
102. Chae, J. Y.; Buchwald, S. L., Palladium-catalyzed regioselective hydrodebromination of dibromoindoles: Application to the enantioselective synthesis of indolodioxane U86192A. *J Org Chem* **2004,** *69* (10), 3336-3339.
103. Andersen, J.; Madsen, U.; Bjorkling, F.; Liang, X. F., Rapid synthesis of aryl azides from aryl halides under mild conditions. *Synlett* **2005,** (14), 2209-2213.

104. Pianowski, Z.; Rubnicki, L.; Cmoch, P.; Stalinski, K., Radical Cyclizations Leading to the Bicyclo[2.2.1]heptane Framework: A New Radical Approach to (±)-(*Z*)-ß-Santalol. *Synlett* **2005,** *2005* (6), 900-904.
105. Nickon, A., New perspectives on carbene rearrangements: migratory aptitudes, bystander assistance, and geminal efficiency. *Acc Chem Res* **1993,** *26* (3), 84-89.
106. Ong, S. E.; Schenone, M.; Margolin, A. A.; Li, X. Y.; Do, K.; Doud, M. K.; Mani, D. R.; Kuai, L.; Wang, X.; Wood, J. L.; Tolliday, N. J.; Koehler, A. N.; Marcaurelle, L. A.; Golub, T. R.; Gould, R. J.; Schreiber, S. L.; Carr, S. A., Identifying the proteins to which small-molecule probes and drugs bind in cells. *PNAS USA* **2009,** *106* (12), 4617-4622.
107. Sche, P. P.; McKenzie, K. M.; White, J. D.; Austin, D. J., Display cloning: functional identification of natural product receptors using cDNA-phage display. *Chem Biol* **1999,** *6* (10), 707-716.
108. Westall, F.; de Wit, M. J.; Dann, J.; van der Gaast, S.; de Ronde, C. E. J.; Gerneke, D., Early Archean fossil bacteria and biofilms in hydrothermally-influenced sediments from the Barberton greenstone belt, South Africa. *Precambrian Research* **2001,** *106* (1–2), 93-116.
109. Hall-Stoodley, L.; Costerton, J. W.; Stoodley, P., Bacterial biofilms: from the Natural environment to infectious diseases. *Nat Rev Micro* **2004,** *2* (2), 95-108.
110. Lawrence, J. R.; Korber, D. R.; Hoyle, B. D.; Costerton, J. W.; Caldwell, D. E., Optical sectioning of microbial biofilms. *J Bacteriol* **1991,** *173* (20), 6558-6567.
111. Stoodley, P.; Sauer, K.; Davies, D. G.; Costerton, J. W., Biofilms as Complex Differentiated Communities. *Annu Rev Microbiol* **2002,** *56* (1), 187-209.
112. Bjarnsholt, T.; Jensen, P. Ø.; Fiandaca, M. J.; Pedersen, J.; Hansen, C. R.; Andersen, C. B.; Pressler, T.; Givskov, M.; Høiby, N., Pseudomonas aeruginosa biofilms in the respiratory tract of cystic fibrosis patients. *Pediatr Pulm* **2009,** *44* (6), 547-558.
113. Herzberg, M. C., Platelet-Streptococcal Interactions in Endocarditis. *Crit Rev Oral Biol M* **1996,** *7* (3), 222-236.
114. Percival, S. L.; Emanuel, C.; Cutting, K. F.; Williams, D. W., Microbiology of the skin and the role of biofilms in infection. *International Wound Journal* **2012,** *9* (1), 14-32.
115. Ceri, H.; Olson, M. E.; Stremick, C.; Read, R. R.; Morck, D.; Buret, A., The Calgary Biofilm Device: New technology for rapid determination of antibiotic susceptibilities of bacterial biofilms. *J Clin Microbiol* **1999,** *37* (6), 1771-1776.
116. Stewart, P. S., Theoretical aspects of antibiotic diffusion into microbial biofilms. *Antimicrob Agents Ch* **1996,** *40* (11), 2517-2522.
117. Brown, M. R. W.; Allison, D. G.; Gilbert, P., Resistance of bacterial biofilms to antibiotics a growth-rate related effect? *J Antimicrob Chemoth* **1988,** *22* (6), 777-780.
118. Adams, J. L.; McLean, R. J. C., Impact of rpoS Deletion on Escherichia coli Biofilms. *Appl Environ Microb* **1999,** *65* (9), 4285-4287.

119. Molin, S.; Tolker-Nielsen, T., Gene transfer occurs with enhanced efficiency in biofilms and induces enhanced stabilisation of the biofilm structure. *Curr Opin Biotech* **2003,** *14* (3), 255-261.
120. Archibald, L.; Phillips, L.; Monnet, D.; McGowan, J. E., Jr.; Tenover, F.; Gaynes, R., Antimicrobial resistance in isolates from inpatients and outpatients in the United States: increasing importance of the intensive care unit. *Clin Infect Dis* **1997,** *24* (2), 211-215.
121. Page, C. P.; Bohnen, J. M. A.; Fletcher, J. R.; Mcmanus, A. T.; Solomkin, J. S.; Wittmann, D. H., Antimicrobial Prophylaxis for Surgical Wounds - Guidelines for Clinical Care. *Arch Surg-Chicago* **1993,** *128* (1), 79-88.
122. Lembke, C.; Podbielski, A.; Hidalgo-Grass, C.; Jonas, L.; Hanski, E.; Kreikemeyer, B., Characterization of Biofilm Formation by Clinically Relevant Serotypes of Group A Streptococci. *Appl Environ Microb* **2006,** *72* (4), 2864-2875.
123. Rohde, H.; Burandt, E. C.; Siemssen, N.; Frommelt, L.; Burdelski, C.; Wurster, S.; Scherpe, S.; Davies, A. P.; Harris, L. G.; Horstkotte, M. A.; Knobloch, J. K. M.; Ragunath, C.; Kaplan, J. B.; Mack, D., Polysaccharide intercellular adhesin or protein factors in biofilm accumulation of Staphylococcus epidermidis and Staphylococcus aureus isolated from prosthetic hip and knee joint infections. *Biomaterials* **2007,** *28* (9), 1711-1720.
124. Barth, E.; Myrvik, Q. M.; Wagner, W.; Gristina, A. G., In vitro and in vivo comparative colonization of Staphylococcus aureus and Staphylococcus epidermidis on orthopaedic implant materials. *Biomaterials* **1989,** *10* (5), 325-328.
125. Vuong, C.; Otto, M., Staphylococcus epidermidis infections. *Microbes Infect* **2002,** *4* (4), 481-489.
126. Zimmerli, W.; Trampuz, A.; Ochsner, P. E., Prosthetic-Joint Infections. *New Engl J Med* **2004,** *351* (16), 1645-1654.
127. Zhang, Y.-Q.; Ren, S.-X.; Li, H.-L.; Wang, Y.-X.; Fu, G.; Yang, J.; Qin, Z.-Q.; Miao, Y.-G.; Wang, W.-Y.; Chen, R.-S.; Shen, Y.; Chen, Z.; Yuan, Z.-H.; Zhao, G.-P.; Qu, D.; Danchin, A.; Wen, Y.-M., Genome-based analysis of virulence genes in a non-biofilm-forming Staphylococcus epidermidis strain (ATCC 12228). *Mol Microbiol* **2003,** *49* (6), 1577-1593.
128. Mulligan, M. E.; Murray-Leisure, K. A.; Ribner, B. S.; Standiford, H. C.; John, J. F.; Korvick, J. A.; Kauffman, C. A.; Yu, V. L., Methicillin-resistant Staphylococcus aureus: A consensus review of the microbiology, pathogenesis, and epidemiology with implications for prevention and management. *The American Journal of Medicine* **1993,** *94* (3), 313-328.
129. Holden, M. T. G.; Feil, E. J.; Lindsay, J. A.; Peacock, S. J.; Day, N. P. J.; Enright, M. C.; Foster, T. J.; Moore, C. E.; Hurst, L.; Atkin, R.; Barron, A.; Bason, N.; Bentley, S. D.; Chillingworth, C.; Chillingworth, T.; Churcher, C.; Clark, L.; Corton, C.; Cronin, A.; Doggett, J.; Dowd, L.; Feltwell, T.; Hance, Z.; Harris, B.; Hauser, H.; Holroyd, S.; Jagels, K.; James, K. D.; Lennard, N.; Line, A.; Mayes, R.; Moule, S.; Mungall, K.; Ormond, D.;

Quail, M. A.; Rabbinowitsch, E.; Rutherford, K.; Sanders, M.; Sharp, S.; Simmonds, M.; Stevens, K.; Whitehead, S.; Barrell, B. G.; Spratt, B. G.; Parkhill, J., Complete genomes of two clinical Staphylococcus aureus strains: Evidence for the rapid evolution of virulence and drug resistance. *PNAS USA* **2004,** *101* (26), 9786-9791.

130. Cosgrove, S. E.; Sakoulas, G.; Perencevich, E. N.; Schwaber, M. J.; Karchmer, A. W.; Carmeli, Y., Comparison of Mortality Associated with Methicillin-Resistant and Methicillin-Susceptible Staphylococcus aureus Bacteremia: A Meta-analysis. *Clinical Infectious Diseases* **2003,** *36* (1), 53-59.
131. Christensen, G. D.; Simpson, W. A.; Younger, J. J.; Baddour, L. M.; Barrett, F. F.; Melton, D. M.; Beachey, E. H., Adherence of Coagulase-Negative Staphylococci to Plastic Tissue-Culture Plates - a Quantitative Model for the Adherence of Staphylococci to Medical Devices. *J Clin Microbiol* **1985,** *22* (6), 996-1006.
132. Ma, Y.; Xu, Y.; Yestrepsky, B. D.; Sorenson, R. J.; Chen, M.; Larsen, S. D.; Sun, H., Novel inhibitors of Staphylococcus aureus virulence gene expression and biofilm formation. *PLoS One* **2012**, e47255.
133. Wang, J.; Cady, S. D.; Balannik, V.; Pinto, L. H.; DeGrado, W. F.; Hong, M., Discovery of spiro-piperidine inhibitors and their modulation of the dynamics of the M2 proton channel from influenza A virus. *J Am Chem Soc* **2009,** *131* (23), 8066-8076.
134. Abdel-Magid, A. F.; Carson, K. G.; Harris, B. D.; Maryanoff, C. A.; Shah, R. D., Reductive Amination of Aldehydes and Ketones with Sodium Triacetoxyborohydride. Studies on Direct and Indirect Reductive Amination Procedures. *J Org Chem* **1996,** *61* (11), 3849-3862.
135. Somers, P. K.; Wandless, T. J.; Schreiber, S. L., Synthesis and analysis of 506BD, a high-affinity ligand for the immunophilin FKBP. *J Am Chem Soc* **1991,** *113* (21), 8045-8056.
136. Yang, B. V.; O'Rourke, D.; Li, J., Mild and Selective Debenzylation of Tertiary Amines Using α-Chloroethyl Chloroformate. *Synlett* **1993,** *1993* (03), 195-196.
137. Klaver, W. J.; Hiemstra, H.; Speckamp, W. N., Synthesis and absolute configuration of the Aristotelia alkaloid peduncularine. *J Am Chem Soc* **1989,** *111* (7), 2588-2595.
138. Gmeiner, P.; Junge, D.; Kaertner, A., Enantiomerically Pure Amino Alcohols and Diamino Alcohols from L-Aspartic Acid. Application to the Synthesis of Epi- and Diepislaframine. *J Org Chem* **1994,** *59* (22), 6766-6776.
139. Calestani, G.; Capella, L.; Leardini, R.; Minozzi, M.; Nanni, D.; Papa, R.; Zanardi, G., Synthesis and X-ray characterisation of a new polycondensed heterocycle obtained by a novel Mn(III)-mediated cascade reaction of 2-cyanophenyl isothiocyanate. *Tetrahedron* **2001,** *57* (33), 7221-7233.
140. Urleb, U., The reactions of heterocyclic isothiocyanates bearing an ortho ester group with aminoalcohols. *J Het Chem* **1998,** *35* (3), 693-697.
141. Johnstone, C.; McKerrecher, D.; Pike, K. G.; Waring, M. J. Heteroaryl Benzamide Derivatives for Use as GLK Activators in the Treatment of Diabetes. WO 2005/121110 A1, 2005.

142. Pfeiffer, C. C., Optical Isomerism and Pharmacological Action, a Generalization. *Science* **1956,** *124* (3210), 29-31.
143. Ariëns, E. J., Stereochemistry, a basis for sophisticated nonsense in pharmacokinetics and clinical pharmacology. *Eur J Clin Pharmacol* **1984,** *26* (6), 663-668.
144. Yestrepsky, B. D.; Xu, Y.; Breen, M. E.; Li, X.; Rajeswaran, W. G.; Ryu, J. G.; Sorenson, R. J.; Tsume, Y.; Wilson, M. W.; Zhang, W.; Sun, D.; Sun, H.; Larsen, S. D., Novel Inhibitors of Bacterial Virulence: Development of 5,6-dihydrobenzo[h]quinazolin-4(3H)-ones for the Inhibition of Group A Streptococcal Streptokinase Expression. *Bioorgan Med Chem* **2013,** *21*, 1880-1897.
145. Bjerketorp, J.; Nilsson, M.; Ljungh, Å.; Flock, J.-I.; Jacobsson, K.; Frykberg, L., A novel von Willebrand factor binding protein expressed by Staphylococcus aureus. *Microbiology* **2002,** *148* (7), 2037-2044.
146. Ong, S.-E.; Blagoev, B.; Kratchmarova, I.; Kristensen, D. B.; Steen, H.; Pandey, A.; Mann, M., Stable Isotope Labeling by Amino Acids in Cell Culture, SILAC, as a Simple and Accurate Approach to Expression Proteomics. *Mol Cell Proteomics* **2002,** *1* (5), 376-386.
147. Riesenberg, D., High-cell-density cultivation of Escherichia coli. *Curr Opin Biotech* **1991,** *2* (3), 380-384.
148. Mah, R. A.; Fung, D. Y.; Morse, S. A., Nutritional requirements of Staphylococcus aureus S-6. *Appl Microbiol* **1967,** *15* (4), 866-870.